SCOTTISH NATURAL HERITAGE

COMMISSIONED REPORT

Commissioned Report No. 007

Broad scale mapping of habitats in the Firth of Tay and Eden Estuary, Scotland

(ROAME No. F01AA401D)

For further information on this report please contact:

Dan Harries
Maritime Group
Scottish Natural Heritage
2 Anderson Place
EDINBURGH EH6 5NP
Telephone: 0131–446 2400
E-mail: dan.harries@snh.gov.uk

This report should be quoted as:

Bates, C. R., Moore, C. G., Malthus, T., Mair, J. M. and Karpouzli, E. (2004). Broad scale mapping of habitats in the Firth of Tay and Eden Estuary, Scotland. Scottish Natural Heritage Commissioned Report No. 007 (ROAME No. F01AA401D).

This report was produced for Scottish Natural Heritage by the Sedimentary Systems Research Unit, University of St Andrews, the School of Life Sciences Heriot-Watt University and the Department of Geography, University of Edinburgh on the understanding that the final data provided can be used only by these parties and SNH.

Dr Richard Bates
Sedimentary Systems Research Unit
School of Geography and Geosciences
University of St Andrews
St Andrews

Dr Colin Moore
School of Life Sciences
Heriot-Watt University
Edinburgh

Dr Tim Malthus
Department of Geography
University of Edinburgh
Edinburgh

SUPPORTING INFORMATION:

Scottish Natural Heritage holds all other non-published data products arising from this mapping project including raw sediment PSA data, video footage, raw acoustic data and GIS products.

Please contact SNH Maritime Group for further information.

COMMISSIONED REPORT
Summary

Broad scale mapping of habitats in the Firth of Tay and Eden Estuary, Scotland

Commissioned Report No. 007 (ROAME No. F01AA401D)
Contractors: University of St. Andrews, Heriot-Watt University and Edinburgh University

Background

The Firth of Tay and the Eden Estuary are situated on the east coast of Scotland between Carnoustie in the north and St Andrews in the south and the site has been selected as a candidate Special Area of Conservation (cSAC). The qualifying features include *estuaries, mudflats and sandflats not covered by seawater at low tide, sandbanks which are slightly covered by seawater all the time* and common seals *Phoca vitulina*. It is also an important site for overwintering wildfowl and waders. In order that a comprehensive management plan can be developed to ensure the sustainable use of resources within the marine cSAC it is essential to obtain an understanding of the geographic distribution and extent of the habitats of interest.

A comprehensive biotope mapping survey of the intertidal and subtidal habitats within the cSAC was undertaken in the summer of 2002, by a collaborative research group comprising staff from the University of St Andrews, Heriot-Watt University, Edinburgh University and Scottish Natural Heritage (SNH). Mapping of the intertidal of the cSAC was accomplished principally through the employment of QuickBird satellite imagery. This imagery was *'ground truthed'* by data collected by intertidal surveys. At a selected subset of locations samples were collected for sediment infauna and granulometric analysis. Subtidal areas of the site were surveyed by rapid broad scale remote acoustic mapping techniques, with *'ground truth'* data collected to enable the interpretation of the acoustically classed sea floor maps. The *'ground-truthing'* data were collected in the field using a range of sampling techniques including video imagery collected by remotely operated vehicle (ROV), epifaunal samples collected by naturalists dredge and infaunal samples collected by both pipe dredge and Van Veen grab with subsamples also retained for granulometric analysis. This information supplemented the existing knowledge on the distribution of marine communities and sediments within the Firth of Tay and Eden Estuary cSAC and all this information was used to produce a series of biotope classification maps.

Main findings

- The site is characterised by powerful tidal currents and a high suspended sediment load. It is overwhelmingly dominated by sediment biotopes. The subtidal sediments of the main river channels tend to be mobile with a relatively impoverished fauna. In the middle and outer Tay there are areas of dense mussel bed. In parts of the outer Tay there is an unusually abundant sponge fauna. Intertidal areas within the estuaries tend to be muddy and are commonly dominated by typical estuarine species such as the ragworm *Hediste diversicolor*. The sediments of more exposed shores in the outer part of the site tend to be cleaner, better drained and are commonly dominated by amphipods. Many shores in the outer Tay and in the Eden are composed of mosaics of lugworm dominated muddy sediments, beds of mussels and fucoid algae and transient mats of the green algae *Enteromorpha* sp. These shores also support sparse beds of the eelgrass *Zostera noltii*.

For further information on this project contact:

Dan Harries, Maritime Group, Scottish Natural Heritage, 2 Anderson Place, Edinburgh EH6 5NP.

Tel: 0131–446 2400

For further information on the SNH Research & Technical Support Programme contact:

The Advisory Services Co-ordination Group, Scottish Natural Heritage, 2 Anderson Place, Edinburgh EH6 5NP.

Tel: 0131–446 2400 or **ascg@snh.gov.uk**

Contents

List of tables

List of figures

1 INTRODUCTION

This report details the studies undertaken by the University of St Andrews, Heriot-Watt University and the University of Edinburgh to survey and map littoral and sublittoral communities within the Firth of Tay and Eden Estuary candidate Special Area of Conservation (cSAC). The aim of this project was to generate a record of the sedimentological, faunal and floral characteristics of the site.

The Firth of Tay and Eden Estuary area represents a particular challenge for habitat appraisal because of the existence of very shallow conditions over a large portion of the area to the west in the mid Tay Estuary, in the south over most of the Eden Estuary and for large sections in St Andrews Bay along spits extending westwards on the north and south sides of the mouth of the Tay. These shallow areas severely limited the use of Acoustic Ground Discrimination Systems (AGDS) and thus alternative techniques including airborne and satellite imagery had to be utilised. The collection of data was further complicated by the rapid tidal and river currents and by the high turbidity of the water. The data for the project were collected during multiple cruises conducted from June through August, 2002 using the research vessel *Serpula* (Heriot-Watt University) and *Envoy* (University of St Andrews) with support in the shallow areas from small inflatable boats and land access points.

Ground validation of the acoustic and aerial remote sensing data was provided through drop-video, remotely operated vehicle (ROV), grab and hand sampling methodologies. Specific objectives of the programme were to:

- Obtain full coverage bathymetric charts and acoustic ground discrimination surveys of all areas with water depths greater than 3m (sub 10m bins).
- Acquire and analyse airborne and satellite data of the shallow and intertidal areas utilising groundtruth information for image calibration.
- Acquire groundtruth information for subsequent biotope classification.
- Produce biotope distribution maps calibrated by groundtruth data.

In addition the following research objective was fulfilled:

- An assessment of the sedimentary structures, sediment grain size and their relation to physical water parameters in the Tay Estuary.

1.1 Firth of Tay and Eden Estuary – Site background

The Firth of Tay and Eden Estuary cSAC is situated on the east coast of Scotland north of the Firth of Forth between the coastal towns of St Andrews and Carnoustie, (Figures 1.1 and 1.2). The site is an excellent example of a northern North Sea Estuary. The coastline is characterised by low cliffs cut into Carboniferous and Devonian Sandstones, wave-cut platforms on Pleistocene boulder clays, extensive sand dune complexes, and deep-cut estuaries.

The cSAC consists of a variety of habitats. To the south, cliffs with a rocky shore platform dominate the coast line from Fife Ness to St Andrews often protecting areas of beach head saltmarsh and brackish fen. North of

Figure 1.1 Site location, Firth of Tay and Eden Estuary cSAC

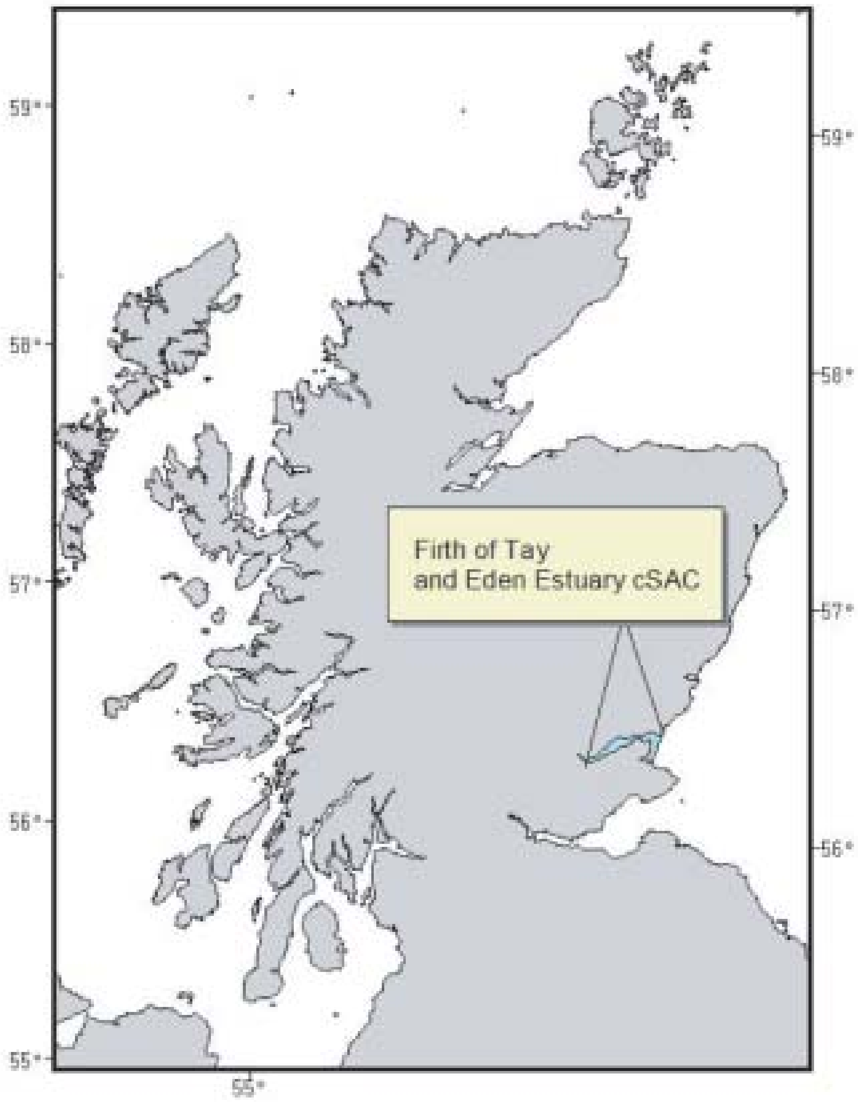

St Andrews, a large spit dune system at West Sands-Outhead protects the entrance to the Eden Estuary. Outhead is a dynamic spit formation which is presently migrating to the north-east across the current course of the river Eden. The Eden estuary consists of extensive mud flats and saltmarsh with a gradation into brackish swamp, freshwater marsh, fen and wet grassland habitat. North of the Eden, Tentsmuir forest covers one of the most extensive sand dune complexes to be found in Scotland. Records of the area show that in the last 5000yrs approximately 4km of seaward migration has occurred. The dunes of Tentsmuir merge into the coastline of the outer Tay Estuary with its foreshore of intertidal sand with some shingle and dunes. Along the south shore of the Firth of Tay, cliffs and a small rock platform are cut into the Devonian sandstone and basalts and overlain by shingle and cobble beaches often with large glacial erratic boulders at the coast edge, however, further west, thick mud sequences dominate the coastline with shingle bars extending to the low water mark. Occasional raised beach deposits with glacial sands and shingles can be seen around Newburgh. Marsh stabilises the thick alluvial muds that have accumulated west of here and the north shore of the estuary has been further stabilised by the planting of extensive reed beds over the last 200 years. The shoreline along the north bank of the Tay to the west and east of Dundee has been protected between

Invergowrie to the east end of Broughty Ferry. To the east discontinuous mussel beds characterize the large expanse of shallow foreshore in Monifieth Bay. Another significant dune sequence at Buddon Ness compliments that at Tentsmuir, however, movement of these dunes has been restricted over the last 20 years by revetment protection schemes on the east shore.

Figure 1.2 Firth of Tay and Eden Estuary cSAC

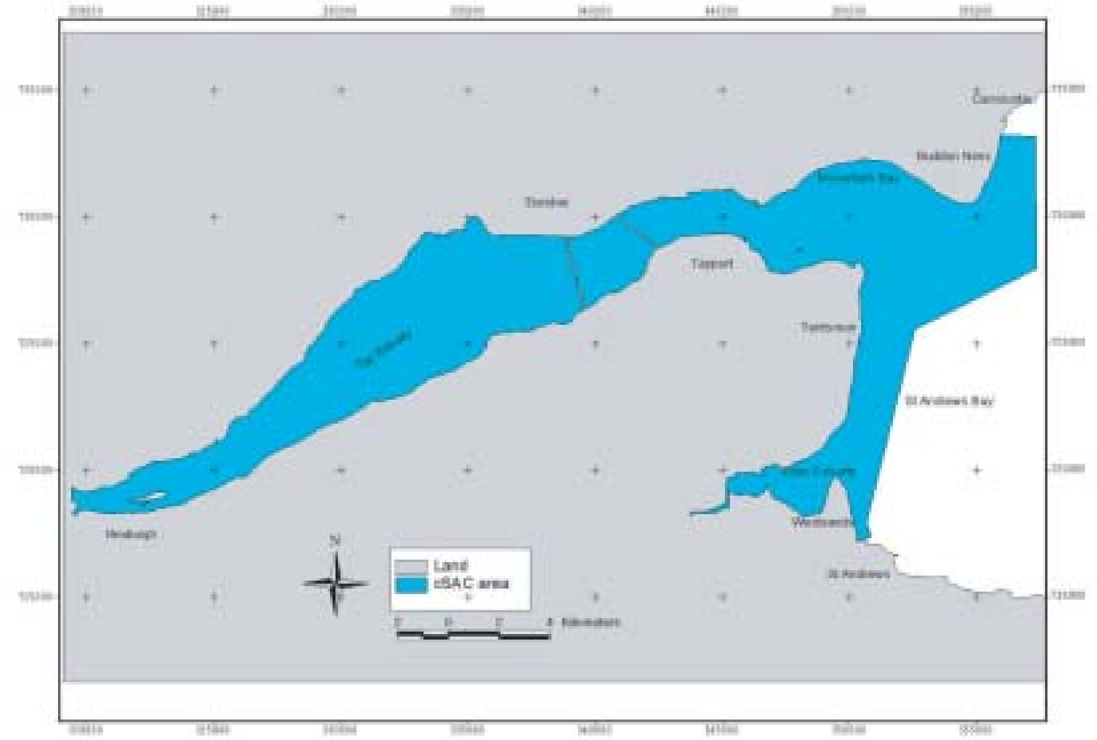

1.2 Site habitat description

The Firth of Tay and Eden Estuary cSAC is made up of the Tay Estuary and the Eden Estuary, and includes the sandy beaches and sandbanks off Buddon Ness, Abertay and Tentsmuir sands. The proposed site is a large, geomorphologically complex area on the east coast of Scotland incorporating a range of estuarine and coastal habitats that stretch from the mouth of the River Earn within the Tay Estuary, east to Barry Sands on the Angus coast and south to St Andrews on the Fife coast. Sedimentary, hydrological and ecological processes indicate that the Firth of Tay, Tay Estuary and Eden Estuary can be regarded as a single unit due to influence of local wave-induced long-shore currents that are a dominant feature of St Andrews Bay. These processes, combined with the large flux from the River Tay result in sand dune complexes and intertidal habitats being continuous between Tayport and the mouth of the River Eden. In addition to this, the common seal population ranges freely within this site from the inner Tay Estuary to the Eden mouth.

The Firth of Tay and Tay Estuary is long and narrow and runs for approximately 42km from the confluence of the rivers Tay and Earn in its south west corner to the Tentsmuir sandbanks in the east. The Tay Estuary has been classified as a partially mixed estuary with moderate tidal range (Williams and West, 1975). The Tay is Scotland's largest river, discharging an average daily flow rate of 198 m^3 s^{-1}. The River Tay is the firth's main source of freshwater and is joined by the River Earn, between them they drain approximately 6000km^2 of land and account for 95% of the freshwater input into the firth. Large intertidal sediment flats with mid-channel sandbank complexes border the firth's channel for most of its length. At the mouth of the firth two large sand flats and shoals extend to the east with the Abertay Sands on the south shore approximately 6km in length. The maximum depth of the channel is 30m at Broughty Ferry but depths for most of the channel range from 2–20m, and the water quality is good although with high turbidity. The smaller Eden Estuary, 10km to the south, by contrast is almost entirely intertidal, comprising a shallow, meandering river channel bordered by muddy sediments in the inner reaches and coarse sandy sediments in the outer estuary.

The inner parts of the Firth of Tay and Eden Estuary cSAC are largely sheltered from wave action, however, outer areas of this system are exposed to strong tidal currents and strong wave activity. The distribution of sediments within the site, together with the gradients of exposure and salinity have a major influence on the composition of the biological communities found within this high quality estuarine area.

This complex site contains a number of important biological features recognised as sub features of the Firth of Tay and Eden Estuary cSAC. Many of these sub features qualify as Annex I features in their own right. These include the extensive tidal reed beds of *Phragmites australis* in the inner Tay Estuary that extend along the north shore over the mudflats. These nationally important beds were established during the 18th century for coastal protection. The mudflats themselves contain large numbers of mud-dwelling invertebrates, particularly the amphipod *Corophium volutator*, mud snail *Hydrobia ulvae* and ragworm *Hediste diversicolor*, which provide rich feeding for over-wintering waders and wildfowl. Saltmarsh communities fringe both estuaries with communities primarily composed of *Juncus gerardii*, *Scirpus* spp. and *Schoenoplectus* spp. on the inner Tay and *Puccinellia* spp. with *Festuca* spp. on the Eden Estuary Sparse beds of eelgrass *Zostera angustifolia* can also be found to some extent in both estuaries. Reefs of the mussel *Mytilus edulis* are common in intermittent subtidal beds in the Tay Estuary and on intertidal banks in both the Tay and Eden Estuary main channels. The reefs support the common starfish *Asterias rubens* in the subtidal, and stands of fucoids in the intertidal areas. A population of the nationally rare fish the smelt or sparling *Osmerus eperlanus* occurs within the Tay. Within the Eden Estuary the mussel reefs are confined to the intertidal muddy areas where they support ephemeral green algae such as *Enteromorpha* sp. that extend over the mid shore as thick mats during the summer months.

The intertidal sandflats of Abertay Sands, the banks west of the Tay Bridge, Broughty Ferry, Buddon and Eden mouth consistently support approximately 600 common seals. This represents about 2% of the UK and 1% of the EU populations of the species. Large colonies are important in maintaining overall population size and are significant as sources of emigration to smaller or newly established groups.

Several species listed in Annex II of the Habitats and Species Directive occur regularly in the Firth of Tay and Eden Estuary cSAC. There is a non-breeding population of grey seals (*Halichoerus grypus*) that haul out within the Firth of Tay and Eden Estuary cSAC. This population contains about 2000 adults, however, no pups have been recorded at this site. Otter *Lutra lutra* occur on the River Eden above Guardbridge and on the inner Tay Estuary. Bottlenose dolphin *Tursiops truncatus* and harbour porpoise *Phocoena phocoena* also occur, mainly in St Andrews Bay, where up to 60 of each species have been seen.

The intertidal sediment flats (to mean low water springs) of the Firth of Tay and the Eden Estuary cSAC are an existing Ramsar site and classified SPA for overwintering wildfowl and waders, as well as for the marsh harrier *Circus aeruginosus* and little tern *Sterna albifrons*. This site stretches from the mouth of the River Earn in the inner Tay Estuary east to Barry Sands on the Angus coast and St Andrews on the Fife Coast. The site includes extensive invertebrate-rich intertidal flats and areas of reedbed, saltmarsh and sand dune contained within the Inner Tay Estuary, Monifieth Bay, Barry Links, Tayport-Tentsmuir Coast and Eden Estuary SSSIs. The upper limit of the site is contiguous with the River Tay cSAC for Atlantic salmon, and the outer part of the site on the north shore borders the Barry Links cSAC dune system.

1.3 Geological background

The solid geology lying beneath the Firth of Tay and Eden Estuary cSAC is dominated by Devonian and Carboniferous sedimentary sequences. These consist of Devonian sandstones of the Upper and Lower Old Red Sandstone, and Carboniferous sandstone, siltstones, limestone and coals. To the north of the area the Highland Boundary Fault, a great fracture that runs across Scotland from Stonehaven to the Clyde, separates these rocks from older metamorphic and igneous rocks that dominate the Grampian Highlands. The Tay Estuary has been developed along the axis of the Sidlaw-Ochil anticline, a line of differential weakness in the basement rocks with the southern shores controlled by the major fault bounding the Carse of Gowrie graben. North of the Firth of Tay, the Lower Old Red Sandstone weathers to give characteristic rich and fertile soils. South of the Tay, sequences of Carboniferous sandstone, siltstones and occasional coal seams are systematically intruded and interbedded with volcanics. The volcanic intrusions give rise to the many of the regions peaks. Across the entire area, glacial deposits of till, sand and gravel record a complex late-glacial and Holocene history. The mark of glaciation in the form of rounded and smoothed landscapes can be seen throughout the area. The most recent of the westward advancing glacial events was that of the Late Devensian ice advance. The most notable landforms produced across the area are those resulting from successive ice retreat when extensive areas of sand and gravel were laid down and there was a widespread marine invasion around the lower ground of the coastal areas. The course of the Tay Estuary shows areas of stable channel over gravels and partially compacted clays and areas of unstable loose, coarse to fine sands. These glacial derived deposits beyond the edge of marginal rock platforms cut into the Fife and Angus shores are composed at the lowest levels of a coarse lodgement till of the Aberdeen-Lammermuir Ice. This is overlain by moraines, outwash gravels and finally laminated silts deposited during ice retreat. Subsequently, these deposits have been deeply eroded to form the valley of the present day Tay Estuary with fluvial fill evidence of two earlier estuarine cycles. In a period of 2000 years, a succession of easterly sloping shorelines formed progressively as the ice retreated to the west with each shoreline having a lower gradient than its predecessor. The resulting raised beach levels can still be seen as relic shorelines around the coast of Fife and Angus, however, many are now covered by extensive deposits of windblown sands with large fluvial deposits in the estuary areas. Recent deposits in the area include deep alluvium deposits associated with the major river systems of the Tay and Earn rivers and the extensive wind blown sands at Tentsmuir and Buddon Ness. The sandy foreland of Tentsmuir has grown 4km in the last 5000 years and even now, Tentsmuir Point continues to extend north-eastwards by an average of 4.8m per year, fed by sand eroding from the flanks of the peninsula.

1.4 Current Patterns and Frontal Systems

The main tidal influence in the Firth of Tay and Eden Estuary cSAC is produced by an amphidromic system centred off the south-west of Norway. The dominant anti-clockwise wave action in this system produces a southward moving tidal wave that travels south to meet with a secondary, and more southerly, system to seaward off the Firth of Forth. The tidal systems together with bathymetric and coastline profiles cause a difference between offshore tidal currents and estuarine tidal currents in the Tay area that result in complex circulation patterns and variations in current strengths at different tidal states. The mean tidal range at Dundee is 5m for spring tides and 2.2m for neap tides. The strength and direction of the tidal currents in the cSAC are strongly controlled by the large shallow mud flats and sand banks. In addition, the maximum height of the tide can be influenced by up to 2m of wind generated increased levels between the outer Tay and Newburgh. Maximum tidal velocities of $1.9ms^{-1}$ have been recorded on the spring ebb and flood in the channel narrows to the west of Broughty Ferry. It has been estimated that up to 60% of the volume of the Tay estuary ebb flow is exchanged with the sea each tidal cycle and that full exchange would be achieved after 5–6 tides (Charlton, 1980).

Numerous recent studies of the Tay Estuary have noted the significant influence of tidal fronts in the mixing of waters over tidal cycles. Tidal fronts are created at the mixing boundary between fresh water and saline water. Not only are there a salinity, density and temperature contrast across the front but they are usually observed at the sea surface by a foam and debris trail. The foam and debris trail is typically located behind the advancing denser salt water flood and the front can exhibit a significant angle with the salt water intruding beneath the fresh water. Alternatively, the foam and debris trial may be located directly above the water boundary where there is significant shear and the water bodies are moving parallel to each other. Thus, fronts are controlled by the dimensions and shape of an estuary, the rate of inflow of fresh and saline water, and the amount of turbulent stirring. Lateral shear is an important element in maintaining fronts and thus strong bathymetric changes such as exist in the Tay Estuary around the many large sandbanks have a significant control on the fronts. A number of significant fronts have been recognised in the Tay Estuary from air photography, satellite studies and temperature/salinity measurements (Anderson *et al.*, 1992; Ferrier and Anderson, 1997a&b; McManus *et al.*, 1998; McManus, 2000). The dominant fronts that have been consistently noted include lateral axial convergent fronts, tailed axially convergent fronts and longitudinal fronts. Longitudinal fronts have been studied in some detail in the Tay Estuary and are thought to exist as a result of rapid bathymetric changes between deep channels and shallow sandbanks. Tailed axially convergent fronts form as the longitudinal fronts that have developed from the marginal waters sweeping off the tidal flats on either side of the estuary meet in the narrow and migrate up estuary with the rising tide (Ferrier and Anderson, 1997a). The influence of the bathymetry has been further confirmed by recent current and density data collected across fronts in the estuary that suggests that the fronts are mainly driven by inertia due to flow over the sandbanks rather than by buoyancy forces (Neill *et al.*, 2000).

The fronts have also been proposed to significantly control the sedimentary bedform character in the estuary. Wewetzer and Duck (1999) have shown that the location of fronts can be correlated with different ripple and dune sizes identified by sidescan sonar surveys between the road and rail bridges. McManus (2000) however noted that only longitudinal fronts give rise to sedimentation in the form of channel parallel sandbanks but that cross-channel fronts associated with the migrating saline wedge were not believed to give rise to substantial deposition.

2 BROAD SCALE HABITAT MAPPING AND MARINE SACs

Survey work in the subtidal marine environment has historically been based on a point sampling approach with often widely distributed locations investigated utilising diving or grab sampling methodologies. Existing data of this nature were sufficient to advise the initial SAC selection process, allowing comparisons of sites to be made across the UK. However, in order that comprehensive and defensible management plans can be developed for important marine sites it is essential to obtain estimates of the geographic distribution and extent of the biological resources – in the form of broad scale habitat/biotope maps (Downie *et al.*, 1999).

Scottish Natural Heritage requires this information on the natural heritage resource for tackling statutory casework issues and for the implementation of the EC Habitats Directive (European Community, 1992) through the identification, selection, management and monitoring of areas of importance. To date 34 marine SACs have been put forward in Scotland for a number of habitat types and certain species that are listed within the Directive.

The site supports the following Annex I marine habitats – estuaries, mudflats and sandflats not covered by seawater at low tide (colonised by estuarine communities that display a transition from predominantly brackish to fully marine species) and sandbanks which are slightly covered by seawater all the time. In addition, the Firth of Tay and Eden Estuary cSAC also supports a nationally important breeding colony of the common (harbour) seal *Phoca vitulina* with around 600 adult hauling out at the site to rest, pup and moult.

To help implement the Habitats Directive in the UK, the Marine SACs LIFE Project was established (1996–2001). One of the key tasks of this project was the identification and development of appropriate methods for recording, monitoring and reporting on the habitats and species present within marine SACs. An important element of this was the testing of acoustic based survey techniques for habitat mapping and the monitoring of long-term habitat change within SACs.

A number of sampling techniques make it possible to create images of large areas of the sea floor and provide broad scale maps of seabed habitats. Broad scale implies that large areas are mapped and show the approximate disposition of broadly defined classes of habitats or biotopes. Fine scale implies that small areas are mapped to a higher level of detail and accuracy (Foster-Smith *et al.*, 2000). Such fine scale mapping would require an intensive and prohibitively expensive survey programme. The approach taken to broad scale mapping in the marine environment is based on remote sensing. An image of an area is obtained using remote sensing techniques (inc. satellite observations, aerial photography or acoustic surveys) and information about certain attributes of the sea bed is then collected by direct or remote sampling at selected sites (a programme of 'groundtruth' validation of the initial remotely sensed data). It must be remembered that every habitat system is in a state of continuous change and that baseline mapping surveys represent the conditions at the time of data acquisition.

Work undertaken through the LIFE project and associated studies demonstrated that the repeat mapping of a near-shore SAC is achievable and that full coverage bathymetric charts can be produced with positional accuracies of 5m or better, object identification at sub-metre scale and habitat identification within 5m grids (EN, 2000; Bates and Whitehead, 2001). In the past, the mapping of areas at such a fine spatial resolution had necessitated the use of acoustic based remote sensing techniques on close line spacings with data extrapolation over areas not covered by the survey (EN *et al.*, 2000).

The broad scale remote sensing and mapping of sublittoral habitats and biota has become common place over the last 5 years with much of the work in the UK initiated in response to the 1992 EC Habitats Directive. The Marine Monitoring Handbook (JNCC, 2001) has synthesised the results from many of the individual studies undertaken.

3 METHODS

Bathymetric sidescan and single beam sonar remote acoustic mapping techniques were utilised at near 100% coverage to develop acoustically classed seafloor maps of the Firth of Tay and Eden Estuary cSAC where water depths were greater than 3m. For shallow areas and intertidal areas airborne and satellite techniques were used to develop classed maps. High fidelity ground validation data were collected in the field using drop-video, ROV, grab, dredge and hand sampling methodologies to enable the subsequent interpretation of the acoustic maps. Each of these methodologies are discussed in further detail in following sections.

3.1 Scientific staff

A number of research scientists from all partner institutes were involved with the field surveys and subsequent data analysis. These individuals together with the SNH staff involved in the survey work are listed in Table 3.1.

Table 3.1 Scientific staff involved in the 2002 Firth of Tay and Eden Estuary mapping survey

Scientist	Field Responsibility	Data Processing Responsibility	Academic Institution
Dr R. Bates	Project Management and Acoustic	Project Management/Acoustic/GIS	St Andrews
Mr C. Cameron		Sediment analysis	St Andrews
Mr D. Oakley	Acoustic Surveying	Sediment analysis	St Andrews
Dr J. Jarvis	Acoustic Surveying		St Andrews
Dr C. Moore	Project Management and groundtruthing	Project Management/Biological/GIS	Heriot-Watt
Dr J. Mair	Groundtruthing	Biological	Heriot-Watt
Dr A. Lyndon	Groundtruthing		Heriot-Watt
Ms S. Hamilton		Biological	Heriot-Watt
Dr T. Malthus	Project Management and Imagery	Satellite Imagery	Edinburgh
Dr D. Harries	Groundtruthing	Biological/GIS	SNH
Mr M. Dalkin	Groundtruthing		SNH
Ms J. Hill	Groundtruthing		JNCC
Mr M Davies	Groundtruthing		JNCC
Ms E. Karpouzli	Groundtruthing	Satellite imagery	Edinburgh

3.2 Acoustic technologies for habitat mapping

Before using any survey technology for either mapping or object identification an appreciation of the system capabilities is needed. A key element is the system resolution or fidelity with which the system can identify objects on the sea floor. The system resolution will dictate the size of object that is recognisable at a particular distance from the survey instrument. The majority of instruments have both theoretical resolution limits and manufacturer defined values from testing under ideal conditions. Unfortunately, these are rarely achieved in real surveys. Achieving a particular resolution will depend on the precision to which the instrument can measure electronic signatures, however, it is the precision with which each measurement of the sea floor is made with a particular instrument that is of real interest to the user. A discussion of an instrument in terms of the accuracy of object identification on the bottom can be misleading as this is a function of not only the sonar instrument specifications but also of all the navigation errors, the location errors for the instrument, the acoustic noise that is recorded and most importantly the identification or interpretation logic. Accuracy in interpretation requires consistent groundtruth information and reliable positioning of both the acoustic data and groundtruth data. The theoretical resolution for each survey instrument is briefly given followed by a discussion of the use of the instrument in SAC habitat mapping.

Acoustic methods for habitat surveying have traditionally relied on single beam echo-sounder type instrumentation and a number of ground discrimination systems have been developed around this method (Greenstreet *et al.*, 1997; Foster-Smith and Sotheran, 1999). More recently, sidescan sonar has been used for not only object identification but also for mapping different areas of the sea floor and classifying them by type (Curran, 1995; EN, 2000; Foster-Smith *et al.*, 2000). In this project the latest development in acoustic techniques, namely bathymetric sidescan, was used as it has been shown to have distinct advantages in habitat mapping through obtaining near full coverage data (Bates and Byham, 2001).

3.2.1 Survey technologies – Echo-sounder or single beam sonar

The echo-sounder or single beam sonar has been used for a number of decades to measure bathymetry and also to record reflecting objects such as fish within the water column. More recently, the acoustic amplitude variations have also been processed for seafloor classification (Chivers *et al.*, 1990; Foster-Smith *et al.*, 2000). An echo-sounder consists of a single sonar transducer that is used to both transmit and record an acoustic energy pulse directly beneath the sonar. The energy pulse or acoustic wave travels from the sonar and is reflected or echoed from boundaries in its path. The intensity of reflection depends on the impedance ratio between water and the reflector and the angle that the reflector makes with the acoustic pulse. For example, a hard, flat sea floor will reflect more energy than a soft sea floor or one that is at an angle to the transmitted acoustic pulse. The sonar produces a number of acoustic energy pulses per second as it passes over the sea floor thus measuring a line track of data.

The range to the bottom and velocity of the acoustic pulse in the water will determine the number of samples or pings off the bottom per second as there is a finite time that must be observed for the energy to travel to, and reflect off, the bottom. The fidelity of recording changes on the bottom is determined by the ping rate with respect to the speed of boat over the bottom. Thus, for most surveys, not only are large areas of the bottom covered with the echo-sounder but there is also significant averaging of data between each ping. Despite this, the echo-sounder has been shown to produce high resolution, repeatable depth data along survey line tracks. However, because the echo-sounder only produces information for targets directly beneath the sonar, it is necessary to extrapolate between survey line tracks in order to produce area coverage maps of the sea floor.

Seafloor classification with single beam sonar

The strength of acoustic energy reflected from the sea floor with single beam sonar has also been used to classify the bottom type. The basis of all these techniques is that different amounts of energy will be reflected or scattered from the sea floor based on the contrast in acoustic impedance between the bottom type and the water column. For example, a soft bottom such as mud will have a different reflection signature than a hard bottom such as rock. In general, a hard surface will produce stronger echoes than a soft bottom or a bottom that is covered in overgrowths of biota. A number of methods have been proposed for this and include those by Jackson and Briggs (1992) who used the backscattered energy from the echo to infer bottom roughness. Orlowski (1984) used a method which integrated parts of the multiple echo signature from the sea floor to provide information on the seafloor characteristics. Burns *et al.* (1985) developed a classification system based on the first echo and the second echo or first multiple echo from energy that bounces between the sea surface and the sea floor. Two commercial systems, RoxAnn and the Echoplus have been developed from this work and it is recommended that the systems are used with transducer beam widths of 8°–25°. The first echo has been related to the roughness of the sea floor with the rougher the sea floor the more energy that is backscattered to the transducer. The second echo is interpreted in two ways. Chivers *et al.* (1990) suggest that the dominant ray paths for the second echo undergo two reflections at the sea bed and a single scattering at the sea surface. The amount of energy returned is related to the acoustic impedance contrast at the sea bed and thus a harder bottom will reflect more energy. A second theory proposed by Heald and Pace (1996) envisages the transmitter-receiver configuration as a bi-static system but with the energy reflected still dependant on the hardness of the bottom. As the second echo is reflected by the sea surface it can be influenced by the sea state especially in rough weather.

QTC View is an alternative system based on single beam echo sounders that uses only the first echo (Simpkin and Collins, 1997; Collins and McConnaghey, 1998). The technique records both transmitted and received waves in order to perform compensations for beam spreading before Principal Component Analysis (PCA) is used to identify key parameters of the echo shape (Collins *et al.*, 1996). This is equivalent to analysis using the Cartesian plot in RoxAnn but with more variables.

A problem that has been experienced in many recent surveys using echosounders for seafloor classification has been the repeatability of measurements during a single survey and between surveys using different sonars and different survey vessels. Numerous authors (for example Foster-Smith *et al.*, 2000) have noted a drift in instruments as temperature and humidity changes, and a different response has been noted from different sonars when used on different vessels. Some of these issues have been addressed with careful quality control during the survey and some issues have been addressed with new instrument development such as the Echoplus. The Echoplus has digital compensation adjustments within the instrument for frequency variations, depth from the bottom (signal strength losses), pulse length differences and power level fluctuations. None-the-less, procedures are recommended where repeat surveys are made over two or more areas of known sea floor in order to calibrate the amplitude response.

Acoustic maps of seabed character from AGDS

The final output of single beam echo sounders is a depth chart and line plot of backscatter or reflection characteristics of the sea bed. In order to produce a map of bottom character it is first necessary to extrapolate the line data into a grid of values. This interpolation marks the point in the interpretation from where the investigator can influence the outcome by their choice of processing parameters. In order to ensure a robust interpretation it is vital at this stage that the processing is conducted under the close scrutiny of both survey and biological experts. The extrapolation can also potentially introduce large errors into the system as the assumption must either be made that conditions vary uniformly between real data points or alternative methods of finding boundaries must be invoked. The numerous methods for achieving full coverage maps and predictions from them on likely distribution of different seafloor types has been extensively studied over the last 5 years (Foster-Smith *et al.*, 2000). While the use of AGDS has been proved highly effective in mapping habitats, this project tested the use of AGDS together with full coverage information from bathymetric sidescan systems so that extrapolation of the AGDS was not necessary across unknown boundaries.

In general, once an acceptable extrapolation of single line track AGDS data has been made, it is possible to apply image processing procedures and modelling with geographic information systems based on acoustic signature correlation to known bottom type. The final step in image classification is the prediction of likelihood of finding similar or dissimilar bottom types across the survey area.

3.2.2 Survey technologies – Bathymetric sidescan

A bathymetric sidescan system is one that is used to measure the depth to sea floor and amplitude of sonar return from the sea floor along a line extending outwards from the sonar transducer at right angles to the direction of motion of the sonar (Geen, 1998). As the sonar platform moves forwards, a profile of sweeps is defined as a ribbon-shaped surface of depth measurements known as a swath in a similar manner to a sidescan image of the sea floor.

The acoustic signal is produced by the sonar in a similar manner to a sidescan acoustic pulse and is narrow in azimuth (that is, viewed from above), and wide in elevation (viewed from the side). The difference between a sidescan and bathymetric sidescan system is in the recording of the acoustic energy. In a bathymetric sidescan system a number of transducers or transducer staves are used to record the returned energy that is back-scattered from the sea floor. When this back-scattered sound is detected at the transducers, the angle it makes with the transducer is measured by recording the phase difference between transducers and a reference signal. Multiple staves ensure that both the angular measurement and the overall phase resolution are measured with high precision. The range for a reflector is calculated from the travel time to the reflector and back and the range and phase angle pair enable the location of the ensonified sea bed patch to be known relative to the sonar transducer thus creating a 3D bathymetry map of the sea bed. A typical far range limit is about 7.5 times the water depth giving a total swath width of approximately 15 times the water depth. In addition to a determination of the location of a reflecting target on the sea floor, the amplitude of the returned signal can be measured with the bathymetric sidescan system. These amplitude data can be used in one of two ways. Either they can be treated as a sidescan record, that is as a time series to produce a qualitative image, or geo-referenced picture of the sea floor or they can be processed using the bathymetric information for the point on the sea floor from which each individual reflection is measured. In this latter case the recorded amplitude is compared with the source signal after compensation for energy losses during the travel path such as loss of signal to the water column, spherical beam spreading and the incidence angle for scatter or reflectance from the sea floor. It is only since the development of this type of sonar with high fidelity co-location of bathymetry and amplitude that these compensations for amplitude loss have been possible.

Acoustic maps of seabed character from bathymetric sidescan

The final output of a bathymetric sidescan is two products – a bathymetric chart and a sidescan or amplitude map (Bates and Byham, 2001). The bathymetric chart is calculated from all of the points on the sea floor where a reflection signal was obtained. In gently undulating sea floor the points form a continuous cover at sub-metre fidelity. However, in areas of large bathymetric variation, some areas will have a higher density of reflection cover than others. Furthermore, it is possible that some areas, those in the shadow of large upstanding features on the sea floor may have no reflection points on them. Great care must be taken in surveying to ensure that this condition is kept to a minimum. For the majority of sites, the bathymetric sidescan technique provides better than 95% coverage of the sea floor. Using a bathymetric map alone, even with the high resolution obtainable with the bathymetric sidescan, for habitat mapping is not recommended as not all seafloor sediment or biological zones are depth defined. However, the broad range of many individual species can be limited by depth and thus the maps provide a very useful additional tool for habitat appraisal. In addition, because the resolution of the bathymetry from these techniques is high, it is possible to use very small scale features to aid in mapping boundaries between contrasting surfaces such as rock to sediment where small slope changes become very apparent.

The second product of the bathymetric sidescan is the amplitude map. This map can be produced in two forms. In the simplest version, only amplitude data are preserved where an acceptable bathymetric value has been recorded. As many of the bathymetric data points are filtered out during processing this decimated data set may loose much of the texture information that is important to a high contrast sidescan image and thus a second data set is usually also preserved where all the amplitude data are saved and separately processed. Again two routes are available for processing these data. In the first, the sidescan recorded is treated like a typical sidescan data set with amplitude correction based on time varied gains or some form of angular corrections (e.g. Danforth, 1997). The single swaths of amplitude data are mosaicked to produce an amplitude map or geo-referenced image that can be overlaid with the bathymetric information thus providing a powerful basis for interpretation of seafloor type. As the exact position and attitude of the sonar are known this approach offers a new way forward for broad scale mapping projects that hitherto was not possible with the sidescan and single beam line track AGDS data of the past.

3.2.3 Acoustic survey equipment

Both AGDS and bathymetric sidescan data were simultaneously acquired during this project with all information collected on a single PC system. An additional PC was used for navigation during the project and this was connected in a mini-network with the acoustic acquisition PC. A further PC was used for regular

Figure 3.1 Schematic of acoustic acquisition hardware

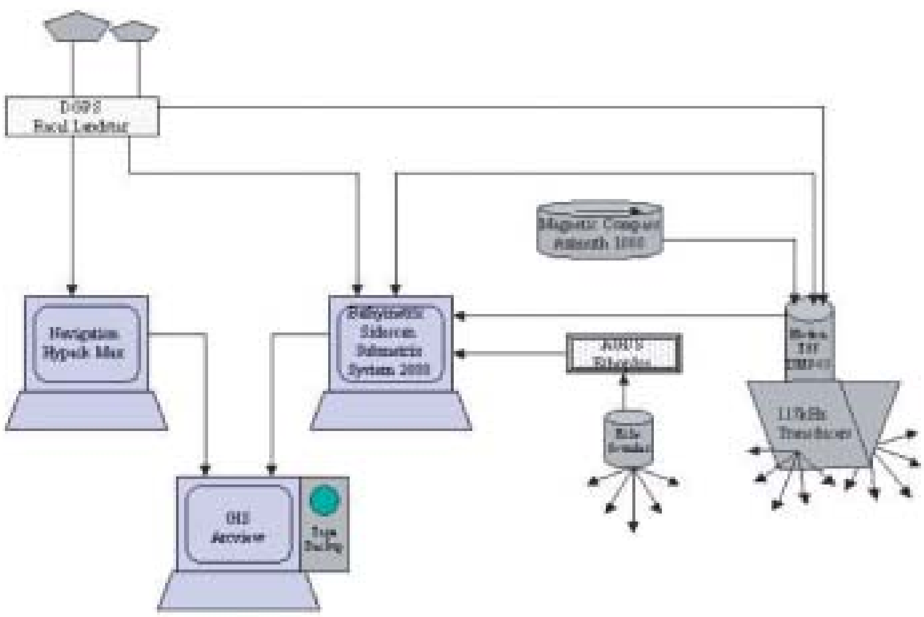

quality control, running the GIS and for downloading the acoustic data at the end of each survey day for processing during the evenings. A block diagram of the acquisition set up is shown in Figure 3.1 and each individual component is discussed in further detail below.

AGDS

The AGDS system chosen for this project was the Echoplus manufactured by SEA Ltd. (Figure 3.2). The Echoplus was chosen in order to have the ability to use more than one frequency echosounder simultaneously for recording AGDS and also as the electronics within the instrument offer the latest in digital signal processing for consistency and repeatability of measurements. The Echoplus was coupled to a Furuno FCV292 dual frequency echosounder with 28kHz and 200kHz transducers.

Figure 3.2 Echoplus AGDS and Hypack Max navigation software

Bathymetric sidescan

The bathymetric sidescan used for this project was a Submetrix System 2000 with 117kHz transducers. Acquisition settings varied with transmit lengths of 18–100cps (77–424µsec), a ping rate of 3–5 per second and 2048 sample receiver length. Sound velocity measurements were acquired at the site but no depth stratification was noted and thus velocities of 1498ms^{-1} were used for ray tracing throughout the site. The transducers were bow-mounted on the survey vessel with the motion reference united permanently fixed immediately above the transducers (Figure 3.3).

The motion reference unit was a TSS DMS-05 dynamic motion sensor which used solid state sensing elements to measure instantaneous linear accelerations and angular rates of motion change to 0.05°. This information is critical to correct positioning of seafloor reflection positions especially at far offsets at the end of each swath. The information from the DMS-05 is supplemented by navigational input from the differential Global Positioning System (dGPS) and also a magnetic compass. The magnetic compass used was a Aximuth 1000 produced by KVH Industries, Inc. This fluxgate digital compass provides azimuth information to 0.5° accuracy after compensation. All data were recorded on a PC with RTS2000 acquisition software (SEA Inc.).

Figure 3.3 Submetrix System 2000 Bathymetric Sidescan, bow mounted together with TSS DMS-05 Motion Reference Unit

Navigation

Navigation was accomplished using Hypack Max Survey software supplied by Coastal Oceanographics Inc. with background charts from C-Map Norway (Figure 3.4). Real-time positioning was accomplished using differential GPS from the Racal Landstar system Mk III receiver. This provided continuous correction data from a sequence of base stations around the coast of Scotland relayed via satellite to the Landstar for positional resolution of less than 2m.

The survey navigation was accomplished on a separate PC that was networked with the sonar acquisition computer and also the QA/QC computer with the GIS (Figure 3.5).

Figure 3.4 Navigation with dGPS, forward looking sonar and echosounder on RV Serpula

Figure 3.5 Submetrix System 2000 and GIS QA/QC

3.2.4 Survey methodology

The survey area was initially divided into a number of zones based on known bathymetric variations and anticipated weather patterns during the survey period. This ensured that natural land features, and the shelter they create, could provide optimum survey conditions with the minimum swell, wave and wind action. The survey line spacing was then chosen that would give a minimum of 50% overlap on the bathymetric sidescan data. The line spacing was further reduced where either the sea floor type changed rapidly or there were specific sea floor biotope characteristics of important interest. Surveys were conducted by the helmsman following a course indicated on the navigation computer. The acoustic data were continually monitored on the acquisition computer and a bottom coverage map produced in real-time in order to ensure full sea floor coverage. No attempt was made to obtain groundtruth information during the acoustic survey rather the groundtruth locations were chosen following preliminary analysis of the acoustic data. All survey data were acquired in the field on the acquisition computer hard drive and also backup disks were made on a magneto-optic drive.

3.2.5 Acoustic survey calibration

If acoustic data are to be acquired over a number of days, and furthermore if the data are to be compared to previous and subsequent acoustic data, it is of paramount importance that careful calibration of the instruments is undertaken on installation. Calibration of the AGDS and bathymetric sidescan was achieved using the following procedures:

AGDS

The AGDS was calibrated for depth by repeat surveying of areas of known depth over different states of the tide. At the beginning and end of each day a 2 minute record was made of these data near the vessel mooring site. Amplitude data for E1 and E2 were also recorded at the beginning and end of each day over the same section of sea floor for comparison of E1/E2 values. An example of the results of these data over a two day period are shown in Figure 3.6.

Bathymetric sidescan – Roll calibration

An area of sea floor that was relatively flat was chosen for the roll calibration. Across this area, 5 survey lines were acquired with 100% overlap of port and starboard transducers between the lines. These data were then processed and compared thus allowing adjustment of the transducer angles to give coincident reflections to less than 0.05°. Skew calibration was accomplished by using recognisable objects on the sea floor and surveying them with both transducers at different offsets. Pitch calibration was achieved by surveying up and down a relatively uniform slope.

Known objects were recognised on the slope and these used to calculate the angular pitch calibration. Once calibrated for roll, pitch and skew, amplitude variations within the Submetrix system are recorded in the data and therefore can be analysed and compensated for at the processing stage. None-the-less, it was still survey practice to record and review data at the beginning and end of each day over known seafloor conditions while the data were being acquired for AGDS calibration.

Figure 3.6 Daily Comparison of Echoplus (AGDS) E2 values. The Echoplus line track data for E2 is colour coded into a range of values between 0.001 and 1.578

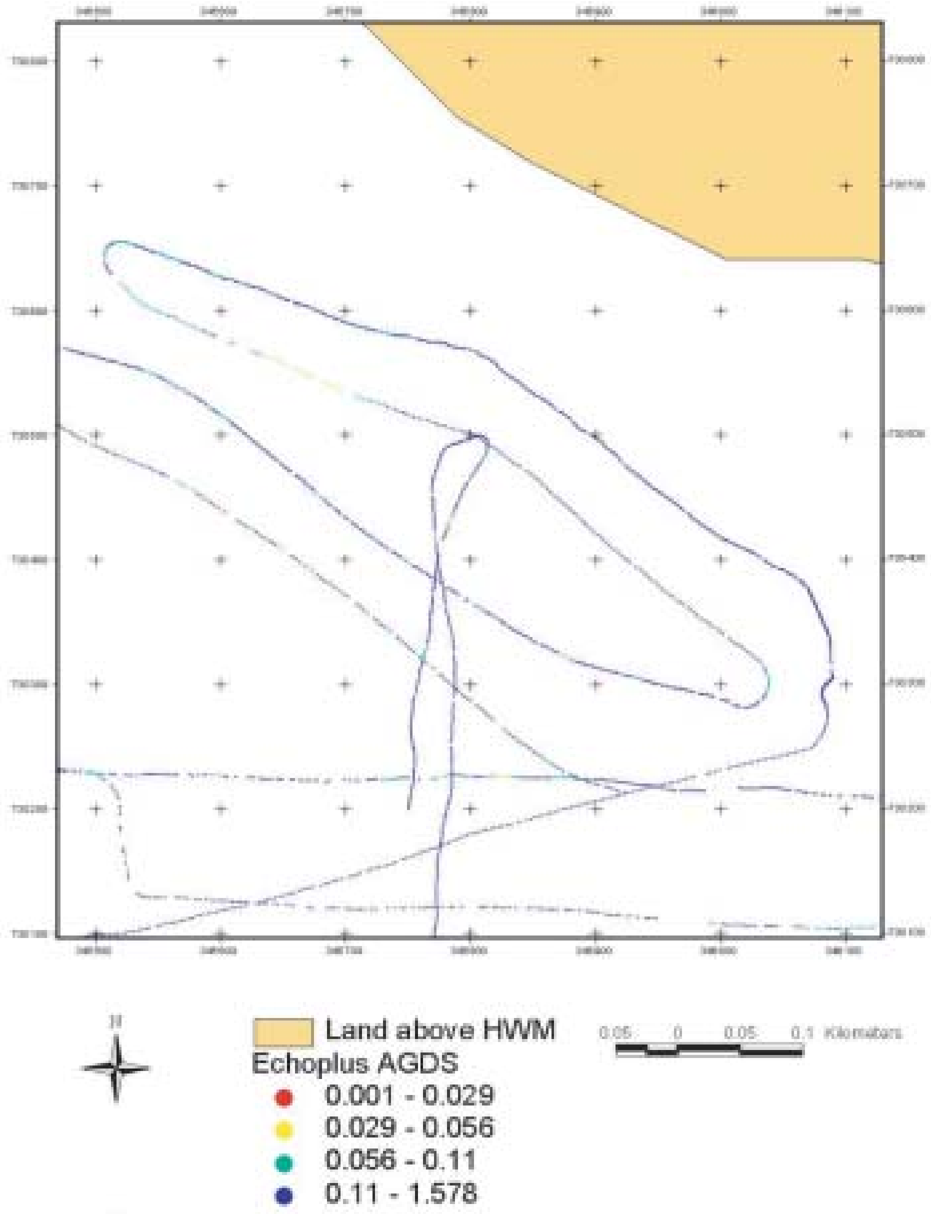

Tidal corrections

Tidal corrections were applied to both the bathymetric sidescan data and the AGDS from 10 minute tide curves modelled using information from the Admiralty Tide Tables and the Hydrographic Office. Previous tidal station recordings for the Tay Estuary and Eden Estuary has noted up to 1hr differences in tidal maximum at different places in the cSAC. Data for tidal differences at three locations along the Tay Estuary are given in Table 3.2. An extrapolation between these was used to correct the acoustic data during survey acquisition with the tidal models entered directly into the navigation computer and to the bathymetric sidescan acquisition software for real-time corrections.

Table 3.2 Tidal heights and delays for stations along the Tay Estuary. Taken from McManus *et al.* (1990)

Station	Datum (m)	Tidal amplitude (m)	Tidal delay Hrs Mins
Tay Rail Bridge	2.32m below O.D.	5	0:00
Flisk Point	2.32m below O.D.	5.4	0:20
Newburgh Quay	1.00m below O.D.	4.2	0:30
Inchyra Pier	0.5m below O.D.	3.8	0:40

3.2.6 Data recording errors

AGDS

There are a number of potential system errors that are generated with AGDS but many of them relate to the particular use of AGDS together with the navigation errors, and style of deployment (line spacing, water depth survey speed). These combined errors are discussed in further detail below.

Table 3.3 Beam width and transducer coverage or ensonified area for different sonar frequency

Beam Width (degree)/sonar frequency (kHz)	Water depth (m)	Radius of ensonified area (m)	Area ensonified (m2)
8/200	3	0.4	0.6
15/28	3	0.8	2.0
8/200	10	1.4	6.2
15/28	10	2.7	22.6
8/200	20	2.8	24.8
15/28	20	5.4	90.2
8/200	30	4.2	55.8
15/28	30	8.0	203

Potential errors resulting from the echosounder and the Echoplus and their impact on final survey resolution are discussed below. There are two main sources of error with the AGDS, namely the precision with which depth can be measured and the resolution of the amplitude measure on the bottom. The depth resolution is a function of the echosounder frequency, pulse width, digitising rate and water depth. For most environmental purposes this typically gives errors of depth well within the overall survey errors for water depths between 3m and 30m. The resolution of the amplitude measure is also a function of the echosounder but is controlled by the beam width and sample rate. The beam width is set by the manufacturer and the sample rate is dictated by the water depth or time of travel for an acoustic pulse between the echosounder and the sea floor. Typical beam widths of between 8° and 20° will result in very different areas of ensonification on the sea floor and thus different degrees of fidelity to which the sounder can map boundaries between different seafloor conditions. With a circular patch of seafloor covered by the sonar, typical beam widths, survey depths and ensonified patch diameters and areas are given in Table 3.3.

Bathymetric sidescan

The range in a bathymetric sidescan is measured using travel times to typically better than 0.05m and transducer angles to better than 0.05°. As the transmit beam spreads in the water away from the sonar in a similar manner to the sidescan, the size of the footprint will also increase. Thus a footprint can be calculated with a 234kHz sonar to about 0.87m at near range and 5.2m at 300m range along track and 5cm across-track. The 117kHz transducer has an along-track footprint of 1.5m at near range and 8.9m at 300m range with a 7.5cm across-track dimension. Because phase difference is recorded, a major advantage is realised with use of the bathymetric sidescan sonar in that there is no footprint spreading along the beam ie in the across-track dimension. However, it should be noted that it may not be possible to achieve these across- track dimensions in practise at far offsets due to energy loss. Details of the bathymetric sidescan resolution are given in Table 3.3.

The maximum range limit is dictated by the nature of the sea floor and the grazing-angle limit where most of the energy is reflected away from the sea floor. Bottom types such as soft mud or peat can reduce the expected range by as much as 30%. Sand, rock and shingle all give good sonar backscattering. For seafloor classification this is an important issue as it is vital that similar size areas of the bottom are surveyed across a sonar record in order to be able to make meaningful comparisons. It should also be remembered that if there are slopes on the sea floor that fall away from the direction of the sonar beam, these areas will fall into shadow zones and it is unlikely that they will be ensonified. Thus once more, obtaining true 100% coverage of the sea floor is rarely achieved.

Similar to the sidescan sonar, the number of pings or hits on a target is defined by the ping rate and speed advance of the sonar over the sea floor of survey. The ping rate is determined by the furthest range limit and speed of beam in the water. High survey speeds will result in poorer target definition or poorer quality images of the target.

Table 3.4 Bathymetric sidescan resolution

Across-track and along-track resolution				
	Across-track range (m)		Along-track range (m)	
Frequency (kHz)/beam width (°)	50	300	50	300
117/1.7	1.5	8.9	0.075	0.075
234/1.1	0.9	5.8	0.050	0.050

Distance between pings (alternate pinging for port and starboard transducers)			
	Range (m)		
Survey Speed (kts)	50	100	200
4	0.26	0.53	1.07
8	0.53	1.07	2.10

3.2.7 Data processing

AGDS

The AGDS data were recorded in line data format using the same PC as for the bathymetric sidescan. In the field these data were extracted from the bathymetric sidescan data for plotting as unedited E1/E2 values in Arcview in near real-time. This allowed for site quality control on the data and also provided information for locating groundtruth sites. Subsequently a number of line editing functions were conducted on the data using simple spreadsheet editing functions.

- Depth Editing - this was used to highlight erratic changes in depth where large jumps in depth (greater than 5m) were evident between individual records.
- Navigation Jumps – instability in dGPS can sometimes cause large navigation errors to be recorded in data. These were removed by comparison of positions along track.
- Erratic Changes in E1/E2 – large changes in E1/E2 were edited together with values at either extreme end of the range of possible values for E1/E2.

Bathymetric sidescan

The bathymetric sidescan data were processed using the acquisition software RTS2000 on-line during acquisition as the speed of sound profiles, calibration settings and tidal information had been calculated and input before commencing the survey. This enabled preliminary bathymetric models of the site to be produced during the field work. In the field, the data were processed using broad bathymetric filters with large depth acceptance windows (+/– 5m) therefore subsequent to acquisition all the data were re-processed in order that the bathymetric filters could be refined. Processing of the data at this stage involved the following steps:

- Input corrected bathymetric data.
- Filter for along-track and across-track anomalies to 1m bins.
- Export navigation filtered data (filters out large navigation jumps)
- Import processed data to mosaic programme – Grid 2000
- Filter and smooth data to 5m bins for broad scale survey, 1m bins for sediment structures
- Export grid data at 5m bin resolution for whole survey area and 1m bin resolution for specific areas of interest

Sidescan

The sidescan data were processed separately to the bathymetry data post-acquisition using SonarWeb Pro (Cheasepeake Inc). SonarWeb Pro uses amplitude corrections to the amplitude time series based on the work of the USGS (Danforth, 1997). The processing method incorporates the following steps:

- Import raw data from the bathymetric sidescan together with the full navigation information. The lines are imported at the desired output resolution to match the bathymetric model – 5m for the whole site with 1m and 0.25m for specific areas of detail.
- Geometrical correction and amplitudes adjustment for offset angles from the transducers. Nadir is removed using bottom tracking algorithms with manual adjustment in areas of rapidly changing bathymetry.
- Line projection onto the relevant datum (OSGB36) and overlapping data is combined to give a mosaic

of the whole site. Overlap data points are averaged to give the mean amplitude values from all crossing tracks

- Final output in the form of geo-referenced TIFF and geo-referenced JPEG files.

3.2.8 Data processing errors/combined survey errors

Mapping error

The production of the final predictive maps is subject to further errors as a result of the individual errors from each system (the acoustics and the groundtruth observations) and the inherent approximations necessary when combining the results. The final error can be thought of as the resolution of the maps. Here resolution is used to refer to the level of detail to which habitats or biotopes are discriminated. This level of detail is therefore a combination of both absolute detail and combined errors within recording systems and the level of interpretative discrimination that it is possible to put to an observation of biotope sequence. Finally, the map output has a finite resolution in both paper form and electronically within a GIS project.

Error in groundtruth position

All of the groundtruth positions are subject to error from the positional error for the dGPS (typically less than 2m) and more importantly from the position of the direct measurement (grab, diver, video or ROV) with respect to the vessel and dGPS. The uncertainty of the position of the groundtruth sampling with respect to the vessel is related to the depth of sampling. In general, the deeper the sampling the greater the uncertainty especially in strong drift conditions arising from currents and wind forces. For typical surveys, the length of cable paid out for a grab, video or ROV is 1.25 times the water depth and a very approximate position for the sampling device might be within a circle centred on the vessel that has a radius of half the water depth.

Track spacing

Prior to it being possible to obtain close to 100% seafloor coverage with acoustic techniques, it was necessary to survey areas with close line tracks in order to record small changes in bottom type across track. Methods for extrapolation between lines were then applied to the data based on the spatial correlation of the data. When lines are close together relative to the heterogeneity of the sea floor then the particular method of extrapolation between lines is of little consequence, however, when the lines are widely spaced or there are significant gaps in the lines then the final results become extremely sensitive to the extrapolation method. Numerous methods of extrapolation have been tested such as distance-weighting and kriging but all must assume some form of averaging and smoothing of change between known data points and thus the mapping of discrete boundaries is difficult. Because of these shortcomings, all the line track data from AGDS acquired in this project were integrated with the bathymetric sidescan which allowed the line data to be extrapolated using knowledge of the seafloor changes from the continuous coverage data. This represents a significant advance in technologies for remote monitoring using acoustic methods.

AGDS

The maximum resolution of the AGDS is a combined function of the particular echosounder used (its frequency and beam width) which defines the acoustic footprint or ensonified area, the water depth and speed of sound in water which defines the number of pings recorded per second, and the vessel speed over the sea floor which defines the spacing between the ensonified patches. Thus for a vessel working in 10m of water at $3ms^{-1}$ with a beam angle of 15° and a dGPS error of less than 2m AGDS values could be recorded 3 times a second giving an ensonified area of $6.2m^2$. Values would be recorded at 1m intervals across the sea floor and overlaps of 30% would be achieved between readings. Thus discrete boundaries on the sea floor could be recorded to +/– 3m. Increases in speed of travel, depth or ping rate will decrease this value.

Bathymetric sidescan

While the minimum seafloor ensonification area is relatively small with bathymetric sidescan sonar (less than $1m^2$), when the sonar is used in practice together with navigation error and with averaging between swaths, it is more practical (in terms of processing size and run time on typical computers) to bin data at a minimum of $2m^2$ for the 117kHz transducers with large areas binned at $5m^2$, $10m^2$ and $20m^2$ for working models. One advantage of the bathymetric sidescan, however, is the fact that this seafloor resolution can be maintained at all water depths for the bathymetric information. The sidescan information can also be presented at a range of scales depending on the size of area that is being analysed. Typically bin sizes of $1m^2$ are used for the study of large areas but this is reduced to $0.25m^2$ for smaller areas of particular interest. As all the bathymetric information is surveyed with the a motion reference unit with angular resolution to less than 0.05°, relative error in positioning within any part of the bathymetric sidescan model is typically less than 0.5m, however, due to dGPS errors, the absolute survey bin position error is less than 2m.

3.2.9 Spatial mapping of acoustics in the GIS – Combination of linetrack data and full coverage data

The output from the ADGS line track data is an edited file containing position, depth, and E1/E2 values. The output from the bathymetric sidescan are an edited file containing position and depth, and a georeferenced amplitude image. These text files are input to the standard GIS package, Arcview, together with other background information such as OSGB land DEM (digital elevation model) and admiralty charts. Following this, a number of procedures are applied to the data in order to produce final maps of acoustics and seafloor type.

Creation of a Digital Bathymetric Model (DBM)

The digital bathymetric model was created using a triangulated irregular network (TIN) to represent the seafloor surface. The TIN represents a surface with vector features (points, lines and faces) and thus it can precisely model discontinuities in the surface with breaklines. This is important in analysis of the sea floor as it is anticipated that many significant changes in seafloor type will occur along discrete boundaries such as breaks of slope for example between a submerged rock reef and a sediment plane. A disadvantage of the TIN is that it cannot represent vertical cliffs, overhangs or caves. However, because the faces in the TIN can be defined as a plane, a slope and a slope direction, it is possible to calculate secondary maps from the TIN for seafloor aspect and slope. Both slope and aspect together with depth can be important for controlling biotope type.

The TIN is produced from the continuous coverage grid file of bathymetric information with a boundary set at low water mark projected from the OSGB DEM. From this map the slope aspect and slope angle are calculated. The slope angle map is defined with a scale range expanded for small slopes (between 1° and 15°).

Sidescan image data

No processing of the sidescan image data was necessary in the GIS as the images are georeferenced raster files at the spatial resolution with which they were originally created using the sidescan sonar mosaic programme. This resolution varied between 1m bins to 0.25m bins for particular areas of interest.

AGDS line track data

The AGDS line track data are entered as a table of values and plotted in the GIS with single data points representing each acoustic set of E1/E2 values. In the field, the E1 and E2 data were combined in order to produce an in-field rapid assessment of the data range. This was achieved by taking the square root of each value, in order to expand the low end values below unity that dominate the acoustic returns over smooth soft seafloor material, and summing these values. This method of analysis does not, however, do justice to the information that is present in the individual variations in E1 and E2. A more critical examination of the data is necessary and it is usual to first produce a scatter plot of E1/E2. The scatter plots typically show a broad trend of data from smooth and soft sea floor to rough and hard sea floor. In the GIS, both the E1 and E2 data are the plotted as separate line tracks and each set of data is classed based on natural breaks in the data that were calculated from variogram analysis of the data ranges. A further discussion of methods for classifying the AGDS data where groundtruth information is assimilated into the classification is given later, however, for the preliminary survey maps it was decided that the acoustic data should be analysed and combined to give a representation and classification of the sea floor based entirely on the acoustic information.

3.2.10 Combining linetrack data with spatial coverage data to produce acoustic classed seafloor maps

The production of final acoustic classed seafloor maps was achieved through combining information from the following set of maps:

- DBM
- Slope angle
- Sidescan image
- AGDS line track.

Changes in AGDS class type were noted and these were compared to the bathymetric model, the slope angle map and the sidescan image. These maps provided an explanation for the change in AGDS such as a textural change from the sidescan image or a change in slope from the bathymetric model and slope map. The feature was then traced to create a separate polygon or Arcview "Shape File" that contained all of that discrete class of AGDS data that fell within this zone defined by the full coverage data. The process was repeated for all changes in AGDS down to the smallest class change that could be identified as a discrete feature on the bathymetric model or sidescan image. The result is a set of shape files of different AGDS class from E1 and E2 projected across the full DBM for the site. This range of classes represents the acoustic final map product but can also be viewed in 3D for better representation of the relationship between seafloor type and bathymetry.

3.3 Groundtruth observations

3.3.1 Field procedures

Groundtruthing of the satellite imagery and the acoustic survey was carried out by a combination of observation and sampling of biotopes from RV *Serpula* and from the shore. From 25th June to 4th July 2002 RV *Serpula* was employed at 68 stations. Most of these were subtidal but this vessel was also used as a base from which to deploy an inflatable for accessing intertidal sites that were difficult or dangerous to access from the shore.

Due to the shallowness of much of the SAC and consequent lack of AGDS data, station selection was greatly aided by the detailed sediment maps that were already available (Buller and McManus, 1975; McManus *et al.*, 1980). These data were incorporated into the GIS of the area. In view of the widespread presence of hard substrates on the sea bed and the presence of strong currents, a variety of sampling techniques was adopted. At most subtidal stations single infaunal samples were taken by either 0.1m^2 Van Veen grab or 10 l pipe dredge. Epifaunal sampling was also performed at most stations, either by naturalist dredge or by deployment of the SNH Highball ROV to collect digital video footage of the sea bed. Samples of the Eden Estuary channel sediments and of the mudflats of the upper Tay Estuary were taken using a 0.05m^2 Van Veen grab from the inflatable. This vessel was also used to land surveyors on Middle Bank and Abertay Sands for the collection of 0.1m^2 box quadrat samples to a depth of 15cm. A subsample of around 100–150ml of sediment was taken from each sediment sample for grain size analysis before sieving the remainder through a 1mm mesh. The screenings were preserved in borax-buffered 10% formalin. Position fixing was by DGPS using differential corrections from the Girdle Ness ground station on RV *Serpula* and the EGNOS satellite on the inflatable. Station details are given in Appendix A (Tables 1 and 2) and their locations mapped in Figures 3.7–3.10.

Groundtruthing of intertidal areas accessible by land was undertaken mainly on 10–11th August and 22–26th August, with some gaps filled in September and December 2002. Concentration was placed on areas for which there was little previous information on the biotopes. Unfortunately for most of this work good quality satellite images were unavailable due to a lack of coincidence between clear skies and low spring tides prior to the fieldwork. Shores were surveyed by recording the physical characteristics and conspicuous biota present at stations chosen to represent the biotopes within an area. Stations were selected both within and on the borderline between biotopes and descriptions were also sometimes made of the region between stations. Video footage was recorded at many of the stations. On sedimentary shores the sediment was dug over to record conspicuous infauna. In total, descriptions were produced at 437 intertidal stations. Sediment samples of approximately 0.1m^2 and 15cm depth were taken at 91 stations. A subsample of around 100–150ml of sediment was taken from most of these sediment sample for grain size analysis before sieving the remainder through a 1mm mesh. The screenings were preserved in borax-buffered 10% formalin. Position fixing was by EGNOS DGPS for all stations apart from those prefaced by the code M, for which non-differential GPS was employed. Station details are given in Appendix A and their locations mapped in Figures 3.7–3.10. The original field station numbers have been retained in this report and so to facilitate locating the positions of stations on Figures 3.7–3.10 the locations of groups of stations from the various field trips are summarised in Table 3.5.

Table 3.5 Locations of groups of stations for the groundtruthing survey. Stations with numerical codes were accessed by sea, whereas stations with codes prefaced by letters were accessed from land. The letters represent the lead surveyor (C, Colin Moore; D, Dan Harries, M, Matt Dalkin) or intertidal location (FE, east of Flisk Point; WS, West Sands)

Stations	Location
1–4	Between Tay road and rail bridges, subtidal
5–7	Upper Tay, R. Earn to Ballinbreich, subtidal
8–11	Upper Tay, Ballinbreich to rail bridge, subtidal
12–16	Between Tay road and rail bridges, subtidal
17	Off Dundee Airport, subtidal
18–22	Tay road bridge to Broughty Ferry, subtidal
23–33	Outer Tay and St Andrews Bay, subtidal
34–38	Eden Estuary channel
39–42	Abertay Sands
43–45	Upper Tay, Flisk to Balmerino, subtidal
46–60	Upper Tay, Port Allen to Invergowrie sediment flats
61	Between Tay road and rail bridges, Middle Bank
62	Upper Tay, Ballinbreich, subtidal
63–64	Upper Tay, sediment flats near Newburgh
65	My Lord's Bank off Dundee airport
C1–C42	Barry Sands
C43–C60	East Monifieth Sands to west Barry Sands
C61–C64	Tay road bridge to Tayport, shore
D1–D52	West Monifieth Sands
D53–D58	Kingoodie shore
D59–D61	Dundee sea wall
D62–D99	Eden Estuary, north bank
D100–D107	Wormit to Tayport shore
D108–D132	South Tentsmuir Sands
D133–D196	West Tayport Beach
D197–D199	Upper Tay, Newburgh shore
D200–D229	Upper Tay, Ballinbreich to Flisk shore
M1–M15	East Monifieth Sands
M16–M33	Stannergate to Broughty Ferry shore
M34–M61	Eden Estuary, south bank
M62–M92	North Tentsmuir Sands
M93–M123	East Tayport Beach
M124–M144	Balmerino to Wormit shore
FE2–FE21	Shore of East Flisk
WS1–WS23	West Sands Beach

Figure 3.7 Groundtruth survey stations in the Inner Tay

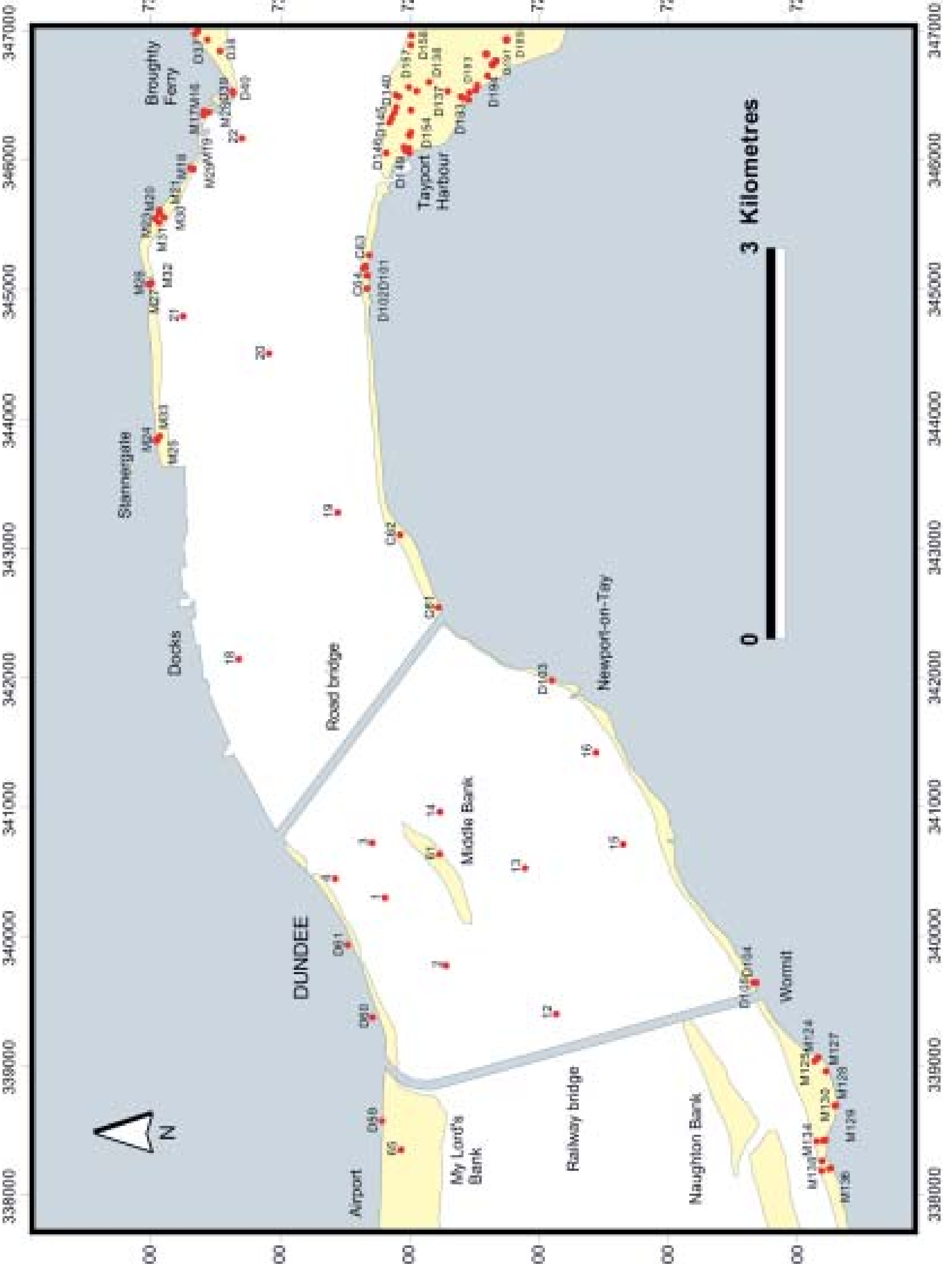

Figure 3.8 Groundtruth survey stations in the Middle Tay

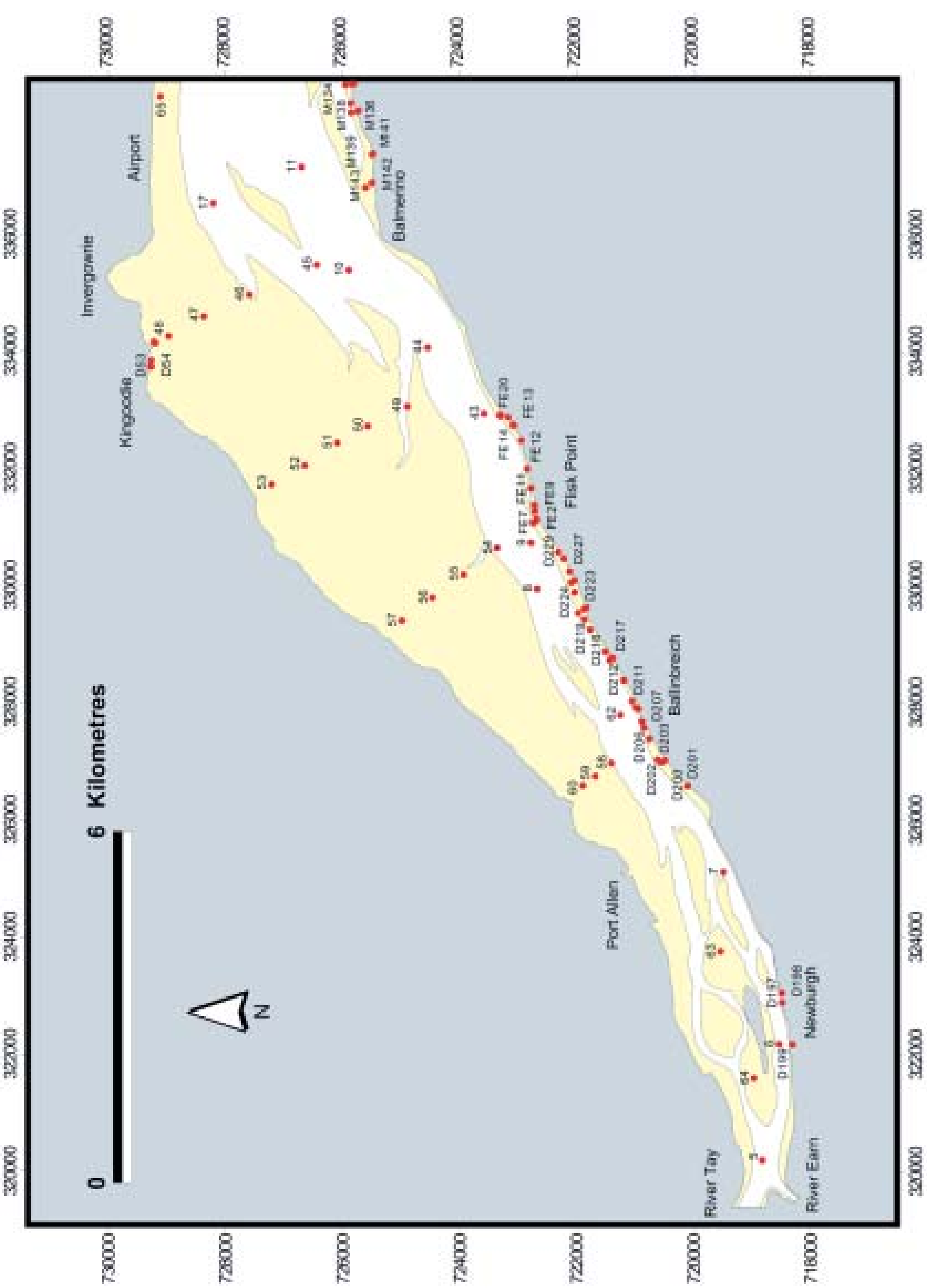

Figure 3.9 Groundtruth survey stations in the Outer Tay

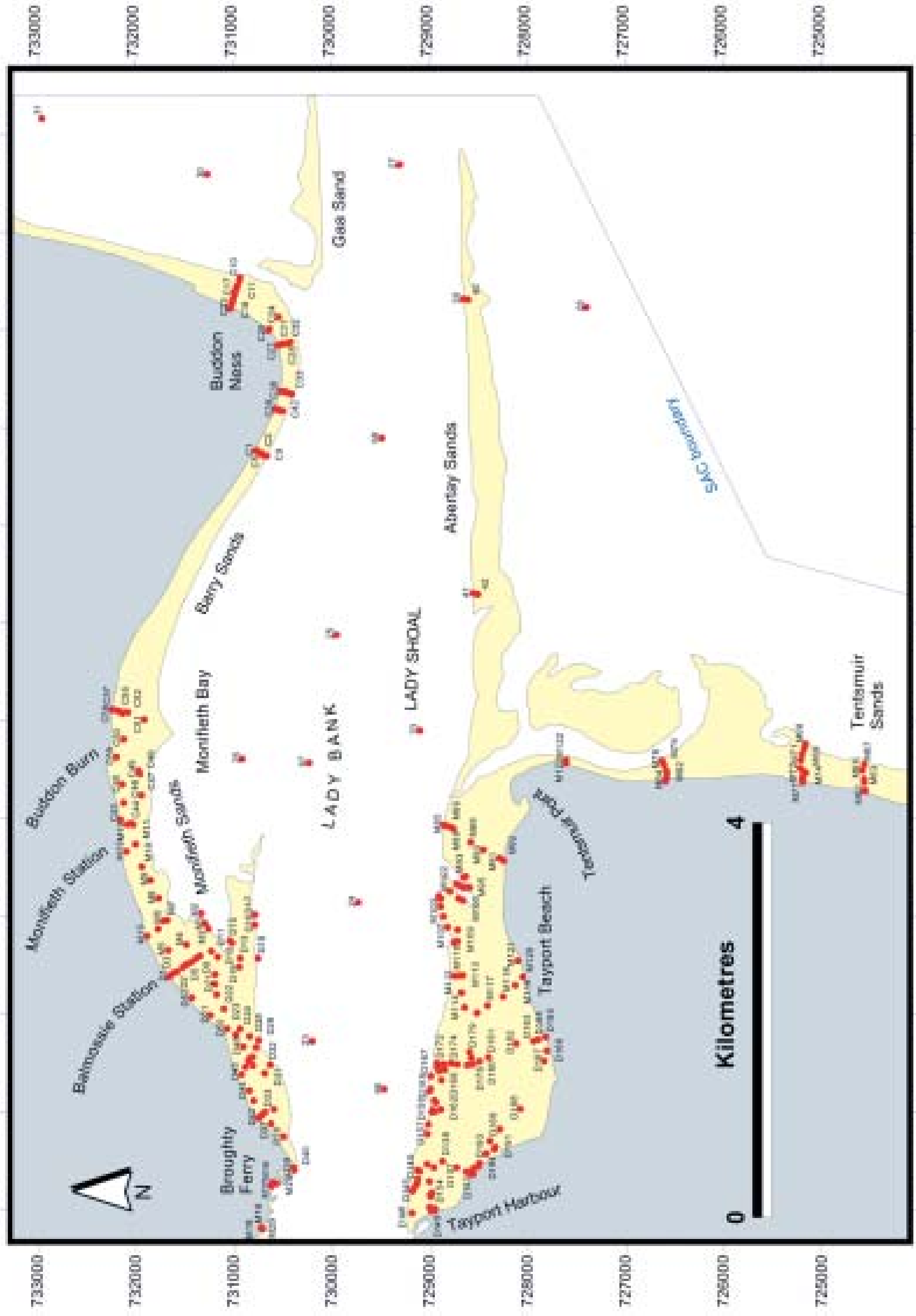

Figure 3.10 Groundtruth survey stations in the Eden Estuary and approaches

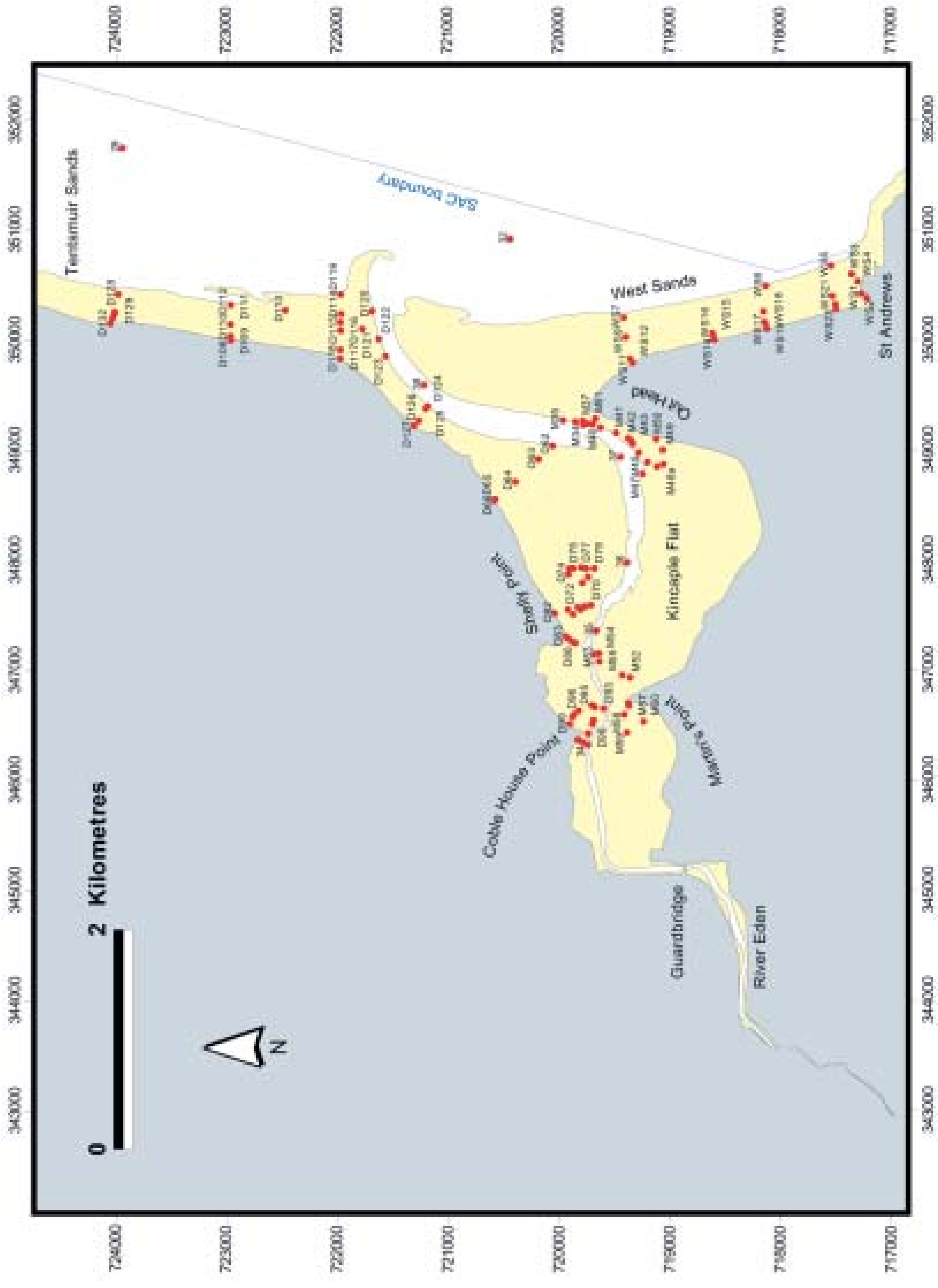

3.3.2 Biological laboratory procedures

Biological material from the infaunal and epifaunal samples was identified to species and enumerated. Station details, including descriptions of the biota, physical characteristics, position, date, sampling gear and surveyors, were entered into an Excel spreadsheet, together with the biotopes present.

Multivariate analysis of the infaunal species abundance data was used to aid the process of biotope identification. As the sampling gear used included both quantitative and semiquantitative methods, the species abundance data were first site-standardized before performing non-metric multidimensional scaling on square root transformed data. The resulting MDS plot was used to highlight possible biotope misidentifications and help resolve uncertainties. Ordinations were also performed on data sets from previous surveys of specific locations to aid in the identification of biotope boundaries and to identify the dominant and characterising species.

Allocation of biotopes was based on the biotope descriptions in Connor *et al.* (1997a,b). Biotope identification took into consideration a number of sources of information, including field notes on biota and physical characteristics, sediment analyses, video material collected on the shore or by ROV, infaunal and epifaunal sample data, known habitat characteristics (eg salinity, wave and current exposure), and multivariate analyses.

The current study was supplemented by information on the distribution of biotopes acquired by examination of the results of previous surveys of the SAC. The major sources were Paterson, Gatty Marine Laboratory (pers. comm.), Johnston *et al.* (1978, 1979), North East Fife District Council (1998), Jones *et al.* (1989, 1992), Bell (1998), Oakwood Environmental Ltd (1998), Marine Ecological Surveys Ltd (1998) and Khayrallah and Jones (1975).

The distribution of biotopes amongst survey stations was tabulated in two ways. The data were ordered by station and then biotope. This list is presented in Appendix 1 (Tables 1 and 2). Table 3 (Appendix 1), on the other hand, lists the stations where each biotope was recorded, together with video frame dumps of most biotopes.

Biotope records and summaries of the physical and biological characteristics for the survey stations was entered into an ArcView GIS. With the aid of the acoustic survey, satellite imagery and sediment maps (Buller and McManus, 1975; McManus *et al.*, 1980), biotope boundaries were drawn as polygons. In view of the absence of current detailed satellite images for the middle and inner Tay, low resolution Landsat images taken on 17th July 2000 and 1st March 2002 and aerial photographs taken on 24th June 1999 assisted in the delineation of some of the major biotope boundaries in these areas.

3.3.3 Sediment laboratory analysis

Particle Size Analysis (PSA)

Initial sediment sorting was conducted on *Serpula* by Heriot Watt University staff. This sorting noted those sites where the grab and dredge samples only contained material that was greater than 32mm and kept material where there was a portion of the sediment that was less than 32mm particle size. This material was preserved for laboratory analysis. The sediment was first divided into subsets of 1–5g with those only containing sediment particle sizes less than 2mm and those that contained a mixture of sizes up to and greater than 2mm. The large particle size sediment was dried and hand sieved through a set of sieves from 32mm to 2mm. Material that remained after sieving to 2mm was re-wet and analysed using a Coulter LS230 Laser Particle Sizer. This particle sizer was also used for the second sub-set of samples that only contained material with a grain size less than 2mm. The <2mm was weighed and the material >2mm was weighed so a percent value was obtained for material <2mm and >2mm (each of the sieves used) The LS230 results for the course sample are then recalculated to represent the percent <2mm. All of the analyses were made at the School of Geography and Geosciences, University of St Andrews.

3.4 Satellite monitoring of intertidal habitats

The extensive nature of Scotland's marine environment necessitates the use of techniques which facilitate the broad-scale mapping of seabed habitats and meet the requirements for monitoring on a routine basis. Remote sensing from satellites and aircraft has been shown to offer a non-invasive technique with which to rapidly monitor changes in the cover and health of submerged habitats in shallower water Scottish environments. In particular, it offered extensive spatial coverage for waters which were too shallow to survey using other techniques (eg acoustic methods). For intertidal mapping, remote sensing offers specific advantage in its ability to obtain temporal and spatial information at scales unmatched by other survey methods and can serve to both reduce and better target time consuming fieldwork.

Mapping of marine intertidal zones requires remotely sensed data at high spatial, spectral and radiometric resolution to match the scale of the variations in subsurface habitat types and to offer the ability to discriminate different habitat types. Furthermore, data should ideally be obtained at low tide when intertidal habitats are exposed. High temporal resolution data are therefore required to maximise the windows of opportunity when low tides coincide with times of satellite overpass. The high spatial resolution (sub 4 m pixel resolution) and rapid frequency of overpass (~ 3 days) of the QuickBird sensor suggests that it offers data most suited to the routine monitoring of intertidal marine habitats (Table 3.5, Figure 3.11). These contrast with the more 'conventional' optical sensors (eg Landsat TM, SPOT) which offer only coarse spatial resolution (20–30m), poor radiometric resolution (256 measured radiance levels) and limited temporal resolution (18–26 days).

3.4.1 Aims and objectives

As part of the wider marine mapping project in the proposed Firth of Tay and Eden Estuary cSAC Scottish marine area undertaken during 2002 this work evaluated QuickBird satellite sensor and other optical data for the mapping of intertidal habitats with the ultimate aim of developing techniques for the routine application of such approaches. The specific objective of this section of the research was to evaluate multispectral high spatial resolution QuickBird data for discriminating and mapping typical intertidal habitats in Scottish coastal waters.

3.4.2 Satellite Imagery

3.4.2.1 QuickBird data acquisition and quality review

Orders were placed for QuickBird image acquisition over the Firth of Tay and Eden Estuary cSAC in April 2002. Due to the size of the estuary and the comparatively narrow swath of the satellite, the acquisition was required in three parts (Figure 3.12). The acquisition was further affected by the need for acquisition during periods of low tide to ensure intertidal regions were exposed, and thus to obtain as complete a mapping as possible. This requirement restricted the acquisition 'window' for any of the three parts to two periods per month of approximately 5 days each.

Table 3.6 Characteristics of the QuickBird satellite and sensor

Characteristic	QuickBird
Launch:	October 18, 2001
Altitude:	450km
Orbit:	98 degrees, sun-synchronous
Imaging modes:	Panchromatic and Multispectral
Spatial resolution:	0.6m (Panchromatic) 2.6m (Multispectral)
Spectral resolution:	Four bands (Blue, Green, Red, Near infrared)
Revisit Frequency:	n/a
Radiometric resolution:	11 bit (2048 radiance levels)
Swath:	16.5km
Other features:	Pointability

Figure 3.11 Sensitivities of the four multispectral QuickBird wavebands (from DigitalGlobe Inc.)

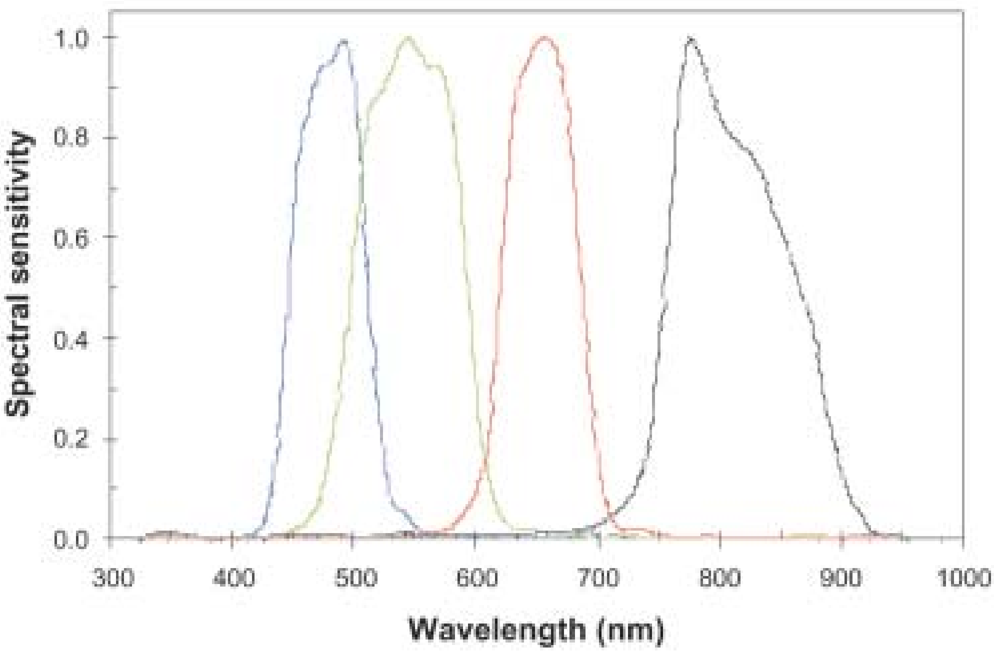

Figure 3.12 Map of Tay estuary showing proposed QuickBird acquisition in three parts. The parts are numbered from 1–3 from east to west

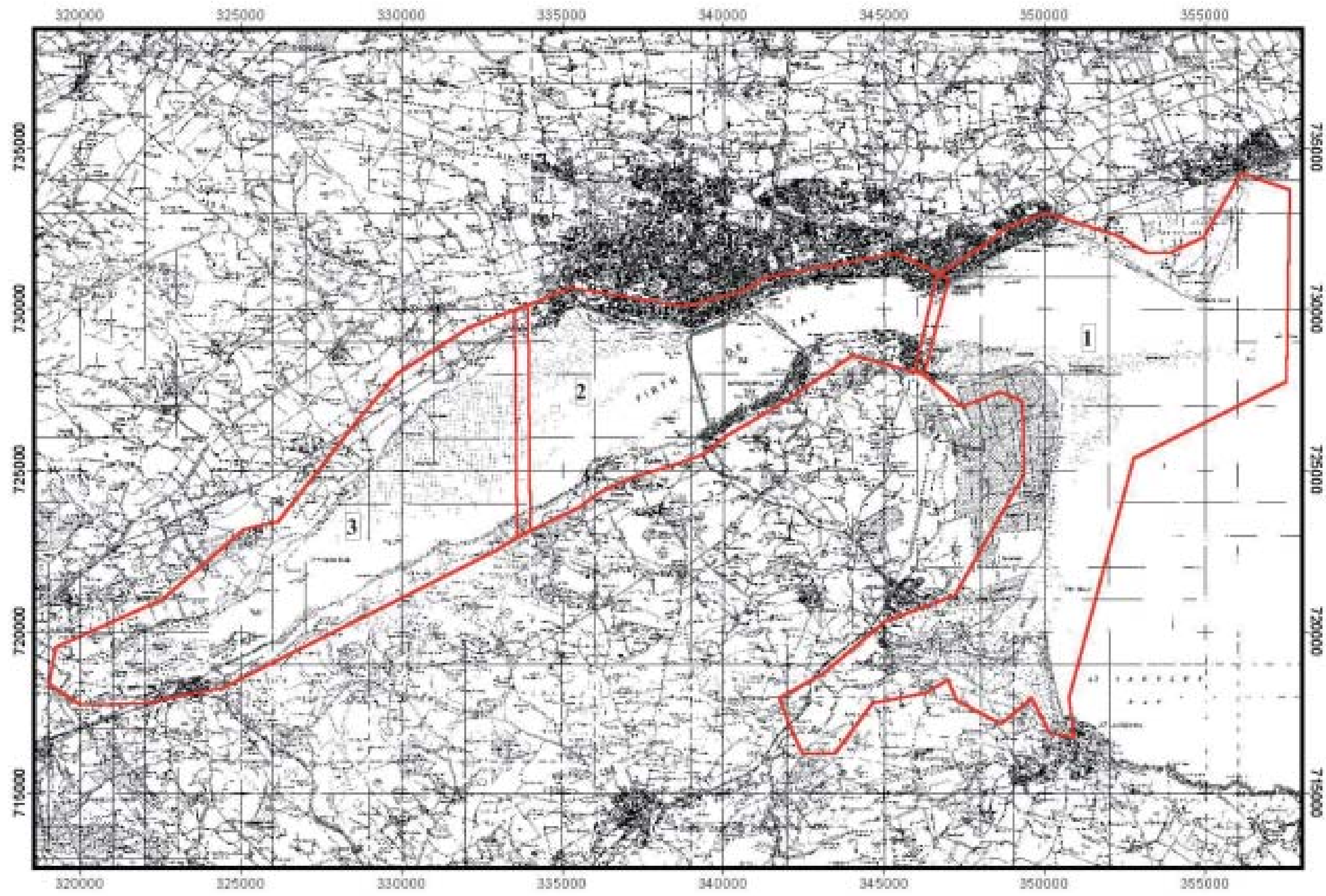

Relatively cloudy weather throughout the summer of 2002, coincident with the narrow acquisition windows, meant that only Part 1 of the Firth of Tay and Eden Estuary cSAC was captured, on 27.08.02. The acquisition characteristics of the image are given in Table 3.6. This part comprises the eastern-most portion of the cSAC extending down the coast from Carnoustie to St Andrews (Figure 3.13).

The image acquired was virtually cloud free. Visual inspection of the data revealed few radiometric problems or other flaws such as missing scan lines etc. This dataset was used in all subsequent processing.

Table 3.7 QuickBird Part 1 image data acquisition characteristics

Acquisition Date:	**27.08.2002**
Acquisition Time:	11:30:29 GMT
Platform altitude:	450km
Orbit:	98 degrees, sun-synchronous
Image Coordinates:	Top Left: 56.49848239°N, -2.94368990°W
	Bottom Right: 56.43756132°N, -2.70174771°W
Geometric Processing Level:	Standard2A
Interpolation Method:	Nearest Neighbour
Bits per Pixel:	11 (2048 brightness levels)
Satellite Azimuth:	335.619°
Satellite Elevation:	64.8515°
Sun Angle Azimuth:	165.673°
Sun Angle Elevation:	43.0064°
Image Quality:	Excellent
Multispectral data spatial resolution:	2.8m
Multispectral bands: Blue Green Red Near Infrared	 450–520nm 520–600nm 630–690nm 760–900nm

3.4.2.2 Geocorrection

The Quickbird imagery was supplied in geocorrected form to a 1:50,000 scale accuracy by DigitalGlobe Inc. To further improve the accuracy for mapping purposes, the imagery was subsequently geocorrected to the corresponding OS LandLine (1:1250 scale) map base using ground control points (GCP's). The ultimate correction of these data is thus to within one pixel (<2.6 m) of true position. The projection used was the Transverse Mercator British National Grid.

Qualitative comparison of our secondary geocorrected image with that of the original image supplied by DigitalGlobe indicated that the original data supplied were accurate only to within 3–4 pixels (approximately 8–12m) of the 'true' location. It may be felt that the level of accuracy of the data originally supplied is of acceptable accuracy to work with, without the need for further geocorrection. Although it is unknown what system or map-base DigitalGlobe use for their original corrections, it is likely that this level of accuracy would be similar for any images obtained from this sensor around the Scottish coastline.

Figure 3.13 Raw QuickBird Part 1 data set obtained from DigitalGlobe Inc., showing the extent of the coverage

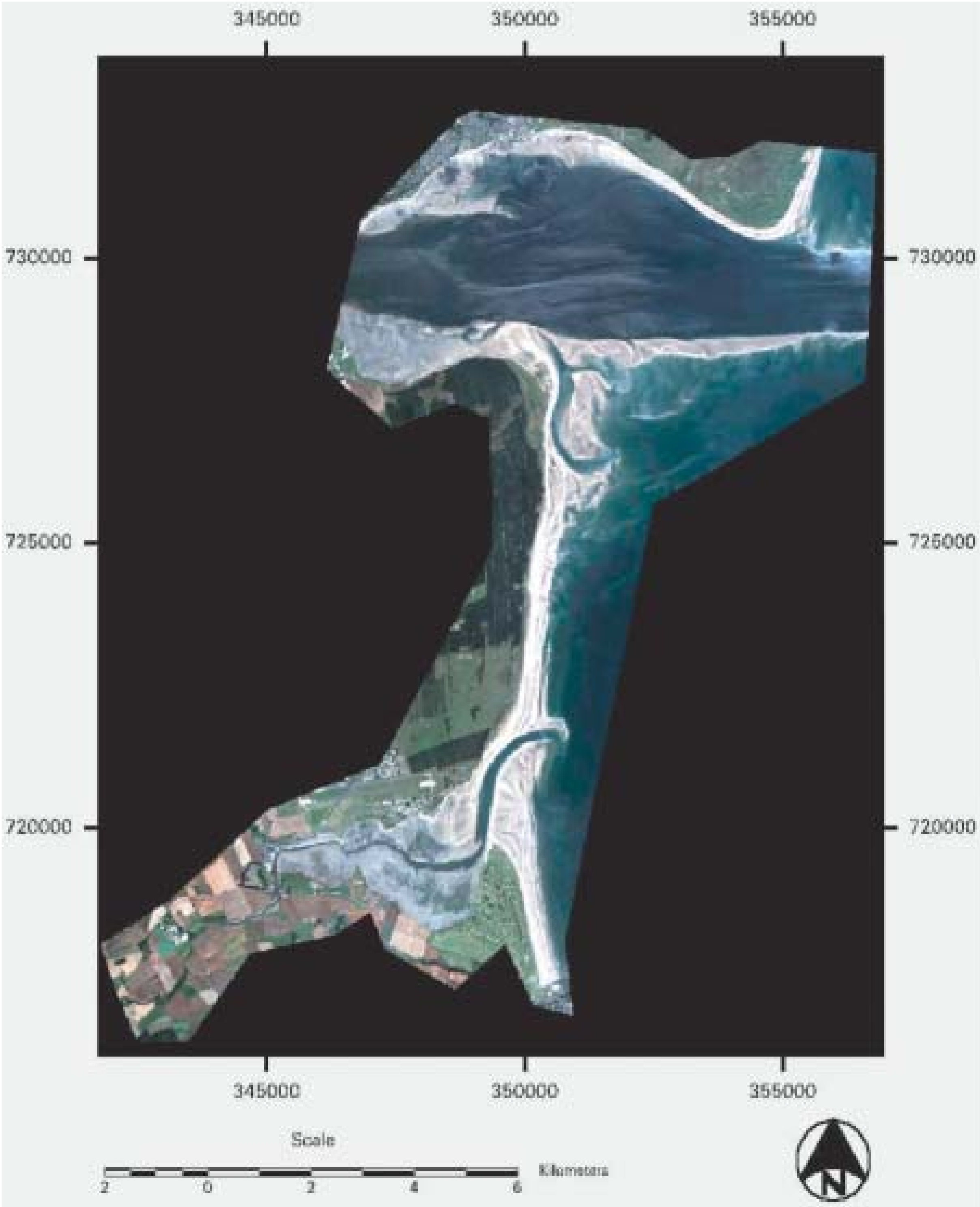

3.4.2.3 Field methods

All field-based measurements were undertaken during a targeted field campaign in the region covered by the Quickbird Imagery during October 2002.

Measurements of land field targets for atmospheric correction

The empirical line method has been shown to provide an accurate method for atmospherically correcting IKONOS imagery (Bates *et al.*, 2002; Karpouzli and Malthus, 2002). To apply this method to the Tay QuickBird data, six large and relatively homogeneous land surface targets of varying brightness were measured for their spectral reflectance properties. The targets selected ranged from a gravelled car park, a sandy beach, a grassed playing field, the 10th tee on the Jubilee course at St Andrews, the driving practice tee at the St Andrews Links Clubhouse and a vehicle park with a light soil substrate. Descriptions and positions of these targets is given in Table 3.8.

Measurements of the spectral reflectance of each target were performed using a GER 3700 spectroradiometer obtained on loan for this research from the NERC Equipment Pool for Field Spectroscopy. This rapid scanning instrument is capable of measuring reflected radiance of targets at very high spectral resolution over the visible, near and middle infrared infrared wavelengths (300–2400nm). The spectroradiometer sensor head was used fitted with a 3° field-of-view lens operated from a height of approximately 1m above the target type, giving a ground footprint of approximately 6cm diameter. Between 10 and 20 spectra were taken at random points over each target depending on the apparent variation visible within the target itself. References to incident irradiance over a calibrated Spectralon™ panel were obtained for every target measurement.

Table 3.8 Description and locations for the ground calibration sites

Target name	Description	Eastings	Northings
Grass	Short grass in ground of caravan park	346384	728533
Sand	Wet sand on beach	349753	719447
Soil	Soil in caravan park	346439	728516
Lsoil	Light soil in carpark	350217	717356
Tee	Short grass in golf course	349542	719488
Drive	Short grass in golf course	350256	717414

Each site was accurately positioned using a 12 channel Garmin III+ GPS unit which recorded the target positions for at least 10 minutes, which, with *Selective Availability* discontinued, gave a positional accuracy of approximately 2m.

The ground-measured spectral data were processed to absolute reflectance. From the averaged reflectance spectra for each target the reflectance values for the QuickBird bandwidths were calculated using filter functions based on the sensor response curves provided by DigitalGlobe Inc (Figure 3.11). Relationships were developed between the calculated ground-based QuickBird reflectance values and related values extracted from the corresponding pixel locations in the multispectral QuickBird dataset (Figure 3.14). The relationships show considerable linearity. Deviations from linearity are probably the result of changes in surface reflectance between image acquisition and measurement of the ground reflectances. It can be concluded that the response of the QuickBird sensor is linear across the range of typical measured earth surface reflectances. The points where the lines would intersect the x-axis indicate the contribution to radiance from background reflectance of light in the atmosphere. This is highest in the blue region where atmospheric scattering is considerable and generally decreases with increasing wavelength.

These empirically-derived relationships were used to atmospherically correct the IKONOS data to percent ground reflectance.

Figure 3.14 Empirical line relationships developed for atmospherically correcting the QuickBird image data

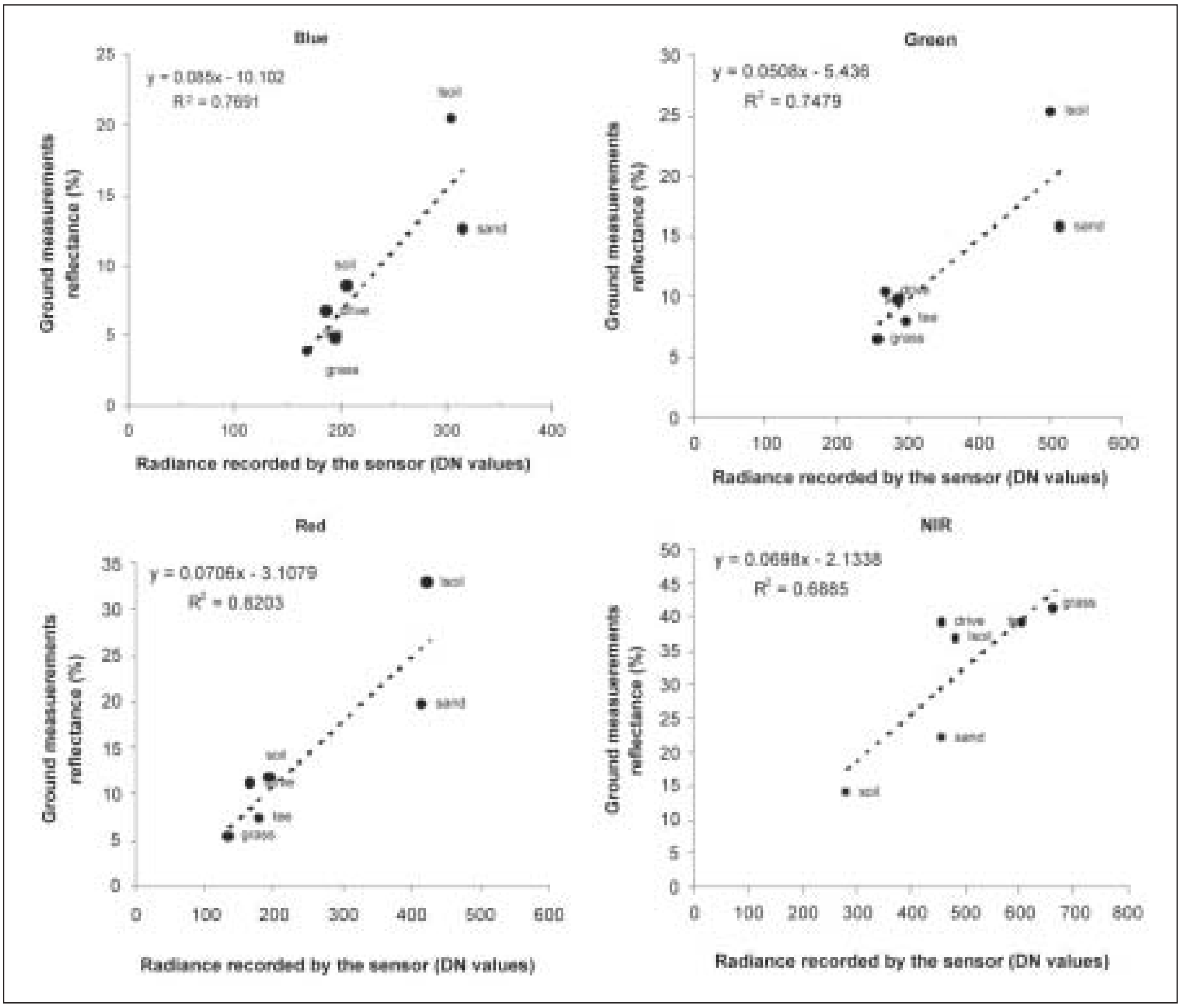

3.4.2.4 Masking

The corrected QuickBird imagery were masked to eliminate all land areas from the image using the digitised Firth of Tay and Eden Estuary cSAC boundary supplied by SNH. Masking is a useful technique in coastal studies to eliminate bright pixels from land such that interpretation can be focussed on the generally darker coastal water features. Eliminating land pixels also allows for any automated classification to focus solely on aquatic features without the need for additional categories to account for land pixels. The resultant masked dataset is shown in Figure 3.15.

Figure 3.15 Masked QuickBird image dataset

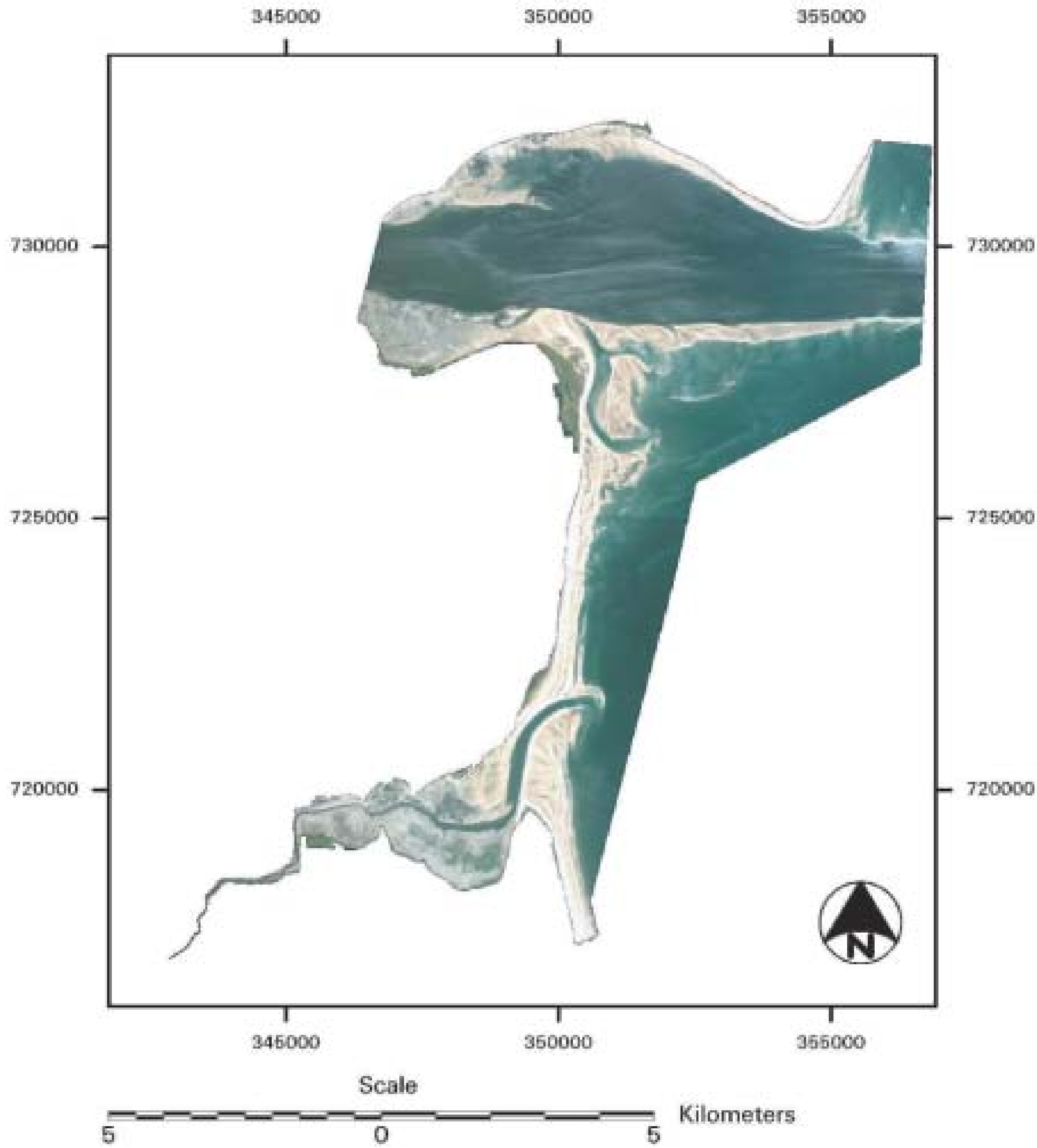

3.4.3 Landsat data

Due to the weather problems encountered which prevented the acquisition of *complete* QuickBird coverage for the Tay, two coarser resolution Landsat TM images were obtained and processed to facilitate mapping of habitats further within the Tay estuary itself. Charactersitics of the two images used are given in Table 3.8. Both images are relatively recent, being obtained by the Landsat 7 Enhanced Thematic Mapper (ETM+) sensor and both were acquired at times of low tide. The ETM+ sensor obtains data in 6 optical bands at approximately 30m spatial resolution, 1 thermal band at 60m resolution and an additional panchromatic band at 15m spatial resolution. Characteristics of the spectral bands for this sensor are given in Table 3.9.

Two Landsat images were used (Table 3.8) because the most recent image, obtained on 01.03.2002, showed some contamination from cloud cover and a limited range of DN brightness values due to low sun angles encountered in early March. The 17.07.2000 image was virtually cloud free and showed a good range of brightness values for the estuarine area. The images were supplied in geocorrected format, but were further corrected to the OS LandLine (1:1250 scale) dataset by manual methods.

Table 3.9 Acquisition characteristics of the two Landsat 7 images used in this study

Product Type	**L1G**	**L1G**
Spacecraft Id	Landsat7 Etm+	Landsat7 Etm+
Acquisition Date	17.07.2000	01.03.2002
WRS Path and Row	205, 021	205, 021
Band Combination	123456678	123456678
Product Upper Left Corner Coordinates	56.9012909, -5.6636882	56.9013519, -5.6608839
Product Lower Right Corner Coordinates	54.9049606, -1.8633730	54.8982430, -1.8573401
Sun Azimuth	150.8694510	157.4846940
Sun Elevation	52.7353241	24.4421246
Reference Datum	WGS84	WGS84
Reference Ellipsoid	WGS84	WGS84
Map Projection	UTM	UTM
Zone	030	030
Pixel Size Panchromatic	14.250	14.250
Pixel Size Thermal band	57.000	57.000
Pixel Size Optical bands	28.500	28.500

Table 3.10 Characteristics of the Landsat ETM+ wavebands

Waveband	**Location**	**Location (nm)**
1	Blue	450 – 520
2	Green	520 – 600
3	Red	630 – 690
4	Near Infrared	760 – 900
5	Middle Infrared	1550 – 1750
7	Middle Infrared	2080 – 2350
6	Thermal	10400 – 12500
Panchromatic	Visible/Nir	–

3.4.3.1 Image merging

The images were used to assist the manual interpretation of upper estuary habitats conducted by the Heriot Watt team and to map general sediment distributions. To facilitate habitat interpretation the multispectral datasets were processed to the 15m panchromatic resolution using an image merge processing technique based on Principal Components Analysis (PCA). This method first transforms the six TM optical bands into the same number of independent principal components. The first principal component image contains the information that is common to all the bands (mostly scene brightness) while spectral information unique to any of the bands is mapped to the other components. To merge the images the first principal component (PC 1) dataset is replaced by TM Panchromatic image, which is first stretched to have the same mean and variance as PC 1. The merged image is then derived by performing an inverse PCA transform. The justification used for replacing the first principal component image with the stretched TM Panchromatic data is that the TM Panchromatic data are approximately equal to the first principal component image. The result is a multiband dataset which can be displayed in false colour composite form. The two merged datasets supplied to the Heriot Watt team are shown in Figures 3.16–3.19 in true and false colour composite forms.

3.4.3.2 Mapping of sediment distribution

The 17.07.2000 TM geocorrected 30m resolution dataset was further processed to maps of sediment distribution throughout the estuary. The image was first masked to eliminate land areas using the SAC boundary shapefile data supplied by SNH. The subsequent masked image was used to better display the contrast of sediments in the Estuary using density slicing techniques applied to the band 2 (green region) spectral band.

Figure 3.16 Resolution merged Landsat TM image from 17.07.00 as true colour composite

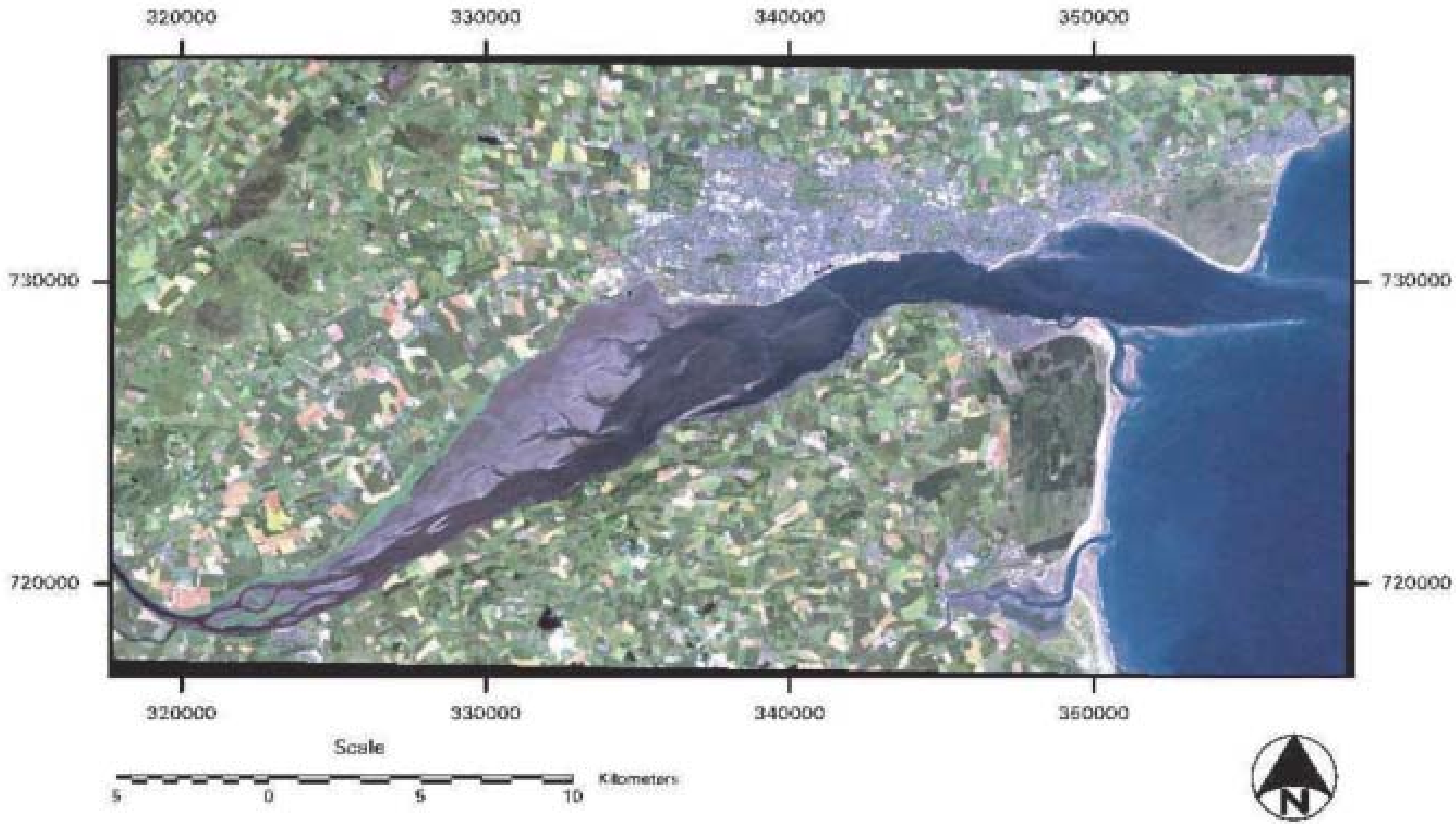

Figure 3.17 Resolution merged Landsat TM image from 17.07.00 as false colour composite

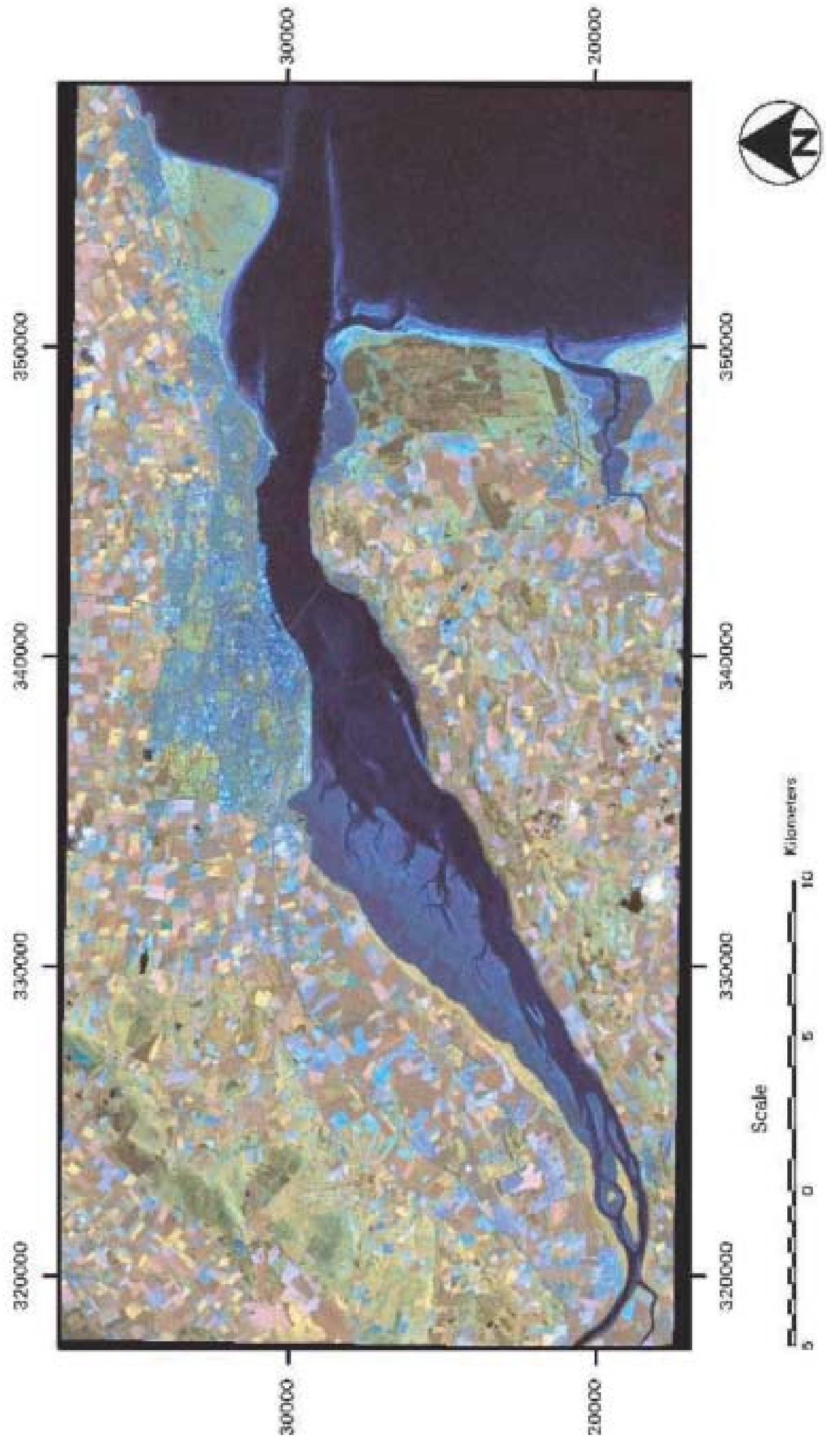

Figure 3.18 Resolution merged Landsat TM image from 01.03.02 as true colour composite

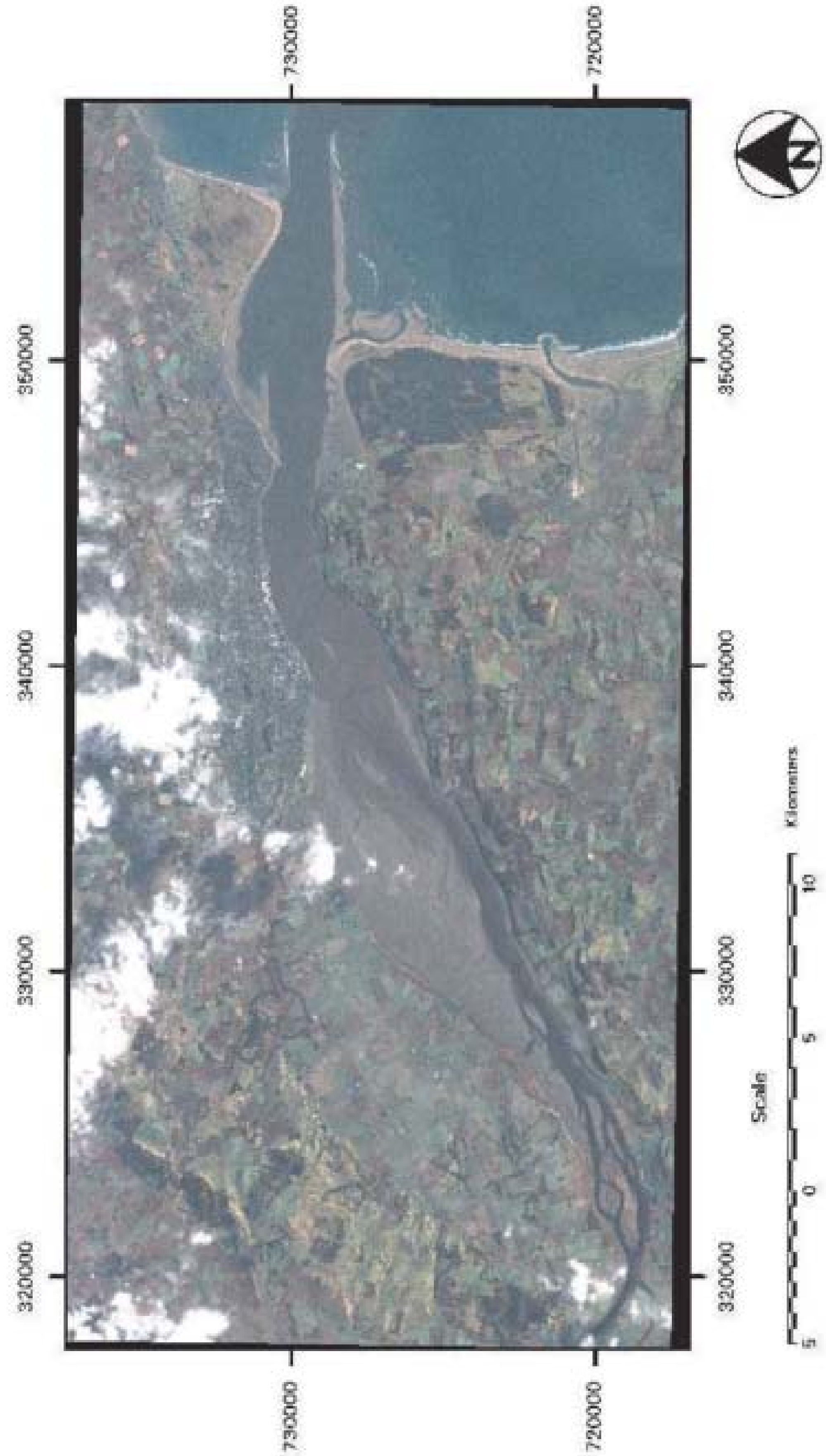

Figure 3.19 Resolution merged Landsat TM image from 01.03.02 as a false colour composit.

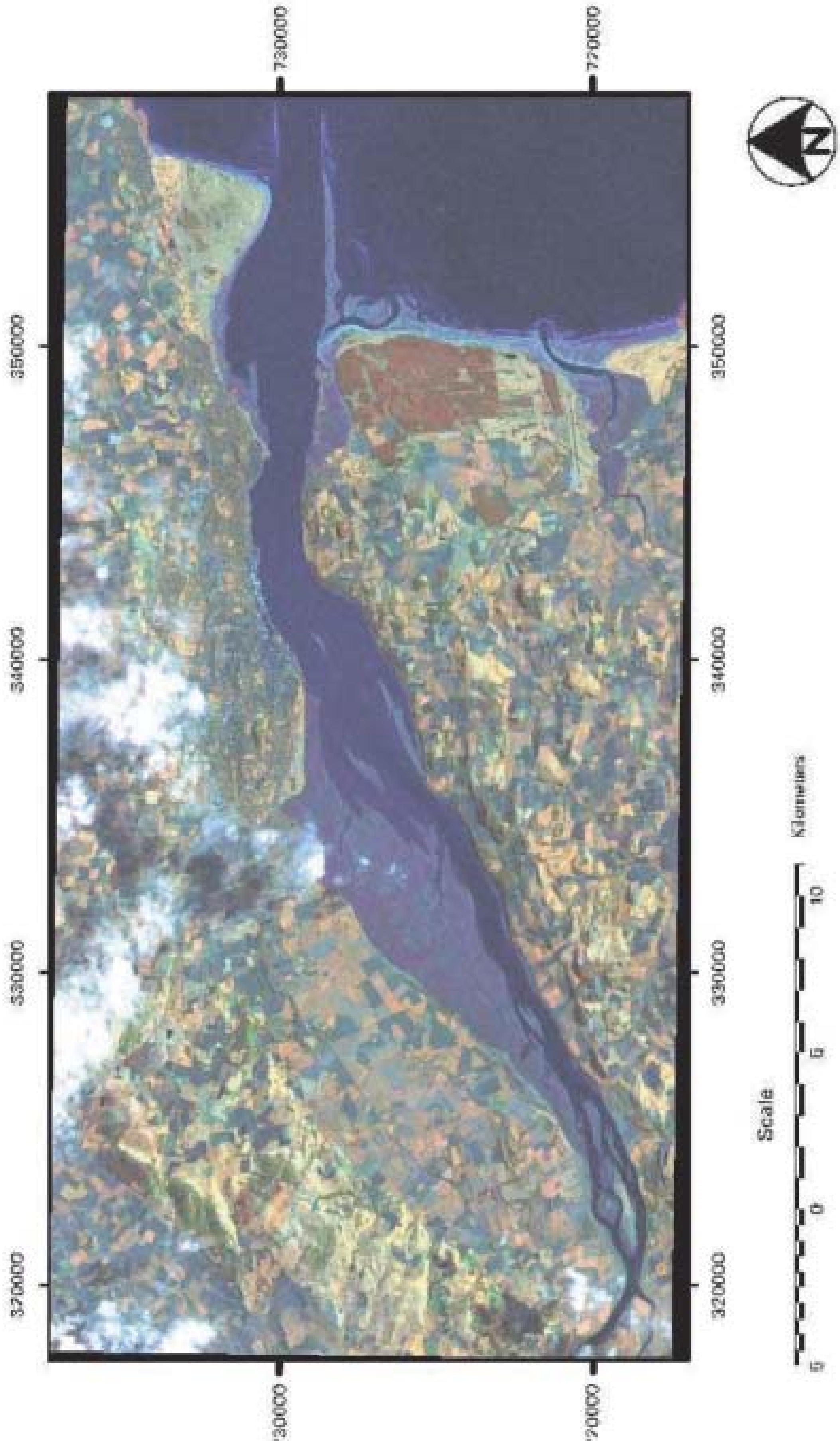

4 RESULTS

4.1 Previous survey results

A considerable number of previous investigations of the sedimentary conditions, currents, and biology have been made in the Firth of Tay and Eden Estuary cSAC. For the Tay Estuary these are summarised in a series of papers published by the Royal Society of Edinburgh (Buller and McManus, 1975; McManus *et al.*, 1980). Figure A1 in Appendix A shows a summary of the mean grain size information recorded by McManus *et al.* (1990) in the Tay Estuary and this is supplemented by information provided by Hamdi (1988) for St Andrews Bay. These maps have been constructed based on over 500 sediment sample data points thus providing a very detailed description of the sediment distribution. Superimposed on this figure are the results of the sediment distribution from the 2002 survey. Each sample data point has been colour coded to the same sediment grain size ranges as used by McManus *et al.* (1980). Also given in Appendix A is sediment distribution information between the Tay Road and Rail bridges presented by Wewetzer (1997). This distribution of sediments was mapped using a combination of sidescan sonar, single beam echosounder and grab samples and represents one of the most recent published data sets for the Tay previous to this investigation.

4.2 Acoustic Maps

4.2.1 Bathymetric results

The results in areas where it was possible to acquire a bathymetric survey using acoustics are shown in Figure 4.1 for the whole area and with an expanded view of the area to the west of the Tay road bridge in Figure 4.2. Bathymetry was corrected for tidal variations during acquisition using Admiralty curves for Dundee adjusted for differences within the Tay Estuary and St Andrews Bay based on the advances and delays given in Table 3.2. Minimum depths of 3m were recorded with the bathymetric sidescan sonar, however, at this lower survey limit some artefacts of the data acquisition and line geometries can be seen in the final bathymetric charts. The maximum channel depth of greater than 30m was recorded to the south of Broughty Ferry. The bathymetry of the area was rendered using a TIN at a final display resolution of 5m bins. The maps are colour coded by depth in 2m intervals. On all the bathymetric maps, but in particular on Figure 4.2, a number of features within the Tay Estuary can be seen such as the large areas covered by sand waves. From the bathymetric chart the scale of these can be measured with maximum sand wave amplitudes of 6m and wavelengths of 250m. Also of note in the area are the numerous sand bars, especially the significant shallow areas of the Abertay Sands and the Gaa Sands, and significant scour associated with both the Tay Estuary road and rail bridges. To the west of the Tay rail bridge, the area that was possible to survey with the bathymetric sidescan was severely restricted to within the central Perth navigation channel. No data could be obtained over the extensive mud flats to the north of the navigation channel. Additional large areas where it was not possible to acquire data due to shallow conditions were present in Monifieth Bay, within the Eden Estuary and along the near shore zone adjacent to Tentsmuir Forest.

4.2.2 Bathymetric slope

Figure 4.3 shows the slope maps derived from the bathymetric TIN with greatest slope change recorded at slope angles between 1° and 15°. The bin size used for this slope map was also 5m. As many of the small

Figure 4.1 Bathymetry for Firth of Tay and Eden Estuary cSAC determined using Submetrix System 2000 bathymetric sidescan

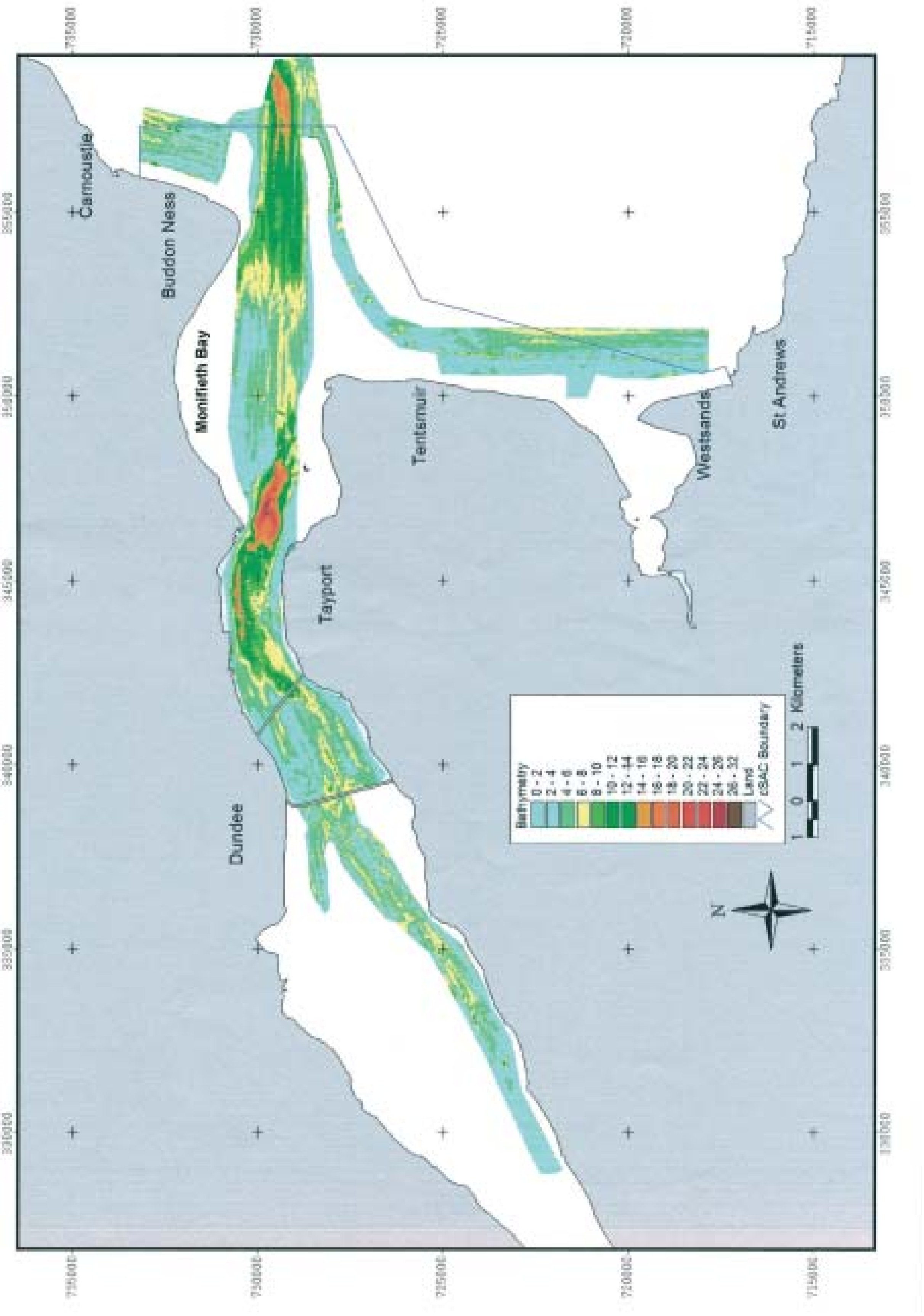

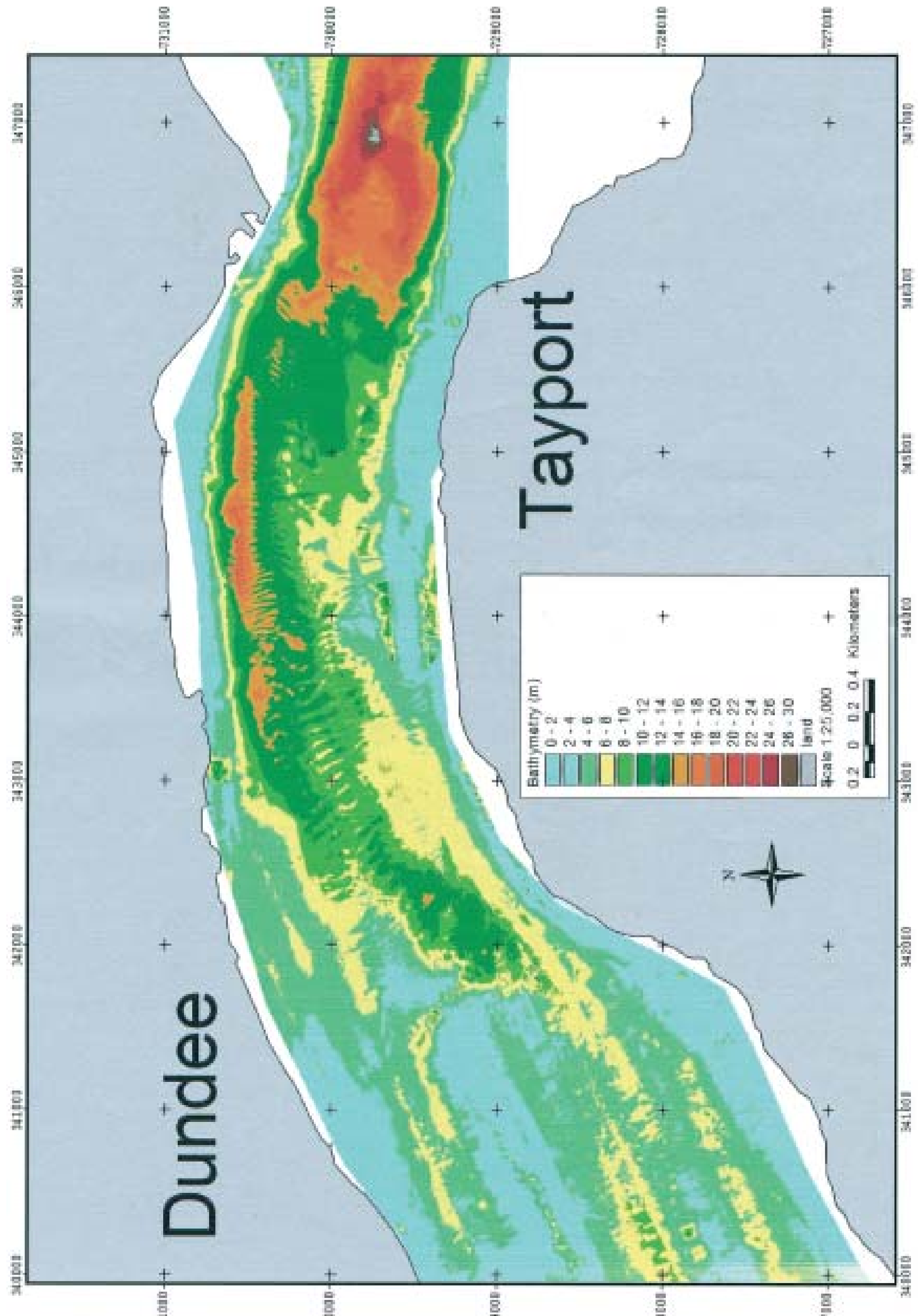

Figure 4.2 Detailed bathymetry for area between Dundee and Broughty Ferry determined using Submetrix System 2000 bathymetric sidescan

Figure 4.3 Slope derived from bathymetry for the Firth of Tay and Eden Estuary cSAC determined using Submetrix System 2000 bathymetric sidescan

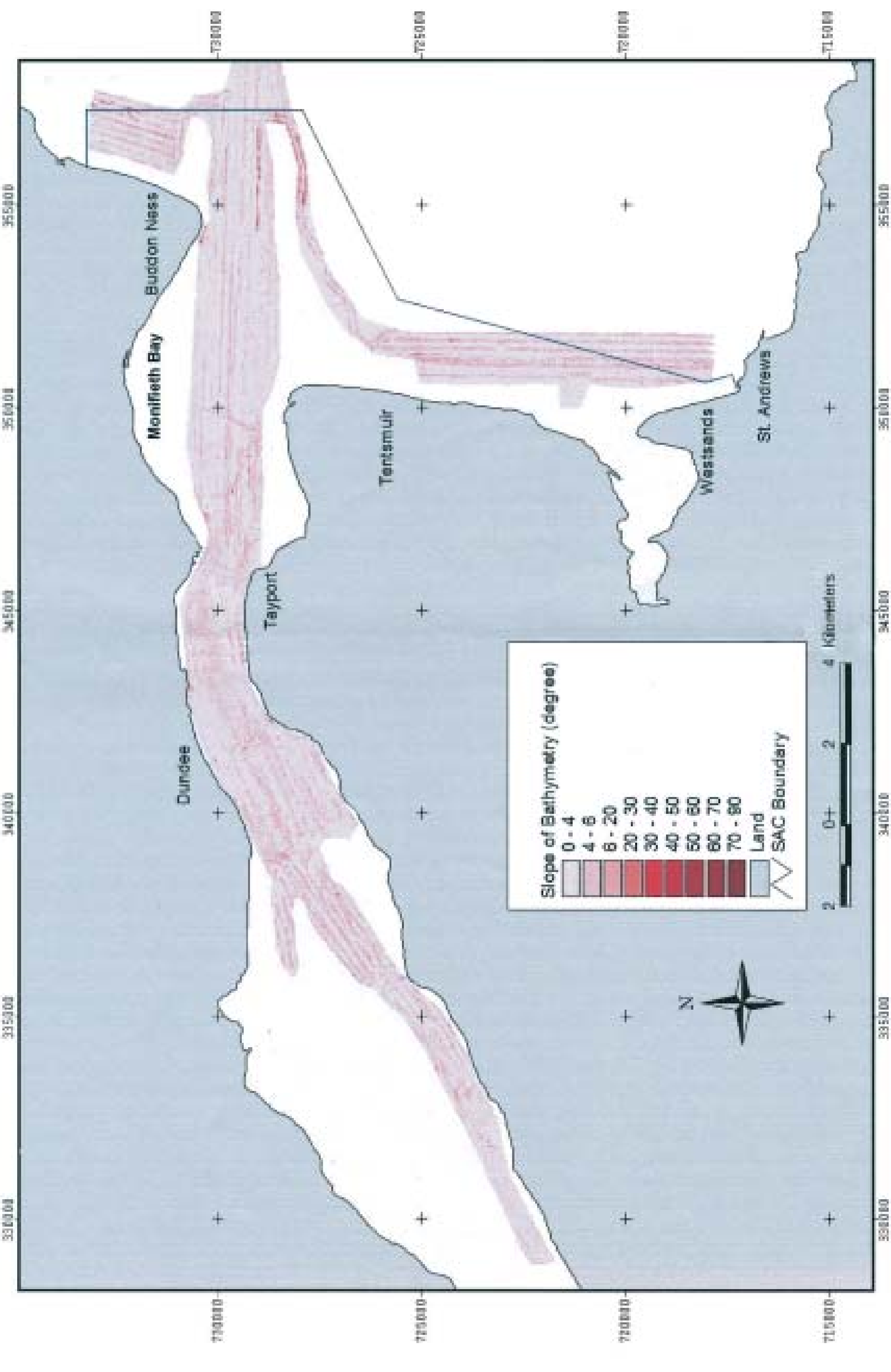

sedimentary structural features within the estuary have wave-lengths and amplitudes less than 5m, the map only shows general areas of slope stability compared to areas of sedimentary feature. Only areas where the sedimentary features are of significant height (greater than 3m) and significant wave-length (greater than 20m) are clearly defined with individually recognisable slope changes.

A number of 3D oblique views of the bathymetry within the Tay Estuary are shown in Figure 4.4. These views clearly show the dramatic range of sand waves that exist within the Tay Estuary in particular east of the Rail bridge and west of Broughty Ferry.

Figure 4.4 3D views of sand waves on the sea floor of the Tay Estuary to the east of the Road bridge

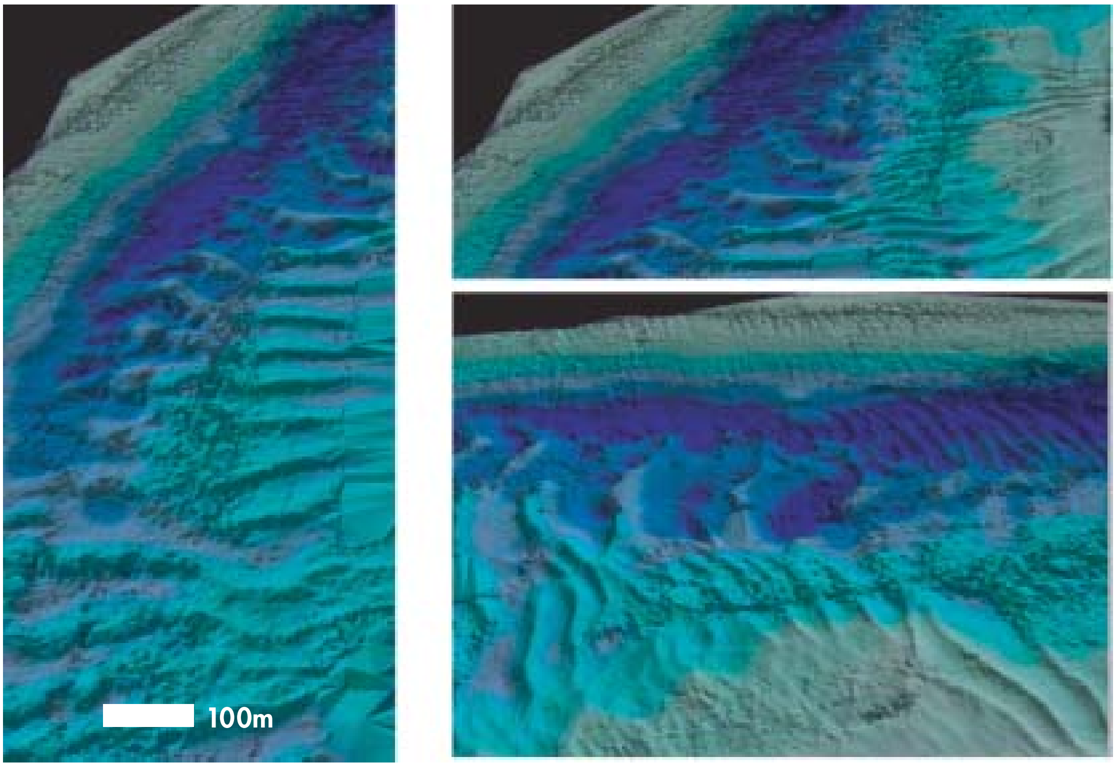

A number of cross-sections have been extracted from the bathymetric maps in order to fully analyse these features. The cross-sections and their locations within the Estuary are presented in Appendix B and an example given in Figure 4.5. Each cross-section has been drawn perpendicular to the wave crests in order that the full wave amplitude (trough to crest height), wave length (crest to crest length) and wave water depth could be measured. From the analysis of these cross-sections it can be shown that a minimum wave height of 75cm can be calculated. The maximum wave height measured in the Estuary was 6m.

4.2.3 Sidescan sonar

Examples of a un-processed sidescan records are given in Figures 4.6 a, c and e. These records have amplitude corrections applied with a time varying gain. Figures 4.6 b, d and f show the same records that have been corrected for true spatial coordinates using transformations from the boat GPS and have also had beam angle corrections applied following the procedures of Danforth (1997). The sidescan records show a number of different seafloor features such as different size sand waves, for example on the port transducer

Figure 4.5 Cross-section of sand wave bathymetry: a) bathymetric chart showing line section; b) cross-section through sand waves

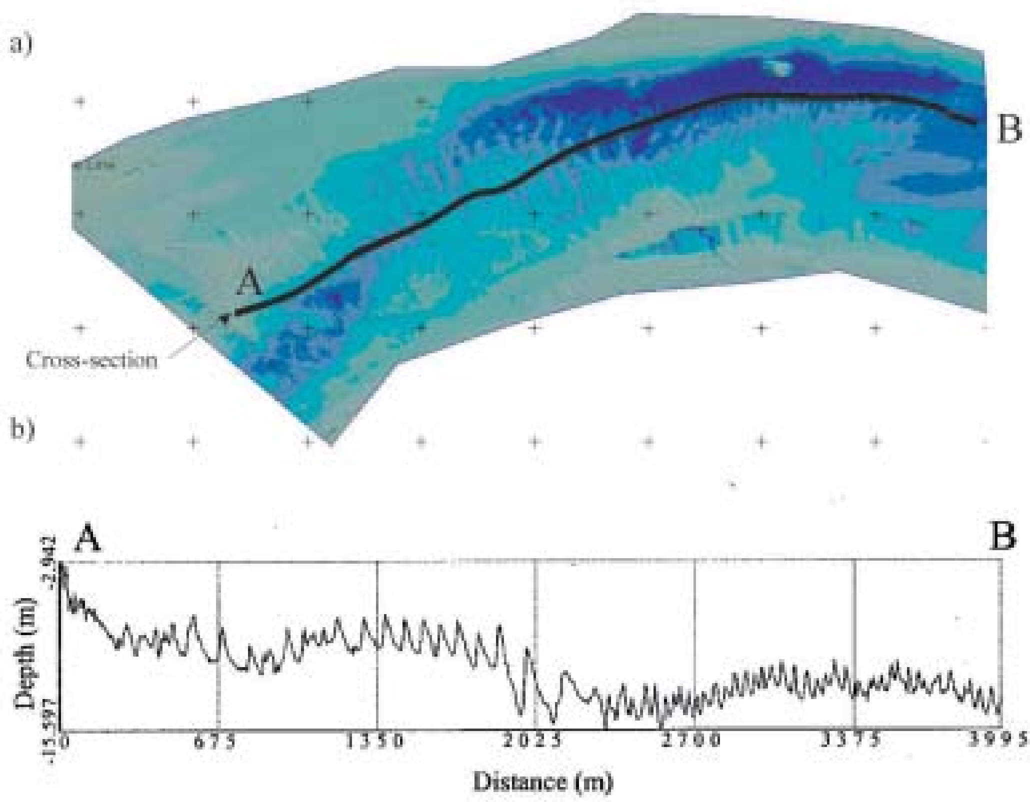

on Figure 4.6 e, features with wavelengths of less than 2m are superimposed on the back of features with wave lengths of greater than 20m. From the sidescan survey it is possible to recognise wave-lengths of 1m or less attributed to individual sand waves.

The sidescan sonar records were acquired over the entire area that the bathymetric survey was effective. In previous surveys using sidescan sonar or bathymetric sidescan it has been common practice to mosaic the individual track lines after corrections for amplitude loss and adjustment for GPS derived position (SNH Laxford/Sunart/Barra). This, however, was not possible for this survey as the numerous sedimentary features caused a mis-match in amplitudes depending on the angle and direction from which they were ensonified. It has been proposed by others and was confirmed with this survey, that in order to mosaic data from areas with complex, upstanding features such as the large sand wave systems that exist in the greater Tay area, it is necessary to acquire sidescan information only in one direction of survey with one ensonificaiton direction using either the port or starboard transducer. Thus final mosaic maps for the whole area are not given for the sidescan survey information. Rather, individual records were analysed for each part of the survey on a line by line basis.

4.2.4 Echoplus AGDS

The results of the Echoplus AGDS are shown as line track data in Figure 4.7 for E1 and Figure 4.8 for E2 of the 200kHz data and Figure 4.9 for E1 and Figure 4.10 for E2 of the 28kHz data. The AGDS data have been filtered and corrected as discussed in the methods section and no attempt was made to extrapolate the data between lines. No AGDS data are presented for areas where the depth was less than 3m as at these depths values become unreliable. Initially, maps were constructed of the AGDS data without the input from

Figure 4.6 Examples of the sidescan sonar results for different seafloor conditions within the cSAC. a), c) and e) are un-corrected images; b), d) and f) are images with beam angle corrections and coordinate transformation to OSGB grid

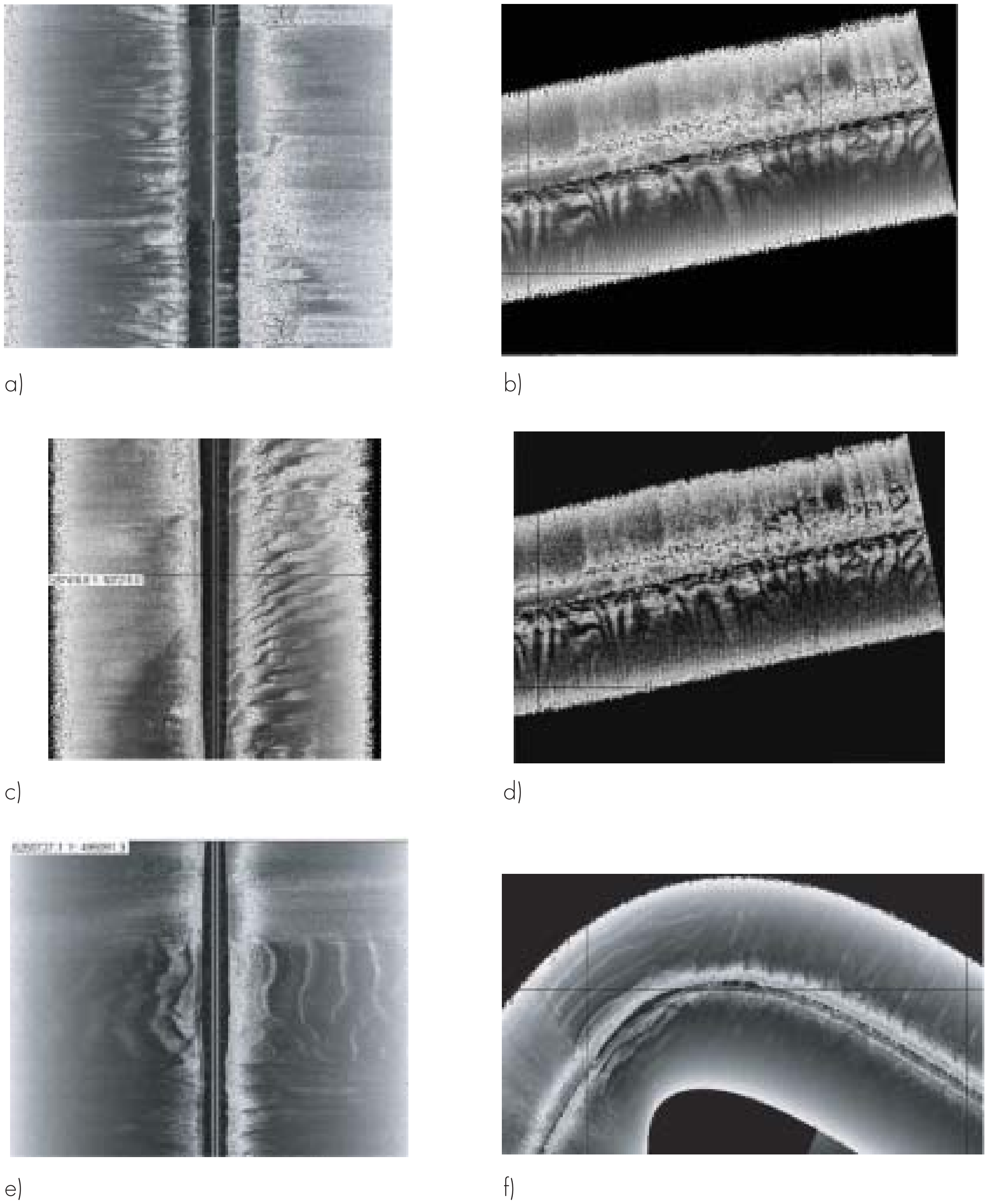

ground control stations containing grain size information. In this manner unbiased acoustic maps could be viewed in the field for directing additional surveying and determining additional groundtruth locations. The size of AGDS footprint was given in Table 3.3. From this and a comparison with information from the sidescan sonar and bathymetric sidescan it is noted that in many places the AGDS footprint crosses sedimentary features. The sedimentary features will in themselves influence the magnitude of AGDS values recorded and thus a simple linear relationship between AGDS values and sediment particle size cannot be found.

Figure 4.7 AGDS line track data for E1, 200kHz echosounder

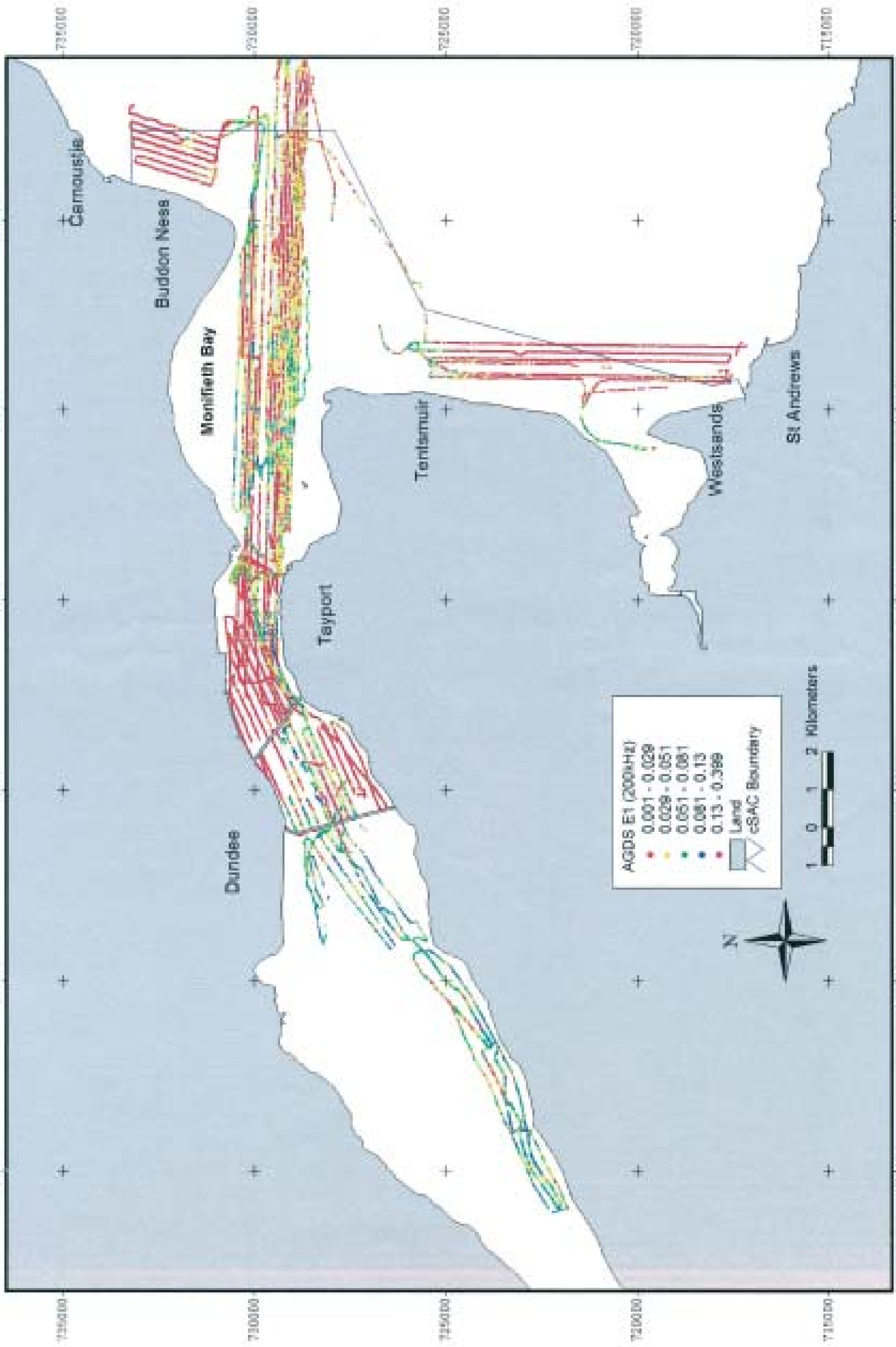

Figure 4.8 AGDS line track data for E2, 200kHz echosounder

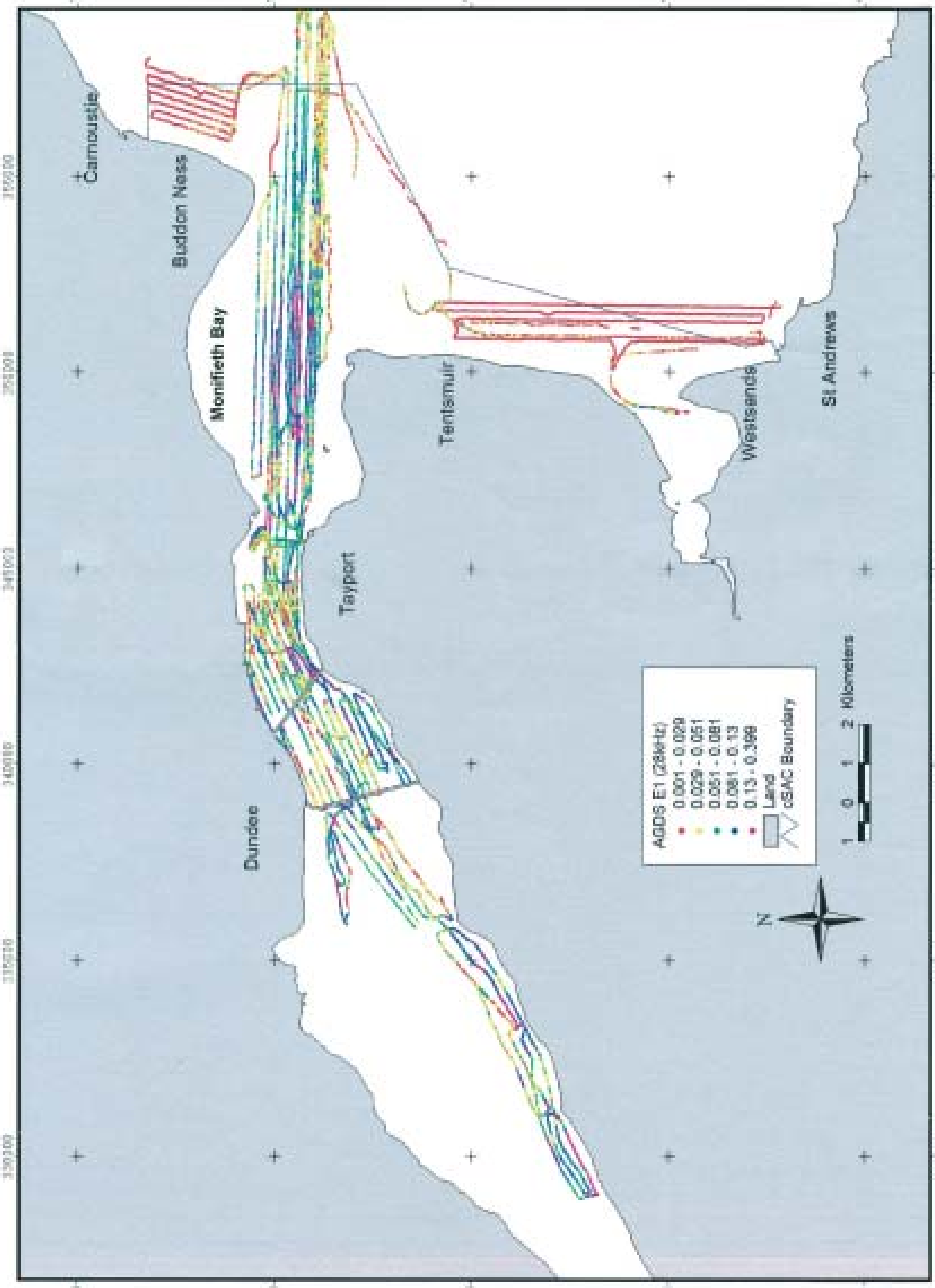

Figure 4.9 AGDS line track data for E1, 28kHz echosounder

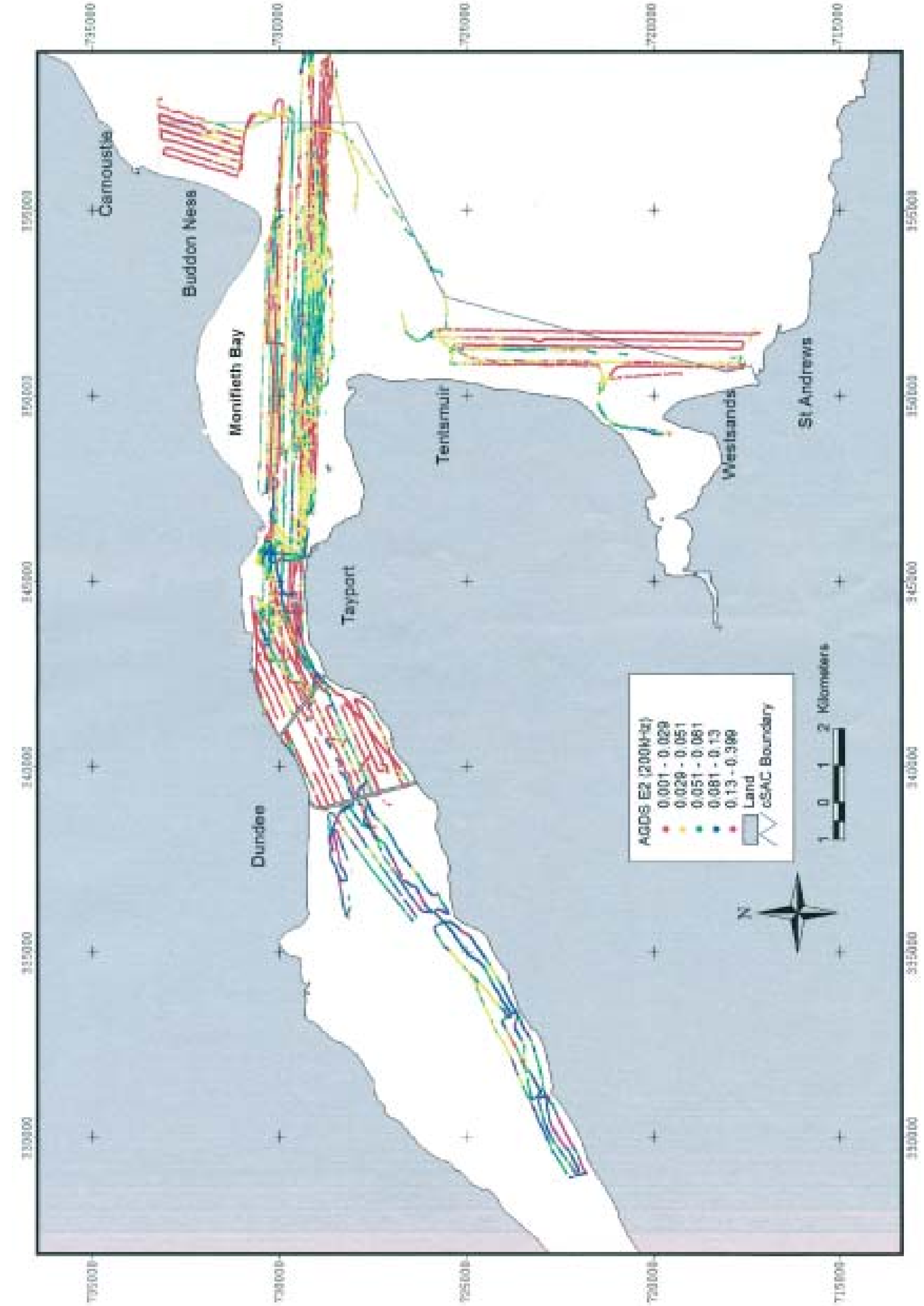

Figure 4.10 AGDS line track data for E2, 28kHz echosounder

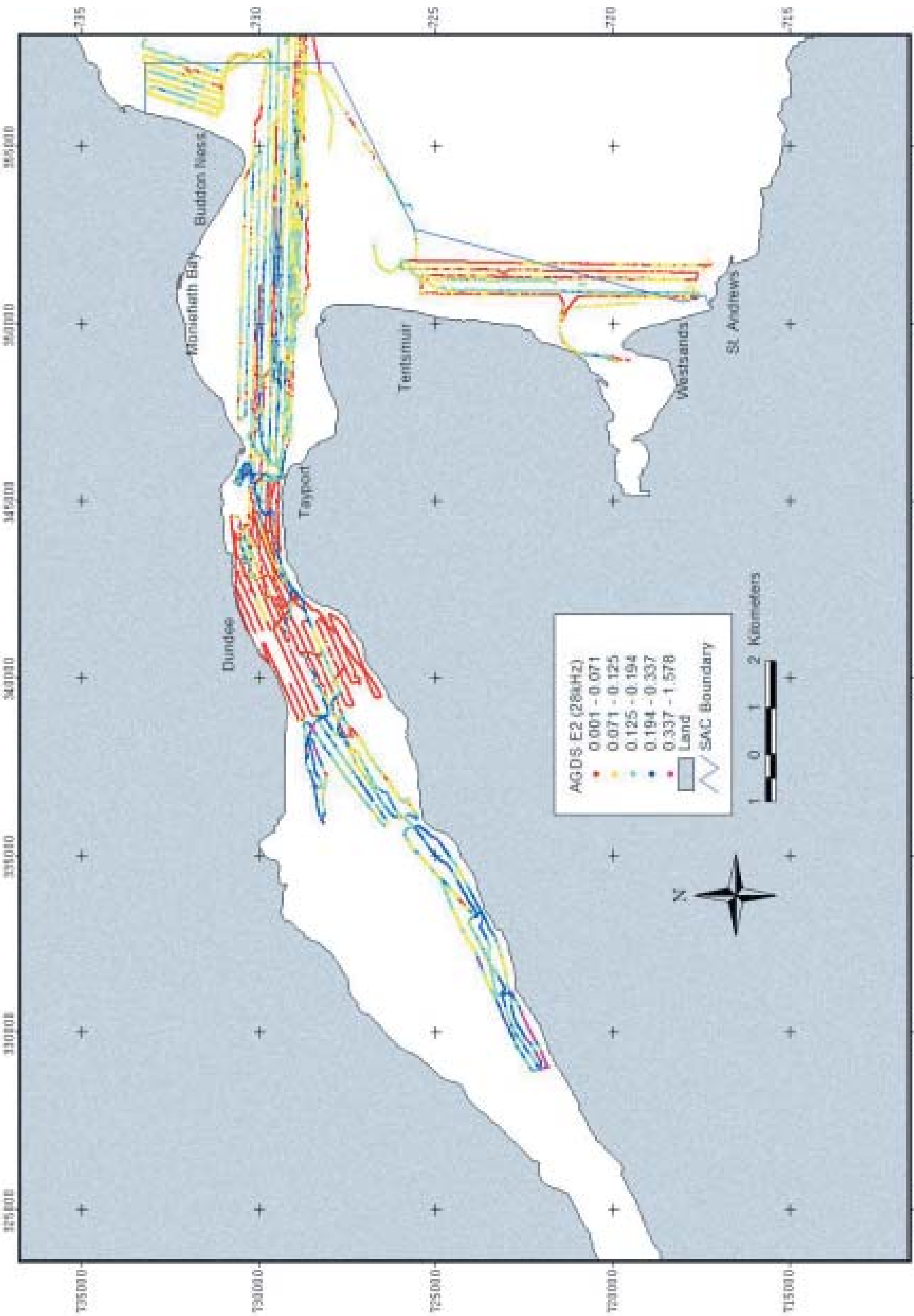

4.3 Sediment grain size analysis

The results of the sedimentary particle size analysis are given in Table 4.1. These show a distribution of sedimentary particles with grain size ranging from fine muds to gravels. Full sediment analysis is given in Appendix B together with summary information on additional sediment sites taken from simultaneous studies by the University of St Andrews. Sites with pebble, cobble and mussel beds did not yield samples that could be retained for full grain size analysis.

Table 4.1 Sediment particle size analysis. Mean particle size and median particle size in μm

Sample Number	Latitude	Longitude	Mean	Median	Silt (%)	Sand (%)	Gravel (%)
C 03	56.46662	-2.75083	297.4	283.7	0	100	0
C 05	56.46644	-2.75103	332	263.3	0	100	0
C 07	56.46606	-2.75134	315.5	292	1	99	0
C 09	56.46581	-2.75149	420.8	303.5	1	99	0
C 11	56.46847	-2.72279	238.4	224.4	0	100	0
C 13	56.46876	-2.72402	307.8	245.3	0	100	0
C 15	56.46886	-2.72464	302.6	244.3	0	100	0
C 17	56.46899	-2.72562	343.1	268	0	100	0
C 19	56.46909	-2.72616	281.3	256.4	1	99	0
C 21	56.46919	-2.72672	388.3	299.5	1	99	0
TAY 01	56.45138	-2.96842	1002	970.5	1	90	10
TAY 02	56.44710	-2.97663	481	426.2	0	100	0
TAY 03	56.45230	-2.96162	830.4	753.2	0	100	0
TAY 04	56.45480	-2.96617	170.9	161.2	5	95	0
TAY 05	56.35508	-3.29133	1111	1077	0	96	4
TAY 06	56.35292	-3.25927	1159	1143	0	76	23
TAY 07	56.36192	-3.21195	606.5	496	1	99	0
TAY 08	56.39123	-3.13452	779.4	661.3	0	100	0
TAY 09	56.39230	-3.12187	1166	1159	0	94	6
TAY 10	56.42095	-3.04702	315.9	274.5	2	98	0
TAY 11	56.42850	-3.01877	855.4	740.2	0	92	8
TAY 12	56.43948	-2.98248	1026	997.3	0	52	47

Table 4.1 *(continued)*

Sample Number	Latitude	Longitude	Mean	Median	Silt (%)	Sand (%)	Gravel (%)
TAY 13	56.44177	-2.96440	409.4	350.2	1	99	0
TAY 14	56.44768	-2.95765	883.9	786.2	1	87	12
TAY 15	56.43503	-2.96138	431.3	217.6	17	55	28
TAY 16	56.43700	-2.94998	164.8	148.5	30	70	0
TAY 17	56.44188	-3.02920	230.5	230.8	12	88	0
TAY 18	56.46167	-2.93907	398.7	113.2	29	48	23
TAY 19	56.45500	-2.92058	403.4	376.6	1	99	0
TAY 20	56.45985	-2.90103	771.8	674.8	1	89	10
TAY 21	56.46582	-2.89648	99.77	28.22	56	19	24
TAY 22	56.46188	-2.87425	683.7	537	7	42	51
TAY 26	56.46772	-2.80128	239.8	234.1	1	68	31
TAY 28	56.43693	-2.72646	329	238.4	0	100	0
TAY 29	56.40573	-2.78150	191.8	188.7	3	97	0
TAY 30	56.47152	-2.70528	225.9	208.1	0	100	0
TAY 32	56.37392	-2.79432	178.6	170.5	3	97	0
TAY 34	56.36707	-2.86882	777	629.6	3	82	15
TAY 35	56.36650	-2.85200	655.4	471.4	1	95	3
TAY 36	56.36405	-2.84183	192.4	190.8	8	92	0
TAY 37	56.36470	-2.82625	225.6	220.1	2	98	0
TAY 38	56.38083	-2.81605	565.8	330.9	1	96	3
TAY 39	56.44815	-2.72537	401.5	388.5	0	100	0
TAY 40	56.44770	-2.72553	369.9	357.8	0	100	0
TAY 41	56.44697	-2.77375	694	585.2	1	99	0
TAY 42	56.44650	-2.77393	858.7	788.1	0	100	0
TAY 43	56.39977	-3.08628	347.3	280.4	1	99	0
TAY 44	56.40865	-3.06808	190.7	183	2	98	0
TAY 45	56.42588	-3.04573	264	71.5	48	52	0
TAY 46	56.43618	-3.05427	183.6	178.1	7	93	0
TAY 47	56.44304	-3.06027	125	128.1	33	67	0
TAY 48	56.44843	-3.06600	122.2	117.2	34	66	0
TAY 49	56.41167	-3.08453	223	217.2	13	87	0
TAY 50	56.41765	-3.09013	176.6	170.7	5	95	0
TAY 51	56.42235	-3.09493	347.8	281.5	8	92	0
TAY 52	56.42725	-3.10120	133.1	135.1	30	70	0
TAY 53	56.43225	-3.10667	111.8	98.98	38	62	0

Table 4.1 *(continued)*

Sample Number	Latitude	Longitude	Mean	Median	Silt (%)	Sand (%)	Gravel (%)
TAY 54	56.39755	-3.12333	660.7	464	1	81	17
TAY 55	56.40255	-3.13080	188.5	188.6	14	86	0
TAY 56	56.40725	-3.13733	96.22	77.33	46	54	0
TAY 57	56.41196	-3.14387	105.8	95.44	42	58	0
TAY 58	56.37941	-3.18240	220.7	195.4	7	93	0
TAY 59	56.38186	-3.18587	134.2	129	29	71	0
TAY 60	56.38373	-3.18880	129.5	117.5	27	73	0
TAY 61	56.44767	-2.96287	312.9	302.7	0	100	0
TAY 62	56.37809	-3.16892	790.7	656.6	0	62	38
TAY 63	56.36218	-3.23395	61.38	35.57	71	29	0
TAY 64	56.35665	-3.26878	968.2	962.4	1	43	55
TAY 65	56.45000	-2.99968	192.3	174.9	3	97	0
TAY 70	56.36695	-2.84832	171.9	162	4	96	0
TAY 71	56.36750	-2.84835	157.9	154.3	0	100	0
TAY 72	56.36805	-2.84855	246.9	170.5	0	100	0
TAY 73	56.36888	-2.84893	188.2	175.6	0	100	0
TAY 74	56.36883	-2.84367	210.5	196.5	0	100	0
TAY 76	56.36842	-2.84282	1202	1178	0	47	53
TAY 77	56.36780	-2.84277	655	534	2	77	21
TAY 78	56.36740	-2.84283	749.2	594.6	3	37	60
TAY 79	56.36677	-2.84288	69.93	52.13	58	42	0
TAY 81	56.36768	-2.84495	81.42	24.86	74	26	0
TAY D11	56.47030	-2.83300	394.3	306.1	1	99	0
TAY D15	56.46868	-2.83122	730.2	564.4	1	99	0
TAY D16	56.46642	-2.82852	482	380.1	1	99	0
TAY D33	56.46448	-2.85877	236.7	226.5	3	97	0
TAY D36	56.46562	-2.85995	406.8	234.6	0	100	0
TAY D49	56.46802	-2.84662	235.8	225.5	0	100	0
TAY D57	56.45047	-3.06808	63.98	33.09	74	27	0
TAY D62	56.37027	-2.82475	306.9	288.8	0	100	0
TAY D64	56.37325	-2.83015	314.3	242	1	99	0
TAY D66	56.37497	-2.83297	450.2	302.9	1	90	9
TAY D70	56.36695	-2.84832	129.1	98.62	37	63	0
TAY D73	56.36888	-2.84893	243.2	236.4	5	95	0
TAY D87	56.36753	-2.86845	90.07	40.11	63	37	0

Table 4.1 *(continued)*

Sample Number	Latitude	Longitude	Mean	Median	Silt (%)	Sand (%)	Gravel (%)
TAY D97	56.36825	-2.86440	184	186.1	27	73	0
TAY D110	56.39672	-2.80942	246.7	235.3	0	100	0
TAY D111	56.39670	-2.80755	384	284.5	1	99	0
TAY D112	56.39673	-2.80453	306.1	214.2	0	100	0
TAY D115	56.38775	-2.80693	252.9	242.6	0	100	0
TAY D119	56.38773	-2.80280	231.5	216.2	0	100	0
TAY D124	56.38050	-2.81927	323.8	240.2	0	100	0
TAY D137	56.44780	-2.86805	369.4	269.9	3	97	0
TAY D140	56.45138	-2.86855	221.7	185.5	5	95	0
TAY D150	56.45075	-2.87512	187	105.1	35	65	0
TAY D167	56.45025	-2.85320	187	105.1	2	98	0
TAY D182	56.44253	-2.84757	206.7	200.5	3	97	0
TAY D200	56.36772	-3.18832	117.9	49.01	33	19	48
TAY D201	56.36767	-3.18813	68.74	29.41	71	29	0
TAY D202	56.37180	-3.18190	349.9	336	0	100	0

4.4 Infaunal analysis

To aid the process of biotope allocation, infaunal species abundance data from 149 stations were subjected to non-metric multidimensional scaling. Figure 4.11 shows the results after the exclusion of several outlier stations that were initially dominating the patterns in the data.

It can be seen that in general there is a strong relationship between biotope allocation and similarity in faunal composition. This relationship is much weaker, however, in the case of biotopes which often have highly impoverished faunas (eg **IGS.MobRS**, **LGS.AEur**). A striking feature of the whole data set was the low species diversity of the biotopes. Although the abundances of 135 taxa in total were recorded, only 20 of the 149 samples contained more than 10 species, the maximum of 26 being found at one of the **IGS.Lcon** stations. The full species abundance data set is given in Table 4 (Appendix 1).

4.5 Satellite results

4.5.1 Mapping overall sediment distribution

The geocorrected TM image from 17.07.2000 that was masked to the SAC boundary is shown in Figure 4.12. This has been contrast stretched only on the water pixels and illustrates well, the variations in sediment colour, reflecting both sediment type and habitat. The clear differences in water colour are also evident from the brown turbid waters at the headwaters of the estuary to the clearer waters of St Andrews Bay. The estuary has the greatest freshwater input of any British estuary being fed by the rivers Tay and Earn. The source of these rivers means that a large amount of sediment enters the estuary. It has been estimated that the amount

Figure 4.11 Multidimensional scaling analysis of infaunal species abundance data. Labels indicate the station code and symbols the allocated biotope

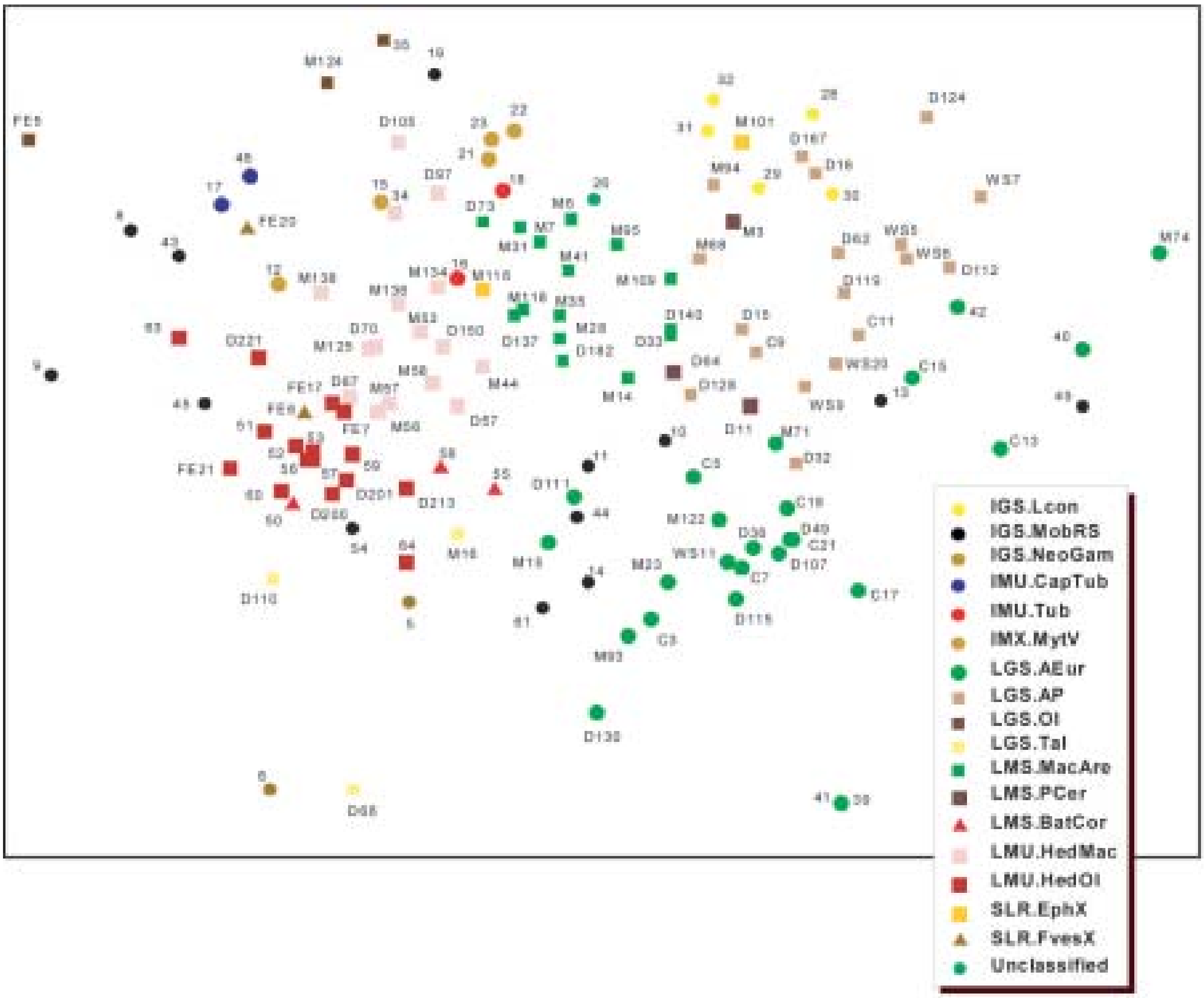

of sediment to enter the estuary varies between 646,000 tons in a dry year and 1,648,000 tons in an average year (Charlton, 1980). Of this load 3-5% of the total solids are carried as bed load and up to 85% as suspended load. As well as the sediment being brought in from freshwater sources a considerable amount of material is deposited in the estuarine channel from the sea, coming from long-shore drift in both northerly and southerly directions from St Andrews Bay and Gaa Sands, respectively. This map also shows that the shape of the sand banks has changed considerably in the inner estuary compared to the SAC sandbank map, derived from OS map data.

Band 2 (green waveband) raw brightness values in the masked image were density sliced to show variations in visible sediment brightness (Figure 4.13). Colours vary from purples and blues indicating inundated areas through green, yellow and red indicating increasing sediment brightness. It is clear that the variation in brightness of the sediments reflects the size of the particles making them up. The density slice is thus a crude form of classification of sediment particle size distribution. The image thus shows larger, brighter particles on the sandbanks at the mouth of the estuary and on the edges of the mud flats declining to the darker, smaller particles further up the estuary and at the boundary of the mud flats and dry land, reflecting the hydrodynamics operating in the estuary.

Figure 4.12 Masked Landsat 7 TM image over Tay Estuary, 17.07.00, displayed as a true colour composite

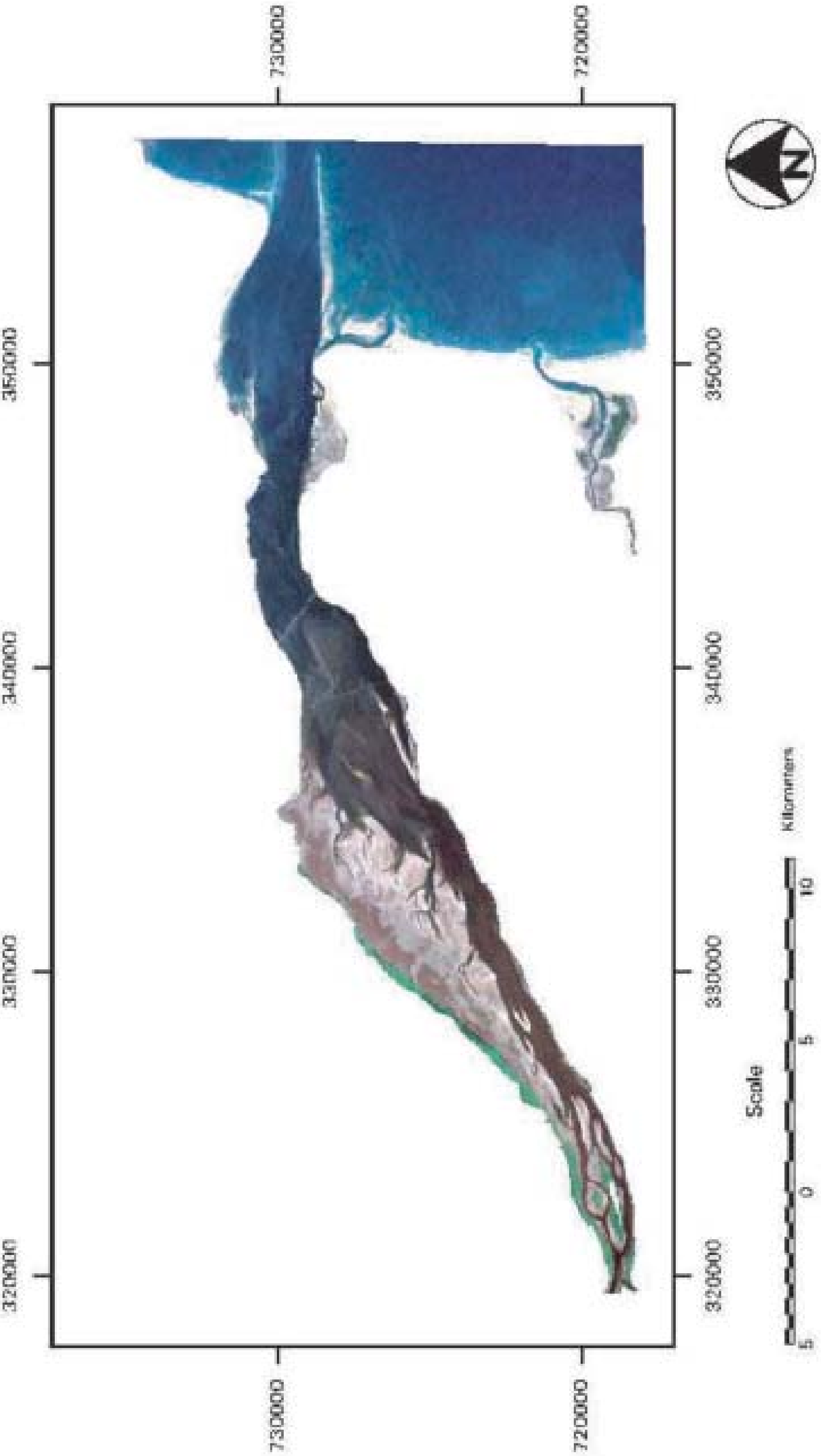

Figure 4.13 Masked Landsat 7 TM image over Tay Estuary, 17.07.00, density sliced to show variations in sediment brightness

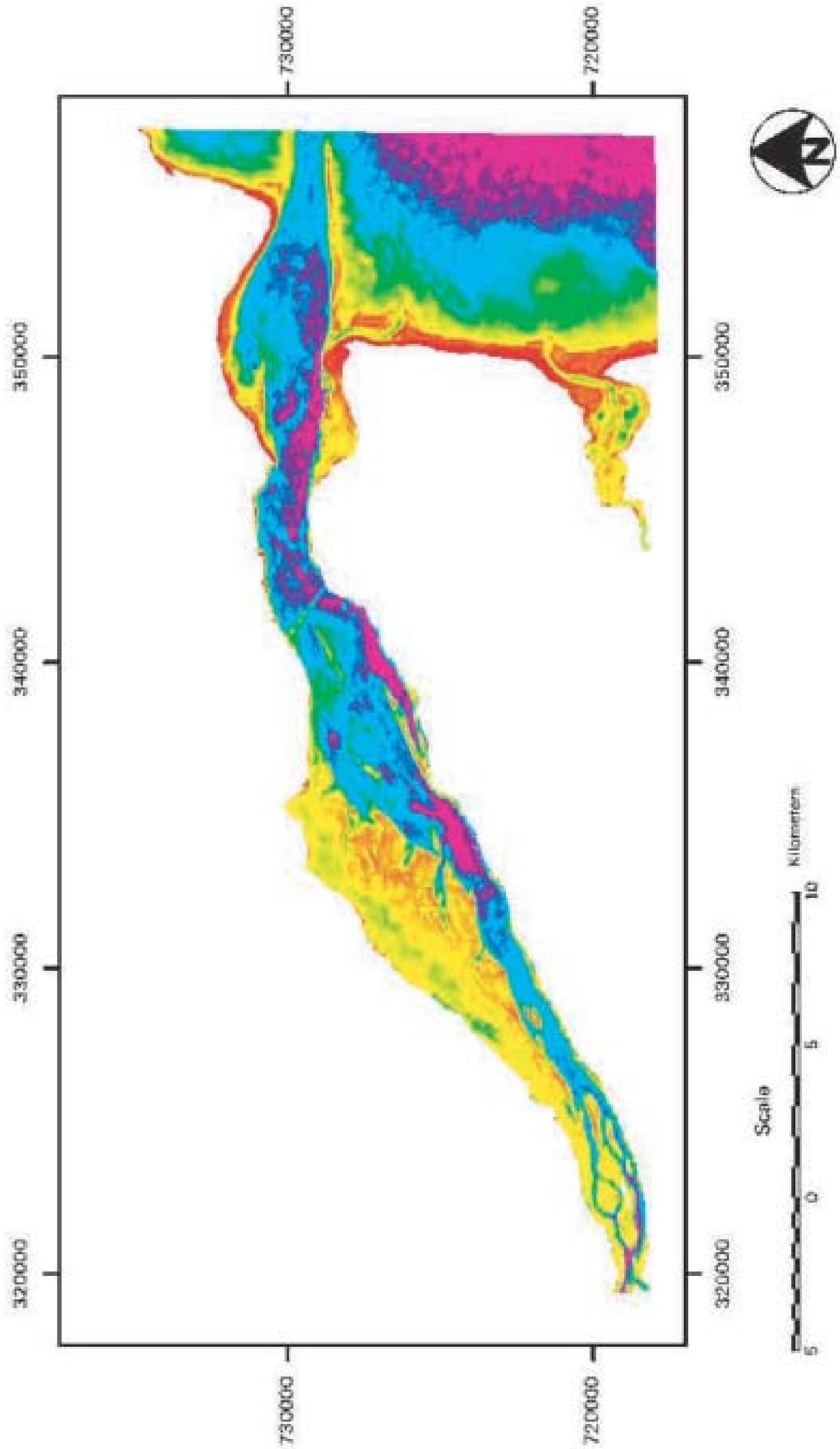

4.5.2 Classification of sediment types in the QuickBird imagery

A supervised classification was performed on the land-masked, atmospherically corrected QuickBird Tay Part 1 image as shown in Figure 3.15. The image was first overlaid with the sample point ID's and locations from the Heriot Watt and SNH field surveys. The biotope polygons produced from the manual interpolation undertaken by the Heriot Watt team were also overlaid. Training areas for each biotope were placed within each polygon and located in homogeneous areas close to actual measurement sites to ensure the correct spectral signatures were chosen. To account for potential variations in spectral signatures, mainly due to variations in wetness of the different habitats, multiple training areas for each biotope class were defined. In total, 249 training sites were defined in a total of 26 biotope classes identified as present in the Part 1 image (NB. the actual number of biotopes for the whole SAC is larger, including habitats only found further up the Tay Estuary).

A maximum-likelihood supervised classification was then performed on the imagery. From the result the individual sub-classes resulting out of the multiple training areas were amalgamated and a median and majority filter passed over the classification to produce a map of 26 classified biotope zones (Figures 4.14 and 4.15). The colour scheme adopted differs from the manually interpreted biotope map, because, as this is a raster map, only solid colours (ie without stippling) can be used.

Figure 4.14 Biotope distributions identified after multispectral classification of the QuickBird dataset. North section

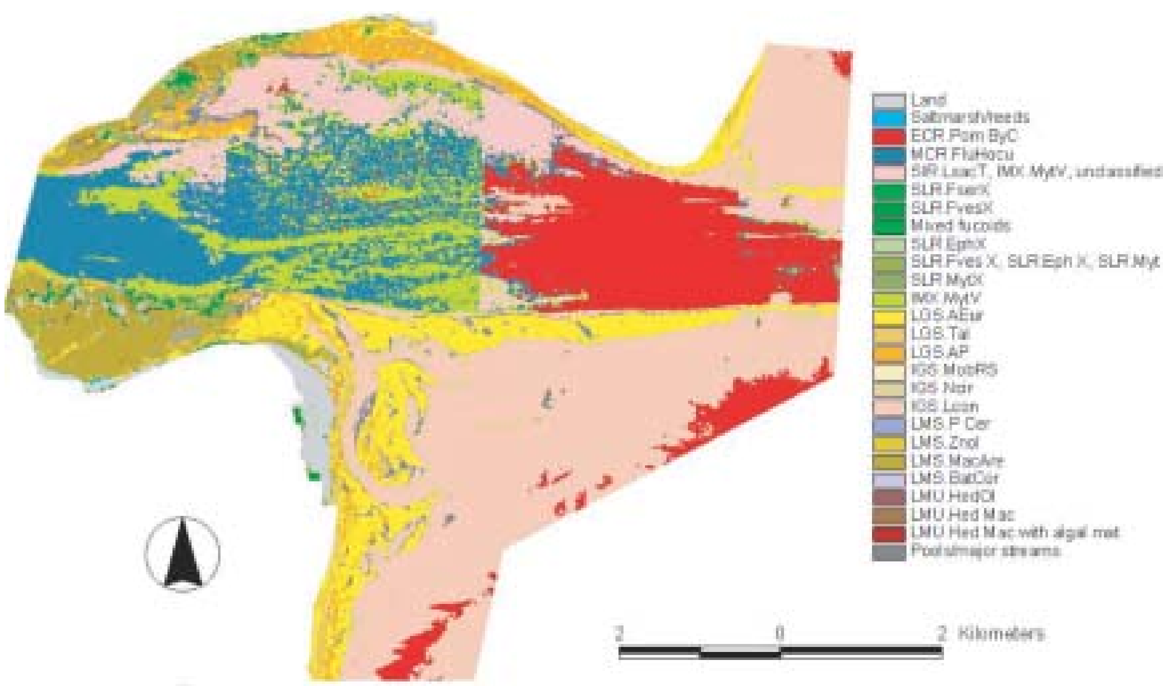

Overall, the distribution of biotopes matches the general distribution shown in the manual interpretation. However, the automatic classification shows considerably greater complexity to biotope structure than the manually interpreted version. Whilst some of this may arise out of confusion between the spectral characteristics of different biotopes, a great deal of the complexity is considered to be real.

Figure 4.15 Biotope distributions identified after multispectral classification of the QuickBird dataset. South section

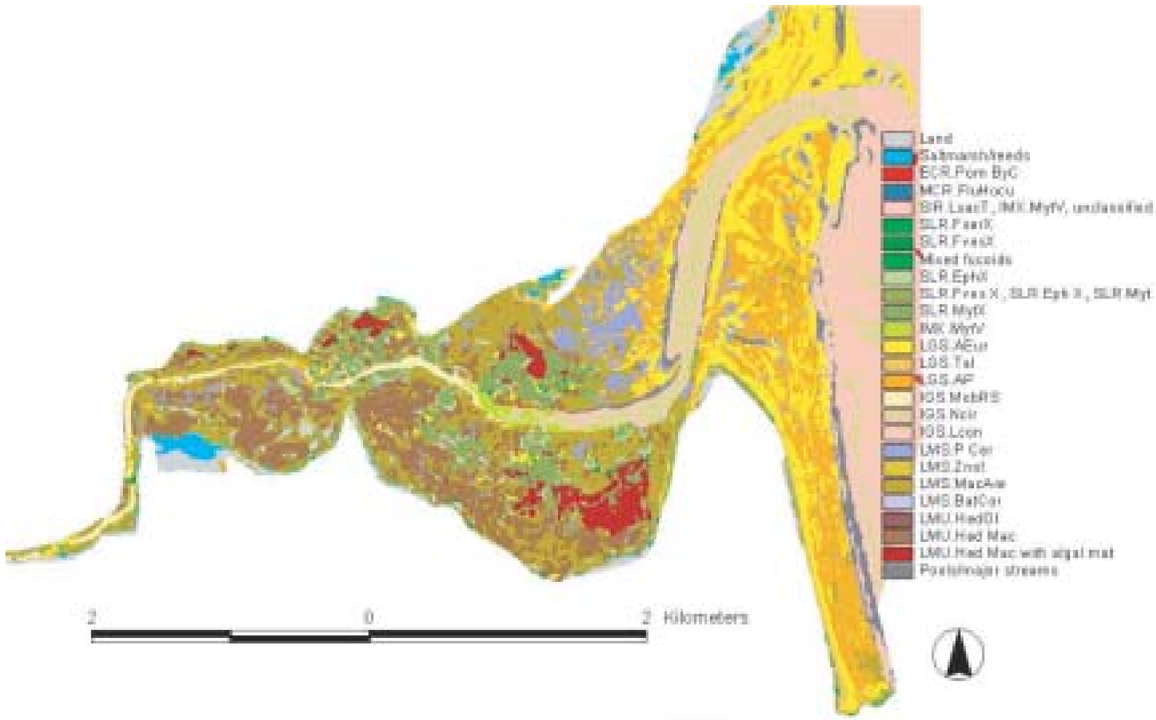

Factors that contribute to the confusion of different biotope zones include that the classification itself is achieved on the basis of spectral data alone and that only four wavebands are available on which to perform the classification. Furthermore, the signatures of some target biotope types may be spectrally similar. This problem is exacerbated in areas of deepwater, where the effects of the water column mask reflectance signals from the bottom substrate. Areas of *Enteromorpha* and mussel beds have been well delineated. On the other hand, areas of exposed sand along Tentsmuir Beach are perhaps overclassified in structural terms. It is apparent what the classification is detecting major variations in sand moisture content. *Zostera* beds have probably also been overclassified, on the basis that as the beds are so sparse, their spectral signature is most likely not that different from surrounding mudflat areas. The line of marked change in class which occurs in the northern section (Figure 4.14) at the mouth of the estuary is the result of broad vertical banding present in the original data. Although not confirmed, it is thought this banding is induced in the imagery as a result of the acquisition process, perhaps reflecting the use of different sets of detectors used to obtained different parts of the image. The use of multiple sets of detectors may be required to meet the demands of the high resolution required.

5 DATA INTEGRATION

5.1 Sedimentary structures

From an analysis of the bathymetric sidescan depth data and the sidescan images maps of sedimentary structures have been derived. The limit in resolution of depth measurements of the bathymetric sidescan is 0.5m thus it is possible to record individual sand waves with amplitudes of 1m. These waves typically have wavelengths of 5–10m. On the sidescan sonar records, sand waves and ripples with wavelengths of less than 5m were visible often as features that were superimposed on the larger sandwaves. However, it was not possible to make quantitative evaluations of the amplitudes of these ripples. Furthermore, these features were not consistently recorded in adjacent sidescan passes when the passes were separated by some hours or more. It is suggested that features of this scale are transitory and migrate throughout the tidal cycle. The sedimentary structure map for the Tay Estuary is shown in Figure 5.1. Four categories of sedimentary feature can be recognised from the acoustic data. These categories include three where sandwaves can be quantified into ranges with small waves showing amplitudes of between 1–2m and wavelengths of 10–30m, medium waves showing amplitudes of between 2–4m and wavelengths of 30–100m and large waves with amplitudes greater than 4m and wavelengths of 100–300m. The type of waves are also subdivided into those that are ebb dominated and those that are flood dominated. One additional category is recognised from the data. Plain conditions describes those areas where some sand ripples were mapped inconsistently with the sidescan sonar but also describes areas where no sedimentary features were recorded with the acoustic techniques (referred to in the figure as "sub-bathy"). In many of these areas it is difficult to determine the grain size of particles where no groundtruth information is available and thus the areas could contain both fine-grained smooth mud flats and areas where there are large grain sizes and rough conditions with patchy mussel beds. For a more complete discrimination of these areas, further high-resolution acoustic surveying and groundtruth sampling is recommended. Where groundtruth information is available, zones have been discriminated on grain size. It is worth noting, however, that it is not possible to discriminate between areas of pebbles, cobbles and boulders and areas of either dead or alive mussel assemblages. Furthermore, the acoustic signature of these areas is often influenced by a cushion of sponges and soft-textured star fish. These cause a reduction in reflection strength of acoustic signatures and make for inconsistent interpretations with the biological mapping.

The larger sedimentary features in the cSAC are seen within the Tay Estuary where the strongest current activity is recorded. In the Tay the maximum currents have been recorded along the central (navigation) channel with velocities up to $2ms^{-1}$ noted on spring tides (Neill *et al.*, 2000). It is also along this channel that the more significant bedforms are seen. The channel contains sandwaves with amplitudes greater than 5m, however, the sand banks to north and south for the most part show features with amplitudes less than 1m. To the west of the Tay rail bridge, the channel bed also shows small sand waves with the amplitudes generally diminishing to the west. Interestingly, the area of largest sand waves is not correlated with the deepest part of the survey area in the main Tay channel to the south of Broughty Ferry. Rather this area contains small to medium sandwaves. It is has been shown that this area contains some of the strongest current activity on both the ebb and the flood tides and it is postulated that this, together with its position at a convergence zone for tailed axially convergent fronts on the flooding tide, results in the over-deepening of the channel and a lack of large stable bedforms. The largest sand waves are seen to the west of this location in a water depth of 8–15m.

An additional feature of the sandwaves that are recorded by the bathymetric sidescan is their symmetry and asymmetry. This can be clearly seen in the cross-sections in Appendix B. All of the measurable waves to the east of the Tay road bridge in the central channel are asymmetric with lee slopes (steep slope angles) facing the west and stoss slopes (gentle slope angles) facing the east. This indicates that they are dominantly formed by the flooding tide. In contrast, to the north of the main channel the sandwaves on the large shallow areas are in general symmetric. To the south of the main channel between the road bridge and Tayport the large shallow area is dominated by asymmetric waves with an ebb or river flow direction. Between the two bridges the sandwaves are symmetric with occasional zones of asymmetric waves with the opposite sense of direction, i.e. ebb or river dominated near the north and south shore. To the west of the rail bridge the sandwaves become dominantly asymmetric indicating ebb tides and the strong current flow from the Tay River. This change in sedimentary conditions noted at the Tay road bridge is marked not only in the nature of sedimentary structures but also in the overall bathymetry. In addition, significant scour exists around many of the bridge pillars. Whether these changes in the sedimentary system have been caused by the presence of the bridges, or more likely that the bridges just represents a significant point in the estuary where necking of the channel causes significant sediment deposition is unclear from the present study. However, a review of historical charts (Buller and McManus, 1971) would suggest that the estuary is perhaps silting-up and that the next stage of this process is a general filling between the bridges. If this is the case then it is likely that the Middle Bank will become a more established feature protecting shallow mud flats behind. The nature of the sedimentary features and the strong frontal systems in the estuary are discussed in further detail in section 6.

A broad summary map of acoustic data is shown in Figure 5.2. This has been constructed based on the AGDS line track data, the bathymetric sidescan bathymetry data and the sidescan images for acoustic boundaries. The map represents a combination of acoustic responses from not only the reflection strength variations due to micro features such as sediment particle size but also to macro features such as biology and to a certain extent the sedimentary structures. Broad categories of grain size equivalent predicted ranges are given for three acoustic classes. However, to fully appreciate the complexity of sediment types in the area it is necessary to combine both maps together thus giving a map of broad sediment grain size ranges and sedimentary structures. This is presented in Figure 5.3 where 15 acoustic categories have been interpreted with increasing grain size and increasing size of sedimentary feature. A comparison of the measured particle grain size ranges for individual sample points that coincide with the acoustic survey is given in Figure 5.4. This figure shows the division of the acoustic classes based on grain size and sediment feature type.

Figure 5.1 Sedimentary features interpreted from the bathymetric sidescan bathymetry map and sidescan images for the Tay Estuary

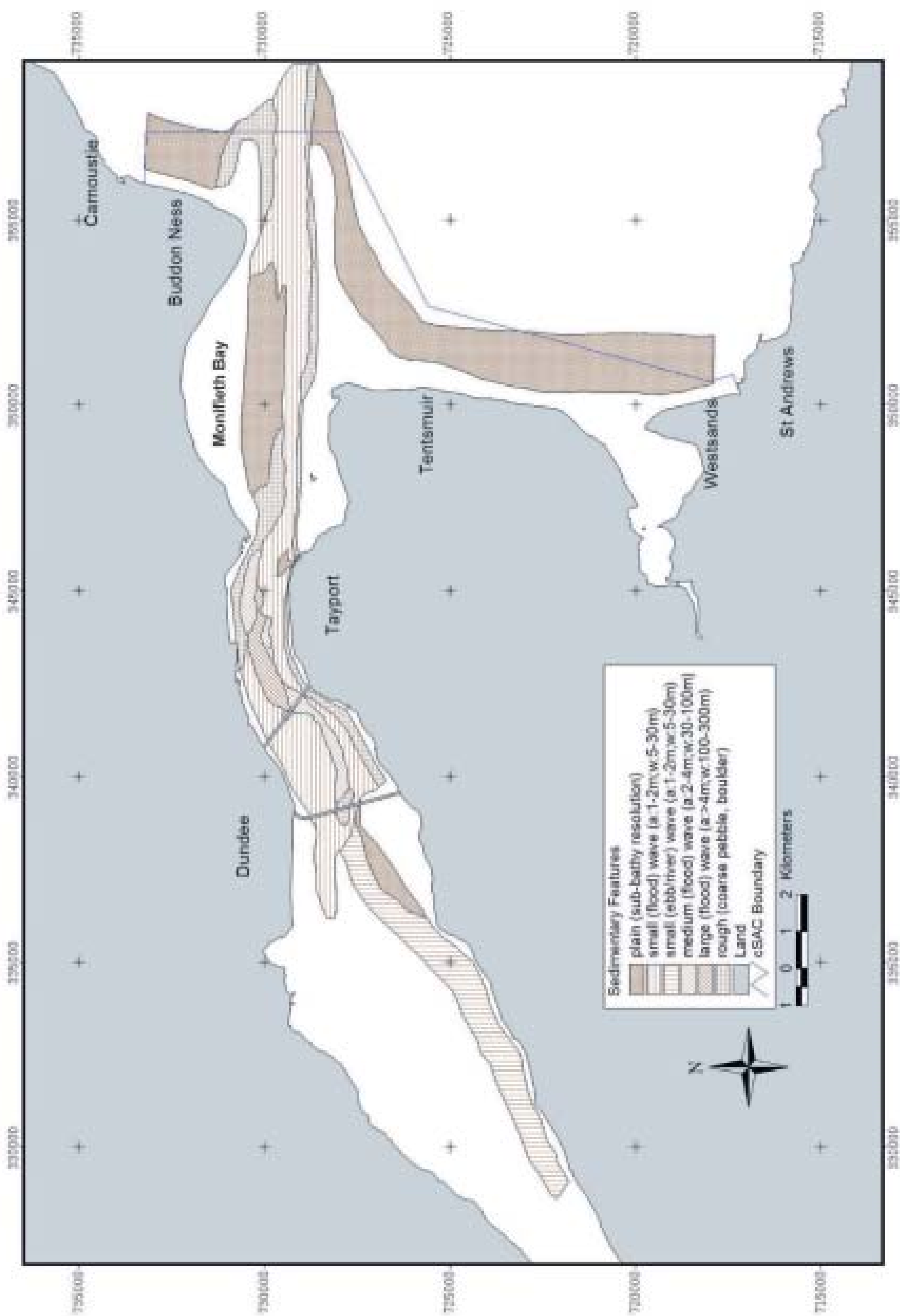

Figure 5.2 Acoustic class interpreted from the bathymetric sidescan, AGDS and sidescan images for the Tay Estuary

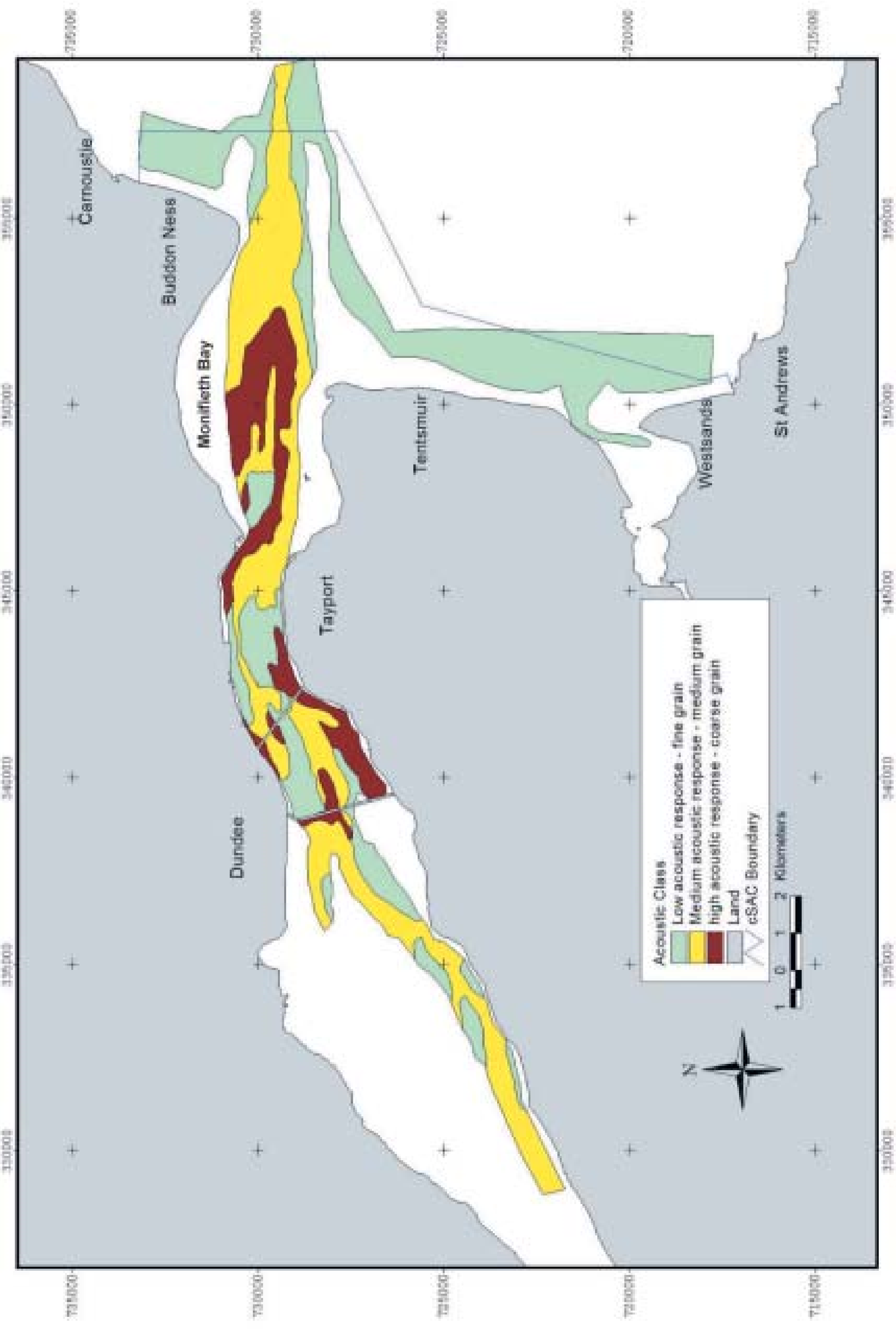

Figure 5.3 Combined sedimentary feature interpretation for the Tay Estuary from acoustic techniques

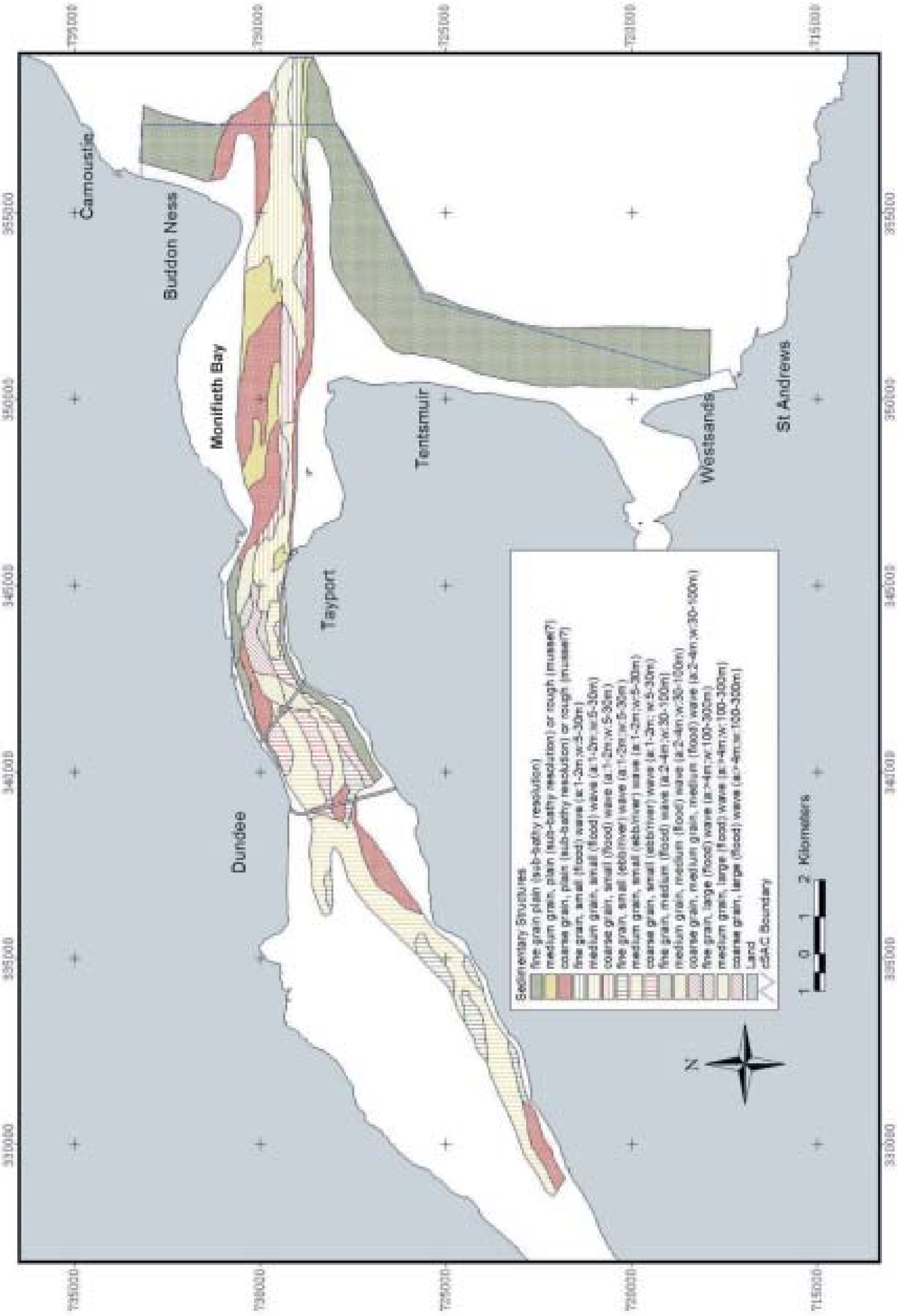

Figure 5.4 Sediment particle grain size and sedimentary structures. Sediment grain size ranges fine <0.250mm, medium 0.250–0.500mm, coarse >0.500mm; a – amplitude of sandwaves; w – wavelength of sandwaves

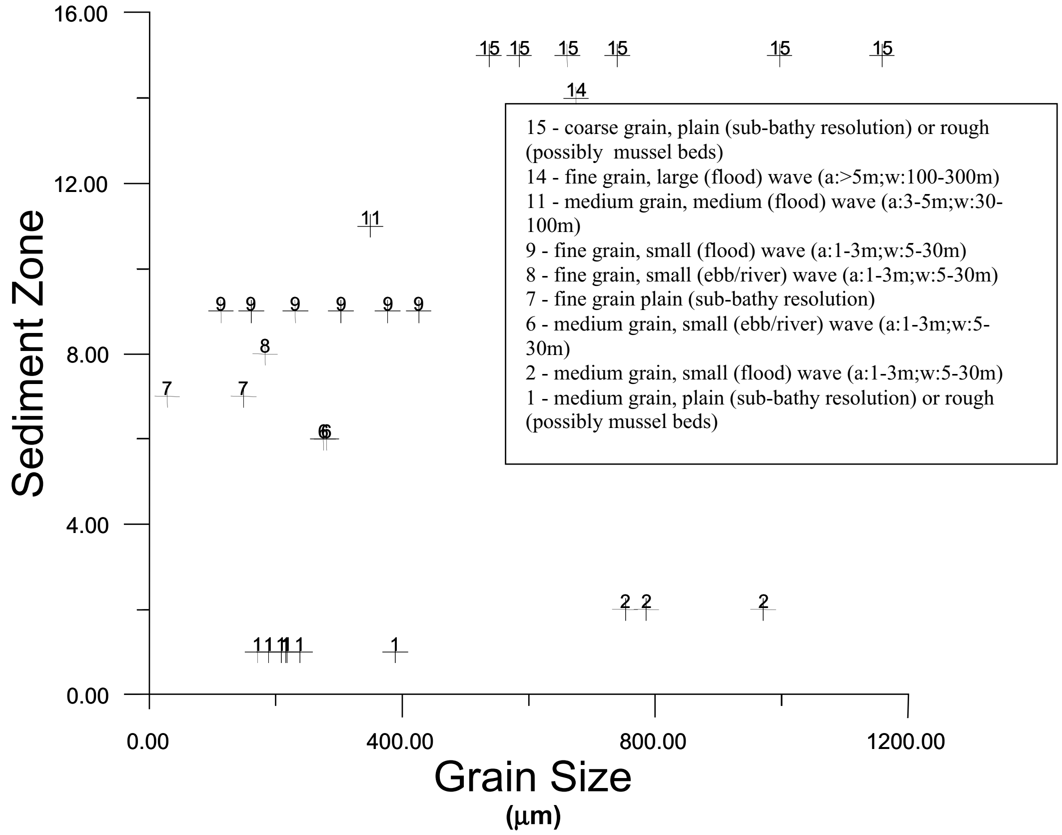

5.2 The distribution of biotopes

5.2.1 Inner Tay: Earn/Tay confluence to Invergowrie/Balmerino *(Figure 5.5)*

The salinity regime in this region of the Tay is characteristic of the upper reaches of estuaries, varying in range from 0.2–21‰ at Balmerino to 0–0.02‰ at Newburgh (Buller *et al*., 1972). Strong currents in the main channel have resulted in coarse and mobile substrates, generally of medium-coarse sand, gravel and pebbles, supplemented in places by cobbles and boulders.

From the mouth of the Earn to the broadening of the estuary at Port Allen/Ballinbreich the coarse channel sediments harbour a species-poor community of amphipods (*Gammarus* spp., *Corophium multisetosum*), oligochaetes and a number of freshwater forms, such as caddis and dipteran larvae (IGS.NeoGam). Large numbers of flounders were collected in the dredge in this area. Below Ballinbreich the freshwater fauna is largely lost and the predominantly coarse sediments are dominated by mobile crustaceans (*Bathyporeia* spp., *Haustorius arenarius*, *Eurydice pulchra*, *Gammarus* spp. and *Crangon crangon*) and the polychaete, *Marenzelleria viridis* (IGS.MobRS).

The river channel runs close to the southern coastline throughout most of this region with extensive sediment flats to the north and steeper, mixed shores to the south. The shores are backed by saltmarsh and reedbeds which cover an extensive area on the north shore from the Earn to Kingoodie but are in the form of narrow broken ribbons along the southern shore. The northern flats consist predominantly of muddy sand becoming coarser towards the river channel and muddier on the upper shore. Over much of this area the muddier sediments harbour a fauna of low diversity, strongly dominated by *Corophium* (both *C. multisetosum* and *C. volutator*) and *Hediste diversicolor*, although *Hediste* is replaced by oligochaetes in the muddier shores upstream of Port Allen (**LMU.HedOl**). In the clean and slightly muddy sands subject to stronger tidal action adjacent to the river channel *H. diversicolor* is lost and amphipods become dominant, especially *Bathyporeia* spp and, in lower numbers, *Corophium* spp. and *Haustorius arenarius* (**LMS.BatCor**). The mobile sandbanks in this region have been allocated to the same biotope, although the amphipods may be accompanied by *Eurydice pulchra*. In fact the infauna of these sandbanks is little different from that of the adjacent sublittoral (**IGS.MobRS**).

Species richness is elevated in the higher salinity conditions off Invergowrie where the basic *Hediste-Corophium* community characteristic of muddy sediments higher up the estuary is supplemented by abundant populations of several polychaetes (eg *Marenzelleria viridis*, *Pygospio elegans*, *Capitella capitata*, *Eteone longa*) and the bivalve mollusc, *Macoma balthica* (**LMU.HedMac**). The mudflat at Kingoodie is backed by a belt of cobbles and boulders dominated by *Fucus vesiculosus* with occasional *Ascophyllum nodosum* (**SLR.FvesX**).

The southern bank of the inner estuary is far steeper and more heterogeneous than the northern flats. At the western limit of the SAC the shore is composed of a very narrow band of soft mud, in places with gravel (**LMU.HedOl**), backed by reed beds, interrupted at Newburgh by stone walls and quays. Below Newburgh to Balmerino there are mixed shores of mud and sand populated by oligochaetes and *Hediste diversicolor* and both *Corophium multisetosum* and *C. volutator* (**LMU.HedOl**) and banks of gravel, pebbles and cobbles on the upper shore supporting *Enteromorpha* sp. and oligochaetes (**LGS.Ol**). These two biotopes have been mapped together as 'Mixed oligochaetes'. From about 1km west of Flisk Point to Balmerino these biotopes continue but are accompanied by patchy *Fucus vesiculosus* on cobbles and boulders on the middle shore (**SLR.FvesX**). The three-biotope complex has been mapped as 'Mixed oligochaetes with FvesX'.

5.2.2 Middle Tay: Invergowrie/Balmerino to Broughty Ferry/Tayport *(Figure 5.6)*

Between Invergowrie and Broughty Ferry the estuary decreases in width leaving only relatively narrow intertidal areas. The salinity range off Newport is 6–30‰ and off Tayport is 11–32‰. Subtidal sediments are predominantly highly mobile medium and coarse sands with an impoverished fauna of small crustaceans (*Gastrosaccus spinifer, Eurydice pulchra, Haustorius arenarius*). This **IGS.MobRS** biotope is also found on the mobile clean medium sand of Middle Bank. The dredge revealed a scattered epifauna of *Carcinus maenas* and several fish, including the smelt, *Osmerus eperlanus*, the greater pipe-fish, *Syngnathus acus* and juvenile gobies, *Pomatoschistus* sp., and the lesser sand eel, *Ammodytes tobianus*.

Just off the northern and southern shores, out of the path of the strongest currents, the sediments become basically muddy sands with a much richer fauna dominated by tubificid oligochaetes and polychaetes such as *Scoloplos armiger, Pygospio elegans* and capitellids (**IMU.Tub**). Mussels, *Mytilus edulis*, are scattered throughout this area and form beds (**IMX.MytV**) on both northern and southern margins. However, the spatial extent of living mussel beds is difficult to determine due to the widespread presence of dead shells and pebbles, which fail to produce a distinctively different AGDS signature. A mussel bed is also present beneath the railway bridge. This may have initially become established on andesite ballast tipped between some of the piers to counteract scouring (Buller and McManus, 1975).

In the shallow sublittoral off Dundee airport there is a region of fine-medium sands apparently influenced by organic pollution from the Invergowrie Burn (Jones *et al.*, 1989). The community here is dominated by *Capitella capitata*, together with abundant populations of the polychaetes, *Marenzelleria viridis, Pygospio elegans*, and oligochaetes (**IMU.CapTub**).

Littoral biotopes in this region reflect the higher salinities experienced here than higher up the estuary. On the southern coastline Balmerino marks the appearance of *Ascophyllum nodosum* and a transition from the **IMU.HedOl** to the **IMU.HedMac** biotope in areas of muddy sediment. From Balmerino to Tayport the upper and middle shores are composed of very mixed substrates (bedrock outcrops, boulders, cobbles and pebbles) with a mixture of fucoid biotopes, especially **SLR.Asc**, **SLR.AscX**, **SLR.FvesX**, **SLR.Fspi** and **SLR.Pel**. A shingle band is also often present on the upper shore (**LGS.Ol**). Over much of this area from Balmerino to just east of the road bridge these hard substrates give way to muddy sediments at the bottom of the shore (**LMU.HedMac**). East of this region the lower shore sediments are predominantly slightly silty sand (**LMS.MacAre**) with some areas of clean sand just west of Tayport harbour (**LGS.AEur**).

Along the northern shoreline the muddy sand flats of Invergowrie Bay (**IMU.HedMac**) become progressively sandier passing eastwards alongside the airfield, where Bell (1998) recorded abundant lugworms, *Arenicola marina*, in fine sandy sediments on My Lord's Bank (**LMS.MacAre**). The lower shore sediments off the airport and the Dundee seafront to the road bridge are backed by a stone seawall, often with cobbles and boulders at the base, which supports a sequence of narrow bands of lichen and fucoid biotopes (**LR.YG**, **SLR.Pel**, **SLR.Fspi**, **SLR.Asc** and **SLR.AscVS**). Between the road bridge and Stannergate natural shores are completely replaced by the vertical stone and wood wharfs of Dundee docks. Beyond Stannergate to Broughty Ferry beaches return and are composed largely of pebbles and cobbles overlying finer sediments (mapped as shingle/cobble beaches). An upper band of shingle (**LGS.Tal** and **LGS.Ol**) is followed by a belt of *Enteromorpha* sp. and *Porphyra* sp. on cobbles and pebbles (**SLR.EphX**). On the lower shore *Fucus vesiculosus* is present on pebbles, cobbles and small boulders over muddy and sandy sediments (**SLR.FvesX**). Patches of sand are also present (**LGS.AEur**, **LMS.MacAre**) and, in the protection of Broughty Ferry harbour, muddy sand (**LMS.MacAre**).

5.2.3 Outer Tay *(Figures 5.7, 5.8)*

The salinity conditions in the outer Tay range from 11–32‰ off Tayport to virtually fully marine conditions off Buddon Ness (32–33‰). Between Tayport and the eastern limit of the SAC at the mouth of the Tay the sea bed is floored predominantly by mixed coarse material of pebbles, cobbles and mussels. Within this area is a mixture of biotopes which unfortunately do not provide distinctive acoustic signatures and so the biotope mapping in this area is unlikely to reflect the detailed biotope heterogeneity and precise biotope boundary positions.

Mussel beds (**IMX.MytV**) occur widely, lining the southern margin of the main channel from Tayport to Tentsmuir Point (McManus *et al.*, 1980) and along the northern margin (Figure 5.7). ROV footage shows the mussels provide an unbroken carpet over extensive areas of the sea bed, including within the channel where it shallows at Lady Shoal. Other conspicuous epifauna includes *Asterias rubens*, which covers 50% of the mussel carpet over large areas, *Carcinus maenas* and the butterfish, *Pholis gunnellus*.

Within the main channel off Tayport Beach and on Lady Bank the pebbles and cobbles have a luxuriant turf of hydroids and sponges. *Halichondria panicea* is the dominant sponge but *Haliclona oculata* is also common off Tayport Beach (MCR.Flu.Hocu). At the eastern extremity of the SAC off Buddon Ness in presumably more dynamic sea bed conditions the soft faunal turf on the cobbles and pebbles is largely replaced by an epifauna dominated by hard calcareous forms, especially *Balanus crenatus, Pomatoceros triqueter* and bryozoan crusts (ECR.PomByC).

The sea bed of Monifieth Bay is composed of a patchy mixture of fine-medium sands and areas of pebbles, cobbles and boulders. There are also a number of scattered mussel beds (IMX.MytV) resulting from the seeding of spat by local fishermen (McManus *et al.*, 1980). The boulders support a flora of the kelp *Laminaria saccharina* with an understorey of foliose red algae and *Halichondria panicea* (SIR.LsacT). From the ROV footage and grab sampling it proved impossible to ascribe the sedimentary areas to a biotope. The fauna has characteristics of MCR.Flu.Hocu, IMX.MytV and IGS.Lcon, all of which occur extensively in the vicinity.

The eastern fringe of the SAC to the north and south of the mouth of the Tay is floored by fine-medium rippled sands in shallow water (<10m), which support dense populations of *Lanice conchilega* (IGS.Lcon).

5.2.4 Monifieth Sands *(Figures 5.7, 5.9)*

Monifieth Sands consists of a large expanse of fine – medium sand up to 1km in width extending from Broughty Ferry to the mouth of the Buddon Burn. No bedrock was observed on the beach but there are scattered patches of pebbles, cobbles and boulders lying on the sand, the major occurrences being 1km east of Broughty Castle, off Balmossie and Monifieth railway stations and near the mouth of the Buddon Burn. The biotope of these areas is principally SLR.FvesX, although there are some patches of cobbles and pebbles dominated by *Enteromorpha* sp. and *Porphyra* sp. in these areas and in bands near the top of the shore (SLR.EphX). Mussels, *Mytilus edulis*, often occur amongst the *Fucus* but form the dominant constituent towards the lower margin of three of the major pebble/cobble areas (SLR.MytX) and in isolated pockets at the bottom of the shore. Visits to the shore in August and December 2002 and comparisons of satellite images taken in July 2002 with aerial photographs from 1999 reveal that this is a region of high temporal change, particularly with respect to the coverage by rocky substrata.

Coarser sediments of predominantly medium sands are found to the east of the region and on the lower shore in the west, probably reflecting the gradients in wave and current exposure. Where these sediments retain a high water content they are dominated by a polychaete infauna with occasional bivalve molluscs such as *Angulus tenuis* and *Cerastoderma edule* (LGS.AP). The other major sedimentary biotope in this area is found in regions of silty sand on the western side of the bay, where *Arenicola marina* is common – superabundant and *Macoma balthica* common (LMS.MacAre). This biotope is modified by the presence of patches of the eelgrass, *Zostera noltii* (with overall coverage of approximately 5–10%) in an upper shore band off Broughty Ferry (LMS.Znol). LMS.Znol is also found in shallow pools on the midshore. Throughout most of this region the shore is backed by well-drained sand supporting parallel bands dominated by *Eurydice pulchra* and *Bathyporeia* spp. (LGS.AEur) and *talitrid amphipods* (LGS.Tal).

East of the Buddon Burn the beach continues as the more exposed Barry Sands, where most of the middle and lower shore is formed into sand waves. From the Buddon Burn for a distance of about 2.5km the waves run obliquely across the shore with a wavelength of around 40m. The waves are composed mainly of moist (crests) or waterlogged (troughs) medium sand supporting a polychaete-dominated infauna (LGS.AP.P), although a few of the higher waves provide the same dry habitat for amphipods and isopods (*Eurydice* *pulchra, Bathyporeia* spp.) that is found along the upper shore (LGS.AEur). Towards Buddon Ness the wave form becomes parallel to the shoreline and the LGS.AEur biotope occupies most of the shore, even in the lows of damp sand. LGS.AP is represented by a very low diversity infauna in fine – medium sands along the lower margin of the shore, with *Bathyporeia pelagica, Scolelepis squamata* and *Nepthys cirrosa* as the dominant taxa.

5.2.5 Tayport Beach *(Figure 5.10)*

Tayport Beach is an extensive embayment stretching eastwards from Tayport Harbour to Tentsmuir Point. It is composed predominantly of slightly silty fine sand that contains abundant populations of *Arenicola marina* and *Macoma balthica* (LMS.MacAre). *Zostera noltii* is widely distributed on these slightly silty sands reaching 40% coverage in a small area near the top of the shore on the eastern side (LMS.Znol). Elsewhere it is generally at much lower density (<10% cover) and is patchily distributed and does not therefore present a discernible satellite signature. Consequently, the individual records of this biotope are shown on the map. Green (1975) only recorded *Zostera* sp. from the western side of the beach. In the more wave sheltered areas of the beach *Corophium volutator*, and often *Hediste diversicolor*, becomes abundant in generally muddier sands (LMU.HedMac.Are).

In the more mobile clean sand of Tentsmuir Point, Green (1975) failed to find any macrofauna below MHWS, although Khayrallah and Jones (1980) recorded the presence of the amphipod, *Bathyporeia pilosa*, in this area (LGS.AEur).

Rock substrates on Tayport Beach are chiefly represented by extensive banks of pebbles, gravel and cobbles, occasionally with boulders, distributed along the lower shore. This provides a substrate for a complex mosaic of biotopes, which have been mapped collectively in Figure 5.10. The predominant biotopes are dominated by *Fucus vesiculosus* (SLR.FvesX), *Enteromorpha* sp. (SLR.EphX) and mussels (SLR.MytX), the latter spilling onto adjacent mudflats. Clear patches of sand occur between the banks (LMS.MacAre, LGS.AP, LGS.Lan).

At the top of the shore hard substrata are largely restricted to the western end of the beach, which is backed by a seawall supporting a range of fucoid biotopes and a belt of boulders, cobbles and pebbles (principally SLR.FvesX and SLR.EphX).

5.2.6 Tentsmuir Beach, Abertay Sands and West Sands *(Figures 5.7, 5.8)*

Tentsmuir Beach stretches from Tentsmuir Point to the mouth of the Eden Estuary and is composed of highly mobile fine – medium sands, backed by sand dunes. Most of the intertidal area is populated by a low diversity fauna of mobile crustaceans (especially *Eurydice pulchra, Bathyporeia sarsi* and *Haustorius arenarius*) with the polychaete, *Scolelepis squamata*, sometimes present (LGS.AEur). Abertay Sands has a similar fauna, with the addition of the amphipods, *Pontocrates* spp.

A narrow fringe of damp sand at the bottom of Tentsmuir Beach supports a richer fauna of polychaetes, especially *Nepthys cirrosa*, amphipods, such as *Bathyporeia pelagica* and *Pontocrates altamarinus*, and the bivalve molluscs, *Angulus tenuis* and *Donax vittatus* (LGS.AP.Pon).

West Sands beach extends from the mouth of the Eden Estuary southwards to St Andrews and is composed of fine sand formed into a series of sand waves running parallel to the coastline. This beach is more sheltered from wave action than Tentsmuir Beach and has a much richer infaunal community. Although polychaetes such as *Nepthys cirrosa* and *Spiophanes bombyx* are common, the lower shore is dominated by amphipods, particularly *Bathyporeia pelagica* and *Pontocrates altamarinus*, and the bivalve molluscs, *Angulus tenuis* and *Donax vittatus* (LGS.AP.Pon). A polychaete-dominated fauna is found above this with *Nephtys cirrosa* and *Scolelepis squamata* common and *Arenicola marina* widely present and locally abundant (LGS.AP.P).

5.2.7 Eden Estuary *(Figures 5.8, 5.11)*

For descriptive purposes the estuary can be usefully divided into an inner section, consisting of the narrow channel upstream of Guardbridge, a middle section between Guardbridge and a line joining Martin's Point and Coble House Point, and an outer section from here to the mouth at Out Head. This categorisation is not necessarily that adopted by previous authors (eg Howson and Chambers, 2000).

In comparison with the Tay, the Eden Estuary is a much higher salinity environment. Salinities recorded on the sediment flats lie between 20–30‰ over most of the estuary but fall to around 10‰ on the mudflats of the inner estuary. At high tide the estuary has a uniform salinity of 28‰ (Johnston *et al.*, 1979). The sediments of the tidal flats are predominantly muddy sand and mud, with some firm sand at the top of the shore in the middle section and over an extensive area on the eastern side of the north bank in the outer section.

Few invertebrate species have colonised the mudflats in the lower salinity conditions above Guardbridge (Johnston *et al.*, 1979), although *Hediste diversicolor* and *Corophium volutator* have been found to be common for at least the first 500m upstream of Guardbridge (LMU.HedOl).

Knowledge of the biotopes present in the middle and outer sections is greatly aided by detailed invertebrate surveys carried out by Johnston *et al.* (1978, 1979) and Professor David Paterson, St Andrews University (pers. comm.), which supplements the limited surveying carried out during the current project.

The extensive mudflats of the middle estuary support a dense diatomaceous surface film (Caudwell and Jones, 1994), visible on the satellite imagery. On the north bank dense green algal mats are present. The green algal mats of the Eden tend to be dominated by species of *Enteromorpha* spp., although *Ulva* sp.and the red alga, *Porphyra* sp., are also often present. The infauna is dominated by abundant oligochaetes, *Corophium volutator* and *Hediste diversicolor*, although the fauna is more diverse than the inner estuary with several additional species being common or abundant including *Spio filicornis, Eteone longa* and *Macoma balthica* and, on the upper shore, *Hydrobia ulvae* (LMU.HedMac). The bivalve, *Scrobicularia plana*, has previously been recorded here and elsewhere in the estuary but it was not found during the current survey and may no longer be present in the estuary (Hatton, pers. comm.).

The sediment flats of the outer estuary support a greater diversity of biotopes. Mussel beds are largely confined to this area and occur in patches along both the north and south banks of the main channel and extend upwards to the midshore, particularly in the vicinity of the major drainage channels (SLR.MytX). *Fucus vesiculosus* is found associated with the mussel beds and also around the edges of the beds and elsewhere on stones and shells overlying the sediment (SLR.FvesX).

Figure 5.5 Distribution of biotopes in the inner Tay Estuary

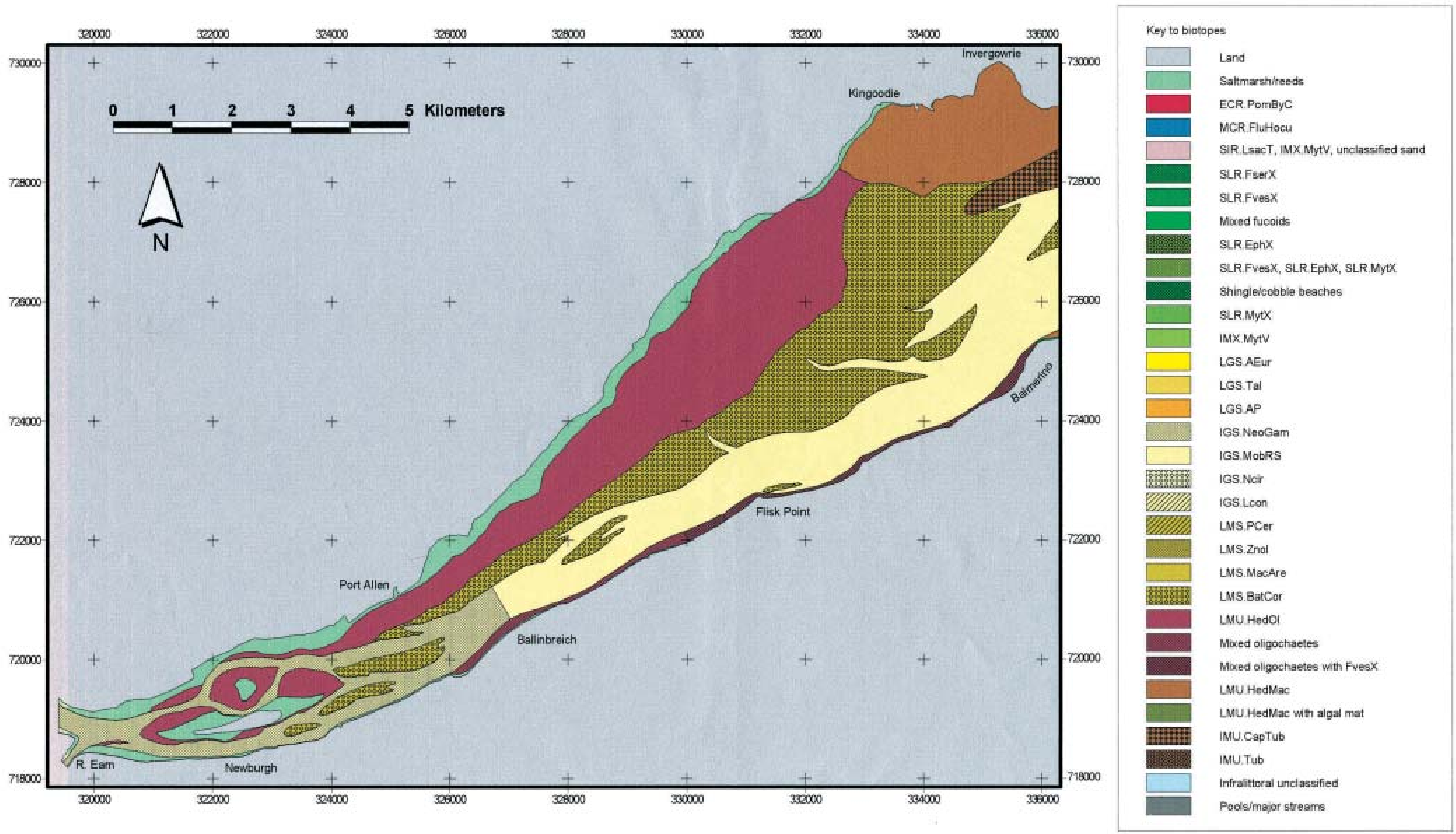

Figure 5.6 Distribution of biotopes in the middle Tay Estuary

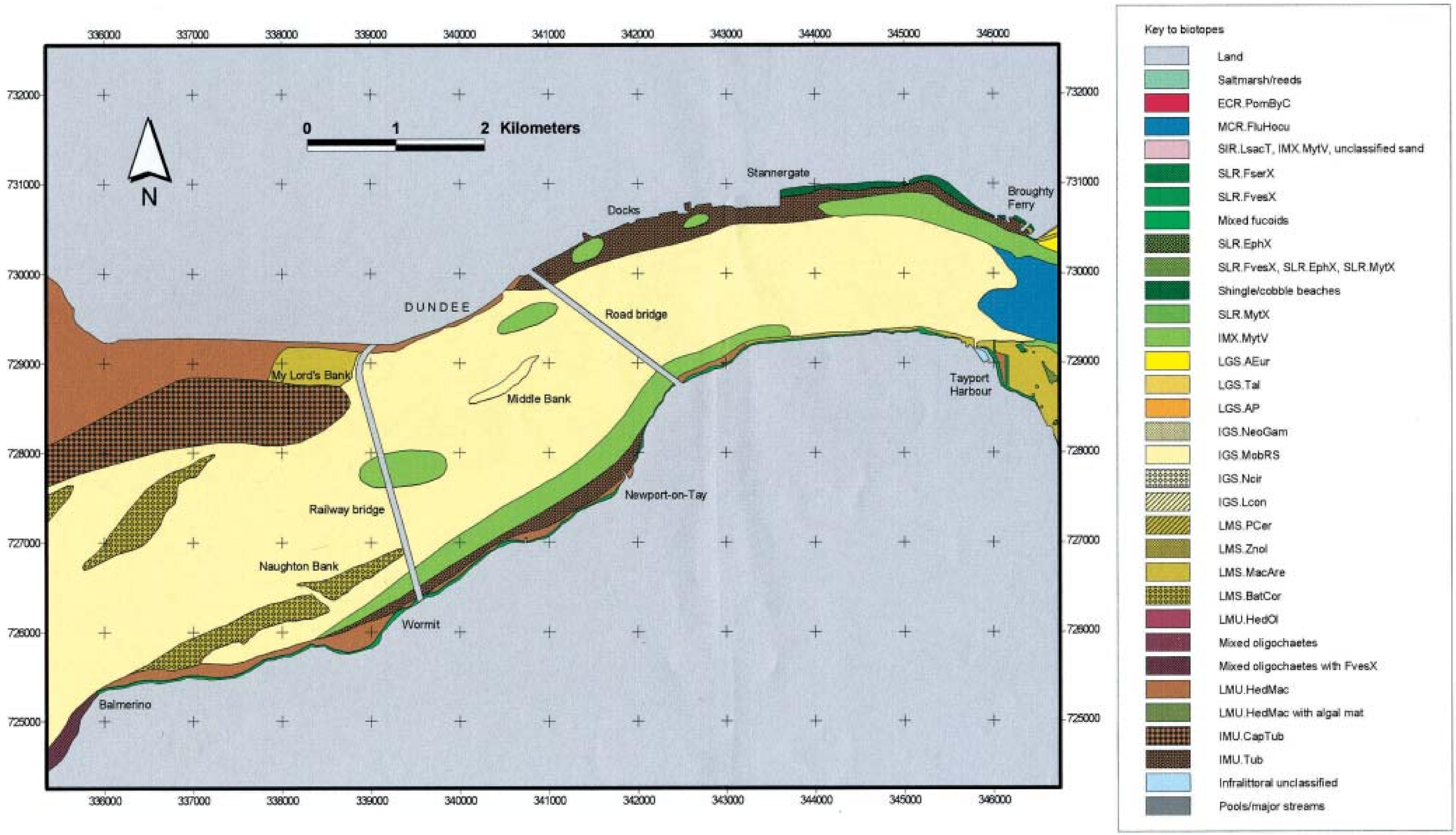

Figure 5.7 Distribution of biotopes in the outer Tay Estuary

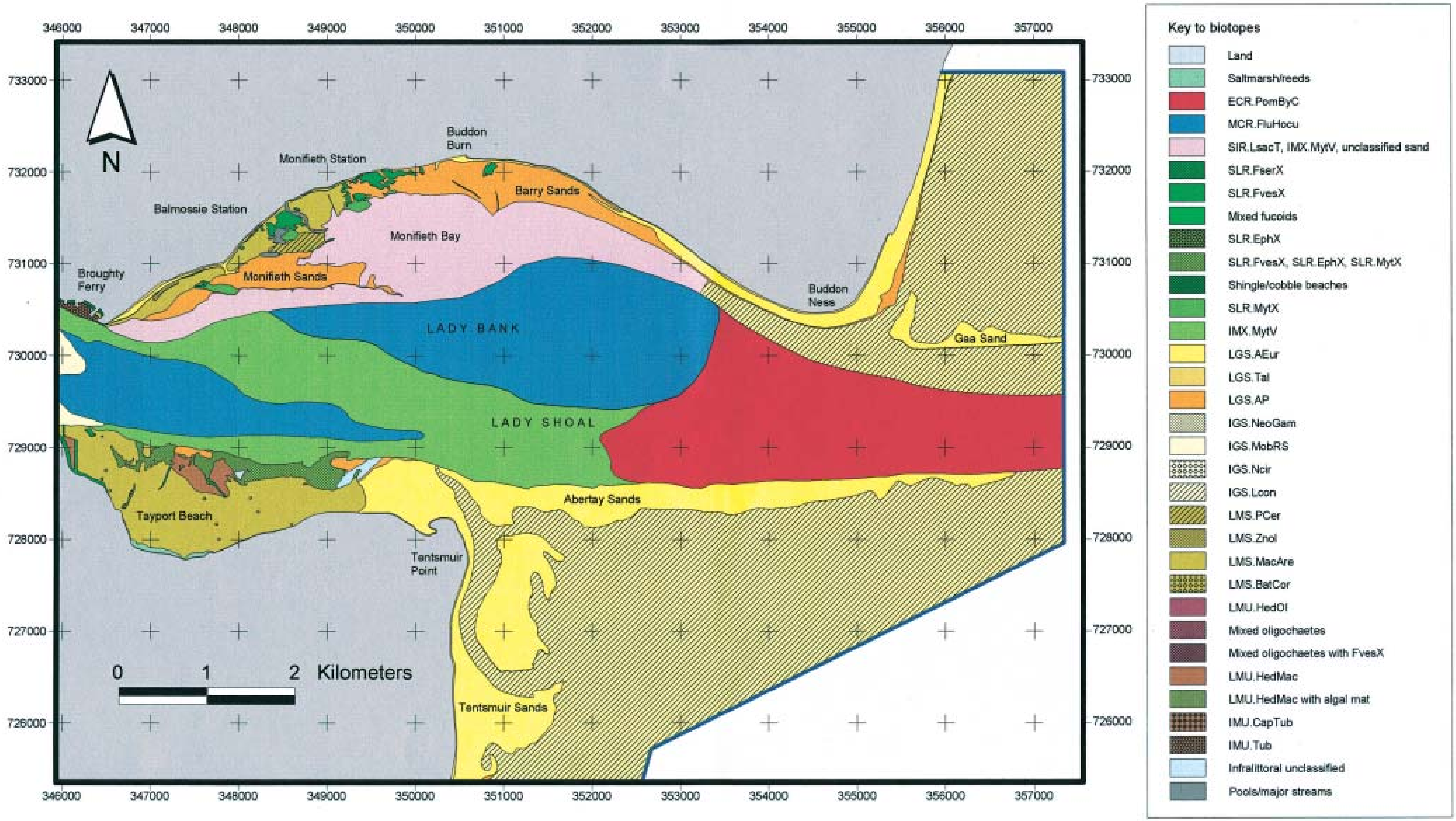

Figure 5.8 Distribution of biotopes in the Eden Estuary and approaches

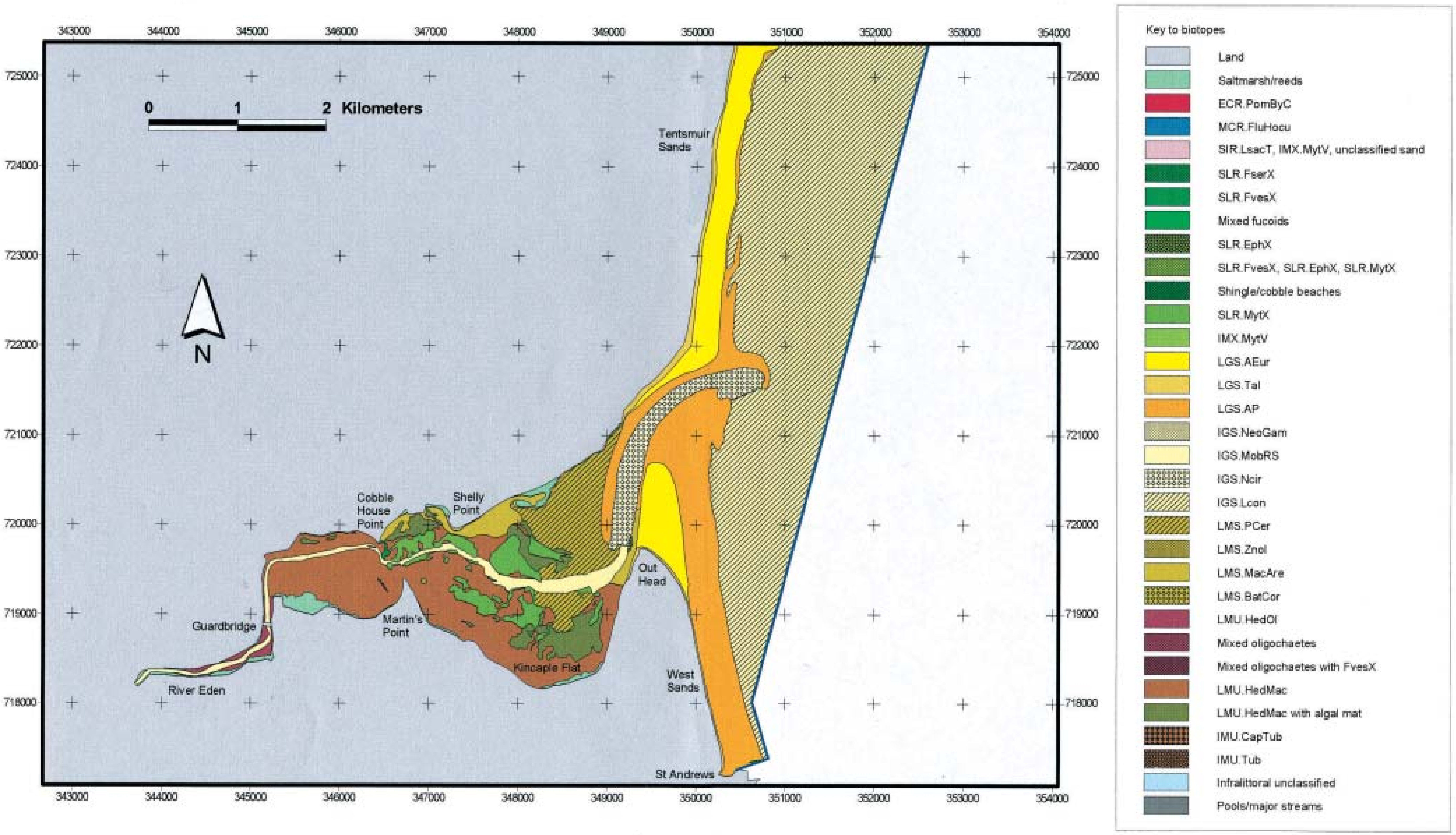

Figure 5.9 Distribution of biotopes in Mountain Sands

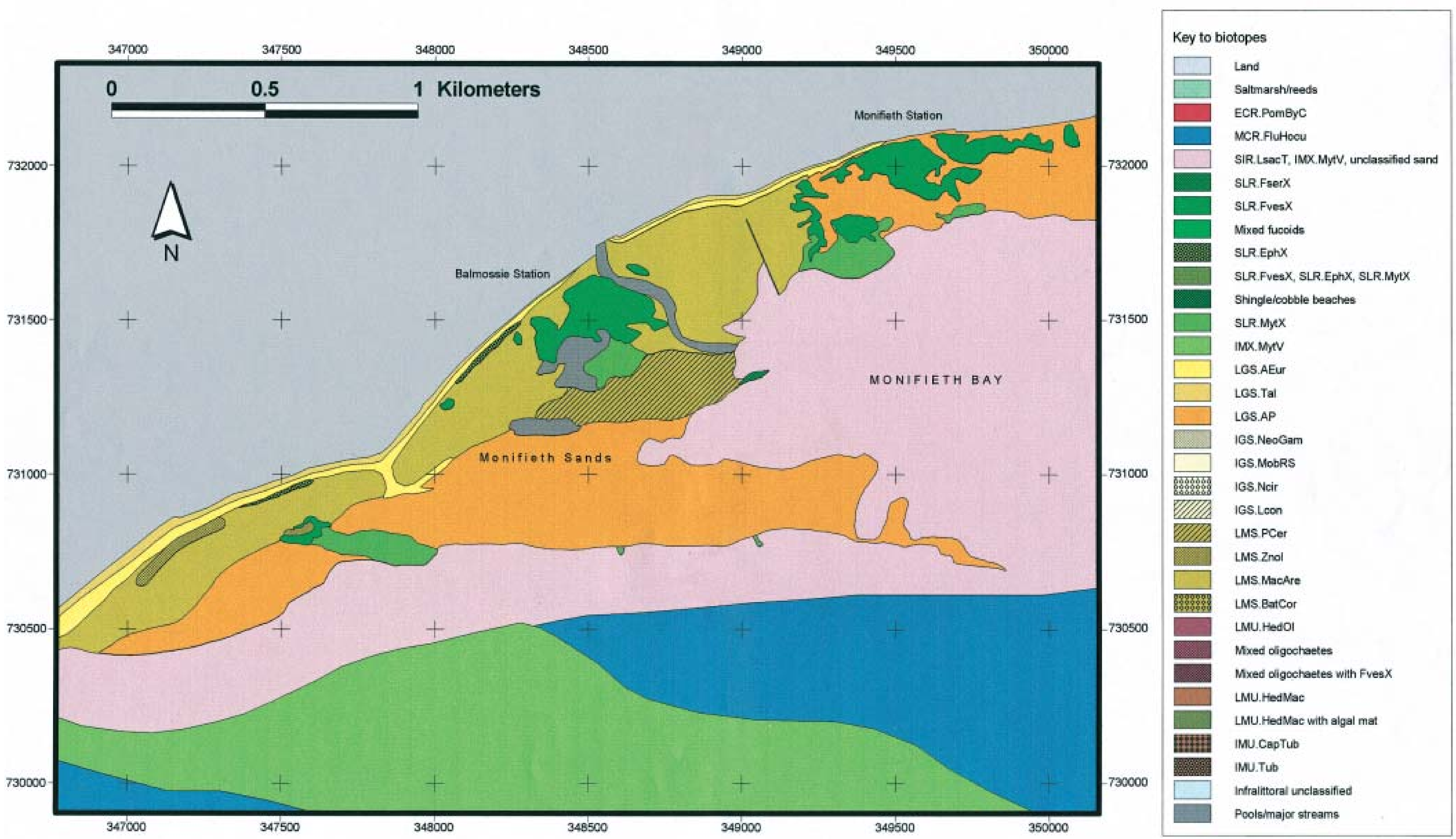

Figure 5.10 Distribution of biotopes on Tayport Beach

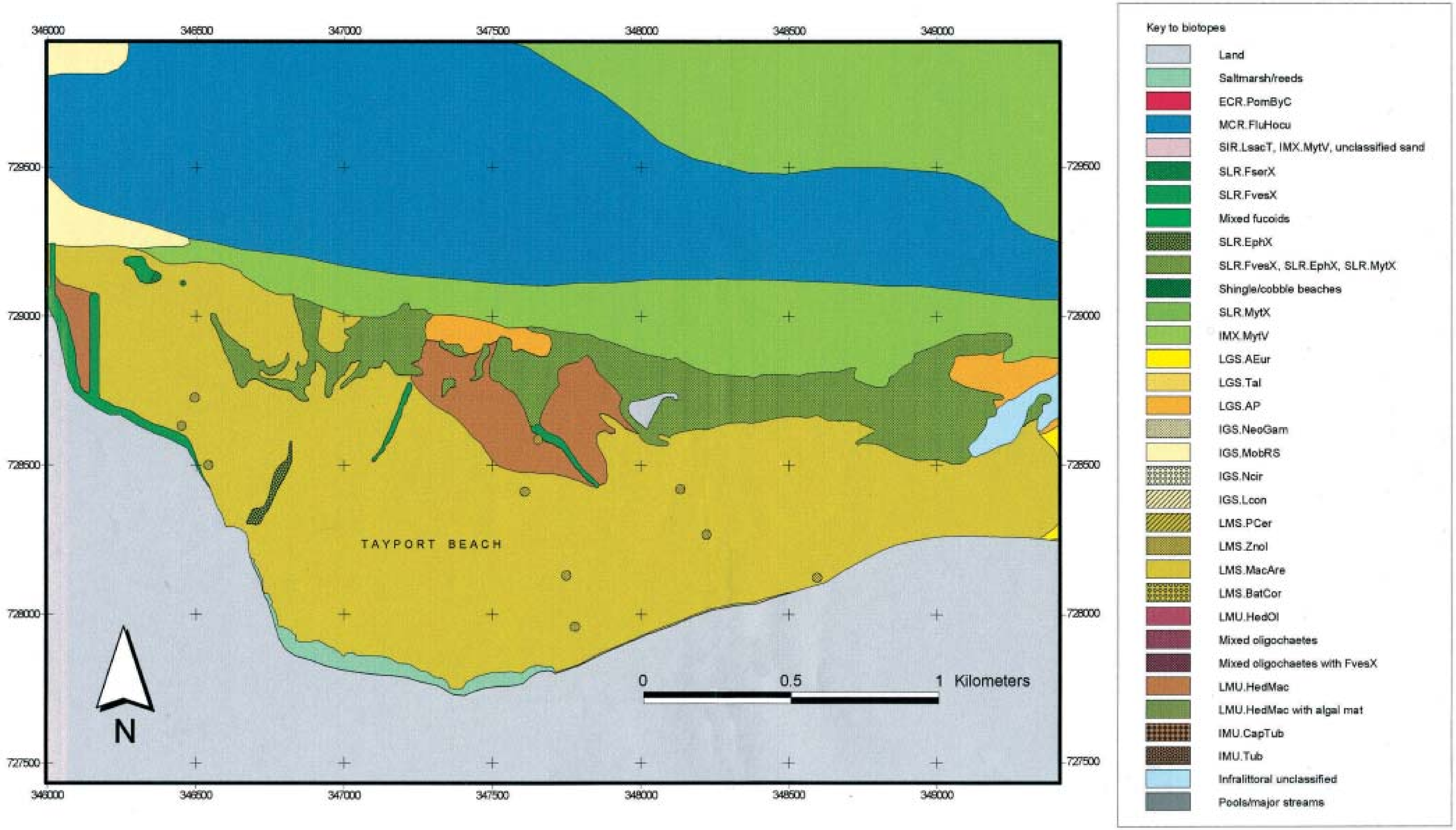

Figure 5.11 Distribution of biotopes in the Eden Estuary

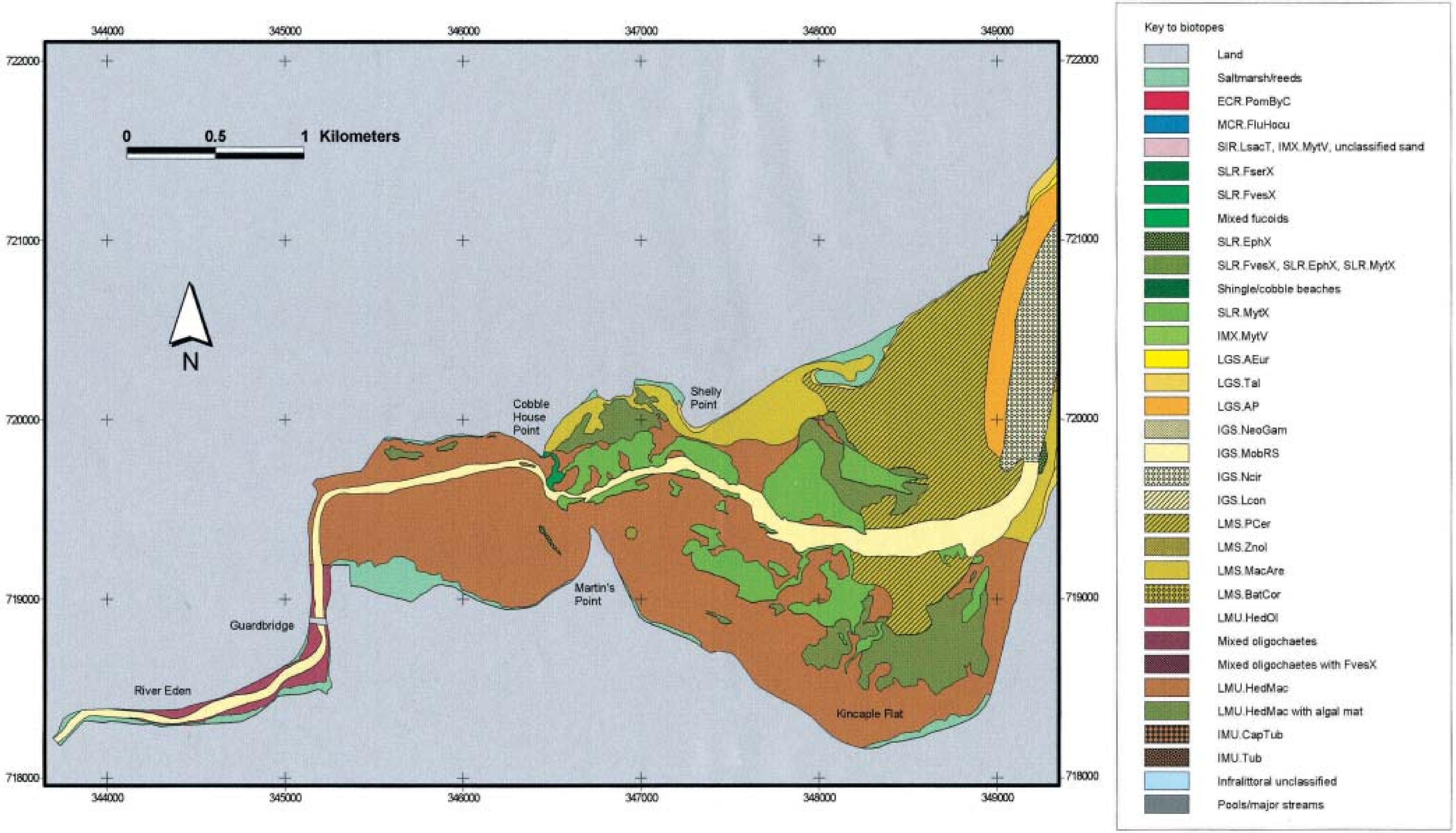

The infauna of the predominant muddy sediments of the outer estuary can be referred to the same biotope as the middle estuary (**LMU.HedMac**), with most of the same dominant taxa, although *Corophium volutator* is present in much lower numbers and *Cerastoderma edule* is considerably enhanced. However, much of this biotope in the outer region is covered by green algal mats during the summer. Figure 5.11 shows the extent of these mats revealed by satellite imagery in August 2002. A Landsat image taken on 17th July 2000 shows the extent of these mats to be considerably greater, appearing as a broad band occupying most of the midshore region of Kincaple Flat.

Firmer, slightly silty sands are found principally just inside the mouth of the estuary both on the north and south banks of the river channel (**LMS.PCer**). The cockle, *Cerastoderma edule*, is common here (as it is elsewhere in the outer estuary) but the infauna differs from the adjacent muddy sand biotope, **LMU.HedMac**, in the presence of high numbers of *Bathyporeia sarsi* and impoverished populations of *Hediste diversicolor* and oligochaetes. Another muddy sand biotope, **LMS.MacAre**, is found on the upper shore of the north bank either side of Shelly Point and along the south bank of the river channel near the mouth.

A century ago *Zostera* spp. were reported to cover vast areas of the estuary (Wilson, 1910) but have now almost disappeared. During the current survey only one small stand with *Zostera* sp. at about 15–20% cover was observed just east of Martin's Point. The position of this record is indicated in Figure 5.8 though not the extent of the bed. Several beds of *Zostera* are known to persist in the estuary, with *Z. noltii* being found mainly on open mudflats on the north side of the estuary, whereas *Z. angustifolia* and *Z. marina* are mainly confined to shallow drainage channels on the south side. The distribution has been mapped by North East Fife District Council (1998).

From the limited number of samples taken from the river channel it would appear that the sediments are generally slightly silty fine, medium and coarse sands supporting an extremely impoverished fauna. Only small numbers of *Carcinus maenas* and oligochaetes were found in the channel upstream of Out Head (**IGS.MobRS**) and only *Nepthys cirrosa* downstream of this point (**IGS.Ncir**).

5.3 Satellite-based biotope mapping

To account for some of the errors after the automatic spectral classification was undertaken, the classification image was enhanced post-classification by simplifying some of the class structure and renaming subclasses. This was undertaken after consultation with the Heriot-Watt team on the appropriateness of the distribution of some of the classes. Membership of some sub-classes were obviously wrong within their context, and were re-assigned. These classes were problematic due to their spectral charateristics not being unique and therefore causing some confusion with other classes with similar spectral signatures.

Several groups were amalgamated on the basis of classes likely to have very similar spectral signatures. These included the Fucoid classes (**SLR.FserX**, **SLR.FvesX**, were amalgamated to a mixed Fucoid class), on the basis that these brown algae are very similar. Ephemeral green algae (**SLR.EphX**) were also amalgamated with the mixed fucoid class. The *Zostera* (**LMS.Znol**) class was left in, but in some cases was overclassified being potentially mixed with signals from *Enteromorpha* (**SLR.EphX**). A knowledge classifier approach was also used to modify the deepwater class (**ECR.PomByC**), probably mis-classified in the first instance, to infralittoral sand (**IGS.Lcon**). Elements of the 'Pools and major streams' category, classified inappropriately in the region of West Sands, were also renamed to infralittoral sand.

The major changes made to the classification were:

- As stated above, the combination to a single class of the biotopes: **SLR.FvesX, SLR.EphX, SLR.MytX.**
- The single biotope class **SLR.FvesX** was occasionally found in the upper eulittoral zone since the fucoids, ephemeral seaweeds and mussel beds were occasionally confused with the freshwater (saltmarsh) or land vegetation. Since it was unlikely these biotopes were found so far up the shores they were removed.
- The **Pools and major streams** class was sometimes found at the sea edge of the clean sand shores (**LGS.AP**), being confused with the intertidal biotope **IGS.Lcon**. Since it is unlikely to find permanent pools or freshwater streams along the lower shore, these classes were removed from these areas and renamed to the latter.
- The fine sand and muddy sand class with polychaetes and cockles (**LMS.PCer**) were sometimes mixed up with the classes **LGS.AEur** and **LGS.AP** (burrowing amphipods and polychaetes in clean sand shores) due to the similarity of the substrate, and was removed from the areas where fieldwork data showed it was not present.
- The *Zostera* biotope (**LMS.Znol**) was in some cases mis-classified as ephemeral green algae (**SLR.EphX**) but overall was successfully classified considering the sparcity of this biotope.
- The reduced salinity infralittoral mobile sand biotope (**IGS. Ncir**) was in places mis-classified as **IGS.Lcon**, (tideswept infralittoral sand with *Lanice* and polychaetes). This problem would have been overcome if extensive salinity data were available in a form of a GRID covering the full extend of the SAC, to incorporate into the classification. The **IGS. Ncir** polygons that found in areas of open seawater were removes since this biotope is unlikely to be encountered under such conditions.
- The deeper water biotopes **ECR. PomByC** (Pomatoceros, Balanus and bryozoan on mobile circalittoral cobbles and pebbles), **MCR.Flu.Hocu** (Haliclona and Flustra with rich faunal turf on tide swept circalittoral cobbles and pebbles) as well as the infralittoral biotopes **IGS.Lcon** and **SIR.LsacT** (Laminaria, foliose red algae, sponges ascidians on tide swept infralittoral rock) were often confused, possibly in areas where water column attenuation was highest, since no water column correction was applied to the data. The classes in these cases were re-assigned manually guided by the fieldwork data.
- The **LMU. HedMac** (Hediste and Macoma in sandy mud shores) and **LMS.MacAre** (Macoma and Arenicola in mudy sand shores) were often confused due to the fact they are such similar classes spectrally. They were manually edited in places following field data and distribution indicated by Patterson's quadrat network.

The result of the post-classification clean-up, done on the basis of sound biological sense, has resulted in an improved map of biotopes which better reflects reality (Figures 5.12, 5.13 and 5.14).

Figure 5.12 Biotope distributions identified from multispectral classification of the QuickBird dataset and following post-processing North section

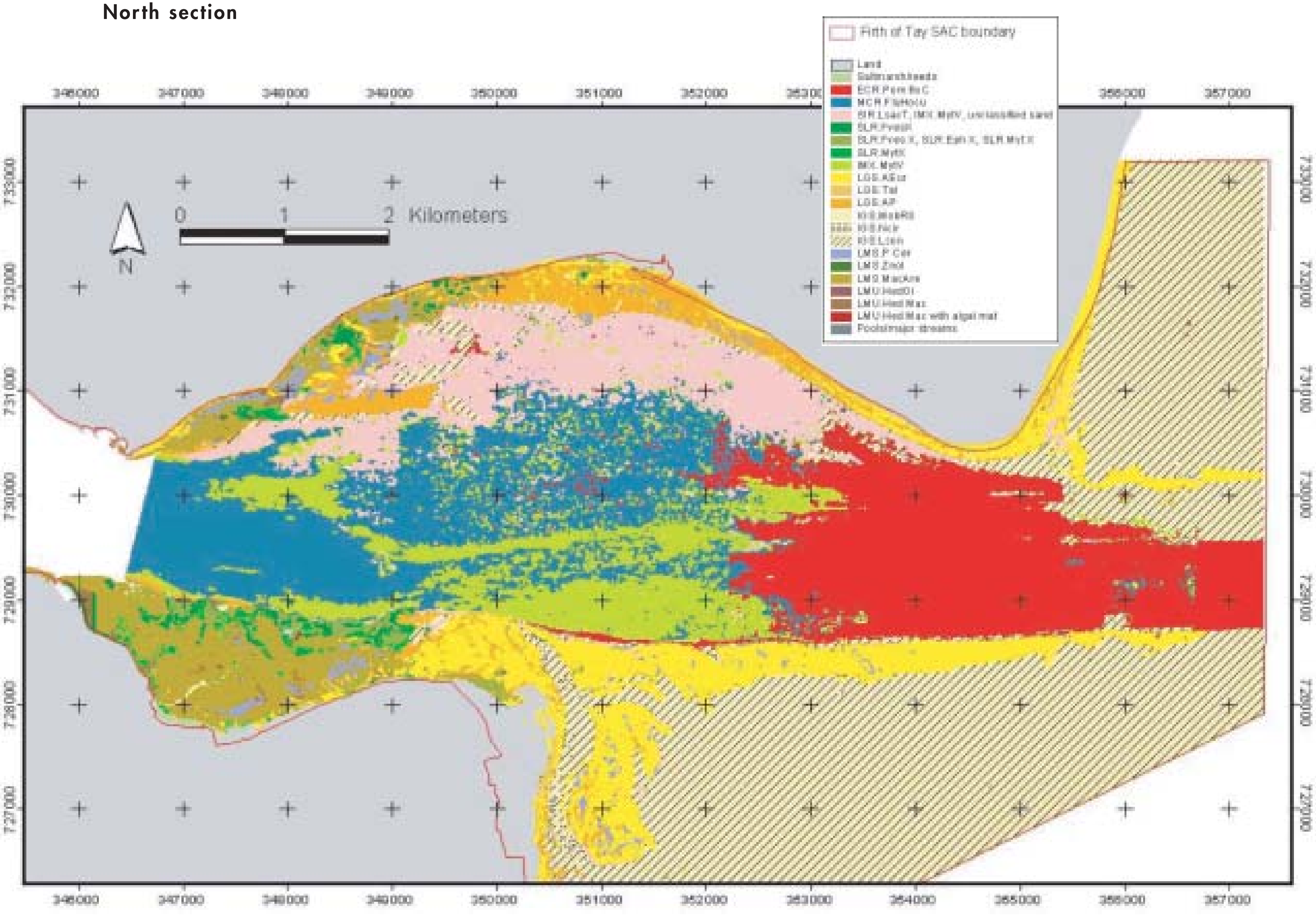

Figure 5.13 Biotope distributions identified from multispectral classification of the QuickBird dataset and following post-processing South section

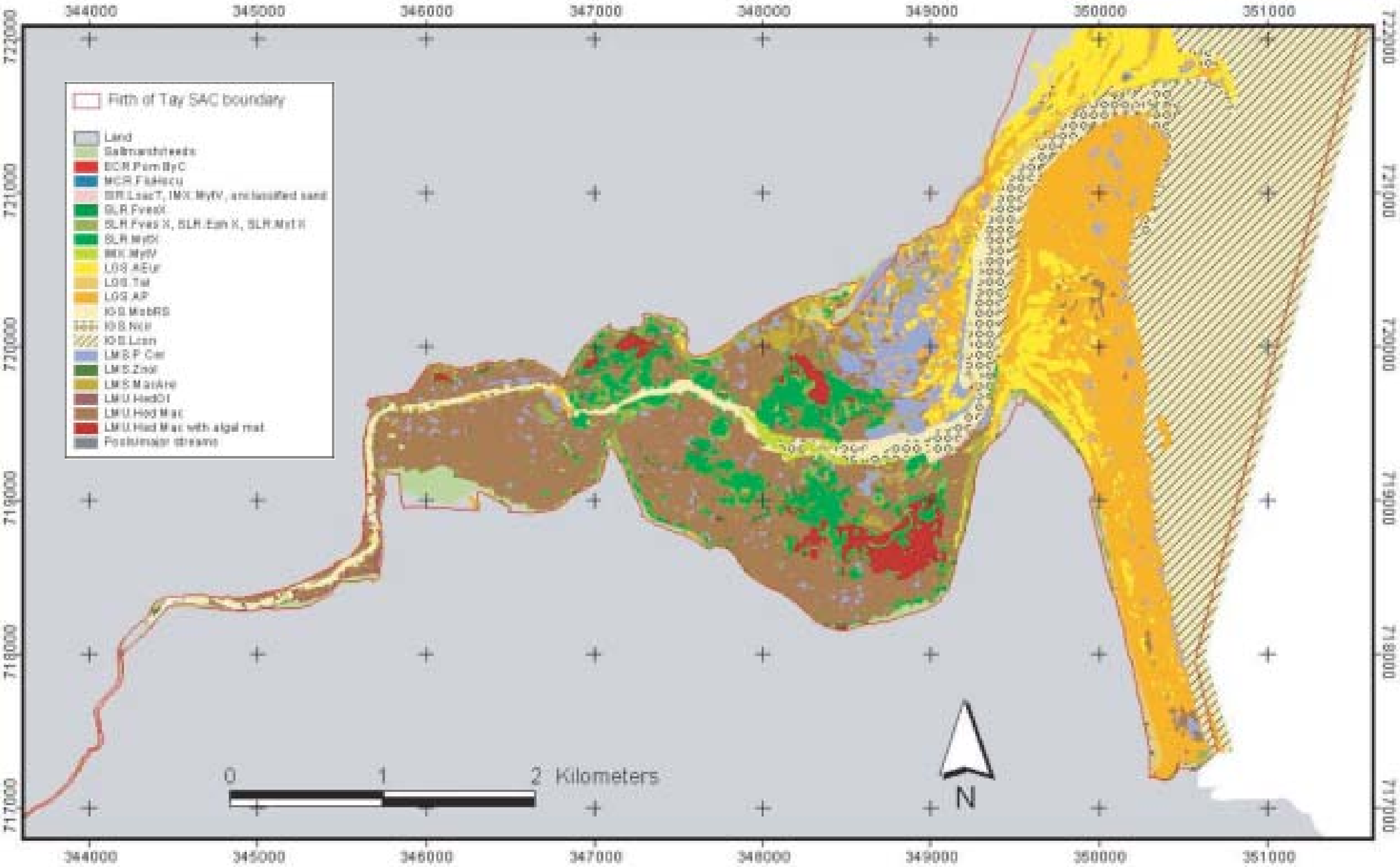

Figure 5.14 Biotope distributions identified from multispectral classification of the QuickBird dataset and following post-processing – full image

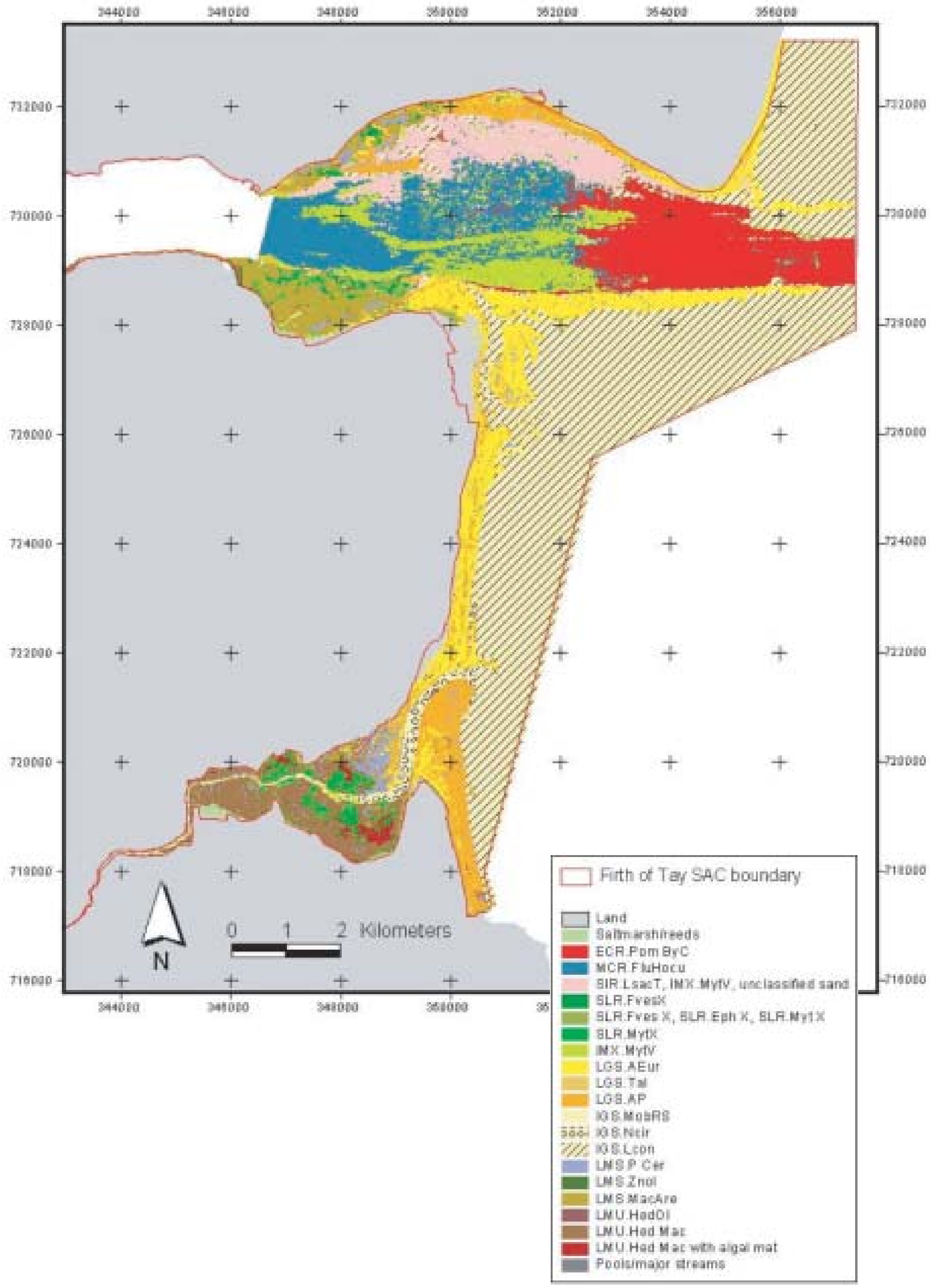

6 DISCUSSION

6.1 General

The combination of acoustic based techniques below 5m water depth and satellite based techniques for 0–10m water depth for biotope mapping proved to be a useful and powerful method of marine habitat appraisal. The satellite based techniques are anticipated to have applicability in similar habitat settings within clear, shallow water. Both acoustic and satellite techniques gave full coverage information with no extrapolation necessary. However, both techniques also required extensive groundtruth information from sediment analysis and biotope identification by trained biologists. Automated habitat discrimination (unsupervised classification) without such informed guidance is not recommended.

6.2 Acoustic mapping

The broad scale mapping of the sublittoral biotopes within the Firth of Tay and Eden Estuary cSAC was accomplished using an acoustic based approach providing complete 3D coverage of the south area and the deeper water portion of the north area combined with high fidelity groundtruth observations derived through ROV, dredge and grab sampling methodologies. The acoustic mapping was completed during a number of cruises due to variable weather conditions using the research vessel *Envoy*. The results of the survey illustrated the complex nature of the bathymetry within the cSAC. This complexity, with significant depth variations over metres from large sandwaves and bars, was particularly significant within the Tay Estuary. This localised heterogeneity would not have been adequately mapped using traditional single beam echo-sounders working on a track spacing of 25–50m demonstrating the value of full coverage, bathymetric sidescan or multi- beam techniques to the habitat mapping process. The value of simultaneous use of traditional AGDS techniques was demonstrated throughout the area for depths greater than 2–3m water depth, where most acoustic based techniques give suspect results due to transducer limitations. The AGDS survey used the Echoplus (SEA Ltd.) and this proved to be a stable acoustic platform that did not suffer from changes in values throughout the surveying (daily or between days). The Echoplus also proved to be stable at different survey speeds and under a wide range of sea states. The sidescan data acquired using the Submetrix System 2000 proved vital to the seafloor classification process for sedimentary structures especially as the information was co-located with bathymetry. Some discrepancies were noted between acoustic results and ground biological groundtruth data stations especially over areas of coarse material and where there were sponges and soft starfish. At these locations a cushioning affect was likely resulting in lower acoustic reflection signatures that would have been recorded in the absence of biological signatures. It is also likely that over areas where mussel patches existed, the acoustic techniques were discriminating different signatures from surrounding sea bed where the mussel areas contained higher portion of sediment. This, however, could not be fully tested with the current data set and further, more intense, data acquisition (both groundtruth and acoustic) would be necessary to resolve this.

The size of sedimentary features such as sand waves has been correlated with water depth by a number of workers and much of this work is summarised by Flemming (2000). Flemming found that the dimensional parameters of height and spacing of subaqueous flow-traverse bedforms, such as those found in the Tay Estuary, define a highly correlated exponential relationship for the global situation with local variations based on prevailing local conditions. Local conditions that cause perturbations of the global trend were cited as changing flow depths, frontal systems and storm wave action. In depth-limiting flow conditions, dune height and water depth are inherently correlated. The results of over 260 measurements of sand wave height were plotted against the global curves derived by Flemming and are shown in Figure 6.1 with a correlation coefficient for the Tay of 0.5. This compares favourably with many studies in the literature where correlation coefficients are typically in the range 0.3–0.6.

Figure 6.1 Sand wave amplitude and wave depth for the Firth of Tay and Eden Estuary and global curves from Flemming (2000) and Allen (1968)

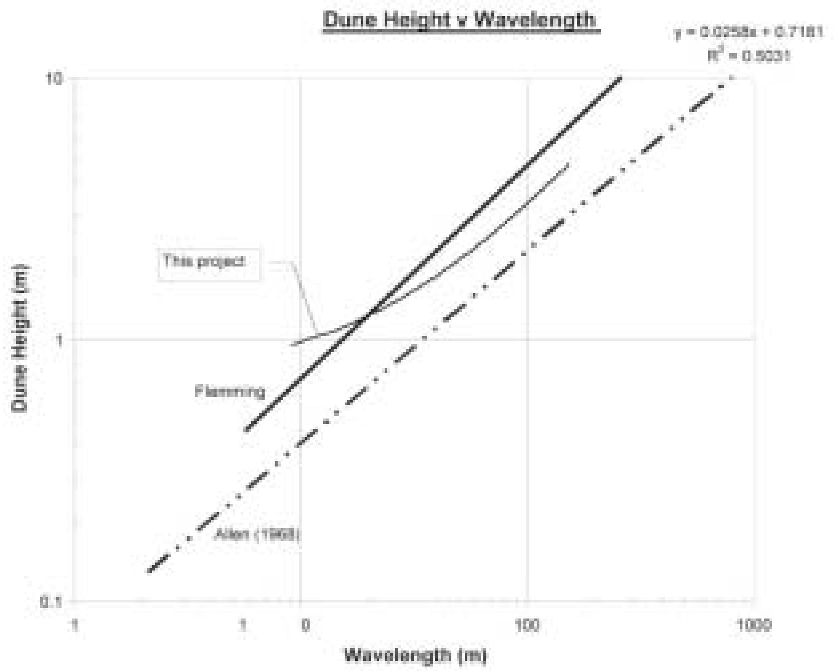

Flemming also reported on the upper limit dune sizes as a function of grain size with respect to wavelength. The results of this type of analysis for the same bedform features as were plotted in Figure 6.1 are shown on Figure 6.2. While there is a considerable scatter for the data, there is still a clear relationship with large sandwaves within coarser grain size sediment up to pebble sizes. Thereafter, as the sediment grain size increases to cobbles and boulders, the size of the sand waves does not increase because it becomes difficult for the average energy (velocity) of currents within the Tay to move this material.

A number of studies have been made of the frontal systems in the Tay Estuary with the most recent work conducted using airborne imagery and mathematical modelling by Ferrier and Anderson, (1997 a & b). Their work clearly demonstrated the complex tidal mixing within the estuary and throughout the tidal cycle. The orientation, location and relatively short time scale for the formation and decay of the fronts suggests an origin related to intratidal and lateral salinity balances. During the flood tide, saline water enters the estuary dominantly along the north side with flood water cascading over the shallow flats of Monifieth Bay, while along the southern shore, discharge of the fresh water from the Tay is still taking place. As tidal flooding continues the fronts move up the estuary with the contrast in waters between the freshwater discharge causing a series of "Y-shaped" fronts on the rising tide. The progress of these fronts has been shown at 2.5hr before high tide, 1hr before high tide and 10min after high tide on Figure 6.3 taken from Ferrier and Anderson (1997 a & b). The fronts marked on this figure represent the position of the surface foam lines that are usually

Figure 6.2 Dune height versus dune spacing as a function of grain size following Flemming (2002)

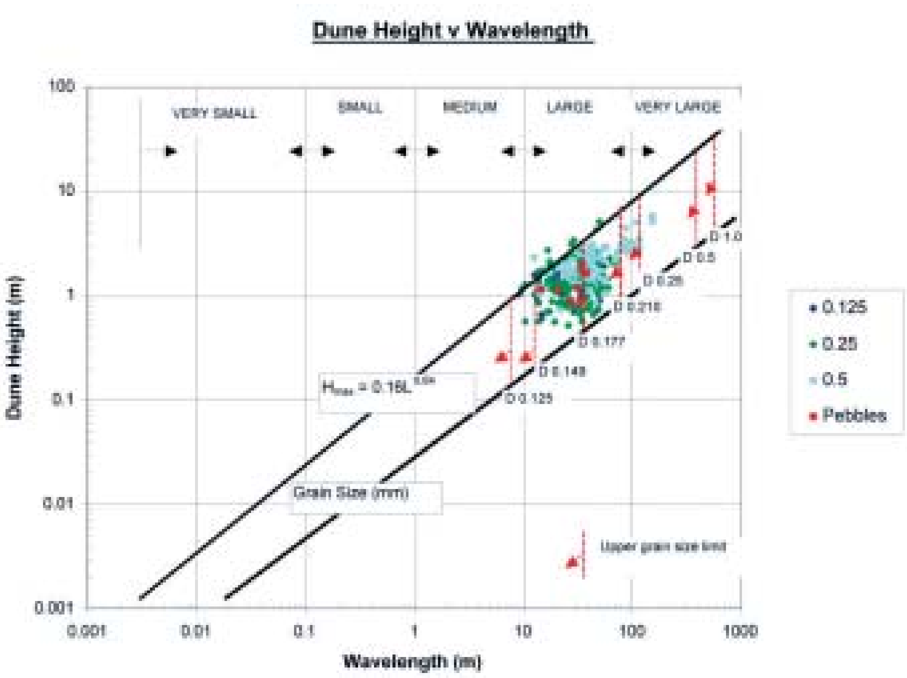

some distance behind the denser saline wedge of bottom water travelling up the main channel. The front moves into the estuary at a velocity similar to the rising tide (1–1.5ms^{-1}). On a large spring tide these fronts can reach as far as the Tay rail bridge but on smaller neap tides they more commonly turn between the bridges. A close correlation can be seen between the bedforms and the position of the fronts in the estuary. In Figure 6.3, the bedforms have been summarised into those where flood flow can be clearly seen, those where ebb flow can be seen and areas where there is either no asymmetry to the bedforms or there are no bedforms mapped. The main Y-front sweeps along the main channel with the largest flood bedforms formed to the north side of the frontal system in the main channel. On the south side of the main front the river dominated bedforms persist over the shallow areas where there is less mixing of the denser saline water with the fresh water. Between the bridges, the river water and ebb currents dominate with flood sandwaves only seen in the main channel. West of the rail bridge, no further flood waves are recorded at the scale of observation possible with the bathymetric sidescan. It must be remembered however that the minimum feature recordable with this system in the current study was 75cm and that it is known from the sidescan sonar, other work and the video recordings that sedimentary features smaller than this exist in the estuary. It is likely that these smaller features, and likely more mobile features are influenced by the flood/ebb state of the tide over much greater areas of the estuary than the larger sedimentary waves described here.

The results of this work represent an important baseline description of the quality and extent of the features for which the site has been selected and contribute to other programmes of work that will assist in a better understanding of the implications of long-term climate change and the development of more refined and cost-effective survey methodologies.

In order that marine habitat information can underpin overall integrated marine resource management it is essential that the results of mapping studies are easily integrated, visualised and useable by the scientific

Figure 6.3 Summary of fronts and large sedimentary structures in the middle Tay Estuary. Front information from Ferrier and Anderson (1997a & b)

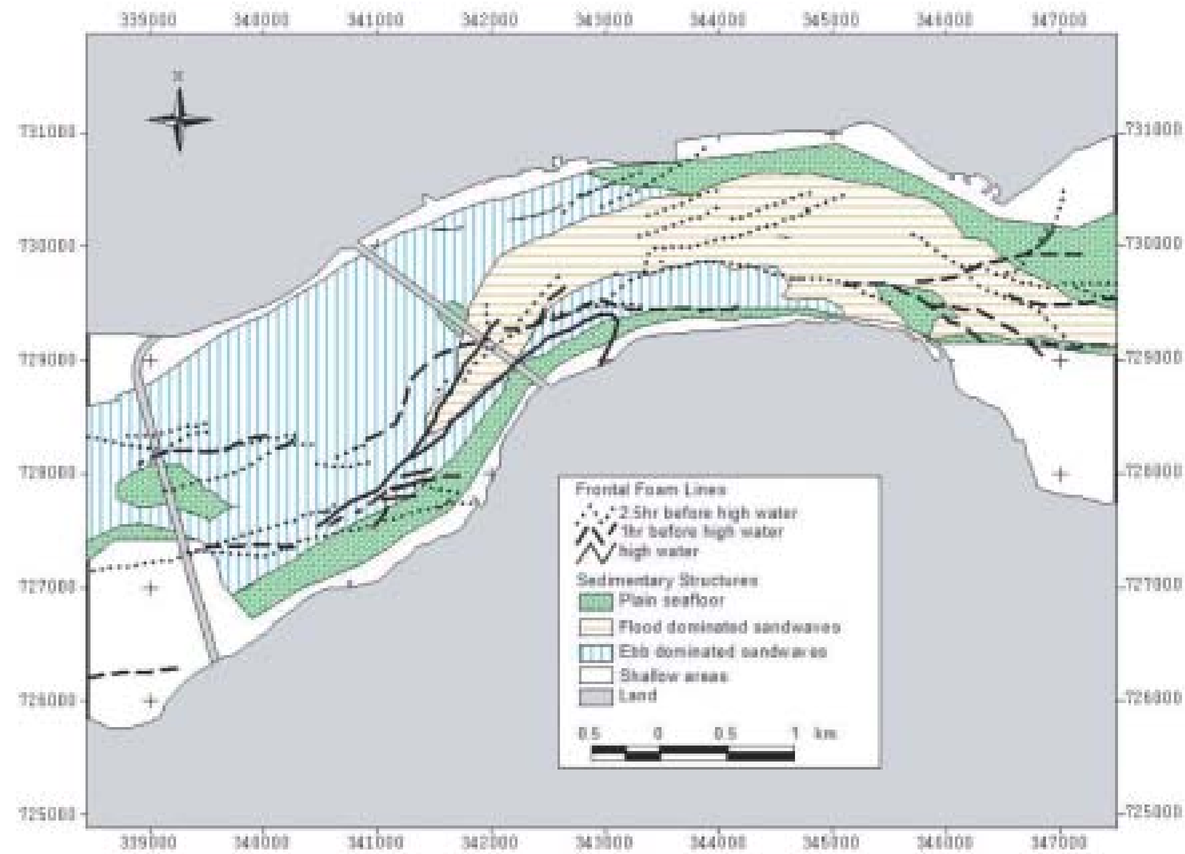

community and wider stakeholder groups. This is made possible where the results of any mapping work are produced in a Geographic Information System (GIS) format. The architecture of a GIS enables relationships to be established and tested between broad scale and small scale features on a site. The presentation of map and database information in a GIS format allows the significance of the data to be fully appreciated and built into ecosystem models. This might lead to the identification of the triggers or stressors that can often initiate large scale change of habitat condition. For example with the ability to tie together land and sea data, interactions between the two can be assessed and the potential of land based anthropogenic activities adversely affecting the marine environment evaluated.

A GIS is an ideal medium for hypothesis testing and survey planning and can also be used as a predictive tool where data can be analysed to estimate the likelihood of finding certain features or biotopes at given locations within the site. This form of analysis and prescribed data presentation has been undertaken in a number of previous studies (c.f. Davies, 1999).

The current study goes beyond the simple production of biotope distribution maps and data bases in attempting to understand not only the distribution of habitat types but also some of the changes that may have occurred historically within the area. This wider work, together with issues relating to site resource management and the further development of mapping techniques form the subject of ongoing research at the universities involved in this project and will be presented in future publications.

The Firth of Tay and Eden Estuary cSAC has received considerable scientific attention over the past 80 years, although the cSAC has only been defined in the recent past, with significant studies undertaken on a periodic basis. These studies have included bathymetry, sedimentary features and biology. The methods of study used in the past have been more extensive in some surveys, for example the number of sediment samples acquired by McManus *et al.* (1980) is considerably more than the current study, however, the whole cSAC has not been surveyed over its full extent with the detail used in this study. As the area contains extremely dynamic conditions that are very susceptible to future climatic induced perturbation it is recommended that a relatively high frequency of monitoring is made on the conditions that are liable to most change.

6.3 Biotope mapping

Although it is believed that the final biotope maps produced during this project broadly reflect the distribution of biotopes within the cSAC, the resolution of the biotope mapping exercise was constrained by a number of factors. The time constraint precluded the acquisition of full high-resolution satellite coverage for the area in conditions of low cloud cover and low spring tides. This resulted in the production of higher definition biotope maps of shores in the outer Tay and Eden Estuary, where satellite coverage was good, compared to the Tay upstream of Tayport where only low resolution Landsat images were available. The reduction in survey detail in the middle and upper Tay was partly resolved by the mapping of combinations of narrow biotopes.

The timescale of the project was insufficient to permit the acquisition and subsequent processing of satellite and acoustic data to the stage where this information could provide the basis for the groundtruthing exercise. However, this problem was lessened by the availability of the detailed sediment maps of much of the area by Buller and McManus (1975) and McManus *et al.* (1980) and the existence of previous biological surveys at several locations within the cSAC. Notwithstanding these mitigating factors, interpretation of the acoustic and satellite results would have been facilitated by planning the groundtruthing on the basis of the results of these remote surveys. This would have been particularly beneficial in the outer Tay, where the heterogeneity revealed by the acoustic survey is not reflected in the previous sediment survey of the area. A higher intensity of groundtruth surveying in this area may well reveal a more heterogeneous biotope distribution pattern.

Over much of the Tay there appears to be a low correlation between estuary bed morphology and sediment type on the one hand, as revealed by acoustic surveying, and biotope distribution on the other. This is largely due to the overwhelming influence of the strong currents and low salinities on the biota. The resultant impoverished biotope, IGS.MobRS, is of widespread occurrence throughout the estuary, being associated with a wide range of substrates, which share the characteristic of instability. A further cause for a lack of correspondence between the acoustic classification and the distribution of biotopes is the presence of biotopes presenting similar acoustic targets. This is particularly marked in the outer Tay where an extensive area is occupied by mixtures of coarse substrates, particularly pebbles, cobbles and mussels. Precise delineation of the different biotopes within such areas, if indeed possible, can probably only be achieved with the assistance of a high resolution groundtruthing programme. Such a programme could not be rapidly accomplished, given the strong tidal currents in the area.

6.4 Biotopes of the cSAC

The Firth of Tay and Eden Estuary has been proposed as an SAC on the basis that the area contains a nationally important colony of the Annex II species *Phoca vitulina*, the common seal, as well as several Annex 1 habitats, including representative estuaries in south-east Scotland. Most of the permanent channels of the estuaries (7596 ha) are considered to be examples of the habitat 'sandbanks which are slightly covered by seawater all the time', whilst much of the intertidal areas (6700 ha) are considered as 'mudflats and sandflats not covered by seawater at low tide'. The biotopes found within these broad habitat types are of low species diversity, as might be expected for such estuarine environments and most of the ground occupied by the subtidal sandbanks and intertidal flats is composed of common biotopes.

The estuary channels support an impoverished fauna (**IGS.MobRS**) for most of their area, although one of the two known Scottish breeding populations of the smelt, *Osmerus eperlanus*, occurs in the Tay. Biomass is considerably enhanced in the mussel beds (**IMX.MytV**) of the middle and outer Tay and on the tideswept banks of pebbles and cobbles in the more wave-sheltered regions of the mouth of the Tay where the nationally uncommon **MCR.Flu.Hocu** biotope is found. The physical conditions here are a good fit to this biotope and the rich sponge and hydroid turf a reasonable fit, although apparently lacking the characterising bryozoan, *Flustra foliacea*. It is likely that there will be high temporal variability in the distribution of biotopes in the outer Tay as a consequence of scour and burial of substrates and biota.

The intertidal areas of both estuaries are strongly dominated by sediment biotopes, especially **LMU.HedOl, LMU.HedMac** and **LMS.MacAre**, which provide feeding habitats for the nationally and internationally important populations of wading birds (Bell, 1998). Extensive areas of the lower sediment flats of the upper Tay, adjacent to the river channel, appear comparatively faunally impoverished (**LMS.BatCor**) and are probably less important as feeding grounds.

The shores of the outer Tay support significant areas of the nationally scarce eelgrass biotope, **LMSZnol**. *Zostera noltii* occurs widely over Tayport Beach and in apparently discrete patches in the more sheltered western end of Monifieth Sands. However, the density of the plant is generally too low to be detectable by satellite and aerial photographic imaging and so it has not been possible to map the detailed distribution of the biotope in the current survey. Even at high plant density, remote mapping is complicated by the similarity in signature between *Z. noltii* and green algae, such as *Enteromorpha* sp. Successful mapping in the area would necessitate *ad hoc* ground-based surveying. Beds of *Z. noltii, Z. angustifolia* and *Z. marina* are also known from the Eden Estuary and have been recently mapped by North East Fife District Council (1998).

The shores of the outer Tay (Tayport Beach and Monifieth Sands) and the Eden Estuary support ecologically important beds of the mussel, *Mytilus edulis* (**SLR.MytX**). Mussel density varies greatly and the beds often support and form mosaics with algal communities (especially *Fucus vesiculosus* and *Enteromorpha* spp.). As a consequence the precise delineation of the mussel beds is a complex task. In this survey satellite imagery has been used in an attempt to map these beds, although precise areal coverage is only likely to be achieved through lengthy *ad hoc* field survey. As with eelgrass, time constraints did not permit such an approach during the current survey.

The low salinity muddy sediment in the upper Tay Estuary (**LMU.HedOl**) supports a small burrowing crustacean of considerable interest. Khayrallah and Jones (1975), quoting the observations of McLusky

(1968) that the amphipod *Corophium volutator* had a lower salinity tolerance of 2‰, drew attention to the presence of an 'unusually euryhaline' population upstream of Newburgh, where the recorded maximum salinity is only 0.26‰. In the present survey only *C. multisetosum* was recorded in this region. This species is of very similar morphology to *C. volutator* and indeed was first recognised as a distinct species by Stock (1952). *C. multisetosum* was first recorded in Britain in 1963 but is still only known from rivers in the south of England. It has recently been recorded in Ireland (De Grave and Wilkins, 1994). Thus this is the first record of the species in Scotland and pushes considerably northwards its known distribution in the UK. Although it is possible that the apparently recent appearance of the species in a new area could merely be a result of previous taxonomic confusion, Janta (1995) has summarised the known distribution of the species within Europe and comes to the conclusion that the species is a new element of the fauna of Polish waters. Although the previous record of *C. volutator* by Khayrallah and Jones in virtually freshwater conditions in the Tay could be interpreted as evidence for the presence of *C. multisetosum* in the Tay for at least the last 30 years, it is most surprising that there have been no UK records for this species between Norfolk and the Tay. One explanation might be that *C. multisetosum* has not reached the Tay by natural spread but is an alien introduction through shipping. Such an explanation has also been suggested as a possible cause for the presence of the alien North American polychaete, *Marenzelleria viridis*, in the Tay (Atkins *et al.*, 1987). Alexander (1930) also recorded *C. volutator* (as *C. longicorne*) from the Newburgh area in 1930 but did not provide an indication of abundance. Thus this record may have related to drift specimens and could have been of either species.

6.5 Satellite mapping

6.5.1 Suitability of the QuickBird imagery for intertidal mapping

Satellite imagery of extremely high quality of part of the Tay Estuary SAC was obtained for this project and indicates the potential for fairly routine acquisition of such data over targeted areas of Scotland's coastline. The narrow swath of the QuickBird sensor necessitated the acquisition of the entire SAC in three parts. Due to the cloudiness of the summer period it was not possible to obtain the remaining images for Parts 2 and 3. Although pointability of the QuickBird sensor, which enables the sensor to be directed to into neighbouring orbit paths), increases the chances of obtaining cloud free data, the acquisition period is further restricted by the need to obtain data at low tide. This restricted suitable acquisition windows to just two periods per month of about 5 days duration each.

The geocorrection undertaken by Digital Globe Inc. was found to be accurate to within about 8–12m of locations measured in the field using GPS that may be acceptable to SNH for further processing without the need for further more accurate correction. However, more accurate geometric correction should be undertaken using independent datasets including field-based measurements of prominent targets using GPS and OS Landline data, the latter of which was used in this study.

Atmospheric correction was employed in this study to process the data from radiometric data to reflectance. The empirical line method gives an acceptable result for correcting such narrowly focussed and localised datasets. Although this correction could be eliminated from the processing chain, it is recommended to retain it, particularly to allow a standardised comparison of different satellite datasets acquired over the same region of interest, as well as to ensure comparison to any reflectance measurements made in the field.

Costs for the QuickBird data purchased for this project were at US$25 per km^2 for multispectral data set (Table 6.1). There is a minimum order size of $64km^2$. These data were purchased at the basic rectification level guaranteed to 1:50,000 accuracy by the data distributors. The relative level of accuracy was good to within 8–12m which may be acceptable for management purposes.

Costs of the imagery increase markedly for increased accuracy of rectified QuickBird data (to US$105 per km^2 for 1:10,000 ortho data). The costs of higher precision data may be less justified in economic terms when, if such precision were needed, it would be cheaper either to acquire ground control points over a suitable number of target features in the field using GPS or locate a suitable number ground control points from precision digital OS field boundary data. At 2.8m pixel resolution, the data came close to that of high quality aerial photographic coverage of a similar target area.

Table 6.1 Costs for varying levels of QuickBird multispectral data acquisition (from Space Imaging Inc. and Eurimage, respectively) for the standard 60 day acquisition window

Product	Accuracy (m)	per km^2 (USD)	per $100km^2$ £ approx.
Standard	na	$25	£1750
Ortho 1:50,000	na	$52.50	£3675
Ortho 1:25,000	na	$67.50	£4725
Ortho 1:10,000	na	$105	£7350

Although minimum order sizes for both IKONOS and QuickBird datasets are set ($100km^2$ and $64km^2$, repectively), polygons of any shape may be defined by the purchaser. This allowed for the acquisition to be tailored to suit the convoluted boundaries of the Firth of Tay and Eden Estuary cSAC such that coverage is maximised at the expense of areas of little interest (as may be the case with more regularly shaped acquisition polygons, eg for SPOT or Landsat data).

6.5.2 Landsat-7 data

In the absence of complete QuickBird coverage for the entire cSAC, two recent Landsat 7 datasets were obtained to facilitate the mapping of both biotopes and sediments within the Estuary itself. Both were obtained close to low tide such that intertidal areas are exposed. The 30m resolution of the multispectral datasets was enhanced by merging them to the 15m resolution of the panchromatic dataset using Principal Components Analysis. Copies of these datasets were supplied to the Heriot Watt team to assist in the manual interpretation of biotope distributions. These images proved valuable in assisting the manual mapping to identify the low tide boundary, and in biotope delineation on the sediment flats of the inner Tay.

One of the Landsat datasets, obtained on 17.07.00, was further processed by masking. It showed the clear differences in water and sediment colour across the cSAC. It also highlighted the significant changes in position of the major sandbanks in the estuaries from those represented in the cSAC spatial datasets (derived from OS data). This emphasises the need for frequent update of sandbank positions, which can only be rapidly derived from remotely sensed data.

Density slicing was applied to green band raw brightness information to produce a map of sediment brightness across all intertidal areas. Sediment brightness was shown to be largely related to sediment size.

Coarser sand sediments, bright and large in size, show up as bright (red) features in the density sliced image. Finer, siltier inorganic and organic sediments are smaller in size and darker and show up less bright in the image data. The distribution of sediment outwith and within the estuary is explained by the relative energies of the river inputs and tidal motions. Longshore drift largely contributes to the patterns of bright and hence coarse sand encountered on Tentsmuir beach and on Abertay sands. Within the Estuary coarser sediments are first deposited out of suspension in input river water as the energy of the river flow decreases. Finer and lighter siltier sediments are carried further in suspension. The tidal flow serves to redistribute sediments such that coarser, brighter sediments are deposited on the sides of the channel banks and finer sediments are carried out over the mudflats as the tide rises and deposited there (Charlton, 1980; Neil *et al.*, 2000).

Thus, despite having a coarser resolution than the fine resolution QuickBird data, the availability of the TM data proved useful in informing both the manually interpreted habitat classification and on indicating larger scale fluvial processes leading to the distribution of sediment zones, which likely influence biotope distributions.

6.5.3 Classification of biotopes by satellite data

The availability of satellite data (both complete Landsat TM coverage for the entire cSAC and QuickBird data for the eastern portion) proved highly valuable to manual mapping of biotope distributions performed by the Heriot-Watt team. The Landsat data assisted in the remapping of the low tide mark, sand bank locations and in separating upper and lower shore sediment types within the Estuary. The QuickBird data, of extremely high resolution, showed the fine structure of dynamic features evident in the cSAC and has undoubtedly led to a more accurate manual mapping of biotopes at the mouth of the Tay as well as in the Eden Estuary.

Whilst the satellite data were used to inform the manual interpretation of biotope distributions, the automatic spectral classification perfomed on the QuickBird imagery was as equally informed by the field survey. Field survey results were used as the basis with which to establish the large number of training samples for each biotope. The resulting smoothed classified image showed considerable patchiness, a great deal of which is probably real but which also arises out of other factors. Both intertidal and shallow subtidal biotopes were classified. Difficulties arose in the classification of intertidal sand biotope types (eg LGS.AP, IGS.Ncir, IGS.Lcon) illustrated well in West Sands and Tentsmuir beach. This is perhaps not surprising when the biotopes are defined by the presence of animal species which will have little influence on overall pixel reflectances. A comparison of the raw image and classified image data shows that the classification on the sandy beaches is more influenced by the relative moisture content of the sand, which has the strongest influence on sand brightness.

Other sources of mis-classification included problems induced by spectral similarities between classes. For example the fucoid classes (SLR.Fser X and SLR.Fves X) are likely to have highly similar reflectances. Misclassification of each is likely to result. For greater accuracy, these classes were subsequently amalgamated into a broader mixed fucoid class.

Similarly, some of the patchiness evident on some muddy sediments in the Eden may have been overestimated. Higher density sampling data supplied by the Sediment Ecology Research Group from the University of St Andrews, suggests that these surfaces are more homogeneous. As these sediments are also colonised by thin films of diatom communities on the sediment surface, it is possible that this contributed to some spectral confusion.

Improvements in the classification could be achieved with improved classification methods incorporating other sources of data. The availability of finescale elevation data and salinity data may well have improved the classification of certain biotopes, particularly the beach biotopes where the class is largely based on organisms with little influence on sand reflectance.

Thus, for this study, two classified images have been produced, a manually mapped biotope distribution and one produced from automated spectral-based classification of the satellite data. Both differ in a number of respects. Firstly, the manually interpreted map is in vector format while the classification is initially produced in raster format; the latter needs later conversion to polygon data. Secondly, whilst informed by the satellite data, the manual interpretation represents a simplification of the probable heterogeneity in biotope distributions which exist in the cSAC. The image-based classification, whilst not without its problems in terms of errors associated with spectrally similar classes as well as classes whose definition is largely unrelated to organisms that have a major impact on reflectance, shows greater heterogeneity in biotope distributions. This heterogeneity is likely to be encountered in the field, but the image data perhaps overrepresents it in parts.

REFERENCES

Adams, J. A. and Grierson, R. J. 1974. *The Eden Estuary. Internal report No. 4.* Marine Laboratory, Department of Agriculture and Fisheries for Scotland, Aberdeen.

Alexander, W. B. 1930. The natural history of the Firth of Tay. *Transactions of the Perthshire Society of Natural Science*, **9**: 35–42.

Allen, J. R. L. 1968. The nature and origin of bedform hierarchies. *Sedimentology*, **10**:161–182.

Atkins, S. M., Jones, A. M. and Garwood, P.R. 1987. The ecology and reproductive cycles of a population of *Marenzelleria viridis* (Annelida: Polychaeta: Spionida) in the Tay Estuary. *Proceedings of the Royal Society of Edinburgh*, **92B**: 311–322.

Austin, E. E. N and Evans, J. R. 2000. NE Atlantic benthic foraminifera: modern distribution patterns and palaeoecological significance. *Journal of the Geological Society, London*, **157**: 679–691.

Bates, C. R. and Byham, P. 2001. Swath-sounding techniques for near shore surveying. *Hydrographic Journal*, **100**: 13–18.

Bates, C. R. and Whitehead, J. 2001. Echoplus measurements in Hopavagen Bay, Norway. Sea Technology, **42**, No. 6: 34–43.

Bates C. R., Moore C. G., Malthus T., Harries D. B., Austin W., Mair J. M. and Karpouzli E. 2002. *Broad scale mapping of sublittoral habitats in The Sound of Barra*, Scotland. Edinburgh: Scottish Natural Heritage. ROAME no F01AA401B.

Bell, D. and Munford, J. 1990. *Mussel farming on the Eden Estuary*. Report to the Eden Estuary LNR Management Committee.

Bell, D. 1992. *Tay Estuary Study Report Parts 1 and 2*. Report to Scottish Natural Heritage, Perth & Kinross District Council and The City of Dundee City Council.

Bell, D. 1996. *A review of the natural heritage of the Tay Estuary*. Report to Scottish Natural Heritage.

Bell, D. 1998. Riverside Land-claim Ecological Statement, Second Draft. Ecos Countryside Services.

Buller, A. T. and McManus, J. 1971. Channel Stability in the Tay Estuary: Controls by bedrock and unconsolidated post-glacial sediment. *Engineering Geology*, **5**: 227–237.

Buller, A. T. and McManus, J. 1975. Sediments of the Tay Estuary. I. Bottom Sediments of the Upper and Upper Middle Reaches. Proceedings of the Royal Society of Edinburgh, **75B**: 41–64.

Buller, A. T., Charlton, J. A. and McManus, J. 1972. Data from Physical and Chemical Measurements in the Tay Estuary for Neap and Spring Tides, June 1972. Tay Estuary Research Centre report.

Burd, F. 1987. *Salt Marsh Survey of Great Britain: Scotland Regional Report South East*, Nature Conservancy Council.

Burns, D., Queen, C.B. and Chivers, R. C. 1985. An ultrasonic signal processor for use in underwater acoustics. *Ultrasonics*, **23**: 189–191.

Caudwell, C. and Jones, A. 1994. *Survey of green algal mats on the Eden Estuary Local Nature Reserve.* University of Dundee Environmental Advisory Unit report.

Charlton, J. A. 1980. The tidal circulation and flushing capability of the outer Tay Estuary. *Proceedings of the Royal Society of Edinburgh*, **78B**: 33–46.

Chivers R. C., Emerson, N. and Burns, D. 1990. New acoustic processing for underway surveying. *Hydrographic Journal*, **42**: 8–17.

Collins, W. and McConnaghey, R. A. 1998. Acoustic classification of the sea floor to address essential fish habitat and marine protected area requirements. In: *Proceedings of the 1998 Canadian Hydrographic Conference*, pp. 361–368. Victoria, Canada.

Collins, W., Gregory, R. and Anderson, J. 1996. A Digital Approach to Seabed Classification. *Sea Technology*, **37**: 83–88.

Connor, D. W., Brazier, D. P., Hill, T. O. and Northen, K. O. 1997a. Marine Nature Conservation Review: marine biotope classification for Britain and Ireland. Volume 1. Littoral biotopes. Version 97.06. *JNCC Report No. 229.*

Connor, D. W., Dalkin, M. J., Hill, T. O., Holt, R. H. F. and Sanderson, W. G. 1997b. Marine Nature Conservation Review: marine biotope classification for Britain and Ireland. Volume 2. Sublittoral biotopes. Version 97.06. *JNCC Report No. 230.*

Connor, D. W. and Little, M. 1998. Outer Hebrides (MNCR Sector 14). *In: Marine Nature Conservation Review. Benthic Marine Ecosystems of Great Britain and the North-east Atlantic, ed. by K. Hiscock,* 371–383. Peterborough, Joint Nature Conservation Committee. (Coasts and seas of the United Kingdom, MNCR series).

Curran, T. 1995. *Remote Sensing Technology for Subtidal Classification*. Kitasoo First Nations Fisheries Program Resources Inventory Committee of British Columbia, Victoria, Canada.

Danforth, W. W. 1997. Xsonar/Show Image: A Complete System for Rapid Side Scan Sonar *Processing and Display, U. S. Geological Survey Open File Report*, pp. 97–686.

Davies, J. 1999. Broad Scale Remote Survey and Mapping of the Sublittoral Habitats and their Associated Biota in the Firth of Lorn. *Scottish Natural Heritage Research, Survey and Monitoring Report, No. 157.*

DEFRA. 2002. *Safeguarding our seas. A strategy for the conservation and sustainable development of our marine environment.* London.

De Grave, S. and Wilkins, H. K. A. 1994. *Corophium multisetosum* (Crustacea), an amphipod new to Ireland. *Irish Naturalists' Journal,* **24**: 366–367.

Dougall, T.W. 1979. *Wildfowl and wader populations of the Eden Estuary, Fife.* Report to the Nature Conservancy Council.

Downie, A.J., Donnan, D.W. and Davison, A.J. 1999. A review of Scottish Natural Heritage's work in subtidal marine biotope mapping using remote sensing. *International Journal of Remote Sensing*, **20**, No. 3: 585–592.

Dunn, M.D. 1939. The marine algae of St Andrews Bay. *Transactions and Proceedings of the Botanical Society of Edinburgh,* **32(4)**: 488–501.

EN, SNH, CC, EHS (DoE(NI)), JNCC and SAMS. 2000. *Guidelines for Developing Conservation Objectives for Marine SACs – Learning from the UK Marine SACs Project 1996–2001*. Peterborough, English Nature.

EN. 2000. Acoustic Seabed Survey Techniques for Monitoring Marine SACs: A trial of Three Systems. *English Nature Report No. 411*, Peterborough.

European Community. 1992. EC Council Directive 92/43/EEC on the conservation of natural habitats and of wild fauna and flora. *Official Journal of the European Communities,* L206: 43.

Ferentius, G. and McManus, J. 1981. Nearshore processes and shoreline development in St Andrews Bay, Scotland. *Special Publication of the Association of Sedimentologists,* 5: 161–174.

Ferrier, G. and Anderson, J. M. 1997a. The application of remotely sensed data in the study of frontal systems in the Tay Estuary, Scotland, UK. *International Journal of Remote Sensing,* 18: 2035–2065.

Ferrier, G. and Anderson, J. M. 1997b. A Multi-disciplinary Study of Frontal Systems in the Tay Estuary, Scotland. *Estuarine, Coastal and Shelf Science*, 45: 317–336.

Flemming, B. W. 2000. The role of grain size, water depth and flow velocity as scaling factors controlling the size of subaqueous dunes. *In Trentesaux, A. and Garlna, T. (eds.), Marine Sandwave Dynamics*, Lille, France, 22–24 March.

Foster-Smith, R. L, Davies, J. and Sotheran, I. 2000. Broad Scale Remote Survey and Mapping of Sublittoral Habitats and Biota: Technical Report of the Broadscale Mapping Project. *Scottish Natural Heritage Research, Survey and Monitoring Report, No. 167.*

Foster-Smith, R. L. and Sotheran, I. 1999. Broad Scale Remote Survey and Mapping of Sublittoral Habitats and Biota of the Wash and the Lincolnshire and North Norfolk Coasts. *Report of the Broadscale Mapping Project.* Peterborough, English Nature.

Geen, M. 1998. Interpreting bathymetry and sidescan displays from an interferometric swath bathymetry system. *Ocean News and Technology*, 4 (4) (July/August 1998): 22–23.

Green, C.D. 1975. Sediments of the Tay Estuary III. Sedimentological and faunal relationships on the southern shore at the entrance to the Tay. *Proceedings of the Royal Society of Edinburgh*, 75B: 91–112.

Greenstreet, P. R., Tuch, I. D., Grewar, G. N., Armstrong, E. Reid, D. G. and Wright, P. J. 1997. An Assessment of the Acoustic Survey Technique RoxAnn, as a Means of Sampling Seabed Habitat. *ICES Journal of Marine Science*, 54: 939–959.

Hatten, L. 1992. *Eden Estuary Local Nature Reserve Management Plan 1993–1998*. North East Fife District Council. 136 pp.

Heald, G. J. and Pace, N. G. 1996. Implications of a bi-static treatment for the second echo from a normal incidence sonar. In: *Proceedings 3rd European Conference on Underwater Acoustics*, pp. 649–654.

Hogarth, B. 1989. *Habitat survey of the Eden Estuary SSSI*. Nature Conservancy Council, Cupar.

Howson, C. M. and Chambers, S. J. 2000. Inventory and Information Reviews of Three Marine Sites: Firth of Tay and Eden Estuary, Loch Laxford and the Isle of May. Report to Scottish Natural Heritage. 50 pp.

Jackson, J. R. and Briggs, K. B. 1992. High frequency bottom scattering: roughness versus volume scattering. *Journal of the Acoustical Society of America*, **92** (2): 962–977.

Janta, A. 1995. Distribution of *Corophium multisetosum* Stock, 1952 (Crustacea, Amphipoda) in European waters with some notes on its ecology. *Polskie Archiwum Hydrobiologii*, **42**, 395–399.

Jarvis, J. and Riley, C. 1987. Sediment transport in the mouth of the Eden Estuary. *Estuarine and Coastal Marine Science*, **24**: 463–481.

JNCC, 2001. *Marine Monitoring Handbook*. Joint Nature Conservation Committee. Editor, Davies, J.

Johnston, J., Cobb, J. L. S. and Bell, P. 1979. Survey of Shorebird Feeding Distribution and movements on the Eden Estuary, North East Fife., Including a Study of the Invertebrate Food Source. Report to the Nature Conservancy Council from the Gatty Marine Laboratory, University of St. Andrews.

Jones, A. M., Atkins, S. M. and Caudwell, C. M. 1992. Environmental Impact Assessment for Proposed Extension to Riverside Landfill, Dundee. University of Dundee.

Jones, A. M., Herbert, R. A. and McManus, J. 1989. Environmental Investigations in the Tay Estuary, July 1989. University of Dundee.

Karpouzli, E., and Malthus, T. J. 2002. The empirical line method for the atmospheric correction of IKONOS imagery. *International Journal of Remote Sensing*, **24**: 1143–1150.

Khayrallah, N. and Jones, A. M. 1975. A survey of the Benthos of the Tay Estuary. *Proceedings of the Royal Society of Edinburgh*, **75B**: 113–135.

Khayrallah, N. and Jones, A. M. 1980. The ecology of Bathyporeia pilosa (Amphipoda: Haustoriidae) in the Tay Estuary. I. Factors influencing the distribution on Tayport and Tentsmuir beaches. *Proceedings of the Royal Society of Edinburgh*, **78B**: 109–119.

Leach, S. J. and Phillipson, P. H. 1985. Saltmarsh and brackish swamp vegetation of the Fife Peninsula. *Transactions of the Botanical Society of Edinburgh*, **44**: 357–373.

Marine Ecological Surveys. 1998. *Biological resources of the Tay Estuary*. Report prepared for Oakwood Environmental Ltd. Confidential report Ref SA/Tay Estuary.

McLusky, D. S. 1968. Some effects of salinity on the distribution and abundance of *Corophium volutator* in the Ythan estuary. *J. mar. biol. Ass. U.K.*, **48**: 443–454.

McManus, J. 1999. Ballast and the Tay Eiderduck population. *Environmental History*, **5**: 1–8.

McManus, J. 1999. Coarse estuary mouth ballast gravel deposits: A sourcing case history. *Estuarine and Shelf Science* **48**: 677–682.

McManus, J. 2000. Sedimentation associated with estuarine frontal systems. Pye, K and Allen, J. (eds) Coastal and Estuarine Environments: sedimentology, geomorphology and geoarchaeology. Geological Society, London, Special Publications, v. 175, pp. 5–11.

McManus, J., Buller, A. T. and Green C. D. 1980. Sediments of the Tay Estuary. VI. Sediments of the lower and outer reaches. *Proceedings of the Royal Society of Edinburgh*, **78B**: 133–153.

McManus, J., Duck, R. W. and Anderson, J. M. 1998. The relative merits and limitations of thermal radiometric measurements in estuarine studies. *International Journal of Remote Sensing*, **19**: 53–64.

Neill, S. P., Copeland, G. J. M. and Folkard, A. M. 2000. Dynamics of Tidal Fronts in the Tay Estuary, Scotland. Presented at 10th Annual Conference on Physics of Estuaries and Coastal Seas, Norfolk Virginia.

North East Fife District Council. 1992. *Eden Estuary Local Nature Reserve Management Plan 1993–1998.* North East Fife District Council. 136 pp.

Oakwood Environmental Ltd. 1997. *Upper Tay Estuary: appraisal of biological resources. September 1997.*

Oakwood Environmental Ltd. 1997. *Upper Tay Estuary: sand resources survey. October 1997.*

Oakwood Environmental Ltd. 1998. *Product Application for Tay Estuary Dredging Licence Renewal. Draft Environmental Statement with Non-Technical Summary.* Oakwood Environmental Ltd, Godalming, Surrey.

Orlowski, A. O. 1984. Application of multiple echoes energy measurement for evaluation of seabottom type. *Oceanlogica*, **19**: 61–78.

Scottish Environment Protection Agency. 1992. *Tay Estuary Benthos Survey.* Unpublished data.

Simpkin, P. G. and Collins, W. T. 1997. Results from the use of broad-band, sub-bottom seismic data with statistically based sediment classificaiton techniques. In: *Saclantcen Conference Proceedings Series CP-45,* Pace, N. G., Pouliquen, E., Bergem, O. and Lyons, A. P. (eds).pp. 493–500.

Stock, J. H. 1952. Some notes on the taxonomy, the distribution and the ecology of four species of the genus *Corophium* (Crustacea, Malacostraca). *Beaufortia*, **21**: 1–10.

Tay Estuary Research Centre. 1997. *Tay Estuary resource survey – Stage 1 report.* Confidential Report prepared for Oakwood Environmental Ltd.

Wewetzer, S. F. K. 1997. Bedforms and sediment transport in the Middle Tay Estuary, Scotland: A sidescan sonar investigation. Unpublished Ph.D. thesis, University of St. Andrews.

Wewetzer, S. F. K. and Duck, R. W. 1996. Side-scan sonograph from the middle reaches of the Tay Estuary, Scotland. *International Journal of Remote Sensing,* **17**: 3539–3540.

Wewetzer, S.F.K. & Duck, R.W. 1999. Bedforms of the middle reaches of the Tay Estuary Scotland. *International Association of Sedimentologists Special Publication*, **28**: 33–41.

Williams, D. J. A. and West, J. R. 1975. Salinity distribution in the Tay Estuary. *Proceedings of the Royal Society of Edinburgh*, **75B**: 29–39.

Wilson, J. H. 1910. Nature Study Rambles Round St. Andrews. W. C. Henderson & Son, University Press, St. Andrews.

APPENDIX A – Biotope Ground Truth Data

Table 1 Subtidal and intertidal survey stations accessed by boat. The table shows the position, date, depth in relation to chart datum and biotopes recorded. The following abbreviations are used for faunal sampling gear: P, pipe dredge; N, naturalist dredge; V, 0.1m² Van Veen grab, R, ROV; S, small Van Veen grab (0.05m²); B, 0.1m² box quadrat. For further details see methods section

Station	Gear	Latitude	Longitude	Depth (m)	Date	Biotope
1	P, N	56.451383	-2.968417	5.7	25-Jun-02	IGS.MobRS
2	P, N	56.447100	-2.976633	5.9	25-Jun-02	IGS.MobRS
3	P, N	56.452300	-2.961617	6.4	25-Jun-02	IGS.MobRS
4	P, N	56.454800	-2.966167	2.8	25-Jun-02	IGS.MobRS
5	P, N	56.355083	-3.291333	2.6	04-Jul-02	IGS.NeoGam
6	P, N	56.352917	-3.259267	1.2	04-Jul-02	IGS.NeoGam
7	P, N	56.361917	-3.211950	1.5	04-Jul-02	IGS.NeoGam
8	V, N	56.391233	-3.134517	4.4	01-Jul-02	IGS.MobRS
9	V, N	56.392300	-3.121867	1.7	01-Jul-02	IGS.MobRS
10	V, N	56.420950	-3.047017	2.8	01-Jul-02	IGS.MobRS
11	V, N	56.428500	-3.018767	3.4	01-Jul-02	IGS.MobRS
12	P, N	56.439483	-2.982483	6.5	26-Jun-02	IMX.MytV
13	P, N	56.441767	-2.964400	6.5	26-Jun-02	IGS.MobRS
14	P, N	56.447683	-2.957650	2.4	26-Jun-02	IGS.MobRS
15	P, N	56.435033	-2.961383	4.8	26-Jun-02	IMX.MytV
16	P, N	56.437000	-2.949983	2.7	26-Jun-02	IMU.Tub
17	V	56.441883	-3.029200	2.5	01-Jul-02	IMU.CapTub
18	V	56.461667	-2.939067	5.8	27-Jun-02	IMU.Tub
19	V, N	56.455000	-2.920583	6.5	27-Jun-02	IGS.MobRS
20	V, N	56.459850	-2.901033	5.7	27-Jun-02	IGS.MobRS
21	V, N	56.465817	-2.896483	6.9	27-Jun-02	IMX.MytV
22	V, N	56.461883	-2.874250	13.2	27-Jun-02	IMX.MytV
23	V	56.461083	-2.847650	2.6	30-Jun-02	IMX.MytV
24	R	56.457033	-2.824750	3.2	30-Jun-02	IMX.MytV
25	N, R	56.459300	-2.780783	3.7	28-Jun-02	MCR.Flu.Hocu
26	V, R	56.467717	-2.801283	2.3	30-Jun-02	SIR.Lsac.T, unclassified sand
27	N	56.454062	-2.703394	13.6	30-Jun-02	ECR.PomByC
28	V, R	56.436926	-2.726457	4.2	29-Jun-02	IGS.Lcon
29	V, R	56.405733	-2.781500	3.9	29-Jun-02	IGS.Lcon
30	V, R	56.471517	-2.705283	2.9	30-Jun-02	IGS.Lcon
31	V, R	56.486600	-2.695267	6.2	30-Jun-02	IGS.Lcon

Table 1 *(continued)*

Station	Gear	Latitude	Longitude	Depth (m)	Date	Biotope
32	V, R	56.373917	-2.794317	2.9	29-Jun-02	IGS.Lcon
33	R	56.451583	-2.796317	4.5	30-Jun-02	IMX.MytV
34	S	56.367067	-2.868817	-1.2	29-Jun-02	LMU.HedMac
35	S	56.366500	-2.852000	-0.5	29-Jun-02	IGS.MobRS
36	S	56.364050	-2.841833	1.5	29-Jun-02	IGS.MobRS
37	S	56.364700	-2.826250	0.8	29-Jun-02	IGS.MobRS
38	S	56.380833	-2.816050	1.9	29-Jun-02	IGS.Ncir
39	B	56.448150	-2.725367	-1.3	30-Jun-02	LGS.AEur
40	B	56.447700	-2.725533	-1.8	30-Jun-02	LGS.AEur
41	B	56.446967	-2.773750	-1.2	30-Jun-02	LGS.AEur
42	B	56.446500	-2.773933	-2.3	30-Jun-02	LGS.AEur
43	P, N	56.399767	-3.086283	3.4	01-Jul-02	IGS.MobRS
44	V, N	56.408650	-3.068083	5.4	01-Jul-02	IGS.MobRS
45	S	56.425882	-3.045733	0.6	02-Jul-02	IGS.MobRS
46	S	56.436176	-3.054267	-0.1	02-Jul-02	IMU.CapTub
47	S	56.443039	-3.060267	-1.8	02-Jul-02	LMU.HedMac
48	S	56.448431	-3.066000	-2.1	02-Jul-02	LMU.HedMac
49	S	56.411667	-3.084533	0.5	02-Jul-02	IGS.MobRS
50	S	56.417647	-3.090133	-1.2	02-Jul-02	LMS.BatCor
51	S	56.422353	-3.094933	-1.7	02-Jul-02	LMU.HedOl
52	S	56.427255	-3.101200	-1.6	03-Jul-02	LMU.HedOl
53	S	56.432255	-3.106667	-2.1	03-Jul-02	LMU.HedOl
54	S	56.397549	-3.123333	1.9	02-Jul-02	IGS.MobRS
55	S	56.402549	-3.130800	0.1	03-Jul-02	LMS.BatCor
56	S	56.407255	-3.137333	-1.3	03-Jul-02	LMU.HedOl
57	S	56.411961	-3.143867	-2.2	03-Jul-02	LMU.HedOl
58	S	56.379412	-3.182400	0.3	03-Jul-02	LMS.BatCor
59	S	56.381863	-3.185867	-0.3	03-Jul-02	LMU.HedOl
60	S	56.383725	-3.188800	-2.2	03-Jul-02	LMU.HedOl
61	B	56.447667	-2.962867	-1.8	02-Jul-02	LGS.AEur
62	P, N	56.378090	-3.168925	2.1	04-Jul-02	IGS.MobRS
63	S	56.362183	-3.233950	-1.4	03-Jul-02	LMU.HedOl
64	S	56.356650	-3.268783	-0.9	03-Jul-02	LMU.HedOl
65	S	56.450000	-2.999683	-1.1	03-Jul-02	not defined
66	N	56.454466	-2.855354	12.9	04-Jul-02	MCR.Flu.Hocu
67	N	56.461643	-2.801826	4.2	04-Jul-02	MCR.Flu.Hocu
68	N	56.455399	-2.748453	9.3	04-Jul-02	ECR.PomByC

Table 2 Intertidal survey stations accessed from the shore. The table shows the position, date and biotopes recorded and whether an infaunal sample was taken

Site	Sample	Latitude	Longitude	Date	Biotopes
WS1	no	56.345183	-2.801758	10-Aug-02	SLR.Fspi
WS2	no	56.344733	-2.802375	10-Aug-02	MLR.Ent
WS3	no	56.346016	-2.798924	10-Aug-02	SLR.Fves, MLR.Fser.Fser, MLR.EntPor
WS4	no	56.345516	-2.800008	10-Aug-02	SLR.Fspi, SLR.Fves, MLR.EntPor
WS5	yes	56.347666	-2.797691	10-Aug-02	LGS.AP.Pon
WS6	yes	56.353034	-2.800791	10-Aug-02	LGS.AP.Pon
WS7	yes	56.364585	-2.805758	10-Aug-02	LGS.AP.Pon
WS9	yes	56.364402	-2.808658	10-Aug-02	LGS.AP.Pon
WS11	yes	56.363985	-2.811842	10-Aug-02	LGS.AEur
WS12	no	56.363818	-2.812325	10-Aug-02	LGS.Tal
WS14	no	56.357118	-2.808842	10-Aug-02	LGS.Tal
WS15	no	56.357251	-2.808225	10-Aug-02	LGS.AP.P
WS16	no	56.357301	-2.807858	10-Aug-02	LGS.AP.P
WS17	no	56.353050	-2.806108	10-Aug-02	LGS.AP.P
WS18	no	56.353000	-2.806492	10-Aug-02	LGS.AP.P
WS19	no	56.352900	-2.807108	10-Aug-02	LGS.Tal
WS20	yes	56.353150	-2.804541	10-Aug-02	LGS.AP.Pon
WS21	no	56.347550	-2.802175	10-Aug-02	LGS.AP.P
WS22	no	56.347283	-2.803375	10-Aug-02	LGS.AP.P
WS23	no	56.347216	-2.804108	10-Aug-02	LGS.Tal
FE2	no	56.391526	-3.115163	11-Aug-02	LR.YG
FE3	no	56.391559	-3.115230	11-Aug-02	SLR.FvesX
FE4	no	56.391643	-3.115480	11-Aug-02	SLR.FvesX
FE5	yes	56.391526	-3.115130	11-Aug-02	LGS.Ol
FE6	yes	56.391576	-3.115347	11-Aug-02	SLR.FvesX
FE7	yes	56.392076	-3.116363	11-Aug-02	LMU.HedOl
FE8	no	56.391776	-3.115897	11-Aug-02	LMU.HedOl
FE9	no	56.391826	-3.113063	11-Aug-02	LMU.HedOl
FE10	no	56.391859	-3.111396	11-Aug-02	Reeds
FE11	no	56.392443	-3.106745	11-Aug-02	LMU.HedOl
FE12	no	56.393076	-3.101295	11-Aug-02	SLR.FvesX
FE13	no	56.395243	-3.089343	11-Aug-02	LGS.Tal
FE14	no	56.395326	-3.089376	11-Aug-02	LGS.Ol
FE15	no	56.395359	-3.089293	11-Aug-02	SLR.FvesX

Table 2 *(continued)*

Site	Sample	Latitude	Longitude	Date	Biotopes
FE16	no	56.397476	-3.086643	11-Aug-02	SLR.FvesX
FE17	yes	56.397376	-3.086709	11-Aug-02	LMU.HedOl
FE18	no	56.394126	-3.093477	11-Aug-02	LMU.HedOl
FE19	no	56.396193	-3.087126	11-Aug-02	MLR.Ent
FE20	yes	56.397276	-3.086409	11-Aug-02	SLR.FvesX
FE21	yes	56.391876	-3.113030	11-Aug-02	LMU.HedOl
D1	no	56.474167	-2.837233	22-Aug-02	LGS.Tal
D2	no	56.473983	-2.837017	22-Aug-02	SLR.Fspi
D3	no	56.473783	-2.836767	22-Aug-02	SLR.Fspi
D4	no	56.473450	-2.836450	22-Aug-02	SLR.Fves
D5	no	56.472933	-2.835750	22-Aug-02	SLR.Fves
D6	no	56.472717	-2.835450	22-Aug-02	SLR.Fves, SLR.MytX
D7	no	56.472517	-2.835217	22-Aug-02	SLR.MytX
D8	no	56.472150	-2.834883	22-Aug-02	SLR.Fves, SLR.MytX
D9	no	56.471717	-2.834300	22-Aug-02	SLR.MytX
D10	no	56.471350	-2.833867	22-Aug-02	SLR.MytX
D11	yes	56.470300	-2.833000	22-Aug-02	LMS.PCer
D12	no	56.469783	-2.833917	22-Aug-02	LGS.AP
D13	no	56.467700	-2.834150	22-Aug-02	LGS.AP
D14	no	56.468500	-2.831633	22-Aug-02	SLR.EphX
D15	yes	56.468683	-2.831217	22-Aug-02	LGS.AP
D16	yes	56.466417	-2.828517	22-Aug-02	LGS.AP
D17	no	56.466400	-2.826883	22-Aug-02	SLR.MytX
D18	no	56.466067	-2.834133	22-Aug-02	SLR.MytX
D19	no	56.467767	-2.835483	22-Aug-02	SLR.EphX, LGS.AP
D20	no	56.469983	-2.836850	22-Aug-02	SLR.BLlit, LMS.PCer
D21	no	56.469983	-2.838367	22-Aug-02	MLR.FvesB
D22	no	56.469800	-2.840183	22-Aug-02	MLR.FvesB
D23	no	56.469133	-2.842533	22-Aug-02	MLR.FvesB
D24	no	56.467667	-2.845783	22-Aug-02	LGS.AP, SLR.FvesX
D25	no	56.466750	-2.846933	22-Aug-02	SLR.BLlit, SLR.MytX, SLR.FvesX
D26	no	56.465950	-2.847600	22-Aug-02	SLR.MytX, SLR.BLlit
D27	no	56.466150	-2.848800	22-Aug-02	SLR.MytX
D28	no	56.466467	-2.850283	22-Aug-02	LMS.Znol, SLR.MytX, SLR.Fves
D29	no	56.466750	-2.850633	22-Aug-02	LMS.Znol, SLR.MytX, SLR.Fves

Table 2 *(continued)*

Site	Sample	Latitude	Longitude	Date	Biotopes
D30	no	56.466467	-2.851767	22-Aug-02	LMS.Znol, SLR.MytX, SLR.Fves
D31	no	56.465300	-2.853017	22-Aug-02	LGS.AP, SLR.MytX, SLR.FvesX
D32	yes	56.464883	-2.851583	22-Aug-02	LGS.AP
D33	yes	56.464483	-2.858767	22-Aug-02	LMS.MacAre
D34	no	56.465250	-2.859400	22-Aug-02	LMS.Znol, LMS.MacAre
D35	no	56.465500	-2.859750	22-Aug-02	LMS.MacAre, LGS.AEur
D36	yes	56.465617	-2.859950	22-Aug-02	LGS.AEur
D37	no	56.464717	-2.861333	22-Aug-02	LMS.MacAre, LGS.AEur
D38	no	56.463583	-2.863367	22-Aug-02	LMS.MacAre, LGS.AEur
D39	no	56.462600	-2.868383	22-Aug-02	MLR.EntPor, SLR.Asc, SLR.Fves, SLR.Fspi, SLR.Pel, LR.YG
D40	no	56.462533	-2.868733	22-Aug-02	SLR.Asc, MLR.FvesB, SLR.Fspi, SLR.Pel, LR.YG
D41	no	56.465700	-2.860117	22-Aug-02	LGS.Tal
D42	no	56.465883	-2.860383	22-Aug-02	LGS.Tal
D43	no	56.466317	-2.857500	22-Aug-02	LMS.Znol, LMS.MacAre
D44	no	56.466733	-2.855933	22-Aug-02	LMS.Znol, LMS.MacAre
D45	no	56.467450	-2.853200	22-Aug-02	SLR.EphX, LMS.MacAre, LGS.AEur
D46	no	56.467117	-2.851950	22-Aug-02	SLR.FvesX, LMS.MacAre
D47	no	56.466817	-2.850933	22-Aug-02	LMS.Znol, SLR.MytX, SLR.Fves
D48	no	56.467333	-2.848700	22-Aug-02	LGS.AP, LMS.MacAre
D49	yes	56.468017	-2.846617	22-Aug-02	LGS.AEur
D50	no	56.468833	-2.845750	22-Aug-02	LMS.MacAre
D51	no	56.470317	-2.843567	22-Aug-02	SLR.Fves, LMS.MacAre
D52	no	56.472067	-2.840717	22-Aug-02	SLR.EphX, LMS.MacAre
D53	no	56.451150	-3.074600	22-Aug-02	SLR.FvesX, MLR.Ent, saltmarsh, LR.YG
D54	no	56.450983	-3.074500	22-Aug-02	LMU.HedMac, SLR.FvesX
D55	no	56.451100	-3.072967	22-Aug-02	LMU.HedMac, Reeds
D56	no	56.450550	-3.068133	22-Aug-02	LMU.HedMac, SLR.FvesX, SLR.Pel
D57	yes	56.450467	-3.068083	22-Aug-02	LMU.HedMac
D58	no	56.450667	-3.067717	22-Aug-02	SLR.FvesX, saltmarsh
D59	no	56.451367	-2.996200	22-Aug-02	SLR.Asc.VS, SLR.Asc, SLR.Fspi, SLR.Pel, LR.YG
D60	no	56.452083	-2.983283	22-Aug-02	SLR.Asc, SLR.Fspi, SLR.Pel, LR.YG
D61	no	56.453900	-2.974350	22-Aug-02	SLR.Asc.VS, SLR.Asc, SLR.Fspi, SLR.Pel, LR.YG
D62	yes	56.370267	-2.824750	23-Aug-02	LGS.AP
D63	no	56.371383	-2.826800	23-Aug-02	LMS.PCer, LGS.AP

Table 2 *(continued)*

Site	Sample	Latitude	Longitude	Date	Biotopes
D64	yes	56.373250	-2.830150	23-Aug-02	LMS.PCer
D65	no	56.374933	-2.832900	23-Aug-02	LGS.Tal, LMS.PCer
D66	yes	56.374967	-2.832967	23-Aug-02	LGS.Tal
D67	no	56.368433	-2.849600	23-Aug-02	LMS.MacAre
D68	no	56.367833	-2.848883	23-Aug-02	SLR.MytX, LMU.HedMac.Are
D69	no	56.367467	-2.848517	23-Aug-02	SLR.MytX, LMU.HedMac
D70	yes	56.366950	-2.848317	23-Aug-02	LMU.HedMac
D71	no	56.367500	-2.848350	23-Aug-02	SLR.MytX, LMU.HedMac
D72	no	56.368050	-2.848550	23-Aug-02	SLR.MytX, LMU.HedMac.Are
D73	yes	56.368883	-2.848933	23-Aug-02	LMS.MacAre
D74	no	56.368833	-2.843667	23-Aug-02	Algal mat, LMU.HedMac.Are
D75	no	56.368783	-2.842800	23-Aug-02	Algal mat, LMU.HedMac
D76	no	56.368417	-2.842817	23-Aug-02	Algal mat, LMU.HedMac
D77	no	56.367800	-2.842767	23-Aug-02	SLR.FvesX, SLR.MytX
D78	no	56.367400	-2.842833	23-Aug-02	SLR.FvesX, SLR.MytX
D79	no	56.366767	-2.842883	23-Aug-02	SLR.MytX
D80	no	56.367250	-2.844050	23-Aug-02	SLR.FvesX, SLR.MytX
D81	no	56.367683	-2.844950	23-Aug-02	LMU.HedMac.Are, SLR.FvesX, SLR.MytX
D82	no	56.369917	-2.849550	23-Aug-02	LGS.Tal, LMS.MacAre
D83	no	56.369017	-2.852983	23-Aug-02	LGS.Tal
D84	no	56.368783	-2.853250	23-Aug-02	LMS.MacAre, LGS.Tal
D85	no	56.368433	-2.853683	23-Aug-02	SLR.MytX, LMU.HedMac.Are
D86	no	56.368200	-2.853867	23-Aug-02	SLR.MytX
D87	yes	56.367533	-2.868450	23-Aug-02	LMU.HedMac
D88	no	56.367867	-2.868150	23-Aug-02	SLR.Pel, SLR.Fspi, SLR.AscX
D89	no	56.367933	-2.868067	23-Aug-02	SLR.Pel, SLR.Fspi, SLR.AscX
D90	no	56.367067	-2.867117	23-Aug-02	SLR.FvesX, LMU.HedMac
D91	no	56.366733	-2.865817	23-Aug-02	SLR.FvesX
D92	no	56.366633	-2.865100	23-Aug-02	SLR.FvesX
D93	no	56.365867	-2.863467	23-Aug-02	SLR.MytX, LMU.HedMac.Are
D94	no	56.366550	-2.863317	23-Aug-02	SLR.MytX, LMU.HedMac.Are
D95	no	56.366800	-2.862983	23-Aug-02	SLR.MytX
D96	no	56.367833	-2.863800	23-Aug-02	Algal mat, SLR.MytX, LMU.HedMac.Are
D97	yes	56.368250	-2.864400	23-Aug-02	Algal mat, LMU.HedMac.Are
D98	no	56.368367	-2.864817	23-Aug-02	LMS.MacAre, Algal mat

Table 2 *(continued)*

Site	Sample	Latitude	Longitude	Date	Biotopes
D99	no	56.368583	-2.865867	23-Aug-02	reeds, LMS.MacAre
D100	no	56.453300	-2.889900	23-Aug-02	SLR.FvesX, SLR.Asc, SLR.Fspi, SLR.Pel, LR.YG
D101	no	56.453133	-2.891167	23-Aug-02	SLR.Asc, SLR.Fspi, SLR.Pel, LR.YG
D102	no	56.453150	-2.892767	23-Aug-02	SLR.FvesX, SLR.Asc, SLR.Fspi, SLR.Pel, LR.YG
D103	no	56.440100	-2.941117	23-Aug-02	SLR.AscX, SLR.Asc, SLR.EphX, SLR.Fspi, SLR.Pel
D104	no	56.425733	-2.978350	23-Aug-02	SLR.FvesX, SLR.AscX, SLR.Asc, SLR.Fspi, SLR.Pel, LR.YG
D105	yes	56.425933	-2.978367	23-Aug-02	LMU.HedMac
D106	no	56.453283	-2.890083	23-Aug-02	SLR.FvesX
D107	yes	56.453483	-2.890233	23-Aug-02	LGS.AEur
D108	no	56.396700	-2.809800	24-Aug-02	LGS.Tal
D109	no	56.396700	-2.809167	24-Aug-02	LGS.Tal
D110	yes	56.396717	-2.809417	24-Aug-02	LGS.Tal
D111	yes	56.396700	-2.807550	24-Aug-02	LGS.AEur
D112	yes	56.396733	-2.804533	24-Aug-02	LGS.AP.Pon
D113	no	56.392233	-2.805267	24-Aug-02	LGS.AP, LGS.AEur
D114	no	56.387717	-2.805683	24-Aug-02	LGS.AP, LGS.AEur
D115	yes	56.387750	-2.806933	24-Aug-02	LGS.AEur
D116	no	56.387733	-2.808117	24-Aug-02	LGS.AEur
D117	no	56.387700	-2.811033	24-Aug-02	LGS.Tal
D118	no	56.387750	-2.812350	24-Aug-02	LGS.Tal
D119	yes	56.387733	-2.802800	24-Aug-02	LGS.AP.Pon
D120	no	56.385167	-2.805217	24-Aug-02	LGS.AP
D121	no	56.385933	-2.807917	24-Aug-02	LGS.AP, LGS.AEur
D122	no	56.384583	-2.809383	24-Aug-02	LGS.AP
D123	no	56.384017	-2.811917	24-Aug-02	LGS.AP
D124	yes	56.380500	-2.819267	24-Aug-02	LGS.AP
D125	no	56.380650	-2.819550	24-Aug-02	SLR.Fspi, SLR.Pel
D126	no	56.381233	-2.821333	24-Aug-02	LGS.AEur, LGS.Tal
D127	no	56.381633	-2.822117	24-Aug-02	LGS.Tal
D128	yes	56.405950	-2.803150	24-Aug-02	LGS.AP.Pon
D129	no	56.406183	-2.805800	24-Aug-02	LGS.AEur
D130	yes	56.406200	-2.806117	24-Aug-02	LGS.AEur
D131	no	56.406367	-2.806733	24-Aug-02	LGS.Tal
D132	no	56.406567	-2.807650	24-Aug-02	LGS.Tal

Table 2 *(continued)*

Site	Sample	Latitude	Longitude	Date	Biotopes
D133	no	56.446317	-2.869100	25-Aug-02	SLR.FvesX, SLR.Fspi, SLR.Pel
D134	no	56.446400	-2.869067	25-Aug-02	SLR.FvesX, SLR.EphX, LMS.Znol
D135	no	56.446717	-2.868867	25-Aug-02	LMS.MacAre, SLR.FvesX, SLR.EphX, LMS.Znol
D136	no	56.446900	-2.868733	25-Aug-02	LMS.MacAre, LMS.Znol
D137	yes	56.447800	-2.868050	25-Aug-02	LMS.MacAre, LMS.Znol
D138	no	56.449067	-2.866967	25-Aug-02	LMS.MacAre
D139	no	56.449900	-2.868100	25-Aug-02	LMS.MacAre
D140	yes	56.451383	-2.868550	25-Aug-02	LMS.MacAre
D141	no	56.451133	-2.868833	25-Aug-02	SLR.FserX
D142	no	56.451333	-2.870150	25-Aug-02	SLR.FserX, LMS.MacAre
D143	no	56.451417	-2.870817	25-Aug-02	SLR.EphX, SLR.BLlit, SLR.FvesX
D144	no	56.451633	-2.871517	25-Aug-02	LMS.MacAre, SLR.FvesX, SLR.EphX
D145	no	56.451750	-2.872050	25-Aug-02	LMS.MacAre
D146	no	56.451950	-2.875833	25-Aug-02	SLR.FserX, SLR.FvesX, LMS.MacAre
D147	no	56.450667	-2.875517	25-Aug-02	SLR.FvesX, LMU.HedMac, LMS.MacAre
D148	no	56.450433	-2.875567	25-Aug-02	SLR.FvesX
D149	no	56.450367	-2.875800	25-Aug-02	SLR.Asc, SLR.Fspi, SLR.Pel, LR.YG
D150	yes	56.450750	-2.875117	25-Aug-02	LMU.HedMac
D151	no	56.450383	-2.875283	25-Aug-02	SLR.FvesX, LMU.HedMac
D152	no	56.450383	-2.873750	25-Aug-02	SLR.FvesX, LMU.HedMac, LMS.MacAre
D153	no	56.450400	-2.873583	25-Aug-02	SLR.FvesX, SLR.Fspi
D154	no	56.450317	-2.873300	25-Aug-02	LMS.MacAre
D155	no	56.450300	-2.870500	25-Aug-02	LMS.MacAre
D156	no	56.450467	-2.867667	25-Aug-02	LMS.MacAre
D157	no	56.450517	-2.862683	25-Aug-02	SLR.MytX, SLR.FvesX, LMS.MacAre
D158	no	56.450433	-2.861133	25-Aug-02	SLR.MytX, SLR.FvesX, LMS.MacAre
D159	no	56.450133	-2.859050	25-Aug-02	SLR.MytX, LMS.MacAre
D160	no	56.450050	-2.858683	25-Aug-02	SLR.MytX
D161	no	56.449800	-2.858900	25-Aug-02	SLR.FvesX
D162	no	56.449267	-2.858633	25-Aug-02	SLR.EphX
D163	no	56.449800	-2.857433	25-Aug-02	SLR.EphX, SLR.FvesX
D164	no	56.449883	-2.857150	25-Aug-02	SLR.MytX, SLR.FvesX
D165	no	56.450400	-2.855633	25-Aug-02	SLR.MytX, SLR.FvesX
D166	no	56.450250	-2.855183	25-Aug-02	LGS.AP, SLR.EphX, SLR.MytX, SLR.FvesX
D167	yes	56.450250	-2.853200	25-Aug-02	LGS.AP

Table 2 *(continued)*

Site	Sample	Latitude	Longitude	Date	Biotopes
D168	no	56.449283	-2.853767	25-Aug-02	SLR.MytX
D169	no	56.449017	-2.852050	25-Aug-02	SLR.MytX
D170	no	56.449483	-2.852250	25-Aug-02	SLR.MytX
D171	no	56.449667	-2.851633	25-Aug-02	LGS.AP
D172	no	56.449700	-2.851050	25-Aug-02	SLR.MytX
D173	no	56.449100	-2.851117	25-Aug-02	SLR.MytX
D174	no	56.448433	-2.851017	25-Aug-02	SLR.MytX, SLR.FvesX
D175	no	56.447900	-2.851117	25-Aug-02	SLR.MytX
D176	no	56.446983	-2.851267	25-Aug-02	LMU.HedMac
D177	no	56.446483	-2.851050	25-Aug-02	LMU.HedMac
D178	no	56.446600	-2.850050	25-Aug-02	LMU.HedMac
D179	no	56.446767	-2.849133	25-Aug-02	SLR.FvesX, LMS.Znol, LMU.HedMac.Are
D180	no	56.445883	-2.850600	25-Aug-02	LMU.HedMac.Are, LMU.HedMac
D181	no	56.445067	-2.849967	25-Aug-02	LMS.Znol, LMS.MacAre
D182	yes	56.442533	-2.847567	25-Aug-02	LMS.Znol, LMS.MacAre
D183	no	56.441000	-2.847117	25-Aug-02	LMS.Znol, LMS.MacAre
D184	no	56.440517	-2.846933	25-Aug-02	LMS.MacAre
D185	no	56.439917	-2.846533	25-Aug-02	LGS.Tal
D186	no	56.439767	-2.848783	25-Aug-02	LMS.MacAre, reeds
D187	no	56.440000	-2.850450	25-Aug-02	LMS.MacAre
D188	no	56.442100	-2.858267	25-Aug-02	LMS.MacAre
D189	no	56.443950	-2.861750	25-Aug-02	LMS.MacAre
D190	no	56.444850	-2.863733	25-Aug-02	SLR.EphX
D191	no	56.444317	-2.864667	25-Aug-02	LMU.NVC SM8, SLR.EphX
D192	no	56.444433	-2.864983	25-Aug-02	LMU.NVC SM8
D193	no	56.445150	-2.865733	25-Aug-02	LMS.MacAre
D194	no	56.445750	-2.867283	25-Aug-02	LMS.Znol, LMS.MacAre
D195	no	56.445867	-2.867883	25-Aug-02	SLR.FvesX
D196	no	56.446300	-2.868250	25-Aug-02	SLR.FvesX, SLR.EphX
D197	no	56.352650	-3.245100	25-Aug-02	LMU.HedOl, reeds
D198	no	56.352600	-3.247717	25-Aug-02	LMU.HedOl, reeds
D199	no	56.350833	-3.259267	25-Aug-02	LMU.HedOl, reeds
D200	yes	56.367717	-3.188317	26-Aug-02	LMU.HedOl, reeds
D201	yes	56.367667	-3.188133	26-Aug-02	LMU.HedOl
D202	yes	56.371800	-3.181900	26-Aug-02	LGS.Ol

Table 2 *(continued)*

Site	Sample	Latitude	Longitude	Date	Biotopes
D203	no	56.372417	-3.181250	26-Aug-02	LGS.Ol
D204	no	56.371483	-3.181600	26-Aug-02	LMU.HedOl, LGS.Ol
D205	no	56.371250	-3.181250	26-Aug-02	LMU.HedOl, reeds
D206	no	56.373667	-3.175433	26-Aug-02	LMU.HedOl, reeds
D207	no	56.374450	-3.172317	26-Aug-02	LMU.HedOl, reeds
D208	no	56.374850	-3.170800	26-Aug-02	LGS.Ol, LMU.HedOl, reeds
D209	no	56.375383	-3.167350	26-Aug-02	LGS.Ol
D210	no	56.375783	-3.166950	26-Aug-02	LMU.HedOl
D211	no	56.376350	-3.165133	26-Aug-02	LMU.HedOl
D212	no	56.377717	-3.159433	26-Aug-02	LMU.HedOl
D213	yes	56.380000	-3.153900	26-Aug-02	LMU.HedOl
D214	no	56.379667	-3.153400	26-Aug-02	LMU.HedOl, reeds
D215	yes	56.379567	-3.153283	26-Aug-02	saltmarsh, SLR.FvesX, LGS.Ol
D217	no	56.379433	-3.153150	26-Aug-02	terrestrial
D218	no	56.380567	-3.151483	26-Aug-02	saltmarsh, SLR.FvesX, LMU.HedOl
D219	no	56.383083	-3.145550	26-Aug-02	reeds, saltmarsh, SLR.FvesX, IMU.HedOl
D220	yes	56.383900	-3.142667	26-Aug-02	LMU.HedOl, SLR.FvesX, IMU.HedOl
D221	yes	56.384917	-3.140900	26-Aug-02	LMU.HedOl
D222	no	56.384050	-3.139833	26-Aug-02	LMU.HedOl
D223	no	56.383650	-3.139367	26-Aug-02	reeds, saltmarsh, LMU.HedOl
D224	no	56.385533	-3.135183	26-Aug-02	SLR.FvesX, LMU.HedOl
D225	no	56.386067	-3.132600	26-Aug-02	LMU.HedOl
D226	no	56.385467	-3.131917	26-Aug-02	LMU.HedOl, SLR.FvesX, LGS.Ol
D227	no	56.386367	-3.129333	26-Aug-02	LMU.HedOl, SLR.FvesX, LGS.Ol
D228	no	56.387267	-3.125867	26-Aug-02	LMU.HedOl, SLR.FvesX, LGS.Ol
D229	no	56.388067	-3.124217	26-Aug-02	LMU.HedOl, SLR.FvesX, LGS.Ol
M1	no	56.470917	-2.828450	22-Aug-02	SLR.EphX, LMS.PCer
M2	no	56.471317	-2.826883	22-Aug-02	SLR.FserX
M3	yes	56.470633	-2.829350	22-Aug-02	LMS.PCer
M4	no	56.472617	-2.832050	22-Aug-02	LMS.MacAre, SLR.MytX, SLR.Fves
M5	no	56.474250	-2.832950	22-Aug-02	SLR.MytX, SLR.Fser, SLR.Fves
M6	yes	56.474700	-2.828133	22-Aug-02	LMS.MacAre
M7	yes	56.474350	-2.827900	22-Aug-02	LMS.MacAre
M8	no	56.475200	-2.824450	22-Aug-02	SLR.MytX, SLR.FvesX
M9	no	56.475917	-2.821433	22-Aug-02	SLR.FvesX

Table 2 *(continued)*

Site	Sample	Latitude	Longitude	Date	Biotopes
M10	no	56.476783	-2.819333	22-Aug-02	SLR.FvesX
M11	no	56.477317	-2.815500	22-Aug-02	SLR.FvesX
M12	no	56.478083	-2.812367	22-Aug-02	SLR.FvesX, SLR.EphX
M13	no	56.478150	-2.816767	22-Aug-02	SLR.FvesX
M14	yes	56.475200	-2.829483	22-Aug-02	LMS.MacAre
M15	yes	56.476167	-2.830633	22-Aug-02	LGS.Tal, LGS.AEur
M16	yes	56.464533	-2.870933	22-Aug-02	LGS.Tal
M17	no	56.464583	-2.871400	22-Aug-02	SLR.FvesX
M18	no	56.465400	-2.877983	22-Aug-02	LGS.Ol
M19	no	56.465300	-2.878167	22-Aug-02	SLR.EphX, SLR.FvesX
M20	no	56.467533	-2.883300	22-Aug-02	LGS.Ol
M21	no	56.467483	-2.883450	22-Aug-02	SLR.EphX
M22	no	56.467467	-2.883700	22-Aug-02	SLR.EphX, SLR.FvesX
M23	yes	56.467800	-2.884383	22-Aug-02	LGS.AEur
M24	no	56.467583	-2.911967	22-Aug-02	LGS.Ol
M25	no	56.467483	-2.911950	22-Aug-02	SLR.EphX, SLR.FvesX
M26	no	56.468200	-2.892550	22-Aug-02	LGS.Ol
M27	no	56.468100	-2.892617	22-Aug-02	SLR.EphX, SLR.FvesX
M28	yes	56.464167	-2.871050	22-Aug-02	LMS.MacAre, SLR.FvesX
M29	no	56.465217	-2.878167	22-Aug-02	SLR.EphX
M30	no	56.467183	-2.884183	22-Aug-02	SLR.FvesX
M31	yes	56.467550	-2.884867	22-Aug-02	LMS.MacAre
M32	no	56.468000	-2.892400	22-Aug-02	SLR.Fser.VS, SLR.FvesX
M33	no	56.467267	-2.911383	22-Aug-02	SLR.FvesX
M34	no	56.367783	-2.821683	23-Aug-02	SLR.FvesX
M35	yes	56.369450	-2.821017	23-Aug-02	LMS.MacAre
M36	no	56.368433	-2.821200	23-Aug-02	SLR.EphX
M37	no	56.367817	-2.821017	23-Aug-02	SLR.EphX
M38	no	56.367467	-2.821500	23-Aug-02	SLR.FvesX, SLR.EphX
M39	no	56.367033	-2.821533	23-Aug-02	SLR.FvesX, SLR.EphX
M40	no	56.366383	-2.822000	23-Aug-02	LGS.Lan
M41	yes	56.365100	-2.822800	23-Aug-02	LMS.MacAre
M42	no	56.364067	-2.823550	23-Aug-02	LMS.MacAre, Algal mat
M43	no	56.363867	-2.823867	23-Aug-02	LMS.MacAre
M44	yes	56.363717	-2.824383	23-Aug-02	LMU.HedMac.Are

Table 2 *(continued)*

Site	Sample	Latitude	Longitude	Date	Biotopes
M45	no	56.363217	-2.825617	23-Aug-02	LMU.HedMac.Are, Algal mat
M46	no	56.362467	-2.827017	23-Aug-02	SLR.MytX, LMU.HedMac.Are
M47	no	56.362883	-2.828800	23-Aug-02	SLR.MytX
M48a	no	56.361700	-2.827700	23-Aug-02	LMU.HedMac, Algal mat
M48b	no	56.361183	-2.827367	23-Aug-02	SLR.FvesX, SLR.MytX
M49	no	56.361250	-2.825200	23-Aug-02	LMU.HedMac.Are
M50	no	56.361800	-2.823650	23-Aug-02	SLR.Fspi
M51	no	56.366783	-2.820683	23-Aug-02	LGS.Tal
M52	no	56.363733	-2.858817	23-Aug-02	LMU.HedMac.Are, LMS.Znol
M53	yes	56.366583	-2.855467	23-Aug-02	LMU.HedMac.Are
M54	no	56.366267	-2.855300	23-Aug-02	SLR.FvesX, SLR.MytX
M55	no	56.366250	-2.856533	23-Aug-02	SLR.MytX
M56	yes	56.364350	-2.858567	23-Aug-02	LMU.HedMac.Are
M57	yes	56.363750	-2.863050	23-Aug-02	LMU.HedMac.Are
M58	yes	56.364150	-2.864367	23-Aug-02	LMU.HedMac.Are
M59	no	56.363900	-2.866967	23-Aug-02	SLR.FvesX, SLR.EphX
M60	no	56.362550	-2.865250	23-Aug-02	SLR.EphX
M61	no	56.363800	-2.862667	23-Aug-02	LGS.Tal
M62	no	56.411167	-2.805500	24-Aug-02	LGS.Tal
M63	no	56.411150	-2.805300	24-Aug-02	LGS.AEur, LGS.Tal
M64	no	56.411217	-2.804017	24-Aug-02	LGS.AEur
M65	no	56.411250	-2.803500	24-Aug-02	LGS.AEur
M66	no	56.411400	-2.801983	24-Aug-02	LGS.AEur
M67	no	56.411267	-2.801083	24-Aug-02	LGS.AEur
M68	yes	56.416600	-2.797783	24-Aug-02	LGS.AP.Pon
M69	no	56.416750	-2.798467	24-Aug-02	LGS.AP, LGS.AEur
M70	no	56.416933	-2.799500	24-Aug-02	LGS.AEur
M71	yes	56.417000	-2.800417	24-Aug-02	LGS.AEur
M72	no	56.417100	-2.801800	24-Aug-02	LGS.AEur
M73	no	56.416883	-2.802183	24-Aug-02	LGS.AEur
M74	yes	56.416533	-2.802600	24-Aug-02	LGS.AEur
M75	no	56.416867	-2.803117	24-Aug-02	LGS.AEur
M76	no	56.416850	-2.803583	24-Aug-02	LGS.Tal
M77	no	56.416850	-2.804083	24-Aug-02	LGS.Tal
M78	no	56.429600	-2.800800	24-Aug-02	LGS.AEur

Table 2 *(continued)*

Site	Sample	Latitude	Longitude	Date	Biotopes
M79	no	56.429500	-2.801233	24-Aug-02	LGS.AEur
M80	no	56.429417	-2.801517	24-Aug-02	LGS.AEur
M81	no	56.429217	-2.802483	24-Aug-02	LGS.AEur
M82	no	56.429133	-2.802867	24-Aug-02	LGS.AEur
M83	no	56.429200	-2.803650	24-Aug-02	LGS.AEur
M84	no	56.429283	-2.804117	24-Aug-02	LGS.Tal
M85	no	56.449350	-2.811817	24-Aug-02	LGS.AP
M86	no	56.449100	-2.811917	24-Aug-02	LGS.AEur
M87	no	56.448783	-2.812133	24-Aug-02	LGS.AEur
M88	no	56.448467	-2.812400	24-Aug-02	LGS.AEur
M89	no	56.446933	-2.814650	24-Aug-02	LGS.AP
M90	no	56.445733	-2.815767	24-Aug-02	LGS.AEur
M91	no	56.444283	-2.817117	24-Aug-02	LGS.AEur
M92	no	56.443867	-2.817433	24-Aug-02	LGS.Tal
M93	yes	56.447317	-2.820233	25-Aug-02	LGS.AEur
M94	yes	56.447517	-2.820500	25-Aug-02	LGS.AP
M95	yes	56.446967	-2.822133	25-Aug-02	LMS.MacAre
M96	no	56.447367	-2.822083	25-Aug-02	SLR.MytX, SLR.FvesX, LMS.MacAre
M97	no	56.447583	-2.822000	25-Aug-02	SLR.MytX, SLR.FvesX
M98	no	56.447933	-2.821750	25-Aug-02	SLR.EphX, SLR.MytX, SLR.FvesX
M99	no	56.448117	-2.821467	25-Aug-02	SLR.EphX
M100	no	56.447533	-2.824200	25-Aug-02	SLR.MytX, SLR.FvesX
M101	yes	56.447950	-2.823917	25-Aug-02	SLR.EphX
M102	no	56.448700	-2.822700	25-Aug-02	LGS.AP
M103	no	56.449567	-2.824050	25-Aug-02	SLR.EphX, LMS.MacAre
M104	no	56.449717	-2.823517	25-Aug-02	SLR.FserX, SLR.EphX, SLR.MytX, SLR.FvesX
M105	no	56.449550	-2.825233	25-Aug-02	?
M106	no	56.449283	-2.826867	25-Aug-02	SLR.MytX
M107	no	56.448900	-2.828583	25-Aug-02	SLR.MytX, SLR.FvesX
M108	no	56.448017	-2.829033	25-Aug-02	SLR.MytX, SLR.FvesX
M109	yes	56.447967	-2.830867	25-Aug-02	SLR.EphX, LMS.MacAre
M110	no	56.448317	-2.831083	25-Aug-02	LGS.Lan, SLR.MytX
M111	no	56.447833	-2.836500	25-Aug-02	SLR.EphX, SLR.FvesX
M112	no	56.448167	-2.836633	25-Aug-02	SLR.MytX, SLR.FvesX
M113	no	56.447483	-2.836517	25-Aug-02	SLR.EphX, SLR.FvesX

Table 2 *(continued)*

Site	Sample	Latitude	Longitude	Date	Biotopes
M114	no	56.447550	-2.839333	25-Aug-02	SLR.FvesX
M115	no	56.447283	-2.841717	25-Aug-02	Algal mat, LMU.HedMac.Are
M116	yes	56.446167	-2.842650	25-Aug-02	SLR.EphX, SLR.FvesX
M117	no	56.445217	-2.841433	25-Aug-02	LMS.Znol, LMS.MacAre
M118	yes	56.443767	-2.839900	25-Aug-02	LMS.Znol, LMS.MacAre
M119	no	56.442717	-2.837983	25-Aug-02	LMS.MacAre
M120	no	56.441983	-2.836667	25-Aug-02	LGS.Tal
M121	no	56.442517	-2.833933	25-Aug-02	LMS.Znol
M122	yes	56.438333	-2.800817	25-Aug-02	LGS.AEur
M123	no	56.438350	-2.801417	25-Aug-02	LGS.Tal
M124	yes	56.421433	-2.987550	26-Aug-02	LGS.Ol
M125	yes	56.421667	-2.987950	26-Aug-02	LMU.HedMac
M126	no	56.421483	-2.987633	26-Aug-02	SLR.AscX, SLR.FvesX
M127	no	56.420833	-2.989233	26-Aug-02	SLR.AscX, SLR.FvesX, SLR.Fspi, SLR.Pel, LR.YG
M128	no	56.420150	-2.993417	26-Aug-02	LGS.Ol
M129	no	56.420217	-2.993433	26-Aug-02	LMU.HedMac
M130	no	56.420250	-2.993517	26-Aug-02	SLR.AscX, SLR.FvesX
M131	no	56.420817	-2.997750	26-Aug-02	SLR.Fspi, SLR.Pel, LR.YG
M132	no	56.420900	-2.997767	26-Aug-02	SLR.AscX, SLR.FvesX
M133	no	56.420983	-2.997817	26-Aug-02	LMU.HedMac, SLR.FvesX
M134	yes	56.421433	-2.997917	26-Aug-02	LMU.HedMac
M135	no	56.421017	-3.000283	26-Aug-02	LMU.HedMac, SLR.FvesX
M136	yes	56.420533	-3.001283	26-Aug-02	LMU.HedMac
M137	no	56.420417	-3.001150	26-Aug-02	SLR.AscX, SLR.FvesX, SLR.Fspi, SLR.Pel
M138	yes	56.421067	-3.001483	26-Aug-02	LMU.HedMac
M139	no	56.419333	-3.008700	26-Aug-02	LMU.HedMac
M140	no	56.419383	-3.008700	26-Aug-02	SLR.AscX, SLR.FvesX
M141	no	56.417583	-3.014750	26-Aug-02	SLR.AscX, SLR.FvesX
M142	no	56.417650	-3.014917	26-Aug-02	LMU.HedMac
M143	no	56.418617	-3.024133	26-Aug-02	LMU.HedMac.Are
M144	no	56.417633	-3.022683	26-Aug-02	SLR.AscX, SLR.FvesX
C1	no	56.466841	-2.750609900	22-Sep-02	LGS.Tal
C2	no	56.466708	-2.750743200	22-Sep-02	LGS.AEur, LGS.Tal
C3	yes	56.466625	-2.750826600	22-Sep-02	LGS.AEur
C4	no	56.466541	-2.750926600	22-Sep-02	LGS.AEur

Table 2 *(continued)*

Site	Sample	Latitude	Longitude	Date	Biotopes
C5	yes	56.466441	-2.751026600	22-Sep-02	LGS.AEur
C6	no	56.466308	-2.751126600	22-Sep-02	LGS.AEur
C7	yes	56.466058	-2.751343300	22-Sep-02	LGS.AEur
C8	no	56.465925	-2.751426700	22-Sep-02	LGS.AP.P, LGS.AEur
C9	yes	56.465808	-2.751493300	22-Sep-02	LGS.AP.P
C10	no	56.468425	-2.722290100	22-Sep-02	LGS.AP.P
C11	yes	56.468475	-2.722790200	22-Sep-02	LGS.AP.P
C12	no	56.468658	-2.723606900	22-Sep-02	LGS.AEur, LGS.AP.P
C13	yes	56.468758	-2.724023600	22-Sep-02	LGS.AEur
C14	no	56.468791	-2.724290300	22-Sep-02	LGS.AEur
C15	yes	56.468858	-2.724640300	22-Sep-02	LGS.AEur
C16	no	56.468908	-2.724973700	22-Sep-02	LGS.AEur
C17	yes	56.468991	-2.725623800	22-Sep-02	LGS.AEur
C18	no	56.469075	-2.726040500	22-Sep-02	LGS.AEur
C19	yes	56.469091	-2.726157200	22-Sep-02	LGS.AEur
C20	no	56.469141	-2.726340500	22-Sep-02	LGS.AEur
C21	yes	56.469191	-2.726723900	22-Sep-02	LGS.AEur
C22	no	56.469241	-2.727057300	22-Sep-02	LGS.AEur, LGS.Tal
C23	no	56.469308	-2.727240600	22-Sep-02	LGS.Tal
C24	no	56.464891	-2.728624300	22-Sep-02	LGS.AEur
C25	no	56.465691	-2.730557800	22-Sep-02	LGS.AEur, LGS.Tal
C26	no	56.465824	-2.730824500	22-Sep-02	LGS.Tal
C27	no	56.464924	-2.733258100	22-Sep-02	LGS.Tal
C28	no	56.464741	-2.733191400	22-Sep-02	LGS.AEur, LGS.Tal
C29	no	56.464458	-2.733058100	22-Sep-02	LGS.AEur
C30	no	56.464158	-2.732958100	22-Sep-02	LGS.AEur
C31	no	56.463974	-2.732908100	22-Sep-02	LGS.AEur
C32	no	56.463774	-2.732774700	22-Sep-02	LGS.AEur
C33	no	56.463608	-2.741225700	22-Sep-02	LGS.AEur
C34	no	56.463974	-2.741042300	22-Sep-02	LGS.AEur
C35	no	56.464208	-2.740925600	22-Sep-02	LGS.AEur
C36	no	56.464341	-2.740858900	22-Sep-02	LGS.AEur
C37	no	56.464524	-2.740825600	22-Sep-02	LGS.AEur, LGS.Tal
C38	no	56.464641	-2.740792200	22-Sep-02	LGS.Tal
C39	no	56.465108	-2.743709200	22-Sep-02	LGS.Tal

Table 2 *(continued)*

Site	Sample	Latitude	Longitude	Date	Biotopes
C40	no	56.464941	-2.743792600	22-Sep-02	LGS.AEur, LGS.Tal
C41	no	56.464708	-2.743909200	22-Sep-02	LGS.AEur
C42	no	56.464424	-2.744009300	22-Sep-02	LGS.AEur
C43	no	56.478717	-2.811500	25-Dec-02	LGS.AP, SLR.Fspi
C44	no	56.477767	-2.812167	25-Dec-02	SLR.EphX
C45	no	56.477517	-2.812333	25-Dec-02	LGS.AP
C46	no	56.478467	-2.808783	25-Dec-02	LGS.AP
C47	no	56.476850	-2.807517	25-Dec-02	LGS.AP
C48	no	56.477050	-2.803917	25-Dec-02	LGS.AEur
C49	no	56.477150	-2.803350	25-Dec-02	LGS.AP
C50	no	56.478517	-2.798283	25-Dec-02	SLR.FvesX
C51	no	56.476667	-2.795050	25-Dec-02	LGS.AP
C52	no	56.478150	-2.793917	25-Dec-02	LGS.AP
C53	no	56.478400	-2.793800	25-Dec-02	LGS.AP
C54	no	56.478667	-2.794083	25-Dec-02	LGS.AP
C55	no	56.478950	-2.793750	25-Dec-02	LGS.AP
C56	no	56.479283	-2.793533	25-Dec-02	LGS.AEur, LGS.AP
C57	no	56.479517	-2.793450	25-Dec-02	LGS.Tal, LGS.AEur
C58	no	56.479600	-2.793467	25-Dec-02	LGS.Tal
C59	no	56.479150	-2.801267	25-Dec-02	LGS.AEur, LGS.AP
C60	no	56.478600	-2.805833	25-Dec-02	LGS.AEur
C61	no	56.447967	-2.932300	25-Dec-02	LR.YG, SLR.Pel, SLR.Fspi, SLR.Asc, SLR.FvesX, LMU.HedMac
C62	no	56.450700	-2.923336	25-Dec-02	LR.YG, SLR.Pel, SLR.Fspi, SLR.Asc, SLR.FvesX, LMU.HedMac
C63	no	56.453050	-2.888600	25-Dec-02	LR.YG, SLR.Pel, SLR.Fspi, SLR.Asc, SLR.FvesX, LMS.MacAre
C64	no	56.453183	-2.891133	25-Dec-02	LR.YG, SLR.Pel, SLR.Fspi, SLR.Asc, SLR.FvesX, LMS.MacAre

Table 3 Biotopes recorded during survey of Firth of Tay and Eden Estuary cSAC. Emboldened stations indicate the origin of the video or still photographic image

Biotope	Station	Video frame
Algal mat on sediment	D74, D75, D76, D96, D97, D98, M42, M45, M48a, **M115**	
ECR.PomByC	27, 68	
IGS.Lcon	26, 28, **29**, 30, 31, 32	
IGS.MobRS	1, 2, 3, 4, **8**, 9, 10, 11, 13, 14, 19, 20, 35, 36, 37, 43, 44, 45, 49, 54, 62	
IGS.Ncir	38	
IGS.NeoGam	**5**, 6, 7	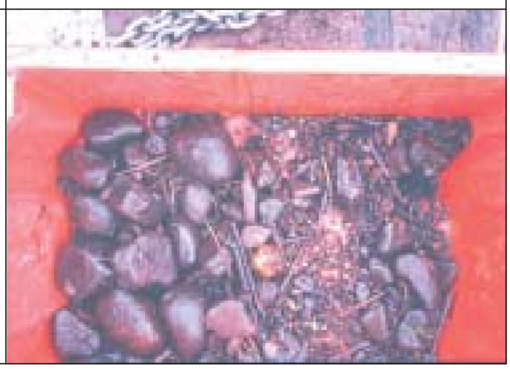

Table 3 *(continued)*

Biotope	Station	Video frame
IMU.CapTub	17, 46	
IMU.HedOl	D219, D220	
IMU.Tub	16, 18	
IMX.MytV	12, 15, 21, 22, 23, 24, **33**	 
LGS.AEur	39, 40, 41, 42, 61, WS11, D35, D36, D37, D38, D45, D49, M15, M23, D107, D111, D113, D114, D115, D116, D121, D126, D129, D130, M63, M64, M65, M66, M67, M69, M70, M71, M72, M73, M74, M75, M78, **M79**, M80, M81, M82, M83, M86, M87, M88, M90, M91, M93, M122, C2, C3, C4, C5, C6, C7, C8, C12, C13, C14, C15, C16, C17, C18, C19, C20, C21, C22, C24, C25, C28, C29, C30, C31, C32, C33, C34, C35, C36, C37, C40, C41, C42, C48, C56, C57, C59, C60	

Table 3 *(continued)*

Biotope	Station	Video frame
LGS.AP	D12, D13, D15, D16, D19, D24, D31, D32, D48, D62, D63, D113, D114, D120, D121, D122, D123, D124, M69, M85, **M89**, D166, D167, D171, M94, M102, C43, C45, C46, C47, C49, C51, C52, C53, C54, C55, C56, C59	
LGS.AP.P	WS15, WS16, WS17, WS18, WS21, WS22, C8, C9, C10, C11, C12	
LGS.AP.Pon	WS5, WS6, WS7, WS9, WS20, D112, D119, D128, M68	
LGS.Lan	M40, **M110**	
LGS.Ol	FE5, FE14, M18, M20, M24, M26, D202, D203, D204, D208, D209, D215, D226, D227, D228, D229, **M124**, M128	

Table 3 *(continued)*

Biotope	Station	Video frame
LGS.Tal	WS12, WS14, WS19, WS23, FE13, D1, D41, D42, M15, M16, D65, D66, D82, D83, D84, M51, M61, D108, D109, D110, D117, D118, D126, D127, D131, D132, M62, M63, M76, M77, **M84**, M92, D185, M120, M123, C1, C2, C22, C23, C25, C26, C27, C28, C37, C38, C39, C40, C57, C58	
LMS.BatCor	50, 55, 58	
LMS.MacAre	D33, D34, D35, D37, D38, D43, D44, D45, D46, D48, D50, D51, D52, D67, D73, D82, D84, D98, D99, M4, M6, M7, M14, M28, M31, M35, M41, M42, M43, D135, D136, D137, D138, D139, D140, D142, D144, D145, D146, D147, D152, D154, D155, D156, D157, D158, D159, D181, **D182**, D183, D184, D186, D187, D188, D189, D193, D194, M95, M96, M103, M109, M117, M118, M119, C63, C64	
LMS.PCer	D11, D20, M1, **M3**, D63, D64, D65	
LMS.Znol	D28, D29, D30, D34, D43, D44, D47, M52, D134, D135, D136, D137, D179, D181, D182, D183, D194, M117, **M118**, M121	

Table 3 *(continued)*

Biotope	Station	Video frame
LMU.HedMac	34, 47, 48, D54, D55, D56, D57, D69, D70, D71, D75, D76, D87, D90, D105, D147, D150, D151, D152, D176, D177, D178, D180, M48a, M125, M129, M133, M134, M135, M136, M138, M139, M142, C61, C62	
LMU.HedMac.Are	D68, D72, D74, D81, D85, D93, D94, D96, D97, M44, M45, M46, M49, M52, M53, M56, M57, M58, D179, D180, M115, M143	
LMU.HedOl	51, 52, 53, 56, 57, 59, 60, 63, 64, FE7, FE8, FE9, FE11, FE17, FE18, FE21, D197, D198, D199, D200, D201, D204, D205, D206, D207, D208, D210, D211, D212, D213, D214, D218, D220, D221, D222, D223, D224, D225, D226, D227, D228, D229	
LMU.NVC SM8	D191, D192	
LR.YG	FE2, D39, D40, D53, D59, D60, D61, D100, D101, D102, D104, D149, M127, M131, C61, C62, C63, C64	

Table 3 *(continued)*

Biotope	Station	Video frame
MCR.Flu.Hocu	25, 66, 67	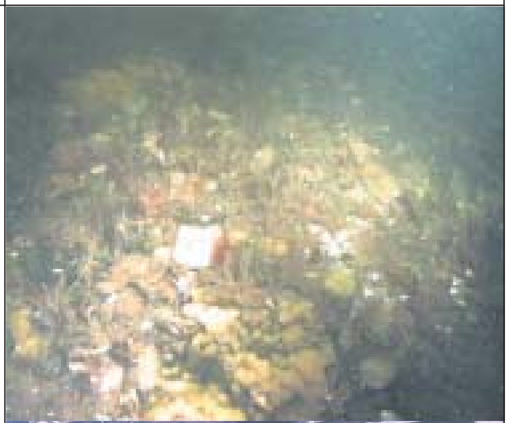 
MLR.Ent	WS2, FE19, D53	
MLR.EntPor	WS3, WS4, D39	
MLR.Fser.Fser	WS3	
MLR.FvesB	D21, D22, D23, D40	
Reeds	FE10, D55, D99, D186, D197, D198, D199, D200, D205, D206, D207, D208, D214, D219, D223	
Saltmarsh	D53, D58, D215, D218, D219, D223	
SIR.Lsac.T	26	
SLR.Asc	D39, D40, D59, D60, D61, D100, D101, D102, D103, D104, D149, C61, C62, C63, C64	
SLR.Asc.VS	D59, D61	

Table 3 *(continued)*

Biotope	Station	Video frame
SLR.AscX	D88, D89, D103, D104, **M126**, M127, M130, M132, M137, M140, M141, M144	
SLR.BLlit	D20, D25, D26, D143	
SLR.EphX	D14, D19, D45, D52, M1, **M12**, M19, M21, M22, M25, M27, M29, D103, M36, M37, M38, M39, M59, M60, D134, D135, D143, D144, D162, D163, D166, D190, D191, D196, M98, M99, M101, M103, M104, M109, M111, M113, M116, C44	
SLR.Fser	M5	
SLR.Fser.VS	M32	
SLR.FserX	M2, D141, D142, D146, **M104**	

Table 3 *(continued)*

Biotope	Station	Video frame
SLR.Fspi	WS1, WS4, D2, D3, D39, D40, D59, D60, D61, D88, D89, D100, D101, D102, D103, D104, M50, D125, D133, D149, D153, M127, M131, M137, C43, C61, C62, C63, C64	
SLR.Fves	WS3, WS4, D4, D5, D6, D8, D28, D29, D30, D39, D47, D51, M4, M5	
SLR.FvesX	FE3, FE4, FE6, FE12, FE15, FE16, FE20, D24, D25, D31, D46, D53, D54, D56, D58, M8, M9, M10, M11, M12, M13, M17, M19, M22, M25, M27, M28, M30, M32, M33, D77, D78, D80, D81, D90, D91, D92, D100, D102, D104, D106, M34, M38, M39, M48b, M54, M59, D133, D134, D135, D143, D144, D146, D147, D148, D151, D152, D153, D157, D158, D161, D163, D164, D165, D166, D174, D179, D195, D196, M96, M97, M98, M100, M104, M107, M108, M111, M112, M113, M114, M116, D215, D218, D219, D220, D224, D226, D227, D228, D229, M126, M127, M130, M132, M133, M135, M137, M140, M141, M144, C50, C61, C62, C63, C64	

Table 3 *(continued)*

Biotope	Station	Video frame
SLR.MytX	D6, D7, D8, D9, D10, D17, D18, D25, D26, D27, D28, D29, D30, D31, D47, M4, M5, M8, D68, D69, **D71**, D72, D77, D78, D79, D80, D81, D85, D86, D93, D94, D95, D96, M46, M47, M48b, M54, M55, D157, D158, D159, D160, D164, D165, D166, D168, D169, D170, D172, D173, D174, D175, M96, M97, M98, M100, **M104**, M106, M107, M108, M110, M112	 
SLR.Pel	D39, D40, D56, D59, D60, D61, D88, D89, D100, D101, D102, D103, D104, D125, D133, D149, M127, M131, M137, C61, C62, C63, C64	

Table 4 Abundance of species in infaunal samples from the Firth of Tay and Eden Estuary cSAC. See methods for samples size. S = superabundant (>1000), A = abundant (100–1000), C = common (20-100), P = present

Taxa	Station																					
	1	2	3	4	5	6	7	8	9	10	11	12	13	14	15	16	17	18	19	20	21	22
HYDROZOA spp				P					P						P							
ACTINIARIA spp																						
NEMERTEA spp											P										21	P
Harmothoe spp indet																						
Harmothoe andreapolis																						
Pholoe synophthalmica																						
Pholoe baltica																						4
Sigalion mathildae																						
Eteone longa															2						1	3
Anaitides mucosa																						1
Eumida bahusiensis																						
Kefersteinia cirrata																					2	
Streptosyllis websteri																						
Autolytus spp																						
NEREIDIDAE spp juv												1						1				
Hediste diversicolor															7	1						
Neanthes virens																						
Nephtys caeca																					1	3
Nephtys cirrosa													1									
Nephtys hombergii																						
Nephtys longosetosa																						
Nephtys assimilis																						
Orbinia spp juv																						
Scoloplos armiger																		11			5	18
Aricidea minuta																						
Paraonis fulgens											2		1									
SPIONIDAE sp juv																		1				
Aonides oxycephala																						1
Malacoceros fuliginosus																						
Marenzelleria viridis								3	5	1	2	16			4		13					
Polydora caeca																		1				
Polydora ciliata																					1	1
Polydora quadrilobata																						3

Table 4 *(continued)*

Taxa	Station																					
	1	**2**	**3**	**4**	**5**	**6**	**7**	**8**	**9**	**10**	**11**	**12**	**13**	**14**	**15**	**16**	**17**	**18**	**19**	**20**	**21**	**22**
Pygospio elegans															7	9		26			8	1
Scolelepis (S) squamata																						
Spio armata																						9
Spio filicornis																						2
Spiophanes bombyx																						
Magelona mirabilis																						
Chaetozone setosa																						
Aphelochaeta sp 'A'																						
Tharyx sp 'A'																3						
Capitella spp																2	2	1				
Mediomastus fragilis																		6			6	7
Arenicola marina																3						
Ophelia sp juv																						
Ophelia borealis																			2	1		
Ophelia rathkei											9											
Travisia forbesii																						
Galathowenia oculata																						
Melinna palmata																						
Ampharete grubei																						
Lanice conchilega																						
Pomatoceros lamarcki																						8
OLIGOCHAETA spp																						
NAIDIDAE spp																						
Paranais littoralis																						
Uncinais uncinata																						
TUBIFICIDAE spp					1							2			35	2		18			5	2
Psammoryctides barbatus																						
Rhyacodrilus coccineus																						
Limnodrilus hoffmeisteri																						
Tubifex costatus																						
Tubificoides benedii															26	8		60	1		581	19
Heterochaeta costata																						
ENCHYTRAEIDAE spp					18	7																
Balanus crenatus												P			P			P				P

Table 4 *(continued)*

Taxa	Station																					
	1	**2**	**3**	**4**	**5**	**6**	**7**	**8**	**9**	**10**	**11**	**12**	**13**	**14**	**15**	**16**	**17**	**18**	**19**	**20**	**21**	**22**
Gastrosaccus spinifer			3																	2		
Neomysis integer																						
Mysidacea sp																						
Bodotria pulchella																						
?Cumopsis goodsiri																						
Cumacea sp																						
Euridice pulchra											3		1	3								
Jaera albifrons															4							
Jaera sp												2										
Idotea linearis																						
Hippomedon denticulatus																						
Leucothoe incisa																						
Talitrus saltator																						
Hyale nilssoni																						
Gammarus duebeni																						
Gammarus locusta																						
Gammarus salinus												85		1	48			5	1		4	158
Melita palmata																					53	14
Melita pellucida																						
Bathyporeia guilliamsoniana																						
Bathyporeia pelagica										4												
Bathyporeia sarsi										5												
Bathyporeia sp																						
Haustorius arenarius														1								
Pontocrates altamarinus																						
Pontocrates arenarius																						
Phoxocephalus holbolli																						
Calliopus laevisculus																						
Atylus falcatus																						
Gammaropsis nitida																						
Microprotopus maculatus																						
Corophium multisetosum/volutator																						
Corophium multisetosum					1							12										
Corophium volutator												2				2						
Corophium insidiosum																						

Table 4 *(continued)*

Taxa	Station																					
	1	2	3	4	5	6	7	8	9	10	11	12	13	14	15	16	17	18	19	20	21	22
Pariambus typicus																						
Crangon crangon																						
Pagurus pubescens																						
Carcinus maenas																			1			
Tectura testitudinalis					1																	
HYDROBIIDAE spp indet																						
?Potamopyrgus jenkinsi						1																
Hydrobia ulvae																						
Nucella lapillus																						
BUCCINIDAE sp juv																						
OPISTHOBRANCHIA spp																						
Polycera quadrilineata																						3
Mytilus edulis (juvs)								7				14			7		3	1			21	341
Mytilus edulis												4			83						2	7
Cerastoderma edule																						
Spisula elliptica																						
Spisula solida																						
Mactra stultorum																						
Ensis arcuatus																						
Angulus tenuis																						
Fabulina fabula																						
Moerella pygmaea																						
Macoma balthica																						
Donax vittatus																						
Abra sp indet																						
Abra alba																						
Chamelea gallina																						
Mya spp juv																						
Mya arenaria												1										11
BRYOZOA spp															P			P				P
Asterias rubens																						
Ammodytes tobianus																				1		
DIPTERA spp						2																
CHIRONOMIDAE spp							1															
TRICHOPTERA spp																						

Table 4 *(continued)*

	Station																			
Taxa	**23**	**26**	**28**	**29**	**30**	**31**	**32**	**34**	**35**	**36**	**37**	**38**	**39**	**40**	**41**	**42**	**43**	**44**	**45**	**46**
HYDROZOA spp																				
ACTINIARIA spp	5																			
NEMERTEA spp	6					3														
Harmothoe spp indet	2																			
Harmothoe andreapolis				1	1	1														
Pholoe synophthalmica		1																		
Pholoe baltica																				
Sigalion mathildae							4													
Eteone longa	3	1				1														
Anaitides mucosa																				
Eumida bahusiensis				2		3	1													
Kefersteinia cirrata	1																			
Streptosyllis websteri																				
Autolytus spp		1																		
NEREIDIDAE spp juv																				
Hediste diversicolor								9												
Neanthes virens																				
Nephtys caeca		2			1															
Nephtys cirrosa			7	17	5	10	9					3				1				
Nephtys hombergii																				
Nephtys longosetosa																				
Nephtys assimilis						2														
Orbinia spp juv				1																
Scoloplos armiger	10	32	1		3	2														
Aricidea minuta																				
Paraonis fulgens																1				
SPIONIDAE sp juv																				
Aonides oxycephala																				
Malacoceros fuliginosus																				
Marenzelleria viridis																	7	3	7	2
Polydora caeca		1																		
Polydora ciliata																				
Polydora quadrilobata																				
Pygospio elegans								1												

Table 4 *(continued)*

Taxa	Station																			
	23	**26**	**28**	**29**	**30**	**31**	**32**	**34**	**35**	**36**	**37**	**38**	**39**	**40**	**41**	**42**	**43**	**44**	**45**	**46**
Scolelepis (S) squamata																				
Spio armata		1																		
Spio filicornis		1				2														
Spiophanes bombyx				1		9	3													
Magelona mirabilis						30	1													
Chaetozone setosa		16				12														
Aphelochaeta sp 'A'																				
Tharyx sp 'A'																				
Capitella spp	16	2						1												5
Mediomastus fragilis	1																			
Arenicola marina																				
Ophelia sp juv																				
Ophelia borealis			4		2															
Ophelia rathkei																				
Travisia forbesii																				
Galathowenia oculata						3														
Melinna palmata																				
Ampharete grubei																				
Lanice conchilega						9														
Pomatoceros lamarcki		14																		
OLIGOCHAETA spp																				
NAIDIDAE spp																				
Paranais littoralis																				
Uncinais uncinata																				
TUBIFICIDAE spp	4																			
Psammoryctides barbatus																				
Rhyacodrilus coccineus																				
Limnodrilus hoffmeisteri																				
Tubifex costatus																				
Tubificoides benedii	92	7					1		1											
Heterochaeta costata																				
ENCHYTRAEIDAE spp																				
Balanus crenatus		P				P														
Gastrosaccus spinifer																				

Table 4 *(continued)*

Taxa	Station																			
	23	26	28	29	30	31	32	34	35	36	37	38	39	40	41	42	43	44	45	46
Neomysis integer																				
Mysidacea sp																				
Bodotria pulchella																				
?*Cumopsis goodsiri*																				
Cumacea sp																				
Euridice pulchra																				
Jaera albifrons																				
Jaera sp																				
Idotea linearis																				
Hippomedon denticulatus						1														
Leucothoe incisa						1														
Talitrus saltator																				
Hyale nilssoni																				
Gammarus duebeni																				
Gammarus locusta																				
Gammarus salinus	346	1		1													1			
Melita palmata	2																			
Melita pellucida																				
Bathyporeia guilliamsoniana																				
Bathyporeia pelagica				1	1	1								1		1				
Bathyporeia sarsi		4																2		
Bathyporeia sp																				
Haustorius arenarius													19		1			4		
Pontocrates altamarinus						3								4						
Pontocrates arenarius																3				
Phoxocephalus holbolli		12																		
Calliopus laevisculus		1																		
Atylus falcatus																				
Gammaropsis nitida						5														
Microprotopus maculatus						1														
Corophium multisetosum/volutator																			1	
Corophium multisetosum																				
Corophium volutator																				
Corophium insidiosum																				

Table 4 *(continued)*

Taxa	Station																				
	23	26	28	29	30	31	32	34	35	36	37	38	39	40	41	42	43	44	45	46
Pariambus typicus						1														
Crangon crangon																				
Pagurus pubescens						1														
Carcinus maenas	7								2	2	1									
Tectura testitudinalis																				
HYDROBIIDAE spp indet																				
?Potamopyrgus jenkinsi																				
Hydrobia ulvae																				
Nucella lapillus	5																			
BUCCINIDAE sp juv		1																		
OPISTHOBRANCHIA spp		2																		
Polycera quadrilineata																				
Mytilus edulis (juvs)		2																		
Mytilus edulis	S																			
Cerastoderma edule																				
Spisula elliptica			1																	
Spisula solida				3																
Mactra stultorum																				
Ensis arcuatus			1																	
Angulus tenuis																				
Fabulina fabula						5	1													
Moerella pygmaea				1																
Macoma balthica																				
Donax vittatus							1													
Abra sp indet																				
Abra alba						4														
Chamelea gallina				1		2	3													
Mya spp juv																				
Mya arenaria																				
BRYOZOA spp																				
Asterias rubens	5					3														
Ammodytes tobianus				P																
DIPTERA spp																				
CHIRONOMIDAE spp																				
TRICHOPTERA spp																	1			

Table 4 *(continued)*

Taxa	Station																			
	47	48	49	50	51	52	53	54	55	56	57	58	59	60	61	62	63	64	65	M3
HYDROZOA spp																				
ACTINIARIA spp																				
NEMERTEA spp																				
Harmothoe spp indet																				
Harmothoe andreapolis																				
Pholoe synophthalmica																				
Pholoe baltica																				
Sigalion mathildae																				
Eteone longa																				
Anaitides mucosa																				
Eumida bahusiensis																				
Kefersteinia cirrata																				
Streptosyllis websteri																				
Autolytus spp																				
NEREIDIDAE spp juv		1			2	1														
Hediste diversicolor					2	3	6			4	4		1							
Neanthes virens																				
Nephtys caeca																				
Nephtys cirrosa																				2
Nephtys hombergii																				
Nephtys longosetosa																				
Nephtys assimilis																				
Orbinia spp juv																				
Scoloplos armiger																				1
Aricidea minuta																				
Paraonis fulgens																				1
SPIONIDAE sp juv																				
Aonides oxycephala																				
Malacoceros fuliginosus																				
Marenzelleria viridis																				
Polydora caeca																				
Polydora ciliata																				
Polydora quadrilobata																				
Pygospio elegans																				1

Table 4 *(continued)*

Taxa	Station																			
	47	48	49	50	51	52	53	54	55	56	57	58	59	60	61	62	63	64	65	M3
Scolelepis (S) squamata																				
Spio armata																				1
Spio filicornis																				
Spiophanes bombyx																				
Magelona mirabilis																				
Chaetozone setosa																				
Aphelochaeta sp 'A'																				
Tharyx sp 'A'																				
Capitella spp																				
Mediomastus fragilis																				
Arenicola marina																				
Ophelia sp juv																				
Ophelia borealis																				
Ophelia rathkei																				
Travisia forbesii																				1
Galathowenia oculata																				
Melinna palmata																				
Ampharete grubei																				
Lanice conchilega																				
Pomatoceros lamarcki																				
OLIGOCHAETA spp																	S			
NAIDIDAE spp																				
Paranais littoralis																	P			
Uncinais uncinata																	P			
TUBIFICIDAE spp													7				P	3		
Psammoryctides barbatus																	P			
Rhyacodrilus coccineus																	P	1		
Limnodrilus hoffmeisteri																	P			
Tubifex costatus										1				3						
Tubificoides benedii																				
Heterochaeta costata																				
ENCHYTRAEIDAE spp																	P	8		
Balanus crenatus																				
Gastrosaccus spinifer															6					

Table 4 *(continued)*

Taxa	Station																			
	47	48	49	50	51	52	53	54	55	56	57	58	59	60	61	62	63	64	65	M3
Neomysis integer								2						1						
Mysidacea sp																				
Bodotria pulchella																				
?Cumopsis goodsiri																				
Cumacea sp																				
Euridice pulchra															6					
Jaera albifrons																				
Jaera sp																				
Idotea linearis																				
Hippomedon denticulatus																				
Leucothoe incisa																				
Talitrus saltator																				
Hyale nilssoni																				
Gammarus duebeni																				
Gammarus locusta																				
Gammarus salinus												1						2		
Melita palmata																				
Melita pellucida																				
Bathyporeia guilliamsoniana																				
Bathyporeia pelagica			1																	
Bathyporeia sarsi									2			1								
Bathyporeia sp																				
Haustorius arenarius															5					
Pontocrates altamarinus																				
Pontocrates arenarius																				
Phoxocephalus holbolli																				
Calliopus laevisculus																				
Atylus falcatus																				
Gammaropsis nitida																				
Microprotopus maculatus																				
Corophium multisetosum/volutator				1	2	8		2	2	68	44	10	10	56	1		1	6		
Corophium multisetosum																				
Corophium volutator							29													
Corophium insidiosum																				

Table 4 *(continued)*

Taxa	**Station**																			
	47	**48**	**49**	**50**	**51**	**52**	**53**	**54**	**55**	**56**	**57**	**58**	**59**	**60**	**61**	**62**	**63**	**64**	**65**	**M3**
Pariambus typicus																				
Crangon crangon								1												
Pagurus pubescens																				
Carcinus maenas																				
Tectura testitudinalis																				
HYDROBIIDAE spp indet																		27		
?Potamopyrgus jenkinsi																	2	9		
Hydrobia ulvae																	2			
Nucella lapillus																				
BUCCINIDAE sp juv																				
OPISTHOBRANCHIA spp																				
Polycera quadrilineata																				
Mytilus edulis (juvs)																				
Mytilus edulis																				
Cerastoderma edule																				
Spisula elliptica																				
Spisula solida																				
Mactra stultorum																				
Ensis arcuatus																				
Angulus tenuis																				
Fabulina fabula																				
Moerella pygmaea																				
Macoma balthica																				
Donax vittatus																				
Abra sp indet																				
Abra alba																				
Chamelea gallina																				
Mya spp juv	1																			
Mya arenaria																				
BRYOZOA spp																				
Asterias rubens																				
Ammodytes tobianus																				
DIPTERA spp																	1			
CHIRONOMIDAE spp																		1		
TRICHOPTERA spp																		1		

Table 4 *(continued)*

Taxa	**Station**												
	M6	**M7**	**M14**	**M15**	**M16**	**M23**	**M28**	**M31**	**M35**	**M41**	**M44**	**M53**	**M56**
HYDROZOA spp													
ACTINIARIA spp													
NEMERTEA spp	12		2										
Harmothoe spp indet													
Harmothoe andreapolis													
Pholoe synophthalmica													
Pholoe baltica													
Sigalion mathildae													
Eteone longa	13	5	5		1			1		2			2
Anaitides mucosa	1												
Eumida bahusiensis													
Kefersteinia cirrata													
Streptosyllis websteri	1												
Autolytus spp													
NEREIDIDAE spp juv													
Hediste diversicolor		2					2				7	3	10
Neanthes virens													
Nephtys caeca	1												
Nephtys cirrosa	1								2	2			
Nephtys hombergii	1									1			P
Nephtys longosetosa													
Nephtys assimilis													
Orbinia spp juv													
Scoloplos armiger	13	16					1	1		12	1		
Aricidea minuta	3												
Paraonis fulgens			1										
SPIONIDAE sp juv													
Aonides oxycephala	1												
Malacoceros fuliginosus													
Marenzelleria viridis													
Polydora caeca													
Polydora ciliata													
Polydora quadrilobata													
Pygospio elegans	415	24	8				14	12		24	22	7	1

Table 4 *(continued)*

Taxa	**Station**												
	M6	**M7**	**M14**	**M15**	**M16**	**M23**	**M28**	**M31**	**M35**	**M41**	**M44**	**M53**	**M56**
Scolelepis (S) squamata											2		
Spio armata		2											
Spio filicornis													
Spiophanes bombyx													
Magelona mirabilis													
Chaetozone setosa	32	1											
Aphelochaeta sp 'A'													
Tharyx sp 'A'													
Capitella spp	2	1	7	1			1	12	4	2	42		1
Mediomastus fragilis	6	4											
Arenicola marina		2						1					
Ophelia sp juv													
Ophelia borealis													
Ophelia rathkei													
Travisia forbesii													
Galathowenia oculata													
Melinna palmata													
Ampharete grubei													
Lanice conchilega													
Pomatoceros lamarcki													
OLIGOCHAETA spp													
NAIDIDAE spp													
Paranais littoralis													
Uncinais uncinata													
TUBIFICIDAE spp	7	2		1			1	2			1		
Psammoryctides barbatus													
Rhyacodrilus coccineus													
Limnodrilus hoffmeisteri													
Tubifex costatus													
Tubificoides benedii	15	1			11			2	1	1	5		C
Heterochaeta costata													
ENCHYTRAEIDAE spp					223	1					1		
Balanus crenatus	P												
Gastrosaccus spinifer													

Table 4 *(continued)*

Taxa	Station												
	M6	**M7**	**M14**	**M15**	**M16**	**M23**	**M28**	**M31**	**M35**	**M41**	**M44**	**M53**	**M56**
Neomysis integer					1								
Mysidacea sp													
Bodotria pulchella													
?*Cumopsis goodsiri*													
Cumacea sp													
Euridice pulchra				2		3							
Jaera albifrons													
Jaera sp													
Idotea linearis													
Hippomedon denticulatus													
Leucothoe incisa													
Talitrus saltator													
Hyale nilssoni													
Gammarus duebeni													
Gammarus locusta	6												
Gammarus salinus													
Melita palmata													
Melita pellucida													
Bathyporeia guilliamsoniana													
Bathyporeia pelagica													
Bathyporeia sarsi			13			6	2						
Bathyporeia sp													
Haustorius arenarius													
Pontocrates altamarinus													
Pontocrates arenarius													
Phoxocephalus holbolli													
Calliopus laevisculus													
Atylus falcatus													
Gammaropsis nitida													
Microprotopus maculatus													
Corophium multisetosum/volutator					6				1	1	39	1	S
Corophium multisetosum													
Corophium volutator													
Corophium insidiosum								1					

Table 4 *(continued)*

Taxa	Station												
	M6	**M7**	**M14**	**M15**	**M16**	**M23**	**M28**	**M31**	**M35**	**M41**	**M44**	**M53**	**M56**
Pariambus typicus													
Crangon crangon			1										
Pagurus pubescens													
Carcinus maenas								1					
Tectura testitudinalis													
HYDROBIIDAE spp indet													
?Potamopyrgus jenkinsi													
Hydrobia ulvae													
Nucella lapillus													
BUCCINIDAE sp juv													
OPISTHOBRANCHIA spp													
Polycera quadrilineata													
Mytilus edulis (juvs)	1												
Mytilus edulis													
Cerastoderma edule	2	1								3	2		
Spisula elliptica													
Spisula solida													
Mactra stultorum													
Ensis arcuatus													
Angulus tenuis													
Fabulina fabula													
Moerella pygmaea													
Macoma balthica	3	5					1	2		1	3		
Donax vittatus													
Abra sp indet													
Abra alba													
Chamelea gallina													
Mya spp juv													
Mya arenaria													
BRYOZOA spp													
Asterias rubens													
Ammodytes tobianus													
DIPTERA spp													
CHIRONOMIDAE spp													
TRICHOPTERA spp													

Table 4 *(continued)*

Taxa	Station											
	M57	M58	M68	M71	M74	M93	M94	M95	M101	M109	M116	M118
HYDROZOA spp												
ACTINIARIA spp												
NEMERTEA spp		2	2									
Harmothoe spp indet												
Harmothoe andreapolis												
Pholoe synophthalmica												
Pholoe baltica												
Sigalion mathildae												
Eteone longa	2	2									12	1
Anaitides mucosa												
Eumida bahusiensis												
Kefersteinia cirrata												
Streptosyllis websteri												
Autolytus spp												
NEREIDIDAE spp juv												
Hediste diversicolor	12	23									29	4
Neanthes virens												
Nephtys caeca									2	1		
Nephtys cirrosa			1				2		4	3		
Nephtys hombergii												
Nephtys longosetosa												
Nephtys assimilis												
Orbinia spp juv												
Scoloplos armiger		2		P				2		2		
Aricidea minuta												
Paraonis fulgens					2				1			
SPIONIDAE sp juv												
Aonides oxycephala												
Malacoceros fuliginosus			1								9	3
Marenzelleria viridis												
Polydora caeca												
Polydora ciliata												
Polydora quadrilobata												
Pygospio elegans	6	1	2				1	18		7	167	1

Table 4 *(continued)*

Taxa	**Station**											
	M57	**M58**	**M68**	**M71**	**M74**	**M93**	**M94**	**M95**	**M101**	**M109**	**M116**	**M118**
Scolelepis (S) squamata												
Spio armata			1				1	5			1	
Spio filicornis												
Spiophanes bombyx												
Magelona mirabilis												
Chaetozone setosa												
Aphelochaeta sp 'A'												
Tharyx sp 'A'												
Capitella spp	1							5	1		1	
Mediomastus fragilis											1	
Arenicola marina	1											P
Ophelia sp juv												
Ophelia borealis												
Ophelia rathkei												
Travisia forbesii												
Galathowenia oculata												
Melinna palmata												
Ampharete grubei												
Lanice conchilega												
Pomatoceros lamarcki												
OLIGOCHAETA spp											C	
NAIDIDAE spp												
Paranais littoralis												
Uncinais uncinata												
TUBIFICIDAE spp		1									P	3
Psammoryctides barbatus												
Rhyacodrilus coccineus												
Limnodrilus hoffmeisteri												
Tubifex costatus												
Tubificoides benedii	13	46	1								P	15
Heterochaeta costata												
ENCHYTRAEIDAE spp						2					P	
Balanus crenatus												
Gastrosaccus spinifer								1				

Table 4 *(continued)*

Taxa	**Station**											
	M57	**M58**	**M68**	**M71**	**M74**	**M93**	**M94**	**M95**	**M101**	**M109**	**M116**	**M118**
Neomysis integer												
Mysidacea sp												
Bodotria pulchella												
?Cumopsis goodsiri												
Cumacea sp												
Euridice pulchra						13						
Jaera albifrons												
Jaera sp												
Idotea linearis												
Hippomedon denticulatus												
Leucothoe incisa												
Talitrus saltator												
Hyale nilssoni												
Gammarus duebeni												
Gammarus locusta									3			
Gammarus salinus												
Melita palmata												
Melita pellucida												
Bathyporeia guilliamsoniana												
Bathyporeia pelagica			2	1								
Bathyporeia sarsi				1		1		1		1		3
Bathyporeia sp												
Haustorius arenarius				P								
Pontocrates altamarinus			1									
Pontocrates arenarius												
Phoxocephalus holbolli												
Calliopus laevisculus												
Atylus falcatus			2									
Gammaropsis nitida												
Microprotopus maculatus												
Corophium multisetosum/volutator	S	S										
Corophium multisetosum												
Corophium volutator												
Corophium insidiosum												

Table 4 *(continued)*

Taxa	Station											
	M57	M58	M68	M71	M74	M93	M94	M95	M101	M109	M116	M118
Pariambus typicus												
Crangon crangon		3	1							1		
Pagurus pubescens												
Carcinus maenas								1		1		
Tectura testitudinalis												
HYDROBIIDAE spp indet												
?Potamopyrgus jenkinsi												
Hydrobia ulvae	3											
Nucella lapillus												
BUCCINIDAE sp juv												
OPISTHOBRANCHIA spp												
Polycera quadrilineata												
Mytilus edulis (juvs)												
Mytilus edulis												
Cerastoderma edule		2							2	1	1	5
Spisula elliptica			1									
Spisula solida												
Mactra stultorum												
Ensis arcuatus												
Angulus tenuis			1									
Fabulina fabula												
Moerella pygmaea												
Macoma balthica	2	17									2	2
Donax vittatus			3									
Abra sp indet												
Abra alba												
Chamelea gallina												
Mya spp juv												
Mya arenaria												
BRYOZOA spp												
Asterias rubens												
Ammodytes tobianus												
DIPTERA spp												
CHIRONOMIDAE spp												
TRICHOPTERA spp												

Table 4 *(continued)*

Taxa	Station											
	M122	**M124**	**M125**	**M134**	**M136**	**M138**	**D11**	**D15**	**D16**	**D32**	**D33**	**D36**
HYDROZOA spp												
ACTINIARIA spp												
NEMERTEA spp	1			1							1	
Harmothoe spp indet												
Harmothoe andreapolis												
Pholoe synophthalmica												
Pholoe baltica												
Sigalion mathildae												
Eteone longa				1	1							
Anaitides mucosa												
Eumida bahusiensis												
Kefersteinia cirrata												
Streptosyllis websteri												
Autolytus spp												
NEREIDIDAE spp juv												
Hediste diversicolor			15	1	63							
Neanthes virens												
Nephtys caeca												
Nephtys cirrosa							2	3	5	2	2	
Nephtys hombergii												
Nephtys longosetosa												
Nephtys assimilis												
Orbinia spp juv												
Scoloplos armiger							5		2		13	
Aricidea minuta												
Paraonis fulgens								1	1			
SPIONIDAE sp juv												
Aonides oxycephala												
Malacoceros fuliginosus												
Marenzelleria viridis				8		7						
Polydora caeca												
Polydora ciliata												
Polydora quadrilobata												
Pygospio elegans				4	8						1	

Table 4 *(continued)*

Taxa	**Station**											
	M122	**M124**	**M125**	**M134**	**M136**	**M138**	**D11**	**D15**	**D16**	**D32**	**D33**	**D36**
Scolelepis (S) squamata	1											8
Spio armata												
Spio filicornis												
Spiophanes bombyx												
Magelona mirabilis												
Chaetozone setosa							2					
Aphelochaeta sp 'A'												
Tharyx sp 'A'												
Capitella spp												
Mediomastus fragilis												
Arenicola marina												
Ophelia sp juv												
Ophelia borealis									1			
Ophelia rathkei												
Travisia forbesii								3				
Galathowenia oculata												
Melinna palmata												
Ampharete grubei												
Lanice conchilega												
Pomatoceros lamarcki												
OLIGOCHAETA spp					C							
NAIDIDAE spp												
Paranais littoralis												
Uncinais uncinata												
TUBIFICIDAE spp								1				
Psammoryctides barbatus												
Rhyacodrilus coccineus												
Limnodrilus hoffmeisteri												
Tubifex costatus		1			P	3						
Tubificoides benedii		2	A	15	P	3						
Heterochaeta costata												
ENCHYTRAEIDAE spp												
Balanus crenatus												
Gastrosaccus spinifer												

Table 4 *(continued)*

Taxa	Station											
	M122	**M124**	**M125**	**M134**	**M136**	**M138**	**D11**	**D15**	**D16**	**D32**	**D33**	**D36**
Neomysis integer												
Mysidacea sp												
Bodotria pulchella												
?Cumopsis goodsiri								1				
Cumacea sp												
Euridice pulchra	1											8
Jaera albifrons												
Jaera sp												
Idotea linearis												
Hippomedon denticulatus												
Leucothoe incisa												
Talitrus saltator												
Hyale nilssoni			1									
Gammarus duebeni												
Gammarus locusta												
Gammarus salinus												
Melita palmata												
Melita pellucida												
Bathyporeia guilliamsoniana												
Bathyporeia pelagica												
Bathyporeia sarsi	5						24	1		41	5	40
Bathyporeia sp												
Haustorius arenarius	3											
Pontocrates altamarinus												
Pontocrates arenarius												
Phoxocephalus holbolli												
Calliopus laevisculus												
Atylus falcatus												
Gammaropsis nitida												
Microprotopus maculatus												
Corophium multisetosum/volutator			A	3	C	2						
Corophium multisetosum												
Corophium volutator												
Corophium insidiosum												

Table 4 *(continued)*

	Station											
Taxa	**M122**	**M124**	**M125**	**M134**	**M136**	**M138**	**D11**	**D15**	**D16**	**D32**	**D33**	**D36**
Pariambus typicus												
Crangon crangon						1					2	
Pagurus pubescens												
Carcinus maenas												
Tectura testitudinalis												
HYDROBIIDAE spp indet												
?Potamopyrgus jenkinsi												
Hydrobia ulvae												
Nucella lapillus												
BUCCINIDAE sp juv												
OPISTHOBRANCHIA spp												
Polycera quadrilineata												
Mytilus edulis (juvs)												
Mytilus edulis												
Cerastoderma edule												
Spisula elliptica												
Spisula solida												
Mactra stultorum												
Ensis arcuatus												
Angulus tenuis												
Fabulina fabula												
Moerella pygmaea												
Macoma balthica			15	9	C						5	
Donax vittatus												
Abra sp indet												
Abra alba												
Chamelea gallina												
Mya spp juv												
Mya arenaria												
BRYOZOA spp												
Asterias rubens												
Ammodytes tobianus												
DIPTERA spp												
CHIRONOMIDAE spp												
TRICHOPTERA spp												

Table 4 *(continued)*

Taxa	Station												
	D49	**D57**	**D62**	**D64**	**D66**	**D70**	**D73**	**D87**	**D97**	**D105**	**D107**	**D110**	**D111**
HYDROZOA spp													
ACTINIARIA spp													
NEMERTEA spp			3					3				2	
Harmothoe spp indet													
Harmothoe andreapolis													
Pholoe synophthalmica													
Pholoe baltica													
Sigalion mathildae													
Eteone longa	1				1	3	1	10					
Anaitides mucosa													
Eumida bahusiensis													
Kefersteinia cirrata													
Streptosyllis websteri													
Autolytus spp													
NEREIDIDAE spp juv													
Hediste diversicolor	103				14	6	53		1				
Neanthes virens						2							
Nephtys caeca													
Nephtys cirrosa		8	3										
Nephtys hombergii					1								
Nephtys longosetosa		1											
Nephtys assimilis													
Orbinia spp juv													
Scoloplos armiger													
Aricidea minuta			1										
Paraonis fulgens													
SPIONIDAE sp juv													
Aonides oxycephala													
Malacoceros fuliginosus						5		1					
Marenzelleria viridis													
Polydora caeca													
Polydora ciliata													
Polydora quadrilobata													
Pygospio elegans			2			27		8					

Table 4 *(continued)*

Taxa	Station												
	D49	**D57**	**D62**	**D64**	**D66**	**D70**	**D73**	**D87**	**D97**	**D105**	**D107**	**D110**	**D111**
Scolelepis (S) squamata	3		1										9
Spio armata													
Spio filicornis													
Spiophanes bombyx													
Magelona mirabilis													
Chaetozone setosa													
Aphelochaeta sp 'A'													
Tharyx sp 'A'													
Capitella spp							3		18				
Mediomastus fragilis									1				
Arenicola marina			1				2		1				
Ophelia sp juv	1												
Ophelia borealis													
Ophelia rathkei													2
Travisia forbesii													
Galathowenia oculata													
Melinna palmata													
Ampharete grubei									4				
Lanice conchilega													
Pomatoceros lamarcki													
OLIGOCHAETA spp						C		A	S				
NAIDIDAE spp										2			
Paranais littoralis													
Uncinais uncinata													
TUBIFICIDAE spp						1			P				
Psammoryctides barbatus													
Rhyacodrilus coccineus													
Limnodrilus hoffmeisteri													
Tubifex costatus		2							P				
Tubificoides benedii				1		39	87	P	P	86			
Heterochaeta costata													
ENCHYTRAEIDAE spp					6								1
Balanus crenatus													
Gastrosaccus spinifer													

Table 4 *(continued)*

Taxa	**Station**												
	D49	**D57**	**D62**	**D64**	**D66**	**D70**	**D73**	**D87**	**D97**	**D105**	**D107**	**D110**	**D111**
Neomysis integer													
Mysidacea sp													
Bodotria pulchella													
?Cumopsis goodsiri													
Cumacea sp													
Euridice pulchra											1		1
Jaera albifrons													
Jaera sp													
Idotea linearis													
Hippomedon denticulatus													
Leucothoe incisa													
Talitrus saltator					18							21	1
Hyale nilssoni													
Gammarus duebeni													
Gammarus locusta													
Gammarus salinus		3											
Melita palmata													
Melita pellucida													
Bathyporeia guilliamsoniana													
Bathyporeia pelagica													
Bathyporeia sarsi	204	1		25							45		4
Bathyporeia sp													
Haustorius arenarius													
Pontocrates altamarinus													
Pontocrates arenarius													
Phoxocephalus holbolli													
Calliopus laevisculus													
Atylus falcatus													
Gammaropsis nitida													
Microprotopus maculatus													
Corophium multisetosum/volutator		4				A		S				4	3
Corophium multisetosum													
Corophium volutator													
Corophium insidiosum													

Table 4 *(continued)*

Taxa	Station												
	D49	**D57**	**D62**	**D64**	**D66**	**D70**	**D73**	**D87**	**D97**	**D105**	**D107**	**D110**	**D111**
Pariambus typicus													
Crangon crangon				2			6		1	3			
Pagurus pubescens													
Carcinus maenas													
Tectura testitudinalis													
HYDROBIIDAE spp indet													
?Potamopyrgus jenkinsi													
Hydrobia ulvae							3						
Nucella lapillus													
BUCCINIDAE sp juv													
OPISTHOBRANCHIA spp													
Polycera quadrilineata													
Mytilus edulis (juvs)													
Mytilus edulis													
Cerastoderma edule							10						
Spisula elliptica													
Spisula solida													
Mactra stultorum													
Ensis arcuatus													
Angulus tenuis													
Fabulina fabula													
Moerella pygmaea													
Macoma balthica		3				2	6	4	5	19			
Donax vittatus													
Abra sp indet				1									
Abra alba						1							
Chamelea gallina													
Mya spp juv													
Mya arenaria													
BRYOZOA spp													
Asterias rubens													
Ammodytes tobianus													
DIPTERA spp													
CHIRONOMIDAE spp					1								
TRICHOPTERA spp													

Table 4 *(continued)*

Taxa	Station										
	D112	D115	D119	D124	D128	D130	D137	D140	D150	D167	D182
HYDROZOA spp											
ACTINIARIA spp											
NEMERTEA spp					1		1				
Harmothoe spp indet											
Harmothoe andreapolis											
Pholoe synophthalmica											
Pholoe baltica											
Sigalion mathildae											
Eteone longa							3		2		
Anaitides mucosa											
Eumida bahusiensis											
Kefersteinia cirrata											
Streptosyllis websteri											
Autolytus spp											
NEREIDIDAE spp juv											
Hediste diversicolor							4		16		3
Neanthes virens											
Nephtys caeca											
Nephtys cirrosa	6		7	1	4					3	
Nephtys hombergii								1	2	2	
Nephtys longosetosa											
Nephtys assimilis											
Orbinia spp juv											
Scoloplos armiger							1	4	24	2	
Aricidea minuta											
Paraonis fulgens					3						
SPIONIDAE sp juv											
Aonides oxycephala											
Malacoceros fuliginosus							6				3
Marenzelleria viridis											
Polydora caeca											
Polydora ciliata											
Polydora quadrilobata											
Pygospio elegans							8	1			39

Table 4 *(continued)*

Taxa	Station										
	D112	D115	D119	D124	D128	D130	D137	D140	D150	D167	D182
Scolelepis (S) squamata		4			1						
Spio armata											
Spio filicornis											
Spiophanes bombyx	1										
Magelona mirabilis											
Chaetozone setosa											
Aphelochaeta sp 'A'									18		
Tharyx sp 'A'	1										
Capitella spp							5		2		2
Mediomastus fragilis									3		
Arenicola marina							P		3		
Ophelia sp juv											
Ophelia borealis											
Ophelia rathkei											
Travisia forbesii											
Galathowenia oculata											
Melinna palmata											
Ampharete grubei											
Lanice conchilega											
Pomatoceros lamarcki											
OLIGOCHAETA spp									C		C
NAIDIDAE spp											
Paranais littoralis											
Uncinais uncinata											
TUBIFICIDAE spp							7				
Psammoryctides barbatus											
Rhyacodrilus coccineus											
Limnodrilus hoffmeisteri											
Tubifex costatus											
Tubificoides benedii							16		P		P
Heterochaeta costata											
ENCHYTRAEIDAE spp						1					
Balanus crenatus											
Gastrosaccus spinifer											

Table 4 *(continued)*

Taxa	Station										
	D112	D115	D119	D124	D128	D130	D137	D140	D150	D167	D182
Neomysis integer											
Mysidacea sp											
Bodotria pulchella	3	1									
?Cumopsis goodsiri											
Cumacea sp											
Euridice pulchra		24				7					
Jaera albifrons											
Jaera sp											
Idotea linearis											
Hippomedon denticulatus											
Leucothoe incisa											
Talitrus saltator											
Hyale nilssoni											
Gammarus duebeni											
Gammarus locusta											
Gammarus salinus							1				
Melita palmata											
Melita pellucida											
Bathyporeia guilliamsoniana											
Bathyporeia pelagica	10		28		6						
Bathyporeia sarsi		6					1	1			49
Bathyporeia sp				1							
Haustorius arenarius		13			2						
Pontocrates altamarinus	1		8		2		1				
Pontocrates arenarius											
Phoxocephalus holbolli											
Calliopus laevisculus											
Atylus falcatus	2										
Gammaropsis nitida											
Microprotopus maculatus	1										
Corophium multisetosum/volutator					1		4		A		
Corophium multisetosum											
Corophium volutator											
Corophium insidiosum											

Table 4 *(continued)*

Taxa	Station										
	D112	D115	D119	D124	D128	D130	D137	D140	D150	D167	D182
Pariambus typicus											
Crangon crangon							3		2		2
Pagurus pubescens											
Carcinus maenas											
Tectura testitudinalis											
HYDROBIIDAE spp indet											
?Potamopyrgus jenkinsi											
Hydrobia ulvae											25
Nucella lapillus											
BUCCINIDAE sp juv											
OPISTHOBRANCHIA spp											
Polycera quadrilineata											
Mytilus edulis (juvs)											
Mytilus edulis											
Cerastoderma edule											6
Spisula elliptica											
Spisula solida											
Mactra stultorum											
Ensis arcuatus											
Angulus tenuis	1		2								
Fabulina fabula											
Moerella pygmaea											
Macoma balthica			1						21		13
Donax vittatus	2									1	
Abra sp indet											
Abra alba											
Chamelea gallina											
Mya spp juv											
Mya arenaria											
BRYOZOA spp											
Asterias rubens											
Ammodytes tobianus											
DIPTERA spp											
CHIRONOMIDAE spp											
TRICHOPTERA spp											

Table 4 *(continued)*

Taxa	Station													
	D200	D201	D213	D221	C3	C5	C7	C9	C11	C13	C15	C17	C19	C21
HYDROZOA spp														
ACTINIARIA spp														
NEMERTEA spp					1	1								
Harmothoe spp indet														
Harmothoe andreapolis														
Pholoe synophthalmica														
Pholoe baltica														
Sigalion mathildae														
Eteone longa														
Anaitides mucosa														
Eumida bahusiensis														
Kefersteinia cirrata														
Streptosyllis websteri														
Autolytus spp														
NEREIDIDAE spp juv														
Hediste diversicolor														
Neanthes virens														
Nephtys caeca														
Nephtys cirrosa								1	2		1			
Nephtys hombergii														
Nephtys longosetosa														
Nephtys assimilis														
Orbinia spp juv														
Scoloplos armiger														
Aricidea minuta														
Paraonis fulgens								1			P		1	
SPIONIDAE sp juv														
Aonides oxycephala														
Malacoceros fuliginosus														
Marenzelleria viridis				19										
Polydora caeca														
Polydora ciliata														
Polydora quadrilobata														
Pygospio elegans								1						

Table 4 *(continued)*

	Station													
Taxa	**D200**	**D201**	**D213**	**D221**	**C3**	**C5**	**C7**	**C9**	**C11**	**C13**	**C15**	**C17**	**C19**	**C21**
Scolelepis (S) squamata						1	7	2	P	1		5	3	
Spio armata								1						
Spio filicornis														
Spiophanes bombyx														
Magelona mirabilis														
Chaetozone setosa														
Aphelochaeta sp 'A'														
Tharyx sp 'A'														
Capitella spp														
Mediomastus fragilis														
Arenicola marina								1						
Ophelia sp juv														
Ophelia borealis														
Ophelia rathkei														
Travisia forbesii														
Galathowenia oculata														
Melinna palmata														
Ampharete grubei														
Lanice conchilega														
Pomatoceros lamarcki														
OLIGOCHAETA spp														
NAIDIDAE spp														
Paranais littoralis														
Uncinais uncinata														
TUBIFICIDAE spp	1	2												
Psammoryctides barbatus														
Rhyacodrilus coccineus														
Limnodrilus hoffmeisteri														
Tubifex costatus														
Tubificoides benedii														
Heterochaeta costata														
ENCHYTRAEIDAE spp	1		20											
Balanus crenatus														
Gastrosaccus spinifer														

Table 4 *(continued)*

Taxa	Station													
	D200	D201	D213	D221	C3	C5	C7	C9	C11	C13	C15	C17	C19	C21
Neomysis integer														
Mysidacea sp														
Bodotria pulchella							1	1	1					
?Cumopsis goodsiri														
Cumacea sp														
Euridice pulchra					4		23	2				45	5	
Jaera albifrons														
Jaera sp														
Idotea linearis														
Hippomedon denticulatus														
Leucothoe incisa														
Talitrus saltator														
Hyale nilssoni														
Gammarus duebeni														
Gammarus locusta														
Gammarus salinus			5	2										
Melita palmata														
Melita pellucida														
Bathyporeia guilliamsoniana														
Bathyporeia pelagica									40	4	2	1	2	
Bathyporeia sarsi						2	23						47	1
Bathyporeia sp														
Haustorius arenarius			1				2				P	1	2	
Pontocrates altamarinus														
Pontocrates arenarius														
Phoxocephalus holbolli														
Calliopus laevisculus														
Atylus falcatus														
Gammaropsis nitida														
Microprotopus maculatus														
Corophium multisetosum/volutator	A	5	S	6										
Corophium multisetosum														
Corophium volutator														
Corophium insidiosum														

Table 4 *(continued)*

Taxa	Station													
	D200	D201	D213	D221	C3	C5	C7	C9	C11	C13	C15	C17	C19	C21
Pariambus typicus														
Crangon crangon			10			1			1					
Pagurus pubescens														
Carcinus maenas														
Tectura testitudinalis														
HYDROBIIDAE spp indet														
?Potamopyrgus jenkinsi														
Hydrobia ulvae														
Nucella lapillus														
BUCCINIDAE sp juv														
OPISTHOBRANCHIA spp														
Polycera quadrilineata														
Mytilus edulis (juvs)														
Mytilus edulis														
Cerastoderma edule														
Spisula elliptica										1				
Spisula solida														
Mactra stultorum														
Ensis arcuatus														
Angulus tenuis														
Fabulina fabula														
Moerella pygmaea														
Macoma balthica														
Donax vittatus														
Abra sp indet														
Abra alba														
Chamelea gallina														
Mya spp juv														
Mya arenaria														
BRYOZOA spp														
Asterias rubens														
Ammodytes tobianus														
DIPTERA spp														
CHIRONOMIDAE spp	1													
TRICHOPTERA spp														

Table 4 *(continued)*

Taxa	Station											
	WS5	WS6	WS7	WS9	WS11	WS20	FE5	FE6	FE7	FE17	FE20	FE21
HYDROZOA spp												
ACTINIARIA spp												
NEMERTEA spp	2	2		1								
Harmothoe spp indet												
Harmothoe andreapolis												
Pholoe synophthalmica												
Pholoe baltica												
Sigalion mathildae	1	P										
Eteone longa												
Anaitides mucosa												
Eumida bahusiensis												
Kefersteinia cirrata												
Streptosyllis websteri												
Autolytus spp												
NEREIDIDAE spp juv												
Hediste diversicolor								3	6	9	4	
Neanthes virens												
Nephtys caeca												
Nephtys cirrosa	10	8	5	4		6						
Nephtys hombergii												
Nephtys longosetosa												
Nephtys assimilis												
Orbinia spp juv												
Scoloplos armiger												
Aricidea minuta												
Paraonis fulgens												
SPIONIDAE sp juv												
Aonides oxycephala												
Malacoceros fuliginosus												
Marenzelleria viridis									3	2	1	
Polydora caeca												
Polydora ciliata												
Polydora quadrilobata												
Pygospio elegans												

Table 4 *(continued)*

Taxa	**Station**											
	WS5	**WS6**	**WS7**	**WS9**	**WS11**	**WS20**	**FE5**	**FE6**	**FE7**	**FE17**	**FE20**	**FE21**
Scolelepis (S) squamata				4	2	2						
Spio armata												
Spio filicornis												
Spiophanes bombyx	11	6	6			1						
Magelona mirabilis		1										
Chaetozone setosa												
Aphelochaeta sp 'A'												
Tharyx sp 'A'												
Capitella spp												
Mediomastus fragilis												
Arenicola marina												
Ophelia sp juv												
Ophelia borealis												
Ophelia rathkei												
Travisia forbesii												
Galathowenia oculata												
Melinna palmata												
Ampharete grubei												
Lanice conchilega	1											
Pomatoceros lamarcki												
OLIGOCHAETA spp							16	9			1	1
NAIDIDAE spp												
Paranais littoralis												
Uncinais uncinata												
TUBIFICIDAE spp												
Psammoryctides barbatus												
Rhyacodrilus coccineus												
Limnodrilus hoffmeisteri												
Tubifex costatus												
Tubificoides benedii												
Heterochaeta costata									3		1	2
ENCHYTRAEIDAE spp												
Balanus crenatus												
Gastrosaccus spinifer												

Table 4 *(continued)*

Taxa	Station											
	WS5	WS6	WS7	WS9	WS11	WS20	FE5	FE6	FE7	FE17	FE20	FE21
Neomysis integer								4				
Mysidacea sp		2										
Bodotria pulchella												
?Cumopsis goodsiri												
Cumacea sp	4											
Euridice pulchra					3							
Jaera albifrons												
Jaera sp												
Idotea linearis		1										
Hippomedon denticulatus												
Leucothoe incisa												
Talitrus saltator					1							
Hyale nilssoni												
Gammarus duebeni											10	
Gammarus locusta												
Gammarus salinus								6	C		5	
Melita palmata												
Melita pellucida											4	
Bathyporeia guilliamsoniana	1	1	3									
Bathyporeia pelagica	17	22	2	2								
Bathyporeia sarsi				6	26	2						
Bathyporeia sp												
Haustorius arenarius					2							
Pontocrates altamarinus	8	8										
Pontocrates arenarius						2						
Phoxocephalus holbolli												
Calliopus laevisculus												
Atylus falcatus	1											
Gammaropsis nitida												
Microprotopus maculatus	1											
Corophium multisetosum/volutator												3
Corophium multisetosum								105	A	C		
Corophium volutator										C		
Corophium insidiosum												

Table 4 *(continued)*

Taxa	Station											
	WS5	WS6	WS7	WS9	WS11	WS20	FE5	FE6	FE7	FE17	FE20	FE21
Pariambus typicus												
Crangon crangon									4	4		
Pagurus pubescens												
Carcinus maenas												
Tectura testitudinalis												
HYDROBIIDAE spp indet												
?Potamopyrgus jenkinsi												
Hydrobia ulvae												
Nucella lapillus												
BUCCINIDAE sp juv												
OPISTHOBRANCHIA spp												
Polycera quadrilineata												
Mytilus edulis (juvs)												
Mytilus edulis												
Cerastoderma edule												
Spisula elliptica												
Spisula solida												
Mactra stultorum		1										
Ensis arcuatus												
Angulus tenuis	17	23	27	4		6						
Fabulina fabula												
Moerella pygmaea												
Macoma balthica												
Donax vittatus	17	21	22									
Abra sp indet												
Abra alba												
Chamelea gallina	1											
Mya spp juv												
Mya arenaria												
BRYOZOA spp												
Asterias rubens												
Ammodytes tobianus												
DIPTERA spp												
CHIRONOMIDAE spp												
TRICHOPTERA spp												

APPENDIX B Supplemental Sediment Information

Table B1 Summary of particle grain size ranges for all sites in the Firth of Tay and Eden Estuary pSAC

Sample Number	Latitude (OSGB)	Longitude (OSGB)	Mean Grain Size	Median (d50) Grain Size	Sample Number	Latitude (OSGB)	Longitude (OSGB)	Mean Grain Size	Median (d50) Grain Size
C 03	56.46662	-2.75083	297.4	283.7	TAY D062	56.37027	-2.82475	306.9	288.8
C 05	56.46644	-2.75103	332	263.3	TAY D064	56.37325	-2.83015	314.3	242
C 07	56.46606	-2.75134	315.5	292	TAY D066	56.37497	-2.83297	450.2	302.9
C 09	56.46581	-2.75149	420.8	303.5	TAY D070	56.36695	-2.84832	129.1	98.62
C 11	56.46847	-2.72279	238.4	224.4	TAY D073	56.36888	-2.84893	243.2	236.4
C 13	56.46876	-2.72402	307.8	245.3	TAY D087	56.36753	-2.86845	90.07	40.11
C 15	56.46886	-2.72464	302.6	244.3	TAY D097	56.36825	-2.86440	184	186.1
C 17	56.46899	-2.72562	343.1	268	TAY D110	56.39672	-2.80942	246.7	235.3
C 19	56.46909	-2.72616	281.3	256.4	TAY D111	56.39670	-2.80755	384	284.5
C 21	56.46919	-2.72672	388.3	299.5	TAY D112	56.39673	-2.80453	306.1	214.2
TAY 01	56.45138	-2.96842	1002	970.5	TAY D115	56.38775	-2.80693	252.9	242.6
TAY 02	56.44710	-2.97663	481	426.2	TAY D119	56.38773	-2.80280	231.5	216.2
TAY 03	56.45230	-2.96162	830.4	753.2	TAY D124	56.38050	-2.81927	323.8	240.2
TAY 04	56.45480	-2.96617	170.9	161.2	TAY D137	56.44780	-2.86805	369.4	269.9
TAY 05	56.35508	-3.29133	1111	1077	TAY D140	56.45138	-2.86855	221.7	185.5
TAY 06	56.35292	-3.25927	1159	1143	TAY D150	56.45075	-2.87512	187	105.1
TAY 07	56.36192	-3.21195	606.5	496	TAY D167	56.45025	-2.85320	187	105.1
TAY 08	56.39123	-3.13452	779.4	661.3	TAY D182	56.44253	-2.84757	206.7	200.5
TAY 09	56.39230	-3.12187	1166	1159	TAY D200	56.36772	-3.18832	117.9	49.01
TAY 10	56.42095	-3.04702	315.9	274.5	TAY D201	56.36767	-3.18813	68.74	29.41
TAY 11	56.42850	-3.01877	855.4	740.2	TAY D202	56.37180	-3.18190	349.9	336
TAY 12	56.43948	-2.98248	1026	997.3	S1	56.36306	-2.85698	185.8	179.3
TAY 13	56.44177	-2.96440	409.4	350.2	S2	56.36376	-2.85465	85.4	80.3
TAY 14	56.44768	-2.95765	883.9	786.2	S3	56.36396	-2.85001	78.2	60.4
TAY 15	56.43503	-2.96138	431.3	217.6	S4	56.36322	-2.84643	81.7	64.6
TAY 16	56.43700	-2.94998	164.8	148.5	S5	56.36162	-2.84625	76.0	49.8
TAY 17	56.44188	-3.02920	230.5	230.8	S6	56.36789	-2.84634	174.6	174.6
TAY 18	56.46167	-2.93907	398.7	113.2	S7	56.35998	-2.84924	149.8	130.5
TAY 19	56.45500	-2.92058	403.4	376.6	S8	56.36221	-2.85008	113.8	87.2
TAY 20	56.45985	-2.90103	771.8	674.8	S9	56.36268	-2.85492	79.8	68.2

Table B1 *(continued)*

Sample Number	Latitude (OSGB)	Longitude (OSGB)	Mean Grain Size	Median (d50) Grain Size	Sample Number	Latitude (OSGB)	Longitude (OSGB)	Mean Grain Size	Median (d50) Grain Size
TAY 21	56.46582	-2.89648	99.77	28.22	S10	56.36858	-2.85401	160.7	143.3
TAY 22	56.46188	-2.87425	683.7	537	S11	56.36024	-2.85643	96.0	75.5
TAY 26	56.46772	-2.80128	239.8	234.1	S12	56.36190	-2.85721	191.9	202.3
TAY 28	56.43693	-2.72646	329	238.4	S13	56.36624	-2.85736	156.2	142.0
TAY 29	56.40573	-2.78150	191.8	188.7	S14	56.36563	-2.85973	204.4	215.1
TAY 30	56.47152	-2.70528	225.9	208.1	S15	56.36558	-2.86649	104.0	104.5
TAY 32	56.37392	-2.79432	178.6	170.5	S16	56.36437	-2.87082	85.1	73.5
TAY 34	56.36707	-2.86882	777	629.6	S17	56.36472	-2.87565	92.4	91.9
TAY 35	56.36650	-2.85200	655.4	471.4	S18	56.36390	-2.87837	144.9	126.4
TAY 36	56.36405	-2.84183	192.4	190.8	S19	56.36228	-2.87558	132.2	102.1
TAY 37	56.36470	-2.82625	225.6	220.1	S20	56.36180	-2.87189	60.5	50.2
TAY 38	56.38083	-2.81605	565.8	330.9	S21	56.36173	-2.86770	66.0	52.9
TAY 39	56.44815	-2.72537	401.5	388.5	S22	56.36018	-2.86077	156.4	144.1
TAY 40	56.44770	-2.72553	369.9	357.8	S23	56.36044	-2.83343	169.7	169.7
TAY 41	56.44697	-2.77375	694	585.2	S24	56.36042	-2.83730	130.7	90.3
TAY 42	56.44650	-2.77393	858.7	788.1	S25	56.36037	-2.83976	35.8	30.3
TAY 43	56.39977	-3.08628	347.3	280.4	S26	56.35840	-2.84029	158.3	145.0
TAY 44	56.40865	-3.06808	190.7	183	S27	56.35748	-2.83848	139.5	126.3
TAY 45	56.42588	-3.04573	264	71.5	S28	56.35738	-2.83495	168.7	157.5
TAY 46	56.43618	-3.05427	183.6	178.1	S29	56.35651	-2.83175	179.3	179.3
TAY 47	56.44304	-3.06027	125	128.1	S30	56.35646	-2.82893	186.0	186.0
TAY 48	56.44843	-3.06600	122.2	117.2	S31	56.35823	-2.82691	208.1	220.9
TAY 49	56.41167	-3.08453	223	217.2	S32	56.36841	-2.84232	175.2	175.2
TAY 50	56.41765	-3.09013	176.6	170.7	S33	56.36684	-2.84211	76.8	45.6
TAY 51	56.42235	-3.09493	347.8	281.5	S34	56.36561	-2.84279	100.5	75.2
TAY 52	56.42725	-3.10120	133.1	135.1	S35	56.36656	-2.84743	42.1	33.4
TAY 53	56.43225	-3.10667	111.8	98.98	S36	56.36859	-2.84797	182.1	182.1
TAY 54	56.39755	-3.12333	660.7	464	S37	56.36812	-2.85340	96.0	82.3
TAY 55	56.40255	-3.13080	188.5	188.6	S38	56.36796	-2.85805	92.7	87.2
TAY 56	56.40725	-3.13733	96.22	77.33	S39	56.36745	-2.86111	70.5	49.6
TAY 57	56.41196	-3.14387	105.8	95.44	S40	56.36718	-2.88218	169.8	152.3
TAY 58	56.37941	-3.18240	220.7	195.4	S41	56.36836	-2.87225	58.4	48.6
TAY 59	56.38186	-3.18587	134.2	129	S42	56.36723	-2.87730	80.6	70.0

Table B1 *(continued)*

Sample Number	Latitude (OSGB)	Longitude (OSGB)	Mean Grain Size	Median (d50) Grain Size	Sample Number	Latitude (OSGB)	Longitude (OSGB)	Mean Grain Size	Median (d50) Grain Size
TAY 60	56.38373	-3.18880	129.5	117.5	S43	56.36448	-2.82369	227.2	210.1
TAY 61	56.44767	-2.96287	312.9	302.7	S44	56.36848	-2.82085	204.0	188.7
TAY 62	56.37809	-3.16892	790.7	656.6	S45	56.37149	-2.82075	218.7	203.6
TAY 63	56.36218	-3.23395	61.38	35.57	S46	56.37417	-2.81952	240.6	224.5
TAY 64	56.35665	-3.26878	968.2	962.4	S47	56.37663	-2.81825	222.5	208.3
TAY 65	56.45000	-2.99968	192.3	174.9	S48	56.37841	-2.81573	241.5	230.9
TAY 70	56.36695	-2.84832	171.9	162	S49	56.38171	-2.81350	253.1	243.3
TAY 71	56.36750	-2.84835	157.9	154.3	S50	56.37948	-2.81144	252.0	243.9
TAY 72	56.36805	-2.84855	246.9	170.5	S51	56.37804	-2.81392	278.7	269.1
TAY 73	56.36888	-2.84893	188.2	175.6	S52	56.37471	-2.81557	255.5	236.1
TAY 74	56.36883	-2.84367	210.5	196.5	S53	56.37495	-2.81190	251.6	200.6
TAY 76	56.36842	-2.84282	1202	1178	S54	56.37154	-2.81141	212.7	199.9
TAY 77	56.36780	-2.84277	655	534	S55	56.36753	-2.81055	200.7	187.6
TAY 78	56.36740	-2.84283	749.2	594.6	S56	56.36748	-2.81455	209.2	191.7
TAY 79	56.36677	-2.84288	69.93	52.13	S57	56.37138	-2.81697	218.7	206.0
TAY 81	56.36768	-2.84495	81.42	24.86	S58	56.36875	-2.81814	193.7	182.4
TAY D011	56.47030	-2.83300	394.3	306.1	S59	56.36729	-2.81823	290.5	199.8
TAY D015	56.46868	-2.83122	730.2	564.4	S60	56.36448	-2.81289	286.3	205.8
TAY D016	56.46642	-2.82852	482	380.1	S61	56.36118	-2.81128	188.6	178.9
TAY D033	56.46448	-2.85877	236.7	226.5	S62	56.36159	-2.80957	181.3	175.6
TAY D036	56.46562	-2.85995	406.8	234.6	S63	56.35882	-2.81061	261.0	200.5
TAY D049	56.46802	-2.84662	235.8	225.5	S64	56.35337	-2.80840	184.3	178.2
TAY D057	56.45047	-3.06808	63.98	33.09					

Figure B1 Depth profiles obtained from the bathymetric sidescan sonar

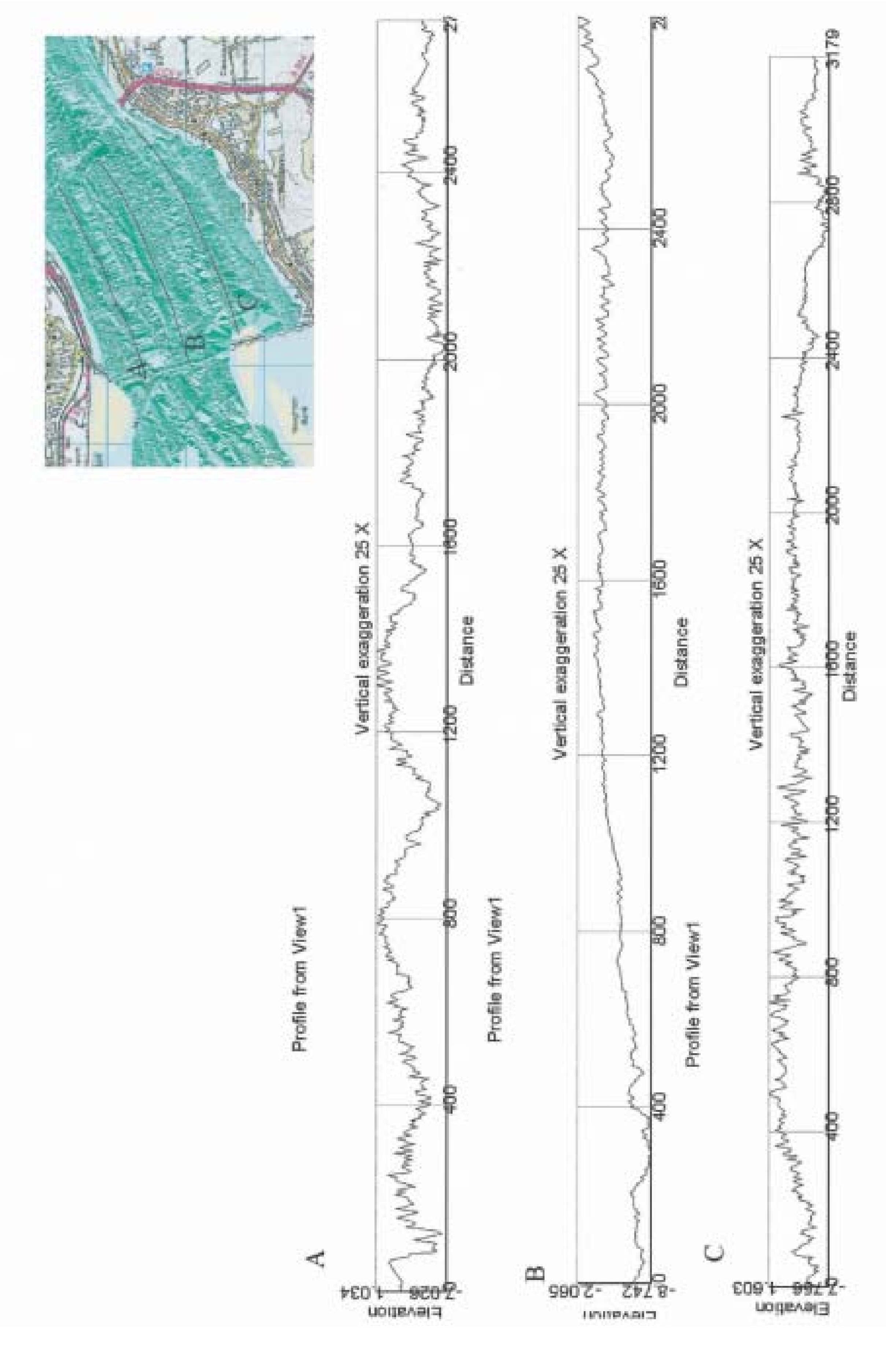

Figure B2 Depth profiles obtained from the bathymetric sidescan sonar

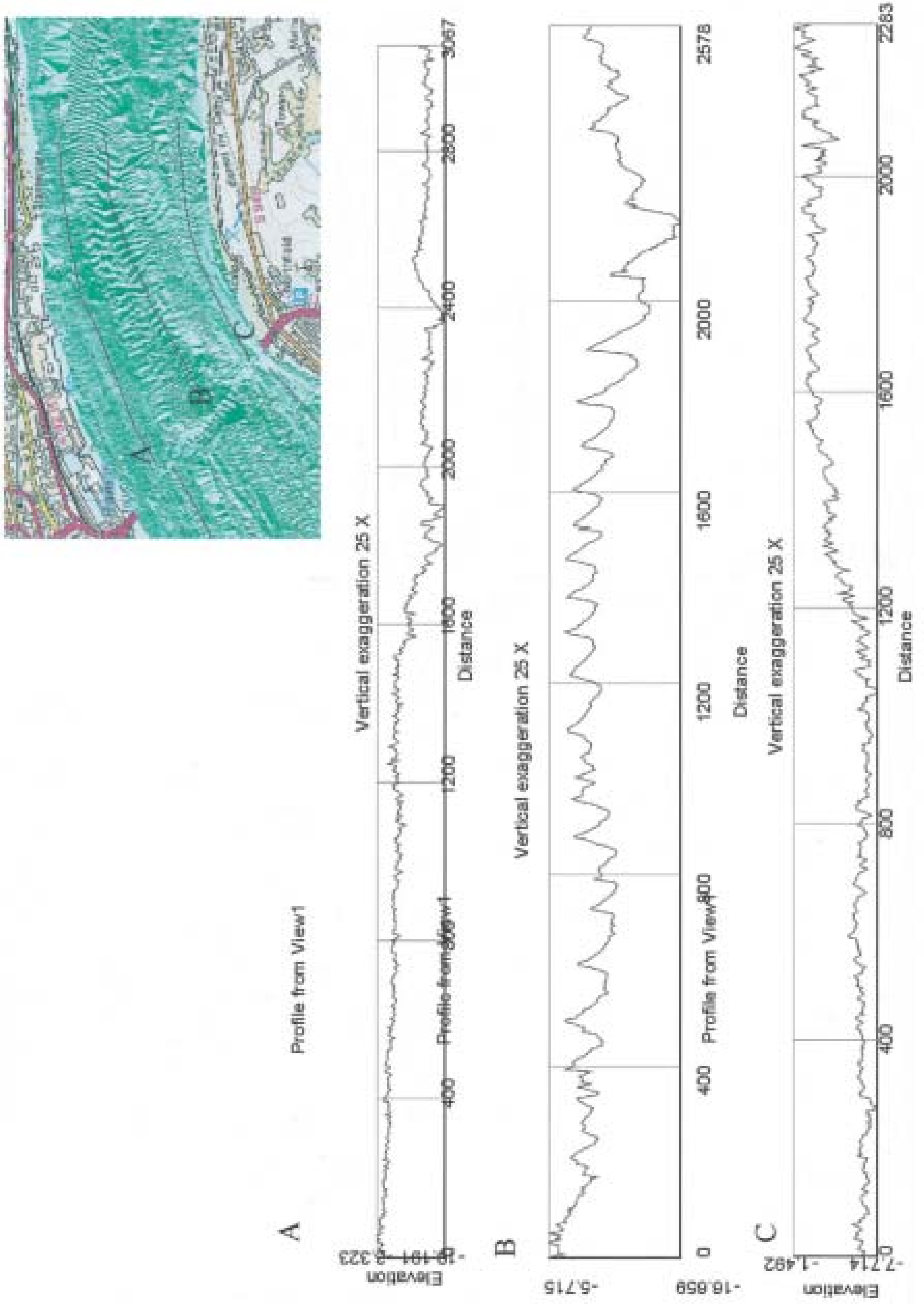

Figure B3 Depth profiles obtained from the bathymetric sidescan sonar

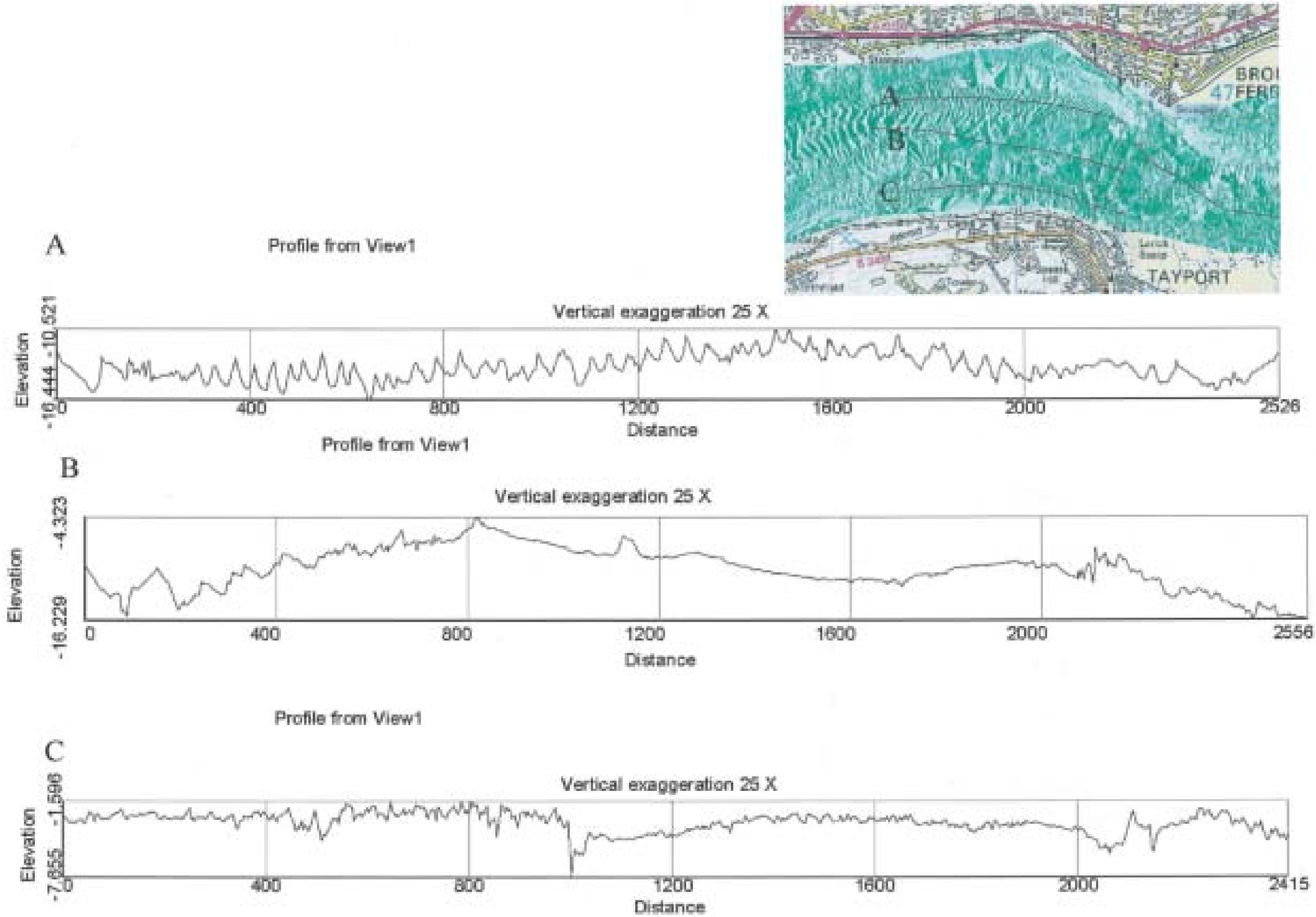

Figure B4 Depth profiles obtained from the bathymetric sidescan sonar

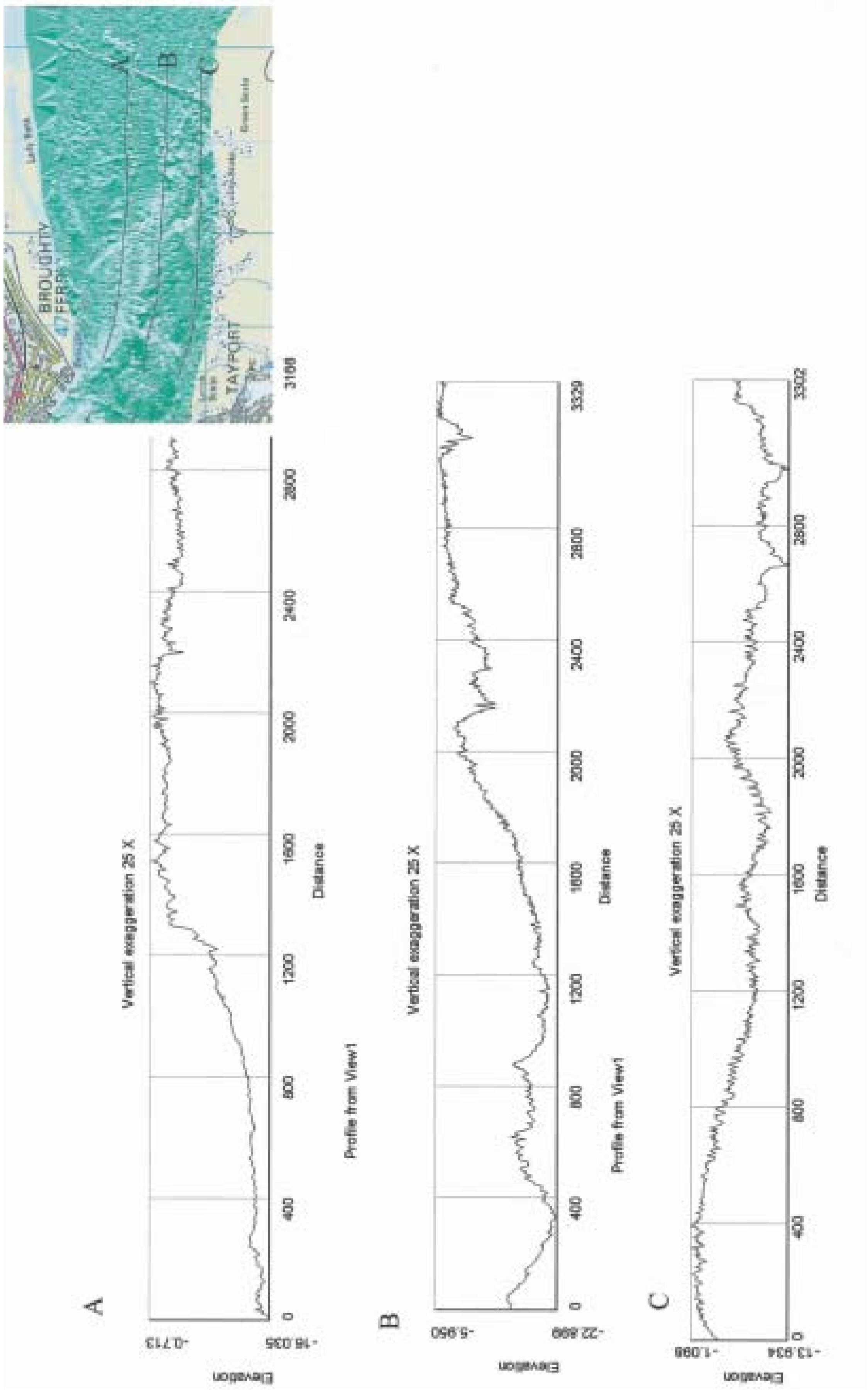

Figure B5 Depth profiles obtained from the bathymetric sidescan sonar

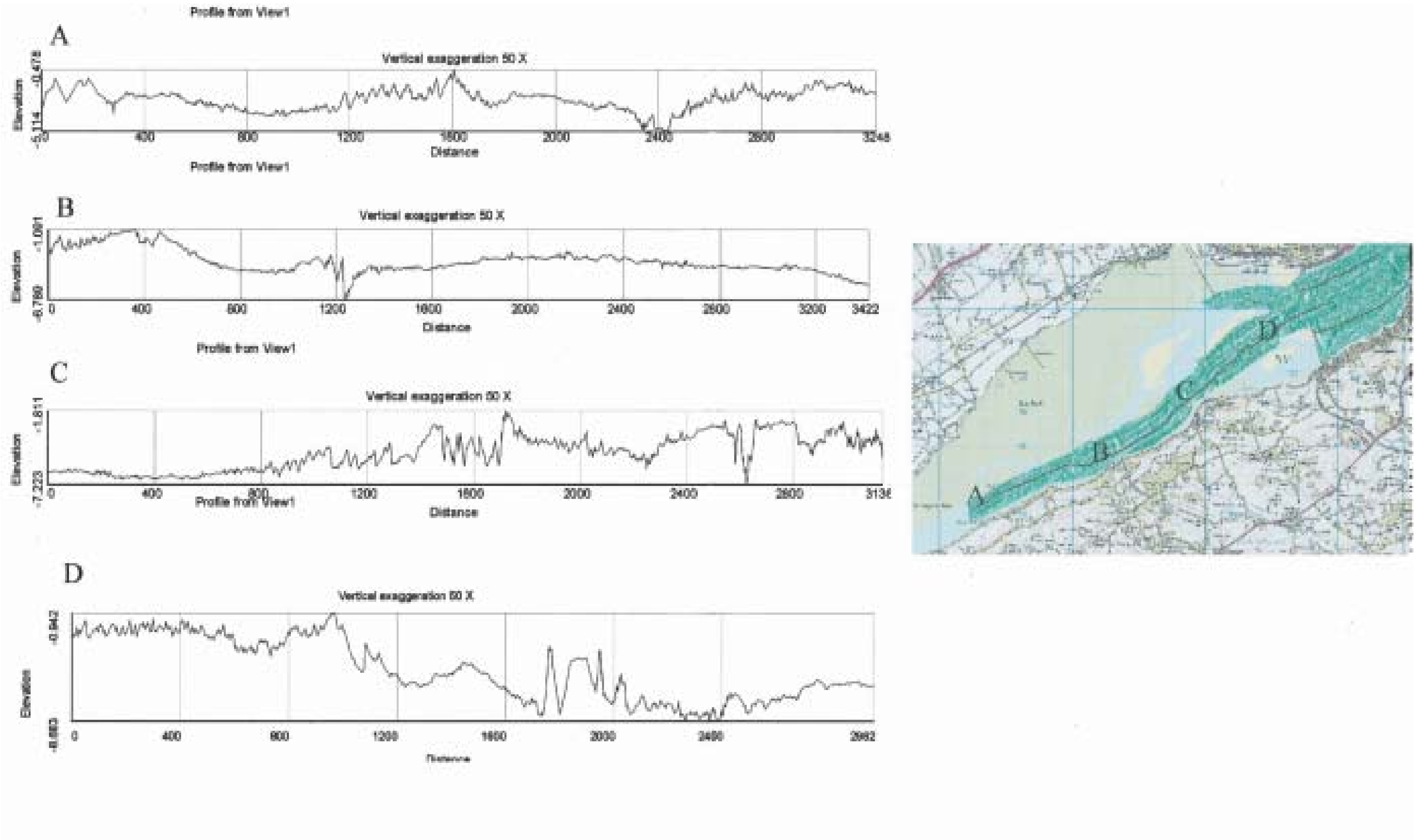

Figure B6 Sediment distribution patterns from McManus et. al, 1990

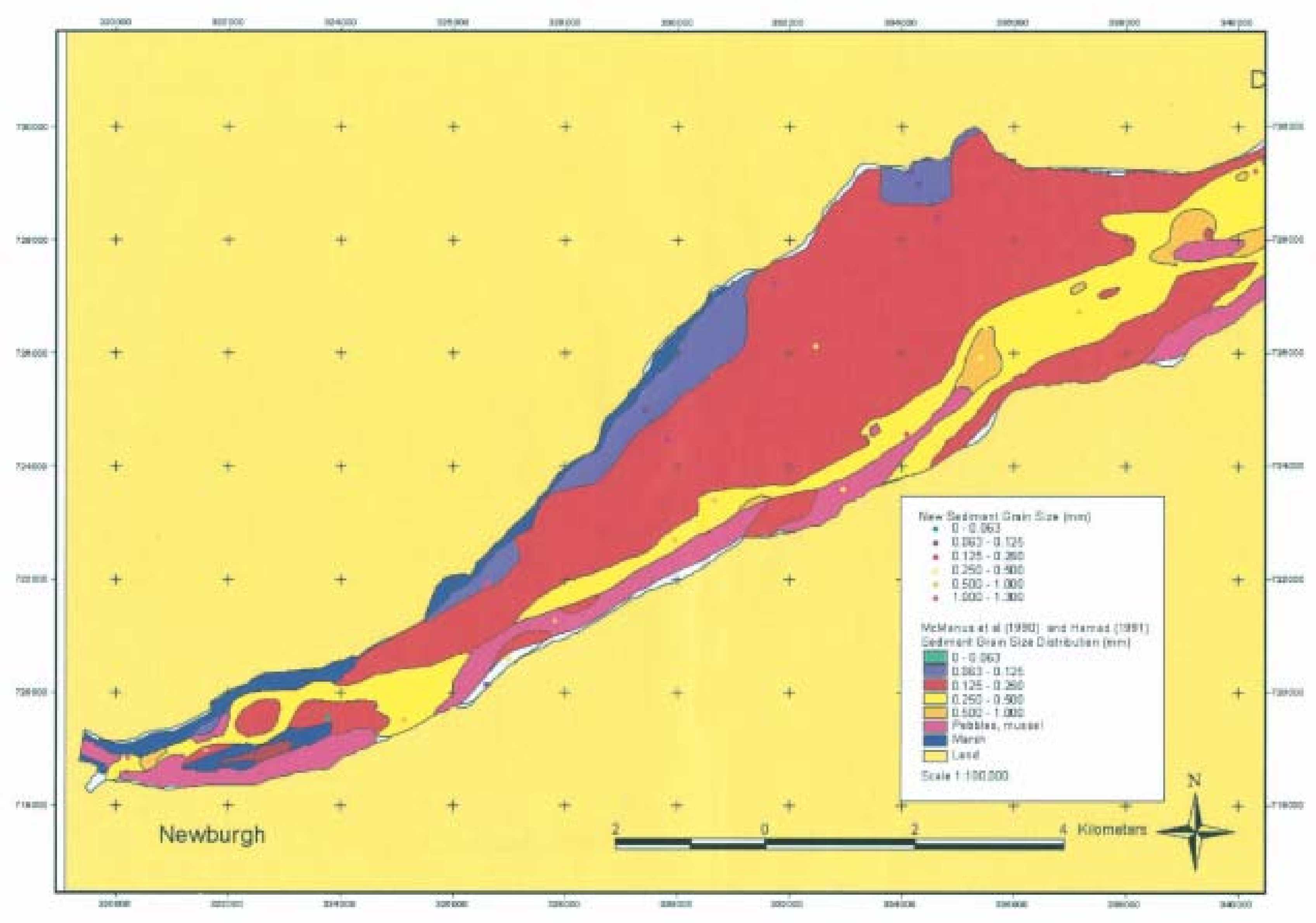

Figure B7 Sediment distribution patterns from McManus et. al, 1990

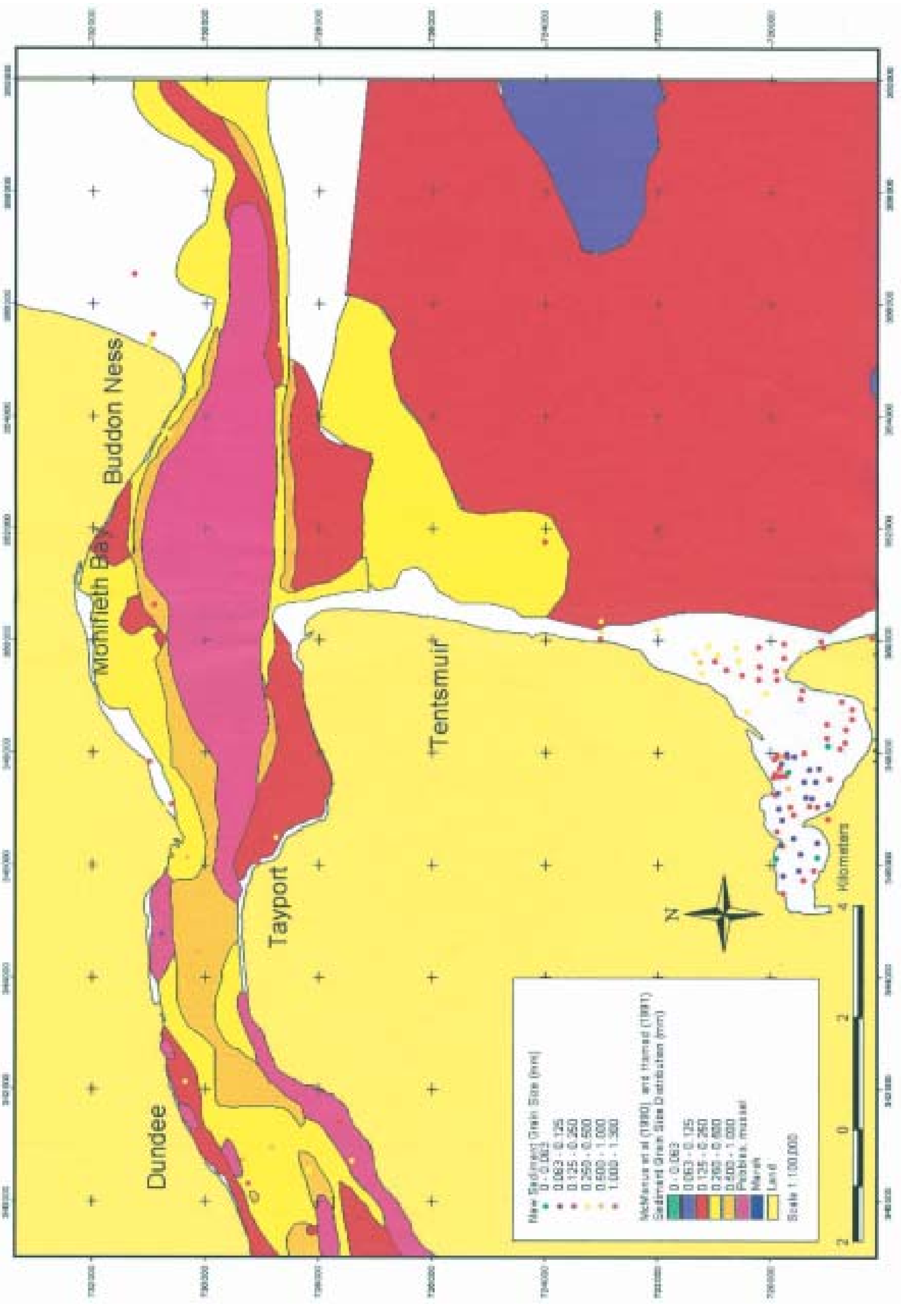

Figure B8 Sediment distribution patterns from Wewetzewr (1998)